

Saúl Vallejos Calzada

TESIS DOCTORAL

Año 2014

POLÍMEROS SENSORES

**APLICACIONES COMO SENSORES QUÍMICOS EN
DETECCIÓN Y CUANTIFICACIÓN DE ANALITOS**

Directores:

Prof. Dr. José Miguel García Pérez

Prof. Dr. Félix Clemente García García

Universidad de Burgos

DEPARTAMENTO DE QUÍMICA

Área de Química Orgánica

Grupo de Polímeros





D. José Miguel García Pérez, Catedrático, y **D. Félix Clemente García García**, Profesor Titular, del Área de Química Orgánica del Departamento de Química de la Universidad de Burgos,

INFORMAN:

La presente Memoria titulada “**Polímeros sensores. Aplicaciones como sensores químicos en detección y cuantificación de analitos**” se ha realizado en el Departamento de Química de la Universidad de Burgos, bajo su dirección, por **D. Saúl Vallejos Calzada**, y autorizan su presentación para que sea calificada como **TESIS DOCTORAL**.

Burgos, 12 de septiembre de 2014.

Fdo.: Prof. Dr. José Miguel García Pérez Fdo.: Prof. Dr. Félix Clemente García García

Agradecimientos

Quisiera expresar mi más sincero agradecimiento a todas las personas que me han apoyado y ayudado, de manera que sin su contribución no hubiera sido posible culminar este trabajo con satisfacción:

A José Miguel García, ya que gracias a él ha sido posible que esté hoy aquí, por su orientación y dirección, sin la cual no hubiera sido posible sacar este trabajo adelante.

A Félix García, por su apoyo, por compartir sus conocimientos conmigo y por los buenos ratos en el laboratorio, sin los cuales no hubiera sido lo mismo.

A Felipe Serna, por darme en su día la oportunidad de conocer de cerca la investigación y el desarrollo dentro de la empresa, y por dirigir de manera impecable mi Tesis de Máster.

A los integrantes del Centro de I+D+i de la Universidad de Burgos, por la ayuda y contribución prestada en este Trabajo de Investigación.

A mis amig@s y a mis compañer@s de laboratorio, tanto a los actuales como a los que ya han terminado, a todos ellos les doy las gracias por su amistad y por los buenos momentos que hemos pasado juntos.

A mis padres, a mi hermano y a Diana, que siempre han estado a mi lado en los momentos más difíciles, les quiero decir que sin ellos nada de lo que hoy en día he logrado hubiera sido posible, ni tampoco tendría sentido.

CAPÍTULO 1 – Introducción general	1
1.1 Antecedentes históricos de los polímeros.....	1
1.2 Sensores y dosímetros químicos.....	7
1.2.1 Sensores químicos ópticos.....	9
1.2.2 Polímeros como sensores químicos y dosímetros	15
1.3 Objetivos	22
1.4 Estructura de la Memoria	23
CAPÍTULO 2 – Polímeros con derivados de fluoreno en su estructura	25
2.1 Fluoreno y sus derivados.....	25
2.2 Polímeros con derivados de fluoreno en la cadena lateral	27
2.3 Resultados	32
<i>Putting to work organic sensing molecules in aqueous media: fluorene-derivative containing polymers as sensory materials for the colorimetric sensing of cyanide in water.....</i>	33
<i>Working with water insoluble organic molecules in aqueous media fluorene derivate-containing polymers as sensory materials for the colorimetric sensing of cyanide in water.....</i>	59
CAPÍTULO 3 – Polímeros con derivados de 2,5-dicetopiperazina en su estructura	63
3.1 2,5-Dicetopiperazina y sus derivados	63
3.2 Polímeros con derivados de 2,5-dicetopiperazina en la cadena lateral	66
3.3 Resultados	70
<i>A selective and highly sensitive fluorescent probe of Hg²⁺ in organic and aqueous media: the role of a polymer network in extending the sensing phenomena to water environments</i>	71
<i>An organic/inorganic hybrid membrane as a solid “turn-on” fluorescent chemosensor for coenzyme a (CoA), cysteine (Cys), and glutathione (GSH) in aqueous media..</i>	103
<i>Methacrylate copolymers with pendant piperazinedione-sensing motifs as fluorescent chemosensory materials for the detection of Cr(VI) in aqueous media</i>	125

CAPÍTULO 4 – Polímeros con derivados de 8-hidroxiquinolina en su estructura	137
4.1 8-Hidroxiquinolina y sus derivados.....	137
4.2 Polímeros con derivados de 8-hidroxiquinolina en la cadena lateral.....	140
4.3 Resultados	143
<i>Solid sensory polymer substrates for the quantification of iron in blood, wine and water by a scalable RGB technique</i>	145
<i>Selective and sensitive detection of aluminium ions in water via fluorescence “turn-on” of both solid and water soluble polymer substrates.....</i>	183
CAPÍTULO 5 – Polímeros con derivados de acilhidrazona en su estructura	209
5.1 Acilhidrazona y sus derivados.....	209
Polímeros con derivados de acilhidrazona en la cadena lateral.....	211
5.3 Resultados	212
<i>Forced solid-state interactions for the rapid, highly sensitive and selective “turn-on” fluorescence sensing of aluminium ions in water using a sensory polymer substrate</i>	213
CONCLUSIONES	253
ANEXOS	255

CAPÍTULO 1

Introducción general

Los polímeros son materiales que se encuentran integrados en nuestra vida cotidiana y que juegan un papel fundamental en la configuración de nuestra actividad. Los avances generales en ciencia y tecnología realizados en las últimas décadas se deben en gran medida a la rápida evolución de la Ciencia y Tecnología de Polímeros, que se ha convertido en un instrumento clave en el desarrollo, seguridad y calidad de vida de los seres humanos. Desde su descubrimiento e incipiente comercialización, hace ya más de un siglo, su empleo se ha ido extendiendo de los ámbitos más básicos, como el envasado y el embalaje, a la más alta tecnología, como la medicina, las comunicaciones, el transporte y la electrónica. En este marco tecnológico se inscribe este trabajo, concretamente en el desarrollo de nuevos sensores poliméricos para aplicaciones avanzadas en la detección de especies químicas de interés.

1.1 Antecedentes históricos de los polímeros

El nacimiento de la Ciencia y Tecnología de Polímeros se asienta sobre las modernas industrias del caucho, de los plásticos, de las fibras, de los recubrimientos, y de los materiales compuestos que tiene su origen a principios del siglo pasado. El primero en proponer una definición correcta de polímero fue Hermann Staudinger, que acuñó el término macromolécula demostrando que las propiedades de las disoluciones de sustancias poliméricas se debían a

la existencia de moléculas de elevadísima masa molecular que poseían el tamaño de partículas coloidales. Staudinger recibió el Premio Nobel en Química en 1953 por su trabajo en este campo. Además esta idea fue confirmada por los trabajos rigurosos de Wallace Carothers^{1,2} en el campo de la policondensación, así como por las extraordinarias aportaciones de Paul Flory³ a la comprensión del comportamiento de los polímeros en disolución y en fundido, por las que le otorgaron el Premio Nobel en Química en 1974, y que pusieron los cimientos científicos, tanto teóricos como experimentales, del desarrollo de la física y la química de las macromoléculas.

El empleo de los polímeros por el hombre se encuentra documentado desde los albores de la humanidad, ya que fueron utilizados por las diferentes civilizaciones como alimento, ropa y refugio. Durante milenios, se fue incrementando la capacidad de manipulación y transformación de estos materiales tan abundantes, aprendiendo a tallar la madera, a hilar el algodón y la lana, y a curtir el cuero. Además de éstos, entre otros hitos notables se pueden citar el desarrollo de la habilidad de los nativos de América Central para convertir el látex del árbol del caucho (*Hevea brasiliensis*) en un material útil, así como la fabricación de papel a partir de fibras vegetales naturales, que se produjo en China hace unos dos mil años. Sin embargo, aunque estos avances fueron significativos para el desarrollo de la civilización moderna, no afectaron realmente a la estructura original de estos polímeros.^{4,5}

Así, en épocas anteriores a 1920, un polímero era considerado un material mal definido y a menudo insoluble, del que se disponía una escasa información estructural, hecho que no impidió la explotación industrial de

¹ W. H. Carothers, G. J. Berchet, *J. Am. Chem. Soc.* **1930**, 52, 5289.

² W. H. Carothers, *J. Am. Soc.* **1929**, 51, 2548; *Chem. Rev.* **1931**, 8, 353; *Collected Papers of Wallace Hume Carothers on High Polymeric Substances*, H. Marck, G.S. Whitby, eds., Wiley-Interscience, New York, 1926.

³ P. J. Flory, *Principles of Polymer Chemistry*, Cornell University Press, Ithaca, 1951.

⁴ H. Morawetz, *Polymers-The Origins and Growth of a Science*, Wiley-Interscience, New York, 1985.

⁵ P. J. T. Morris, *Polymer Pioneers*, Centre for the History of Chemistry, Philadelphia, New York, 1986.

sustancias macromoleculares de origen vegetal y animal, como la celulosa, el caucho o las proteínas, sobre una base eminentemente empírica. La explotación industrial entre 1870 y 1920 de los derivados de la celulosa, como el acetato y el nitrato de celulosa, así como los descubrimientos de la vulcanización del caucho natural por Charles Goodyear a mediados del siglo XIX, y el de la formación de resinas duras y versátiles a partir de la reacción de fenol con formaldehído, por Leo Baekeland en 1908, supusieron el nacimiento de la industria de los plásticos sintéticos.

En 1839 se produjo la primera modificación química de algunas de las macromoléculas citadas anteriormente. Charles Goodyear realizó un salto cualitativo con la vulcanización con azufre del caucho natural, que convertía este material en otro con mejores propiedades mecánicas, sobre todo a altas y bajas temperaturas. Siete años después Christian Friedrich Schönbein consiguió transformar el algodón en nitrocelulosa, que a finales del siglo XIX se convertiría en el material de fabricación de las películas fotográficas y de las pólvoras, y que supondría el inicio de la demanda efectiva de materiales orgánicos por parte de la sociedad, demanda que se ha incrementado exponencialmente hasta nuestros días.

Mas tarde, en 1901, Otto Röhm⁶ realizó los primeros estudios sobre polímeros acrílicos que se comercializaron posteriormente como recubrimientos. El más conocido es el polimetacrilato de metilo (PMMA), que se distribuyó en 1933 bajo el nombre de Plexiglas®^{7,8} por la compañía Röhm & Haas. Su producción aumentó considerablemente durante la Segunda Guerra Mundial al utilizarse como sustituto del vidrio, debido principalmente a su elevada resistencia al impacto y a su transparencia.

En 1908, se produjo otro avance importante en el campo de los polímeros con la síntesis de la *baquelita* por Leo Baekeland, primer polímero sintético de gran éxito comercial. La *baquelita* es un material termoestable,

⁶ O. Röhm, *Ber. Dtsch. Chem. Ges.* **1901**, 34, 573.

⁷ O. Röhm, *Chemische Fabrik* **1936**, 529.

⁸ O. Röhm, E. Trommsdorff, Patente EEUU 2, 171, 765; 1939.

aislante y resistente al agua, a los ácidos y al calor moderado, por lo que se utilizó rápidamente en numerosos objetos de uso doméstico y componentes eléctricos de uso general.

A partir de los pasos preliminares descritos, la Ciencia y Tecnología de Polímeros evolucionó rápidamente. Durante los años 40 y 50 del siglo pasado se desarrollaron las familias de plásticos comerciales de gran consumo, alcanzándose volúmenes actuales de producción muy importantes e intensificándose la investigación en nuevos polímeros y copolímeros, en sus mecanismos de polimerización y en su caracterización. En los años 60 la investigación se derivó hacia la física de polímeros, lo que supuso un avance notable en el conocimiento de la relación de la estructura, la morfología y las propiedades de las macromoléculas. Ésto impulsó la mejora de las propiedades de los polímeros conocidos hasta la fecha, lo que supuso el inicio del crecimiento exponencial que ha tenido este tipo de materiales.

En el año 1963, Karl Ziegler y Giulio Natta recibieron el Premio Nobel por sus estudios en el campo de catalizadores para la polimerización estereoespecífica de alquenos. Sus primeras aplicaciones fueron las polimerizaciones de etileno y de propileno, permitiendo el control de la tacticidad de los polímeros. La relevancia de aquel descubrimiento se refleja en los volúmenes de producción a nivel mundial, 30 y 45 millones de toneladas al año de polietileno de alta densidad y de polipropileno, respectivamente.

Las poliamidas aromáticas, o aramidas, también fueron desarrolladas en los años 60. Estos materiales destacan por su alta resistencia térmica y mecánica, lo que permite que sean utilizadas en aplicaciones de altas prestaciones como trajes para bomberos, chalecos antibalas, ropa de protección anti-corte, etc. Las más conocidas son el Nomex® [poli(*m*-fenilen isoftalamida)] y el Kevlar® [poli(*p*-fenilen tereftalamida)], que se produjeron por primera vez a nivel industrial a principios de la década de 1970.

Los años 70 supusieron la ampliación y consolidación de los conocimientos adquiridos, así como un avance importante de los métodos de

síntesis, transformación y producción de los polímeros generales en sus aplicaciones finales.

Finalmente, en los últimos veinte años del siglo pasado la investigación se ha dirigido hacia la preparación de polímeros con propiedades extraordinarias, sustentada en los conocimientos adquiridos en síntesis de monómeros, procesos de polimerización, caracterización, relación estructura-propiedades, procesado, etc.

Hoy en día, la Ciencia y Tecnología de Polímeros se dirige hacia la obtención y estudio de polímeros especiales, preparados directamente mediante síntesis de nuevos monómeros, o bien a través de modificaciones químicas y físicas de polímeros preexistentes. Se ha convertido en una ciencia puntera, eminentemente interdisciplinaria, que se encuentra en las fronteras de la Química, la Física, la Ingeniería y la Biología, y que además exige conocimientos sobre síntesis, caracterización, estructura, procesado, propiedades y comportamiento de los materiales. Los principales objetivos de esta rama de la investigación científica son materiales con alto módulo, de alta resistencia térmica, electroactivos, fotosensibles, biopolímeros, polímeros con propiedades ópticas no lineales, nanomateriales, sistemas multicomponente con propiedades especiales, materiales selectivos para técnicas de separación o análisis, entre otros.⁹

De esta manera, los polímeros actualmente forman parte de una amplia gama de materiales estructurales, funcionales y de aplicaciones especiales, que encuentran aplicación en la industria de la construcción, aeronáutica, automovilística, del envasado y embalaje, electrónica, en aplicaciones médicas, en aislamientos térmicos y eléctricos, etc., adquiriendo una gran importancia económica y de bienestar social.

⁹ *New Trends in Polymer Sciences*, Macromolecular Symposia, Vol. 283-284, Eds.: K. Matyjaszewski, R. C. Advincula, E. Saldivar-Guerra, G. Luna-Bárcenas, R. González-Núñez, John Wiley & Sons, New York, 2009.

La diversidad de aplicaciones que encuentran los materiales poliméricos se debe a la variedad de propiedades físicas y químicas que pueden presentar, y que están relacionadas intrínsecamente con su estructura, la cual deriva de la naturaleza del monómero y de los enlaces que forman a lo largo de la cadena polimérica, además de los grupos laterales del tipo mono o polifuncional que puedan incorporar. Todos estos factores confieren distintos grados de rigidez a las cadenas y distintas fuerzas de interacción entre las mismas, que determinarán, finalmente, las propiedades que presente el material.

Este extraordinario desarrollo ha impulsado notablemente la investigación en este campo, uno de los más activos desde el punto de vista científico y tecnológico en la actualidad. Los avances generales en ciencia y tecnología realizados en las últimas décadas se deben, en una parte significativa, a la rápida evolución de la Ciencia y Tecnología de Polímeros, que se ha convertido en un instrumento clave en el desarrollo, seguridad y calidad de vida de los seres humanos.^{10,11}

Entre los avances y desarrollos tecnológicos recientes se encuentran los sistemas de detección y cuantificación por reconocimiento molecular (sondas moleculares como sensores y dosímetros químicos), que se desarrollaron inicialmente con moléculas discretas, de pequeña masa molecular, a partir de la evolución de la química supramolecular. Sin embargo, el salto cualitativo en este campo se produjo con la inclusión de subestructuras de reconocimiento molecular en polímeros, tanto ancladas covalentemente como grupos laterales, como formando parte de la estructura covalente de la cadena principal, para dar lugar a polímeros sensores.¹²

¹⁰ J. L. Mateo, *Introducción en Ciencia y Tecnología de Polímeros*, Vol. 1, Instituto de Ciencia y Tecnología de Polímeros (CSIC), Madrid, 2004, Cap. 1.

¹¹ *New Polymeric Materials: Reactive Processing and Physical Properties*, Eds.: E. Martusceli, C. Marchetta, VNU Science Press BV, Utrecht, 1987.

¹² J. M. García, F. C. García, F. Serna, J. L. de la Peña, *Polym. Rev.* **2011**, 51, 341.

1.2 Sensores y dosímetros químicos

El reconocimiento molecular es un fenómeno clave muy extendido en el medio natural, que se da entre dos o más moléculas cuando éstas son químicamente y geométricamente complementarias. Se establece espacialmente debido a interacciones moleculares consideradas débiles, como por ejemplo las electrostáticas e hidrofóbicas, los puentes de hidrógeno y las coordinaciones débiles metal-ligando.^{13,14} En la naturaleza, estos procesos tienen lugar en medios acuosos, en los que generalmente intervienen macromoléculas naturales, o incluso sistemas complejos organizados, como células. Entre los ejemplos de reconocimiento se pueden citar: la interacción enzima/sustrato,¹⁵ fármaco/diana biológica,^{16,17} antígeno/anticuerpo,^{18,19} y la síntesis del ARNm a partir del ADN,²⁰ entre otros.

La Química Supramolecular, término acuñado por Jean-Marie Lehn en 1978, o química *anfitrión-huésped*, se desarrolló observando los fenómenos de reconocimiento molecular en los sistemas biológicos comentados tratando de imitar a la naturaleza en la efectividad, simplicidad y resultados de estos procesos en medios biológicos. Se trata de una disciplina que evolucionó durante los años 60, con estudios como el de la descripción de la interacción de cationes con éteres corona por Charles Pedersen en 1967, o el desarrollo de los criptandos y esferandos por Jean-Marie Lehn y por Donald Cram.²¹ Pedersen, Lehn y Cram fueron galardonados en 1987 con el premio Nobel en Química por su incipiente trabajo en este ámbito.

¹³ N. M. Bergmann, N. Peppas, *Prog. Polym. Sci.* **2008**, 33, 271.

¹⁴ B. N. Chen, S. Piletsky, A.P.F. Turner, *Comb. Chem. High Throughput Screen.* **2002**, 5, 409.

¹⁵ A. Tulinsky, *Sem. Thromb. Hemostasis.* **1996**, 22, 117.

¹⁶ M. Britschgi, S. von Gyerz, C. Burkhardt, W. J. Pichler, *Curr. Drug. Targets.* **2003**, 4, 1.

¹⁷ P. Cudic, D. C. Behenna, J. K. Kranz, R. G. Kruger, A. J. Wand, Y. I Veklich, J. W. Weisel, D. G. McCafferty, *Chem. Biol.* **2002**, 9, 897.

¹⁸ E. J. Sundberg, R. A. Mariuzza, *Adv. Protein. Chem.* **2002**, 61, 119.

¹⁹ R. Jimenez, G. Salazar, K.K. Baldridge, F. E. Romesberg, *Proc. Natl. Acad. Sci. USA* **2003**, 100, 92.

²⁰ S. A. Hofstadler, R. H. Griffey, *Chem. Rev.* **2001**, 101, 377.

²¹ J. W. Steed, J. L. Atwood, *Supramolecular Chemistry*, John Wiley & Sons, Ltd., Chichester, 2000.

El término *reconocimiento* se emplea únicamente cuando la interacción *anfitrión-huésped* es muy específica y, por tanto, el *anfitrión* se puede utilizar para el desarrollo de dispositivos tecnológicos tales como sensores, membranas permselectivas, catalizadores, o sistemas de extracción, por poner algunos ejemplos.

En este sentido, se considera muy importante combinar el fenómeno del reconocimiento con la transducción de la señal para el desarrollo real de sistemas o dispositivos capaces de detectar rápidamente productos químicos o moléculas biológicas. El término *sensor* se reserva para los fenómenos de reconocimiento *anfitrión-huésped* que dan lugar a la variación de una propiedad macroscópica fácilmente detectable y, en definitiva, cuantificable. La IUPAC define un sensor químico como aquel dispositivo que transforma una información química en una señal analítica de utilidad. Desde un punto de vista menos genérico, una molécula sensora es una estructura química con, al menos, dos subgrupos o subunidades integrados, donde uno de ellos actúa como *unidad receptora* y el otro como *subunidad indicadora*. La capacidad para interaccionar reversible y selectivamente (sensor químico o quimiosensor), o incluso reaccionar irreversiblemente (dosímetro químico), con un *analito* dado recae en la *unidad receptora*, mientras que el fenómeno de la detección, relacionado con la variación de una propiedad macroscópica, depende de la *subunidad indicadora*, o *transductora*.

Hoy en día, desde el punto de vista tecnológico, se necesitan sensores selectivos y de bajo umbral de detección para el seguimiento en tiempo y espacio reales de la concentración de *analitos* de interés biológico, clínico, medioambiental, químico o industrial. En relación con la terminología, conviene aclarar que desde el punto de vista práctico cuando se habla de sensores se incluye asimismo a los dosímetros.

En resumen, cuando un determinado *receptor* para aniones, cationes o moléculas neutras está unido a otra agrupación química (covalente o no covalentemente) que es capaz de transformar la interacción que se produce

con el *huésped* en una señal macroscópica detectable, nos encontramos ante un quimiosensor o sonda molecular.^{22,23} En función de la señal que detectamos los sensores pueden ser, entre otros, piezoelectricos, electroquímicos y ópticos.

1.2.1 Sensores químicos ópticos

Cuando además, la transducción de la información se produce a través de un cambio de las propiedades fluorescentes, o mediante un cambio de color, se habla de sondas fluorogénicas o cromogénicas, respectivamente. En este proceso, la información que se produce a nivel molecular, como puede ser la presencia o no de un determinado *analito*, se amplifica y se observa macroscópicamente.

A pesar de ser un área relativamente reciente los sistemas descritos comienzan a materializarse en aplicaciones prácticas reales. Desde el Grupo de investigación, y con materiales descritos en esta tesis, se ha desarrollado un proyecto empresarial para la creación de una empresa de base tecnológica (EBT). El tema tiene ya, entre otros, el atractivo de su interdisciplinariedad, que permite relacionar conceptos como diseño, síntesis, coordinación, propiedades fotofísicas, informática, etc., a fin de obtener productos basados en sondas químicas moleculares con marcadas tendencias selectivas hacia determinados *analitos* de interés, así como nuevos software que permitan su cuantificación automática mediante dispositivos móviles.

En general, hay dos tipos de diseño de sondas moleculares en relación con la naturaleza de la unión entre la unidad coordinante y la indicadora, tal como se muestra esquemáticamente en la Figura 1.1. Si ésta es covalente se habla de *aproximación unidad coordinante-unidad indicadora* y si no lo es, de *aproximación por ensayos de desplazamiento*.

²² J. P. Desvergne, A. W. Czarnik, *Chemosensors for Ion and Molecule Recognition*, NATO ASI Series, Kluwer Academic Publishers, London, 1997.

²³ M. D. Marcos, R. Martínez-Máñez, F. Sancenón, J. Soto, L. A. Villaescusa, *Anales de la Real Sociedad Española de Química* **2004**, 100, 20.

Esta clasificación se basa en los principios de la química de la coordinación y, por tanto, la interacción del *analito* con el *receptor* es en principio reversible. De hecho, la coordinación es una típica reacción química reversible en la cual los cambios en la concentración del *analito* determinan la relación entre las especies coordinada y libre.

Además de los quimiosensores moleculares, hay otra aproximación a la detección química selectiva, como son los sistemas denominados dosímetros químicos o quimodosímetros. En la *aproximación del dosímetro químico*, la idea última no es utilizar sistemas selectivos de coordinación, como en los casos anteriores, sino reacciones químicas altamente específicas, y generalmente irreversibles, inducidas por un determinado *analito*, asociadas a un cambio en alguna propiedad macroscópica medible del sistema, en nuestro caso óptica.²⁴⁻²⁶

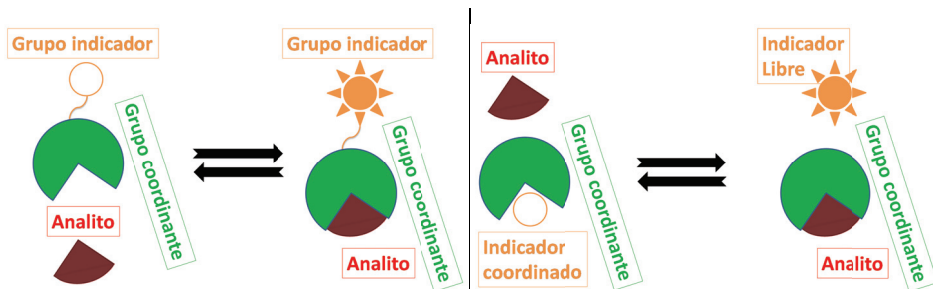


Figura 1.1. Representación esquemática de la *aproximación unidad coordinante-unidad indicadora* (izquierda), y de la *aproximación por ensayos de desplazamiento* (derecha).

Dentro de las propiedades macroscópicas que más se analizan cuando se habla de sensores destacan dos: el color y la fotoluminiscencia. La segunda, se puede definir como la emisión espontánea de radiación, de luz, por parte de cualquier sustancia desde un estado electrónico excitado. Se puede dividir formalmente en dos categorías, fluorescencia y fosforescencia, en función de la naturaleza del mencionado estado excitado. Si la molécula excitada tiene la

²⁴ M. Y. Chae, A. W. Czarnik, *J. Am. Chem. Soc.* **1992**, *114*, 9704.

²⁵ V. Dujols, F. Ford, A. W. Czarnik, *J. Am. Chem. Soc.* **1997**, *119*, 7386.

²⁶ F. García, J. M. García, B. García-Acosta, R. Martínez-Máñez, F. Sancenón, J. Soto, *Chem. Commun.* **2005**, 2790.

misma multiplicidad que la molécula en el estado fundamental se habla de fluorescencia. Se caracteriza porque al irradiar una molécula, ésta emite radiación a longitudes de onda mayores que la empleada para la excitación.²⁷ La subestructura de la molécula responsable de la fluorescencia se denomina fluoróforo.

Existen diferentes procesos que permiten utilizar como señal de respuesta la variación de la intensidad de la fluorescencia tras el proceso de coordinación. Entre otros, se pueden citar:

- ❖ Transferencia electrónica fotoinducida (PET, *Photoinduced Electron Transfer*) y desactivación por transferencia de energía (EET, *Electronic Energy Transfer*).
- ❖ Excímeros.
- ❖ Efectos asociados a variaciones en la rigidez de los fluoróforos.

Los procesos PET y EET asociados a la interacción *anfitrión-huésped* se muestran de forma esquemática en la Figuras 1.2 y 1.3.

En general, los procesos PET (Figura 1.2) pueden dar lugar al desarrollo (*apagado-encendido*, *encendido*, *turn-on*, u *OFF-ON*) o al amortiguamiento (*encendido-apagado*, *apagado*, *turn-off*, u *ON-OFF*) de la fluorescencia. Los primeros se observan en *receptores* con pares de electrones no-enlazantes de alta energía, que amortiguan la emisión por una rápida transferencia electrónica intramolecular (IET, *Intramolecular Electron Transfer*) del *quimiosensor* o *receptor* al estado excitado del fluoróforo. Tras la coordinación del *receptor* a una *molécula objetivo* que se comporta como un ácido de Lewis, disminuye en energía el orbital molecular ocupado de más alta energía (HOMO) del *receptor*, impidiendo la IET y encendiéndola la fluorescencia.

²⁷ J. R. Lakowicz, Cap. 1, Ed. 3, *Principles of Fluorescence Spectroscopy*, Kluwer Academic/Plenum Publishers, New York, 2006.

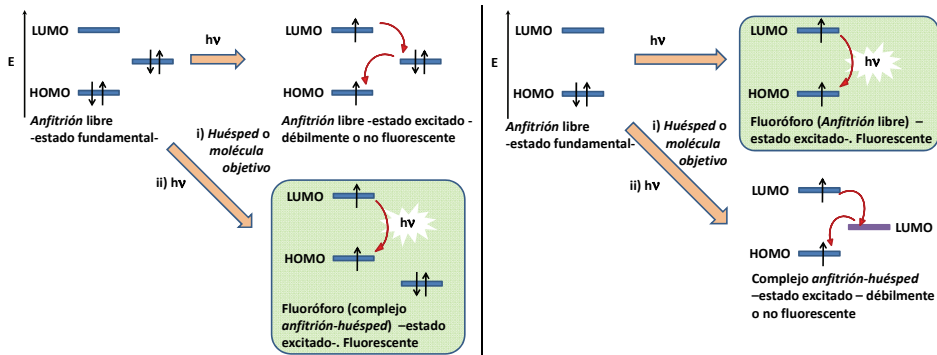


Figura 1.2. Representación esquemática de los procesos PET (izquierda: *encendido*, derecha: *apagado*).

El *apagado* de la fluorescencia (amortiguamiento, *quenching*) se observa cuando la energía del orbital no ocupado de más baja energía (LUMO) del *huésped* se encuentra entre el HOMO y el LUMO del quimiosensor. Así, cuando se produce la interacción se observa la disipación de la energía de excitación por un proceso no radiativo, dando lugar al amortiguamiento de la fluorescencia.

En relación al amortiguamiento por EET, tiene lugar cuando el *analito*, o *huésped*, tiene un orbital molecular vacío o semiocupado entre la energía del HOMO y del LUMO del *receptor*. En ese caso se produce el intercambio síncrono de dos electrones, tal como se muestra en la Figura 1.3.

En cualquier caso, el término amortiguamiento es genérico y se refiere a la disminución de la intensidad de la fluorescencia por cualquier proceso, y se puede analizar globalmente por la ecuación de Stern-Volmer, $I_0/I = 1 + K_{SV}[G]$, donde I_0 e I son la intensidad de la fluorescencia en la ausencia y presencia de *huésped* o *analito*, respectivamente, $[G]$ es la concentración de *huésped* o *analito*, y K_{SV} es la constante de Stern-Volmer, que está relacionada con la eficiencia del *huésped* como amortiguante de la fluorescencia.

Además, hay que tener en cuenta que el amortiguamiento de la fluorescencia proviene de múltiples procesos paralelos de naturaleza compleja. Desde un punto de vista simple, éste se puede describir como una mezcla de

amortiguamiento estático y dinámico, estando el primero asociado a la formación de complejos *anfitrío-huésped*, y el segundo a las colisiones entre el fluoróforo y el *huésped*.

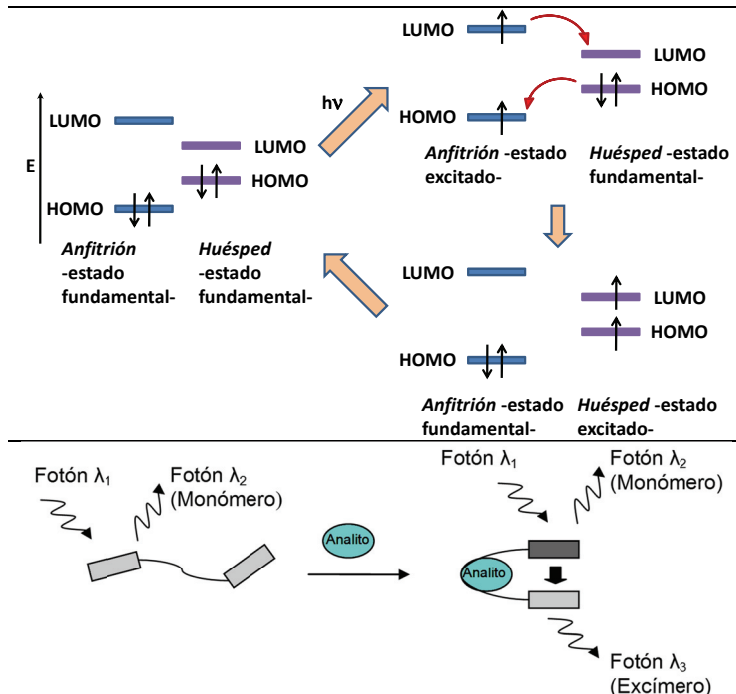


Figura 1.3. Representación esquemática de los procesos EET (arriba) y de un excímero tras la interacción con un *analito* (abajo).

Por otra parte, un excímero es un complejo formado por la interacción de una molécula de fluoróforo en el estado excitado con otra en el estado fundamental (Figura 1.3). Los excímeros presentan bandas de emisión desplazadas hacia el rojo (emisión del excímero) cuando se compara con la emisión del propio fluoróforo (emisión del monómero) y en numerosos casos se observan las dos emisiones (del monómero y del excímero) a la vez. Así, la formación o ruptura de excímeros, como resultado de la adición de un *analito*, sirve para detectar la presencia del mismo. Los excímeros se observan en ocasiones si: (i) se emplean fluoróforos aromáticos y planos; y (ii) cuando dos unidades del fluoróforo estén próximas en el espacio y sean capaces de establecer interacciones, generalmente de apilamiento π .

En cuanto a la rigidez del sistema, si como consecuencia de la coordinación del *analito* se produce un aumento de la rigidez del complejo formado, lo que hace menos probable la desactivación no radiante del estado excitado, se puede observar un aumento en la intensidad de emisión.

Por otro lado, la señal macroscópica que provoca la unión anfitrón-huésped puede ser un cambio de color. La detección y cuantificación de *analitos* a simple vista, a través de variaciones en el color, es clave en el desarrollo de sensores colorimétricos para uso por personal no especializado. Así, por ejemplo, estos materiales serán, en un futuro próximo, extremadamente útiles para el ensayo y detección de moléculas contaminantes *in situ* mediante una sencilla prueba analítica visual que indique al instante si se sobrepasan o no (*pasa / no pasa*) los límites legales de un determinado compuesto en efluentes acuosos. Además, las variaciones en el espectro de absorción de radiación ultravioleta y visible se pueden medir de forma muy precisa y económica con espectrofotómetros de UV/Visible, o con equipos UV/Visible de fotodiódos portátiles conectados asimismo a ordenadores portátiles, a tabletas o a teléfonos móviles.

Los sistemas coloreados están formados por estructuras conjugadas con diferencias de energía entre el HOMO y el LUMO correspondientes a las de la radiación electromagnética visible. Un incremento en la extensión del sistema conjugado disminuye la diferencia de energía HOMO-LUMO dando lugar a un desplazamiento hacia el rojo, o batocrómico, de la banda de absorción. La longitud de onda absorbida se puede variar tanto por el control de la extensión o del diseño del sistema conjugado, como mediante la introducción de grupos dadores (p.ej., -NR₂, -OR, -O⁻, etc.) y aceptores de (p.ej., -NO₂, -CN, -SO₃H, -SO₃⁻, -COR, etc.) de electrones en el sistema conjugado. La conjugación extendida entre un grupo dador y uno aceptor da lugar a complejos de transferencia de carga (CT) que se asocian generalmente a colores intensos debido a que poseen coeficientes de extinción molar elevados. La interacción de la molécula cromófora, que actúa como *anfitrión*,

con un *huésped* varía generalmente las características dadoras o aceptoras de los grupos, modificando al CT, con la consiguiente transducción por cambio de color.

En general, las moléculas sensoras discretas, de baja masa molecular, presentan una limitada resistencia química y térmica, y su separación y recuperación de una disolución es laboriosa y cara, desde un punto de vista aplicado, debido a su solubilidad. Como consecuencia, en aplicaciones finales se requiere su inmovilización en un soporte para la obtención de un material con propiedades mecánicas suficientes y, paralelamente, como una forma de reducir la tendencia a la migración de estas moléculas. El diseño y síntesis de macromoléculas con subunidades *anfitrión* ancladas químicamente a la cadena principal, o como parte integral de ésta, ofrece una vía inmejorable de inmovilización. Es más, los polímeros poseen habitualmente buenas propiedades mecánicas y térmicas, por lo que se pueden transformar de forma sencilla en materiales acabados, como películas o recubrimientos, para la obtención de dispositivos sensores baratos, como por ejemplo filmes sensores colorimétricos, o integrar los mismos en equipos portátiles de espectroscopía de UV/Vis o fluorescencia, empleando fibras ópticas recubiertas en su extremo con los polímeros sensores.²⁸⁻³²

1.2.2 Polímeros como sensores químicos y dosímetros

Como es natural, los fenómenos de detección en sistemas biológicos se dan en medios acuosos. Por ejemplo, los sitios activos en las enzimas tienen la forma requerida para alojar a la *molécula huésped*, o parte de ella, y la interacción se basa en enlaces débiles que tienen lugar debido a los dominios hidrofóbicos en un entorno hidrofilico general, proporcionado por la constitución química y por la estructura cuaternaria de las proteínas. De una forma simplificada, se puede

²⁸ J. M. García, F. C. García, F. Serna, J. L. de la Peña, *Prog. Polym. Sci.* **2010**, 35, 623.

²⁹ K. C. Persaud, *Mater. Today*, **2005**, 8, 38.

³⁰ P. Anzenbacher Jr, Y. Liuand, M. E. Kozelkova, *Curr. Opin. Chem. Biol.* **2010**, 14, 1.

³¹ K. E. Geckeler, *Advanced Macromolecular and Supramolecular Materials and Processes*, Ed., Kluwer Academic/Plenum Publishers, New York, 2003.

³² V. Rotello, S. Thayumanavan, *Molecular Recognition and Polymers. Control of Polymer Structure and Self-Assembly*, Wiley, Hoboken, 2008.

decir que la competitividad de las moléculas de agua para establecer estas interacciones débiles disminuye localmente, o se altera drásticamente, según sea el microentorno de los sitios activos.

En un intento de imitar a la naturaleza, se pueden anclar *receptores* insolubles en agua, lipofílicos, a cadenas lineales o reticuladas de polímeros hidrofílicos, dando lugar a polímeros sensores solubles en agua o a materiales sensores hinchados en este medio, con comportamiento tipo gel. Esta última aproximación al fenómeno sensor permite el control del hinchamiento por medio del incremento o disminución de la densidad de nudos, denominada relación nominal de entrecruzamiento. Es decir, el carácter hidrofílico del polímero, relacionado con la constitución de los monómeros, se puede controlar no sólo mediante la naturaleza de los comonómeros utilizados en la síntesis del material, sino también a través del porcentaje de entrecruzante empleando en la síntesis, facilitando o disminuyendo la absorción de agua. Así, se puede inducir un carácter hidrofóbico a una estructura polimérica hidrofílica mediante la tensión de la red tridimensional en el proceso de hinchamiento con agua, tal como se ha demostrado en trabajos anteriores.^{26,33}

Además de la posibilidad de disponer de polímeros con diferente geometría (lineal, esférica y tridimensional –redes entrecruzadas–), la constitución química de las macromoléculas se puede diseñar de forma que los *receptores* anclados químicamente a la cadena lateral, o formando parte de la cadena principal, posean microentornos hidrofóbicos o hidrofílicos, independientemente de la naturaleza hidrofílica o hidrofóbica del disolvente. Así, la estructura tridimensional del ovillo estadístico en disolución se asemeja a la estructura terciaria y cuaternaria de las proteínas, y se puede expandir o colapsar parcialmente incrementando o disminuyendo su afinidad con el disolvente. Es más, los polímeros hinchados, o geles poliméricos, con *grupos receptores* selectivos, pueden dar lugar al fenómeno de la detección en el estado intermedio sólido-líquido, donde los *analitos* en disolución pueden

³³ B. García-Acosta, F. García, J. M. García, R. Martínez-Máñez, F. Sancenón, N. San José, J. Soto, *Org. Lett.* **2007**, 9, 2429.

interaccionar con la subestructura del *receptor* no disuelta, que puede ser completamente compatible o incompatible con el medio, con la consiguiente transducción de la señal.

Al mismo tiempo, los polímeros, como moléculas de alta masa molecular, muestran propiedades colectivas que son sensibles a perturbaciones menores. Así, por ejemplo, la interacción de una molécula *anfitrío* con un único *grupo huésped*, de los múltiples anclado a una cadena polimérica sensora, puede dar lugar al amortiguamiento completo de la fluorescencia de toda la cadena de un polímero conjugado, con la consiguiente amplificación de la señal en relación a la amortiguación de la fluorescencia de únicamente ese centro, si se tratara de una molécula discreta de baja masa molecular. También se observa, al igual que en las proteínas, el efecto alostérico, que en general conduce asimismo al incremento de sensibilidad a medida que se produce la interacción *receptor-analito*.

Por ello, los quimiosensores poliméricos exhiben generalmente una sensibilidad muy superior a la de las moléculas discretas con *receptores* similares. Es más, tanto la sensibilidad como la selectividad se puede incrementar de forma sencilla modificando las unidades estructurales constitutivas del polímero, así como su forma, o incluso alterando el hinchamiento a través de la modificación de la densidad de entrecruzamiento en redes.

Los polímeros como sensores se pueden clasificar en función del tipo de respuesta asociada al fenómeno de la detección en:

- ❖ Sensores piezoelectricos: la interacción selectiva de una matriz sólida (p.ej.: polímero soportado, polímero de impronta molecular, y materiales híbridos metal-polímero) con una molécula objetivo siempre da lugar a una variación de masa

que se puede detectar por un dispositivo sensible a la misma, como por ejemplo la microbalanza de cuarzo.³⁴

- ❖ Sensores quimio-mecánicos: materiales que dan lugar a variaciones reversibles en su tamaño o forma ante la exposición a estímulos químicos.³⁵
- ❖ Sensores electroquímicos: materiales que varían su conductividad eléctrica en respuesta a la interacción con un *analito* detectable, p.ej., por voltamperometría cíclica, o mediante técnicas potenciométricas.³⁶
- ❖ Sensores colorimétricos: sensores cuya respuesta se debe a cambios en las propiedades de absorción de la radiación electromagnética visible de los materiales, tanto en la variación de la absorbancia a una longitud de onda dada, como a la variación de la longitud de onda de absorción, detectables por espectroscopía UV/Vis. Este es un campo de interés creciente entre los investigadores, ya que permite el diseño y síntesis de moléculas capaces de dar lugar a variaciones de color detectables a simple vista tras la interacción con el *analito*.³⁷⁻³⁹
- ❖ Sensores fluorescentes: se basan en cambios en la vida media, intensidad, longitud de onda, etc., de la fluorescencia de las moléculas sensoras. La espectroscopía de fluorescencia se emplea extensamente debido tanto a la disponibilidad de la técnica como a su sensibilidad.³⁷⁻⁴⁰

³⁴ M. Ávila, M. Zougagh, A. Escarpa, A. Ríos, *Trends Anal. Chem.* **2008**, 27, 54.

³⁵ H. J. Schneider, K. J. Kato, *Mater. Chem.* **2009**, 19, 569.

³⁶ L. J. Fan, Y. Zhang, C. B. Murphy, S. E. Angell, M. F. L. Parker, B. R. Flynn, W. E. Joner Jr., *Coord. Chem. Rev.* **2009**, 253, 410.

³⁷ R. Martínez-Máñez., F. Sancenón, *Coord. Chem. Rev.* **2006**, 250, 3081.

³⁸ H. N. Kim, Z. Guo, W. Zhu, J. Yoon, H. Tian, *Chem. Soc. Rev.* **2011**, 40, 79.

³⁹ A. B. Descalzo, R. Martínez-Máñez, F. Sancenón, K. Hoffmann, K. Rurack, *Angew. Chem. Int. Ed.* **2006**, 45, 5924.

⁴⁰ P. Bosch, F. Catalina, T. Corrales, C. Peinado, *Chem. Eur. J.* **2005**, 11, 4314.

En lo que respecta a este trabajo, se han diseñado materiales quimiosensores colorimétricos y fluorogénicos. Nuestro interés se centra realmente en la detección a simple vista mediante sensores colorimétricos, así como en la cuantificación por espectroscopía UV/Vis y fluorescencia, ya que, como se ha mencionado con anterioridad, éstas son técnicas sencillas, rápidas, baratas y disponibles en la mayoría de los laboratorios, tanto institucionales como de las empresas, puesto que se utilizan habitualmente en control de calidad. En relación con las propiedades y características de los polímeros comentadas anteriormente, así como con las asociadas a los fenómenos de detección selectiva y cuantitativa, para diseñar un polímero que se pueda utilizar eficientemente como material selectivo en un sensor químico se debe tener en cuenta las siguientes características:

- ❖ El polímero ha de poseer una alta capacidad de absorción de los compuestos específicos, y fundamentalmente una selectividad hacia éstos.
 - ❖ En aplicaciones acuosas, el material debe ser resistente a la hidrólisis por agua caliente y disoluciones acuosas ligeramente ácidas y básicas. En otros medios, el polímero ha de ser resistente a disolventes orgánicos y aceites.
 - ❖ En el caso de membranas densas, el material debe presentar una absorción de agua suficiente para permitir la difusión del disolvente en la red tridimensional y de esta forma el acceso de los *analitos* a la *subestructura receptora*. El porcentaje de hinchamiento en agua ideal para este propósito suele variar entre un 50 y un 100%. En general, el contenido en agua del hidrogel, o grado de hinchamiento, está íntimamente relacionado con el transporte de oxígeno, que es un parámetro clave para aplicaciones biomédicas, como por ejemplo lentes oculares. Por este motivo, se llevó a cabo un estudio en profundidad de la permeabilidad frente al oxígeno de estos materiales (Anexo 1).
-

- ❖ Las membranas densas deben tener buenas propiedades macroscópicas en términos de manejabilidad (propiedades mecánicas y térmicas). Con el objetivo de conocer mejor los materiales, se estudian las propiedades dieléctricas de los materiales reticulados con diferentes proporciones de los monómeros utilizados para sintetizar la membrana (Anexo 2).
- ❖ El polímero ha de estar libre de contaminación de cualquier tipo, en particular trazas de metales o iones metálicos.
- ❖ El porcentaje del compuesto específico absorbido en equilibrio debe ser alto, pero ha de mostrar un balance cinético equilibrado en los ciclos de absorción-desorción en medios acuosos u orgánicos. En el caso de los dosímetros, las reacciones con el *analito* han de ser altamente específicas, únicamente con los *subgrupos receptores*.
- ❖ El comportamiento del polímero no debe verse afectado sensiblemente con los cambios de temperatura.

Además, las numerosas posibilidades de diseño de estructuras poliméricas permiten la preparación de materiales con propiedades muy diversas, como materiales químicamente inertes, mecánicamente y térmicamente resistentes, hidrofílicos, hidrofóbicos, solubles en medios acuosos, etc., lo que posibilita, en principio, el empleo de estos polímeros en cualquier tipo de medio y condiciones. Así, desde la experiencia previa se orientó el trabajo hacia un diseño de estructuras poliméricas vinílicas con *unidades receptoras* selectivas introducidas como grupos laterales de monómeros acrílicos (metacrilato y metacrilamida).

Ambas pertenecen a una familia de macromoléculas de gran relevancia, puesto que son materiales tremadamente versátiles con infinidad de aplicaciones en distintos ámbitos tecnológicos. Este tipo de estructuras se emplean en el Grupo para la preparación de materiales solubles en agua y membranas densas con comportamiento de gel y con distintos grados de

hidrofilia, manteniendo buenas propiedades mecánicas tanto en seco como en hinchado.

Los polímeros lineales solubles en agua y los reticulados en forma de membrana densa con alta capacidad de absorción de agua preparados son copolímeros al azar. Se obtienen a partir de la polimerización de un monómero que contiene la *unidad receptora*, que será la responsable de la interacción con los *analitos* a estudiar, y de uno o varios monómeros que constituyen lo que denominaremos la *matriz inerte*, cuya función es la de proveer al material de las propiedades necesarias para permitir el proceso de detección, manteniendo en todo momento unas buenas propiedades mecánicas, tanto en seco como en hinchado.

A la hora de diseñar químicamente los *subgrupos receptores* que van a formar parte de los polímeros quimiosensores se eligieron sistemas basados en los siguientes derivados orgánicos: fluoreno, 8-hidroxiquinolina, 2,5-dicetopiperazina y acilhidrazona. La elección de éstos se realizó por tratarse de estructuras estudiadas como sensores químicos descritos ampliamente en la bibliografía científica.⁴¹⁻⁴⁴ Este hecho garantizaba, de alguna manera, el éxito de los futuros materiales como sensores, aunque hay que indicar que los estudios realizados por otros autores se habían llevado a cabo con las moléculas discretas y actuando casi siempre en disolución, habitualmente en medios orgánicos. Por esta razón, y de forma sistemática, todos los diferentes *subgrupos receptores* que se describen en esta memoria se han probado con todos los cationes y aniones que se enumeran a continuación: cianuro, acetato, fluoruro, perclorato, dodecilsulfato, nitrito, hidrogenoftalato, pirofosfato, persulfato, metanosulfonato, pirofosfato dibásico, trifluorometanosulfonato, *p*-toluenesulfonato, bromuro, tiocianato, oxalato, carbonato, benzoato, dihidrogenofosfato, sulfato, cloroacetato, trifluoroacetato,

⁴¹ J. P. Ma, Y. Yu, Y. B. Dong, *Chem. Comm.* **2012**, 48, 2946.

⁴² S. B. Maity, P. K. Bharadwaj, *Indian J. Chem., Sect A* **2011**, 50, 1298.

⁴³ T. D. Turnquist, E. B. Sandell, *Anal. Chim. Acta* **1968**, 42, 239.

⁴⁴ K. Tiwari, M. Mishra, V. Singh, *RSC Advances* **2013**, 3, 12124.

periodato, aluminio (III), catión amonio, bario (II), cadmio (II), cerio (III), cesio (I), cobalto (II), cobre (II), disprosio (III), lantano (III), plomo (II), litio (I), magnesio (II), manganeso (II), mercurio (II), neodimio (III), níquel (II), platino (II), cromo (III), cromo (VI), potasio (I), rubidio (I), samario (III), plata (I), sodio (I), estroncio (II), estaño (II), zinc (II) y zirconio (IV).

Aplicando la metodología del estudio de la interacción de *analitos* con diversos *grupos receptores* anclados a una matriz polimérica, se han conseguido desarrollar polímeros para aplicaciones diversas, que podemos clasificar de forma general en: materiales sensores y dosímetros químicos, aptos para la detección de iones y moléculas neutras, y en materiales útiles para el transporte y extracción selectiva de *analitos*.

Conviene aquí indicar que el proceso de difusión, ya sea de gases o líquidos, en redes poliméricas es un fenómeno de interés, pues estos procesos se encuentran presentes en muchas aplicaciones que utilizan este tipo de membranas acrílicas y es, además, el medio por el que las moléculas objetivo acceden a los *centros receptores* en los materiales sólidos sensores. También el estudio de las propiedades mecánicas y térmicas de estos materiales siempre constituye una labor ineludible, independientemente de su aplicación final. Por eso en la mayor parte de los casos que se encuentran en esta Memoria, se realizó el estudio de las propiedades de los filmes preparados como *matriz inerte* que soporta el sensor. Algunos resultados obtenidos producto de un estudio más detallado de las propiedades de las membranas se encuentran en los Anexos I y II.

1.3 Objetivos

El trabajo que se describe en esta Memoria está integrado en el realizado hasta el momento en el Grupo de Polímeros, y supone la continuación natural de los llevados a cabo por otros investigadores del Grupo. En este sentido, se encuadra dentro de la línea general de *investigación, diseño, síntesis y caracterización de polímeros para aplicaciones especiales*, que incluye,

implícitamente, el estudio de la relación entre estructura y propiedades de los nuevos materiales.

Más concretamente, la investigación que se presenta está dirigida hacia el diseño, síntesis y caracterización de nuevos polímeros que incorporan *grupos receptores* selectivos en su estructura para su aplicación como polímeros solubles y membranas densas en tecnologías de sensores y dosímetros químicos.

Los objetivos del trabajo se pueden resumir en los siguientes apartados:

- ❖ Diseñar, sintetizar y caracterizar nuevos copolímeros de adición (vinílicos) lineales y entrecruzados, portadores de *grupos receptores* selectivos, como materiales sensores con potenciales aplicaciones en la detección visual y fluorogénica de especies química de interés. Los *receptores* diseñados serán derivados de fluoreno, 2,5-dicetopiperazina, 8-hidroxiquinolina y acilhidrazona. Las moléculas objetivo serán seleccionadas por su interés biológico, medioambiental e industrial.
- ❖ Relacionar la estructura química con las propiedades específicas, como los comportamientos térmico y mecánico, la solubilidad, la absorción de agua, la permeabilidad frente a distintos gases, las propiedades dieléctricas, etc.
- ❖ Relacionar la capacidad sensora de los materiales poliméricos frente a diversos *analitos* (aniones, cationes o moléculas neutras) con la estructura química.

1.4 Estructura de la Memoria

La Memoria se ha ordenado en cinco capítulos, comenzando con esta Introducción General en la que se ha abordado el encuadre del trabajo y la presentación de los objetivos.

Los trabajos realizados para la consecución de estos objetivos se describen en los siguientes capítulos, estructurados por familias de polímeros en relación con la estructura de la *unidad receptora*. Así, en el Capítulo 2 se realiza el estudio de una estructura derivada del fluoreno para la detección de aniones cianuro. El Capítulo 3 trata del estudio de una estructura derivada de la 2,5-dicetopiperazina para la detección de mercurio, cromo (VI) y moléculas neutras presentes en medios biológicos. En el Capítulo 4 se describe el estudio de una estructura derivada de la 8-hidroxiquinolina para la detección de hierro (III) y aluminio (III), y por último, en el Capítulo 5 el estudio de una estructura derivada de la acilhidrazone para la detección de aluminio (III).

Cada capítulo consta de una introducción a la familia de compuestos orgánicos que se han utilizado como *subgrupos receptores*, información relevante que se tuvo en cuenta a la hora de su diseño para la consecución del objetivo concreto del reconocimiento de especies químicas específicas de interés. A continuación se discuten los procedimientos de síntesis de polímeros con esas *subunidades receptoras*. Por su parte, los procedimientos experimentales, los resultados y su discusión, así como las conclusiones parciales se aportan mediante la transcripción íntegra de los artículos científicos publicados.

Por último, la memoria finaliza con las conclusiones a las que se ha llegado tras realizar esta tesis doctoral.

CAPÍTULO 2

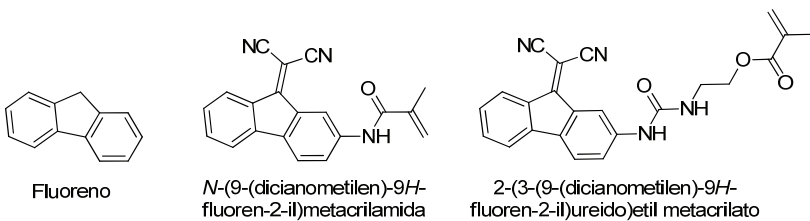
Polímeros con derivados de fluoreno en su estructura

Los polímeros acrílicos se caracterizan por su versatilidad a la hora de diseñar estructuras con características adecuadas para múltiples aplicaciones. Aprovechando este hecho, se han diseñado polímeros acrílicos que contienen en su estructura un receptor químico cromogénico derivado del fluoreno. Estos materiales se comportan como sensores cromogénicos hacia diversos analitos entre los que cabe destacar el anión cianuro en agua, lo que ha permitido preparar tiras de membrana para la detección a simple vista de este anión con límite de detección de 13 ppb, inferior a la concentración máxima admitida para el cianuro en agua potable.

2.1 Fluoreno y sus derivados

Como se ha comentado en la Introducción General, el trabajo descrito en esta Memoria consiste en el diseño y preparación de materiales poliméricos portadores de subestructuras específicas con aplicaciones en la detección y cuantificación de analitos. En este capítulo se describe la preparación de copolímeros acrílicos portadores de subunidades derivadas de fluoreno

(Esquema 2.1), junto con los resultados del estudio de su capacidad sensora hacia cianuro en medios acuosos.



Esquema 2.1. Estructura química del fluoreno y de los monómeros acrílicos sintetizados con derivados de fluoreno en su estructura.

El fluoreno, o 9*H*-fluoreno, es un hidrocarburo policíclico aromático, sus cristales son de color blanco, posee un olor característico similar al naftaleno y una fluorescencia violeta. El fluoreno se utiliza como precursor de otros compuestos de interés, como derivados farmacéuticos, colorantes y productos de química fina. Entre estos últimos destaca el cloruro de 9-fluorenilmetoxicarbonilo (cloruro de Fmoc) que se emplea para introducir el grupo protector 9-fluorenilmetoxicarbonilo (Fmoc) en aminas en la síntesis de péptidos, así como en la protección del grupo amino en reacciones convencionales.⁴⁵

Además, cabe resaltar su empleo como unidad estructural de polifluorenos, polímeros conductores y electroluminiscentes que se están investigando actualmente para su uso en células fotovoltaicas o como diodos orgánicos/polímeros de emisión de luz (PLED o LEP, *Polymer Light-Emitting Diode*),⁴⁶⁻⁴⁸ o incluso para la preparación de membranas para celdas de combustible.⁴⁹ En el ámbito de los sensores, algunos derivados de fluoreno se están estudiando como biosensores basados en polielectrolitos conjugados.^{50,51}

⁴⁵ P. G. M. Wuts, T.W. Greene, *Protective Groups in Organic Synthesis*, 4^a Ed., Wiley-Interscience, New York, 2007.

⁴⁶ L. H. Xie, C.R. Yin, W.Y. Lai, Q.L. Fan, W. Huang, *Prog. Polym. Sci.* **2012**, 37, 1192.

⁴⁷ S. Beaupré, P.L.T. Boudreault, M. Leclerc, *Adv. Mater.* **2010**, 22, E6.

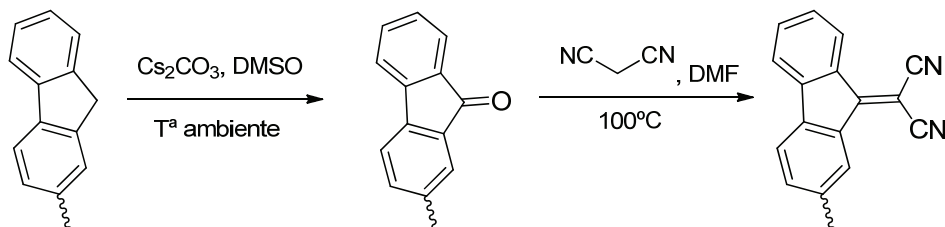
⁴⁸ W. Y. Wong, P.D. Harvey, *Macromol. Rapid Commun.* **2010**, 31, 671.

⁴⁹ K. Miyatake, B. Bae, M. Watanabe, *Polym. Chem.* **2011**, 2, 1919.

⁵⁰ Y. Wang, B. Liu, *Curr. Org. Chem.* **2011**, 15, 446.

En lo que respecta a su reactividad química, la estructura del fluoreno es fácilmente modificable mediante reacciones sencillas, especialmente a través del carbono 9 (C9),⁵²⁻⁵⁴ como por ejemplo la oxidación a fluorenona, que a su vez puede reaccionar con especies con metilenos activos, como el malononitrilo, para dar el correspondiente producto de condensación (Esquema 2.2). De esta forma se obtiene una estructura con conjugación electrónica extendida y, por lo tanto, presumiblemente coloreada, que dará lugar a un cambio de color si se modifica su distribución electrónica.

Así, los monómeros que se muestran en el Esquema 2.1 contienen el subgrupo dicianometileno conjugado con la estructura de fluoreno, por lo que el ataque de un nucleófilo sobre el C9 da lugar a la pérdida de conjugación y al mencionado cambio cromático.⁵⁵ De esta manera, estos monómeros presentaban a priori un gran interés como potenciales sensores cromogénicos, especialmente hacia aniones nucleófilos de interés, como el cianuro.



Esquema 2.2. Derivados de fluoreno sintetizados.

2.2 Polímeros con derivados de fluoreno en la cadena lateral

Desde un punto de vista químico, a la hora de preparar nuevos polímeros se puede seguir una doble vía:

- ❖ Modificación de polímeros comerciales, o preparados previamente en el laboratorio.

⁵¹ M. R. Molina, *Diseño, síntesis y caracterización de nuevos copolímeros de fluoreno con propiedades luminescentes*, Tesis Doctoral, Universidad Miguel Hernández, Elche, 2007.

⁵² A. Schoenberg, *Tetrahedron Lett.* **1983**, 39, 2429.

⁵³ X. Yang, *Chem. Commun.* **2011**, 47, 2053.

⁵⁴ M. Ghandi, *Tetrahedron Lett.* **2008**, 49, 5899.

⁵⁵ H.D. Hartzler, *J. Org. Chem.* **1966**, 31, 2654.

- ❖ Síntesis integral de nuevos monómeros y su posterior polimerización.

Ambas metodologías tienen sus ventajas y sus inconvenientes. La modificación de polímeros implica el diseño y síntesis de un polímero base, o la utilización de uno comercial, a partir del cual se puede preparar de forma rápida y barata una serie de materiales derivados, ya que las reacciones de modificación que generalmente se utilizan son sencillas desde el punto de vista de la química orgánica. Por contra, los polímeros presentan una solubilidad limitada en los disolventes habituales utilizados en la síntesis orgánica, el rendimiento suele estar condicionado por la estructura macromolecular en disolución o en fundido, y los productos secundarios permanecen en la propia estructura de la macromolécula.

En cuanto a la síntesis integral de nuevos monómeros, permite un diseño específico de las estructuras, así como una purificación previa a la polimerización, pero supone un coste más elevado. Otra dificultad añadida, en el caso de monómeros diseñados como sistemas de detección, está relacionada con los subgrupos receptores presentes en el monómero, que pueden ser sensibles a las condiciones de polimerización.

En esta memoria se ha optado en todos los casos por la síntesis integral de los monómeros, en este caso de los derivados de fluoreno. A la hora de preparar éstos monómeros se optimizaron todos los pasos de reacción, obteniéndose de esta manera productos con elevado rendimiento y pureza a partir de reacciones simples y económicas. Por su parte, la síntesis de los polímeros reticulados se llevó a cabo por polimerización radical en bloque de los comonómeros, utilizando como iniciador radical el AIBN (azobisisobutironitrilo) o un iniciador fotoquímico (2,2-dimetoxi-2-fenilacetofenona).

La facilidad de preparación de nuevas estructuras con la funcionalidad adecuada, junto con la versatilidad de la copolimerización, ha hecho que los polímeros acrílicos se encuentren entre los polímeros más estudiados. La

modificación química del ácido (met)acrílico o sus derivados, fundamentalmente el cloruro de (met)acriloilo, es una fuente prácticamente inagotable de monómeros que da lugar a materiales como polimetacrilatos, poliacrilatos, polimetacrilamidas, o poliacrilamidas, cuyas propiedades están condicionadas por la naturaleza química del grupo lateral unido covalentemente al grupo carbonilo, que determina, por tanto, la hidrofilia, la solubilidad y la rigidez del polímero acrílico lineal. Además, la posibilidad de obtener redes entrecruzadas, a partir de la homopolimerización o copolimerización de estos monómeros y un entrecruzante, permite modificar las propiedades del material en función de la aplicación a la que se quiera destinar, pudiendo obtener así sistemas con grados variables de hidrofilia, rigidez o flexibilidad, etc.

Los trabajos previos en el marco del diseño de membranas densas para su empleo como sistemas de detección de analitos han aportado una experiencia valiosa en la preparación de materiales, que además de ser buenos soportes, poseen balances hidrofílicos/hidrofóbicos adecuados, balance que se controla mediante la selección y el empleo de la proporción óptima de comonómeros. Este hecho permite la optimización de la capacidad sensora de la molécula anclada a la matriz polimérica. Así, se han preparado membranas densas que incorporan grupos éter corona y podandos,⁵⁶⁻⁵⁸ triazol,⁵⁹ y grupos laterales derivados del pirilio,^{60,61} entre otros.

Por tanto, y en relación con la experiencia comentada, para este caso y para todos los que se presentan en esta memoria, se ha elegido como soporte (o matriz inerte) del sistema sensor, aquella mezcla de monómeros que permita una buena relación entre las propiedades mecánicas, la manejabilidad y el grado de hinchamiento del material.

-
- ⁵⁶ P. Tiemblo, F. García, J. M. García, C. García, E. Riande, J. Guzmán, *Polymer* **2003**, 44, 6773.
⁵⁷ F. García, J. M. García, F. Rubio, P. Tiemblo, J. Guzmán, E. Riande, *Polymer* **2004**, 45, 1467.
⁵⁸ J. Rey, F. C. García, J. M. García, *React. Funct. Polym.* **2011**, 71, 948.
⁵⁹ A. Gómez-Valdemoro, M. Trigo, S. Ibeas, F. C. García, F. Serna, J. M. García, *J. Polym. Sci. Part A: Polym. Chem.* **2011**, 49, 3817.
⁶⁰ B. García-Acosta, F. García, J. M. García, R. Martínez-Máñez, F. Sancenón, N. San José, J. Soto, *Org. Lett.* **2007**, 9, 2429.
⁶¹ A. Tulinsky, *Sem. Thromb. Hemostasis* **1996**, 22, 117.
-

Con el objetivo de preparar las membranas densas, se diseñó un método que se basa en la inyección de la mezcla de monómeros, del entrecruzante y del iniciador en un molde compuesto por dos vidrios silanizados entre los que se incluye un separador de polietileno del grosor deseado.

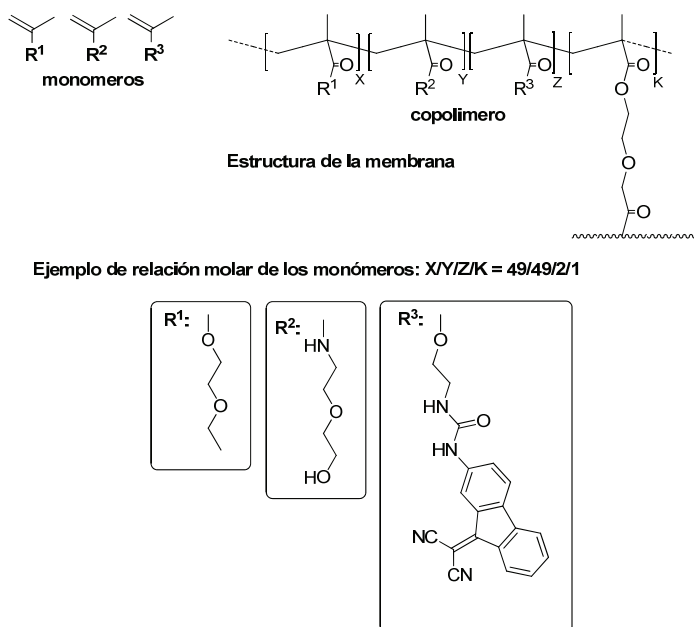
A continuación se discute brevemente la elección de la matriz inerte junto con la estructura, características y mecanismo de detección de los receptores selectivos con estructura de fluoreno.

La matriz inerte por la que se optó en este estudio está compuesta por dos monómeros metacrílicos, el metacrilato de 2-etoxietilo y la metacrilamida de 2-(2-hidroxietoxi)etilo. El primero aporta rigidez e hidrofobia a la membrana, mientras que el segundo aporta flexibilidad e hidrofilia. Se prepararon varias membranas con diferentes proporciones de ambos monómeros. La membrana preparada por polimerización radical en bloque iniciada térmicamente empleando una proporción equimolar de monómeros, entrecruzada con dimetacrilato de etilenglicol, da como resultado un material manejable y con un grado de hinchamiento en agua adecuado para aplicaciones como sensores, donde las moléculas objetivo disueltas en agua han de penetrar en el material por difusión.

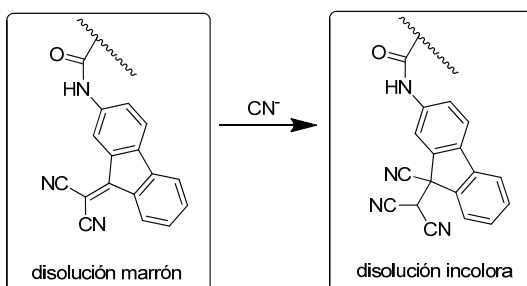
En cuanto a los subgrupos receptores, como se ha comentado previamente los dos monómeros sintetizados presentan un grupo dicianometileno. Además uno de ellos posee un grupo urea (Esquema 2.1). La constitución de uno de estos materiales se muestra de forma gráfica en el Esquema 2.3, que ilustra como ejemplo el que mostró la mejor combinación de solubilidad, manejabilidad, hinchamiento en agua (entorno a un 100%) y respuesta cromogénica ante nucleófilos.

Tras realizar los análisis habituales con una batería de aniones y cationes, se observó que en presencia de aniones cianuro la membrana de color marrón intenso del Esquema 2.3. se decoloraba. Esto se debe al ataque del anión cianuro a través de una adición de Michael al C9, inhibiendo la

conjugación del grupo dicianometileno con la estructura aromática del fluoreno, y dando lugar al cambio de color (Esquema 2.4).⁵⁵ Se trata de una reacción irreversible, por lo que nos encontramos ante un dosímetro químico. Por otro lado, el grupo urea es un receptor reconocido de varios aniones,⁶² pero en este estudio no se observaron evidencias de este tipo de interacciones.



Esquema 2.3. Estructura de una de las membranas sensoras sintetizadas.



Esquema 2.4. Reacción de 2-(9-ciano-9H-fluoren-9-il)malononitrilo con cianuro.

⁶² J. L. Sessler, P. A. Gale, W. Cho, *Anion Receptor Chemistry*, RSC Publishing, Cambridge, 2006, pp 193-205.

2.3 Resultados

A continuación se describen los resultados obtenidos a través de la transcripción íntegra de los trabajos publicados.

- ❖ *Putting to work organic sensing molecules in aqueous media: fluorene derivative-containing polymers as sensory materials for the colorimetric sensing of cyanide in water*
 - ❖ *Working with water insoluble organic molecules in aqueous media: fluorene derivative-containing polymers as sensory materials for the colorimetric sensing of cyanide in water*
-

Putting to work organic sensing molecules in aqueous media: fluorene derivative-containing polymers as sensory materials for the colorimetric sensing of cyanide in water

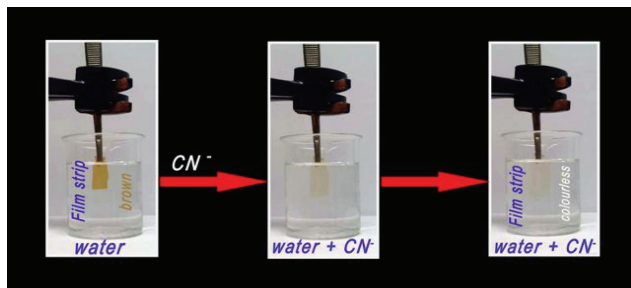
**Putting to work organic sensing molecules in aqueous media:
fluorene derivative-containing polymers as sensory materials for
the colorimetric sensing of cyanide in water[†]**

Saúl Vallejos, Pedro Estévez, Félix C. García, Felipe Serna, José L. de la Peña,
José M. García.*

Departamento de Química, Facultad de Ciencias, Universidad de Burgos. Plaza de Misael
Banuelos s/n, E-09001 Burgos, Spain

Table of contents

A strategy followed to achieve a sensing phenomenon in aqueous media using water-insoluble organic molecules: the hydrophilic polymer membrane.



[†]**Electronic Supplementary Information (ESI) available:** Experimental procedures, intermediates, monomer characterization as well as a movie showing the colorimetric response of a film 4 toward cyanide. See DOI: 10.1039/C0CC02143A

Abstract

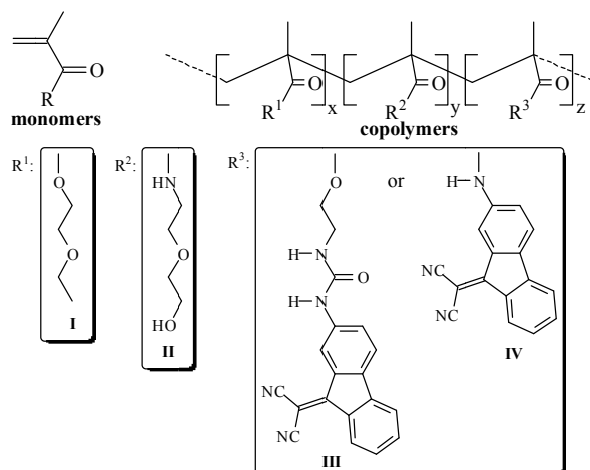
This paper describes a strategy followed to achieve a sensing phenomenon in aqueous media using water-insoluble organic molecules. A sensory polymeric material for the colorimetric sensing of cyanide in water has been developed based on the reactivity of this anion with a fluorene derivative.

Introduction

The development of chemosensors for the detection of target chemicals is a field of current interest.¹ For example, cyanide is a highly toxic, chemical target currently used in many industrial processes.^{2,3} Due to its toxicity, the United States Environmental Protection Agency (EPA) has set the maximum contaminant level (MCL) for cyanide in drinking water at 0.2 ppm, rendering its detection important in terms of both environmental and industrial control.

The detection of cyanide through various supramolecular approaches³ (the binding site-signaling subunit,⁴ the chemodosimeter^{5,6} or the displacement⁷⁻⁹) has been extensively reported. Nevertheless, few examples of sensing of the anion in aqueous solutions,⁶⁻¹⁰ some of them showing detection limits lower than the MCL,^{3,8} have been described. Most cyanide sensing molecules are insoluble in water because of their organic nature, preventing their use in aqueous media. We felt that detection of cyanide by means of changes in optical signals upon interaction of a target guest with a sensor molecule could give rise to the development of inexpensive, portable devices for environmental testing inside or outside the laboratory.^{1,2} Prior to our investigation, few examples existed describing materials exhibiting colorimetric, or fluorescence, recognition with potential use as solid systems or practical kits for “dip-in” naked-eye cyanide detection (e.g., films or membranes,^{10,11} quantum dots¹² or supported materials¹³). We hypothesized that the chemical anchoring of a sensing motif to a hydrophilic polymer chain could provide a water-rich environment to the sensing moiety upon polymer swelling, thus permitting the solvated cyanide ions to reach the guest or the transducer cores, giving rise to the sensing phenomenon, resulting in cyanide detection. To investigate our hypothesis, we prepared two methacrylic and methacrylamide monomers containing a fluorene derivative as a colorimetric cyanide sensing motif (III and IV) and copolymerized them with either a hydrophobic or a hydrophilic monomer (I and II, respectively). The cross-

linking agent 1,2-ethanedioldimethacrylate was used to obtain different, dense polymer films or membranes (Scheme 1, Table 1), which were optically transparent and had good mechanical properties, even after water swelling.



Scheme 1. Chemical structure of monomers and copolymers

Table 1. Composition and properties of polymeric films prepared

	Film I (x) ^a	Film II (y) ^a	Film III (z) ^a	Film IV (z) ^a	WSP ^b	Raw film ^c	Film + CN ^{-d}	Response time (s) ^e
1	100	--	2	--	3	n.a.	n.a.	--
2	80	20	2	--	20	En	its	--
3	60	40	2	--	80	Sc	ion	72
4	50	50	2	--	110	Ag	icy	33
5	--	100	2	--	275	Ag	us	20
6	--	100	--	2	250	proc	of	35
7	50	50	0.2	--	185	soak	ctic	n.a.
8	50	50	--	0.2	160	-9H-	imp	n.a.

^a Molar composition ratio of the monomers used for the preparation of the films. b Water-swelling percentage: weight percentage of water uptake by the films upon soaking until equilibrium, in pure water. c,d Digital picture of the films taken over a written paper upon soaking in pure water and in an aqueous solution of cyanide (10 equiv. per equiv. of the sensing fluorene derivative motif), respectively; the pictures have been taken on written paper to show the transparency and the different shades of the films. e Naked-eye response time (--: without response, n.a.: not applicable).

Depending on the molar composition ratio (MCR) of the monomers

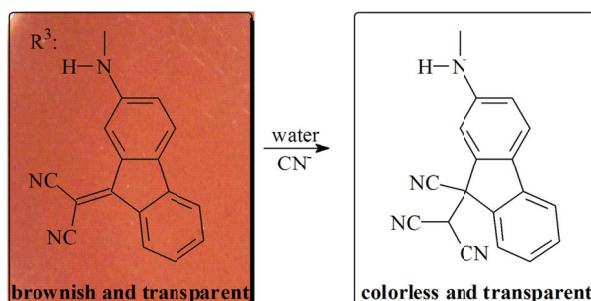
used for preparation of the films, their observed colors were brownish or reddish (films 1 to 6) or light violet (films 7 and 8), both when dry and when water swelled. Upon soaking in aqueous solutions of cyanide, the films turned colorless in less than 72 seconds, which represents a low apparent response time,¹³ the lower values corresponding to the higher hydrophilic character of the membrane, depicted in Table 1 by the water-swelling percentage (WSP).¹⁴

The mechanism of the colorimetric response of the membranes to the cyanide ions is depicted in Scheme 2.¹⁵ To demonstrate the proposed sensing mechanism, we prepared the model molecule 9H-fluorin-9-ylidenemalononitrile and its (9-cyano-9H-fluorin-9-yl)malononitrile derivative, through reaction of the former with cyanide, in a selective and quantitative manner though a Michael reaction (see supporting information for reaction conditions and characterization: Scheme S4).

Membranes prepared with monomers containing the urea subgroup (monomer III, Scheme 1) and without it (monomer IV, Scheme 1) showed a similar response toward cyanide, indicating that this group plays a negligible role in the chemodosimeter response of the fluorene derivative motif. Nevertheless, the fluorene derivative with and without the urea unit influence the UV/Vis spectra of the corresponding membranes, as shown below.¹⁶

To test the colorimetric anion sensing ability of the membranes 1 to 6, different anions were added to a quartz UV/Vis cell containing the films, resulting in a change in the absorption spectra with a gradual diminishment of the absorbance of the 445 nm band with the cyanide concentration. In contrast, the film remained completely silent in the presence of a broad set of other anions. The response to cyanide can be seen in Figure 1, which shows titration of the films with aqueous CN⁻, and the inset shows the corresponding binding isotherm. The best responses in terms of response time and color variation were obtained with film 4, probably due to its moderate hydrophilicity, giving rise to a detection limit lower than 260 ppb,

which is slightly above the MCL. Membranes containing monomer IV do not show a maximum because an intense band centered at 352 nm saturated the UV/Vis spectrometer. A real time movie showing the colorimetric response of a membrane strip (film 4) upon soaking it in a cyanide aqueous solution can be found in the supplementary information.



Scheme 2. Schematic representation of the proposed sensing mechanism (background: digital picture of film 4)

Upon lowering the MCR of the copolymer from 2% (films 1- 6) to 0.2% (films 7 and 8), the absorption bands of the UV region were observed [a maximum at 351 nm (film 7) and two maxima at 290 and 354 nm (film 8)]. The progressive addition of cyanide to the cell containing the copolymer films gave rise to subsequent diminishment of the absorbance intensity of these bands, thus permitting the titration and giving rise to a detection limit lower than 13 ppb for film 8, which is much lower than the MCL (Figure 2).

In summary, water-insoluble organic molecules III and IV, with a chemodosimeter behavior toward the cyanide anion, were chemically incorporated in the lateral chain of a methacrylic copolymer to give different, dense membranes. The design of the membrane composition allows the preparation of a solid material with ‘a la carte’ hydrophilic character. Upon swelling with water, the membrane permits the colorimetric detection of cyanide with an extremely low detection limit. Thus, through diffusion into the swelled membrane the solvated ions reach the highly hydrophobic sensing organic motifs, giving rise to the recognition phenomenon. Following

this procedure, the supramolecular sensing phenomena can be easily carried out by means of anchoring organic sensing molecules to appropriate polymeric nets.

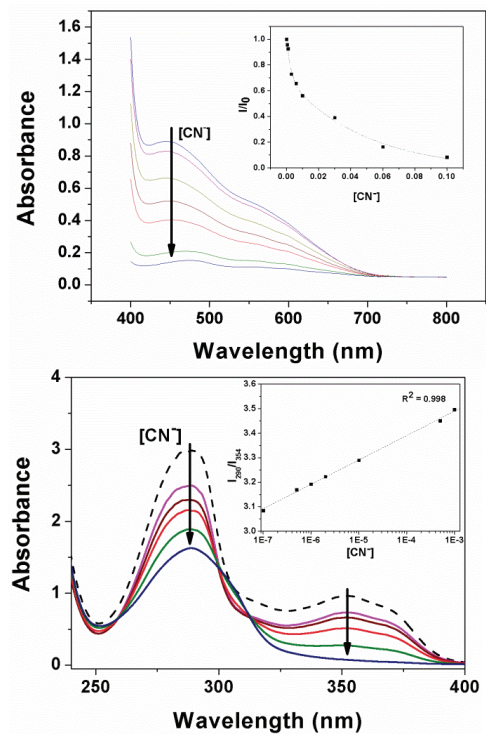


Figure 1. Selected UV/Vis titration curve of film 4 with cyanide in water (inset: cyanide concentration vs. I/I_0 at 445 nm)

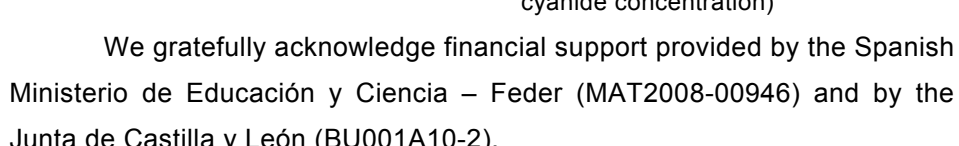


Figure 2. Selected UV/Vis titration curve of film 8 with cyanide in water (inset: absorbance intensity ratio at 290 and 354 nm (I_{290}/I_{354}) vs cyanide concentration)

We gratefully acknowledge financial support provided by the Spanish Ministerio de Educación y Ciencia – Feder (MAT2008-00946) and by the Junta de Castilla y León (BU001A10-2).

NOTES AND REFERENCES

- 1 R. Martínez-Máñez, and F. Sancenón, *Chem. Rev.*, 2003, **103**, 4419.
- 2 K.W. Kulig, In *Cyanide Toxicity*; U.S. Department of Health and Human Services, Atlanta, GA, 1991; Guidelines for Drinking-Water Quality, World Health Organization, Geneva, 1996.
- 3 For a recent review see: Z. Xu, X. Chen, and J. Yoon, *Chem. Soc. Rev.*, 2010, **39**, 127.
- 4 T. Agou, M. Sekine, J. Kobayashi, and T. Kawashima, *J. Organomet. Chem.*, 2009, **694**, 3833; V. Kumar, M.P. Kaushika, A.K. Srivastava, A. Pratap, V. Thiruvenkatam, and T.N. Row, *Anal. Chim. Acta*, 2010, **663**, 77; J. Wang, and C.-S. Ha, *Tetrahedron* 2010, **66**, 1846.

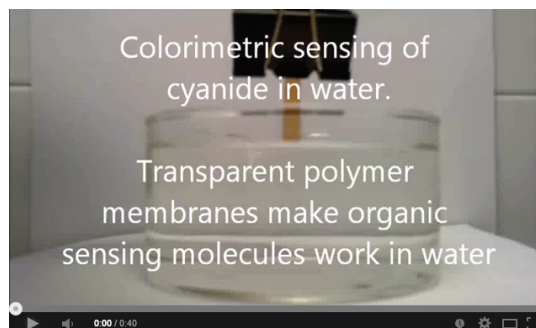
- 5 See, for instance: T. Ábalos, S. Royo, R. Martínez-Máñez, F. Sancenón, J. Soto, A.M. Costero, S. Gil, and M. Parra, *New J. Chem.*, 2009, **33**, 1641; H.-T. Niu, D. Su, X. Jiang, W. Yang, Z. Yin, J. He, and J.-P. Cheng, *Org. Biomol. Chem.*, 2008, **6**, 3038; Y. Sun, G. Wang, and W. Guo, *Tetrahedron*, 2009, **65**, 3480; S.K. Kwon, S. Kou, H.N. Kim, X. Chen, H. Hwang, S.-W. Nam, S.H. Kim, K.M.K. Swamy, S. Park, and J. Yoon, *Tetrahedron Lett.*, 2008, **49**, 4102; D-G. Cho, J.H. Kim, and J.L. Sessler, *J. Am. Chem. Soc.*, 2008, **130**, 12163; J.L. Sessler, and D.-G. Cho, *Org. Lett.*, 2008, **10**, 73; J. Ren, W. Zhu, and H. Tian, *Talanta*, 2008, **75**, 760; S.-J. Hong, J. Yoo, S.-H. Kim, J.S. Kim, J. Yoon, and C.-H. Lee, *Chem. Commun.*, 2009, 189; Y.-K. Yang, and J. Tae, *Org. Lett.*, 2006, **8**, 5721; G. Qian, X. Li, and Z.Y. Wang, *J. Mater. Chem.*, 2009, **19**, 522; J.O. Huh, Y. Do, and M.H. Lee, *Organometallics*, 2008, **27**, 1022; T. Agou, M. Sekine, J. Kobayashi, and T. Kawashima, *Chem. Eur. J.*, 2009, **15**, 5056; M. Jamkratoke, V. Ruangpornvisuti, G. Tumcharen, T. Tuntulani, and B. Tomapatanaget, *J. Org. Chem.*, 2009, **74**, 3919.
- 6 L. Peng, M. Wang, G. Zhang, D. Zhang, and D. Zhu, *Org. Lett.*, 2009, **11**, 1943; Y. Sun, Y.; Liu, and W. Guo, *Sens. Actuators, B*, 2009, **143**, 171; J. Jo, and D. Lee, *J. Am. Chem. Soc.*, 2009, **131**, 16283; Y. Sun, Y. Liu, M. Chen, and W. Guo, *Talanta*, 2009, **80**, 996; H.-T. Niu, X. Jiang, J. He, and J.-P. Cheng, *Tetrahedron Lett.*, 2009, **50**, 6668; K.-S. Lee, H.-J. Kim, G.-H. Kim, I. Shin, and J.-I. Hong, *Org. Lett.*, 2008, **10**, 49.
- 7 J.H. Lee, A.R. Jeong, I.-S. Shin, H.-J. Kim, and J.-I. Hong, *Org. Lett.*, 2010, **12**, 764; R. Guliyev, O. Buyukcakir, F. Sozmen, and O.A. Bozdemir, *Tetrahedron Lett.*, 2009, **50**, 5139; L. Shang, L. Zhang, and S. Dong, *Analyst*, 2009, **134**, 107; F.H. Zelder, *Inorg. Chem.*, 2008, **47**, 1264; C. Mähnel-Croisé, and F. Zelder, *Inorg. Chem.*, 2009, **48**, 1272.
- 8 Lou, L. Zhang, J. Qin, and Z. Li, *Chem. Commun.*, 2008, 5848.
- 9 Z. Xu, J. Pan, D.R. Spring, J. Cui, and J. Yoon, *Tetrahedron*, 2010, **66**, 1678; L. Shang, L. Jin, and S. Dong, *Chem. Commun.*, 2009, 3077; P. Kaur, S. Kaur, and K. Singh, *Inorg. Chem. Commun.*, 2009, **12**, 978; Y. Liu, K. Ai, X. Cheng, L. Huo, and L. Lu, *Adv. Funct. Mater.*, 2010, **20**, 951; X. Lou, J. Qin, and Z. Li, *Analyst*, 2009, **134**, 2071; C. Mähnel-Croisé, B. Probst, and F. Zelder, *Anal. Chem.*, 2009, **81**, 9493; S.-Y. Chung, S.-W. Nam, J. Lim, S. Park, and J. Yoon, *Chem. Commun.*, 2009, 2866.
- 10 N. Gimeno, X. Li, J.R. Durrant, and R. Vilar, *Chem. Eur. J.*, 2008, **14**, 3006.
- 11 Q. Zeng, P. Cai, Z. Li, J. Qina, and B.Z. Tang, *Chem. Commun.*, 2008, 1094; Z. Li, X. Lou, H. Yu, Z. Li, and J. Qin, *Macromolecules*, 2008, **41**, 7433; Z. Ekmekci, M.D. Yilmaz, and E.U. Akkaya, *Org. Lett.*, 2008, **10**, 461; F. García, J.M. García, B. García-Acosta, R. Martínez-Máñez, F. Sancenón, and J. Soto, *Chem. Commun.*, 2005, 2790.
- 12 A. Touceda-Varela, E. I. Stevenson, J. A. Galve-Gasión, D. T. F. Dryden and J. C. Mareque-Rivas, *Chem. Commun.*, 2008, 1998.
- 13 P. Kaur, D. Sareen, S. Kaur, and K. Singh, *Inorg. Chem. Commun.*, 2009, **12**, 272.
- 14 The WSP was obtainain from the weights of a dry (w_d) and a water swelled (the membranes was inmersed in pure water at 20 °C untill the swelled equilibrium was achieved) sample film (w_s) as follows: $100 \times [(w_s - w_d)/w_d]$. See: V. Compañ, P. Tiemblo, F. García, J.M. García, J. Guzmán, and E. Riande, *Biomaterials*, 2005, **26**, 3783.
- 15 H.D. Hartzler, *J. Org. Chem.*, 1966, **31**, 2654.
- 16 The binding characteristics of the urea groups was probably not observed due to the water environment and to the neutral conditions.

SUPPLEMENTARY INFORMATION

**Putting to work organic sensing molecules in aqueous media:
fluorene-derivative containing polymers as sensory materials for
the colorimetric sensing of cyanide in water**

*Saúl Vallejos, Pedro Estévez, Félix C. García, Felipe Serna, José L. de la Peña,
José M. García.**

Departamento de Química, Facultad de Ciencias, Universidad de Burgos. Plaza de Misael
Banuelos s/n, E-09001 Burgos, Spain



S0. Real-time movie showing the colorimetric response of a film 4 toward cyanide anions in aqueous media (<https://www.youtube.com/watch?v=AmHVLx21Wsk>)

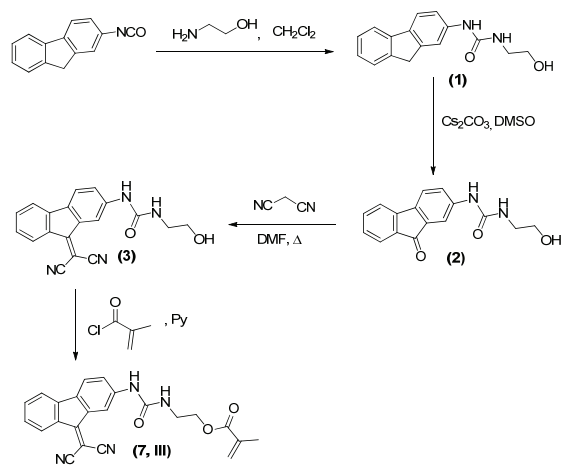
This paper describes a strategy followed to achieve a sensing phenomenon in aqueous media using water-insoluble organic molecules. Thus, we have prepared a methacrylamide and a methacrylate with pendant cyanide chemosensors based on a fluorene-derivative motif, and we have fabricated highly hydrophilic membranes by means of copolymerizing these hydrophobic monomers with others. Therefore, upon absorption of water in the membranes, solvated ions enter the membrane by a simple diffusion mechanism reaching the hydrophobic chemosensor motifs, giving rise to the macroscopic sensing phenomenon. In this way, we have prepared solid materials (dense membranes or films) capable of selectively detecting cyanide, with a extremely low detection threshold, in aqueous solution by means of color changes (naked-eye sensing) (13 ppb).

S1. Materials

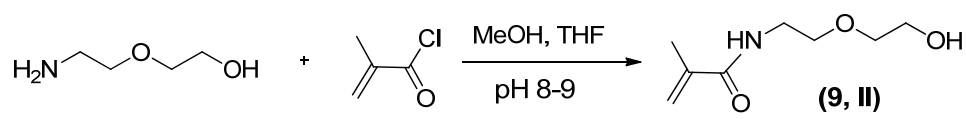
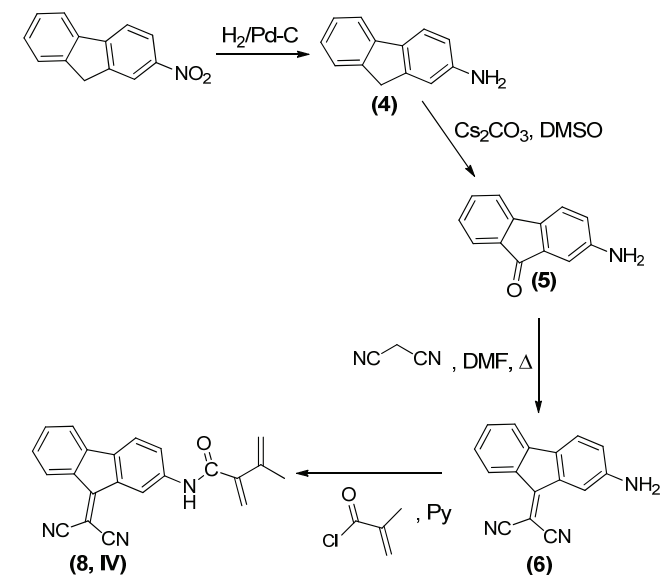
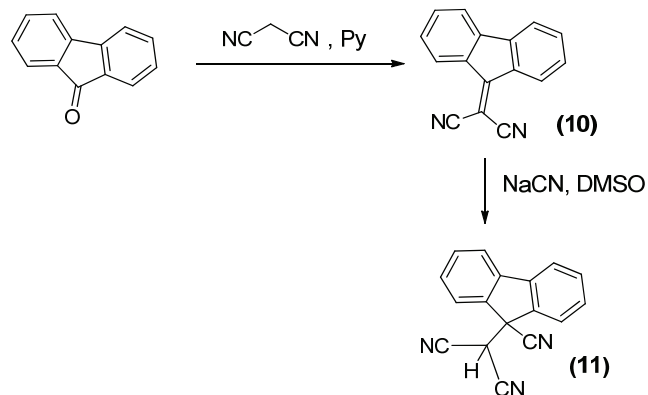
All materials and solvents were commercially available and used as received, unless otherwise indicated including the following: sodium cyanide (Panreac, 98%), 2-Ethoxyethyl methacrylate (Aldrich, 99%), 2-isocyanato-9H-fluorene (Aldrich, 98%), ethanolamine (Merck, 98%), cesium carbonate (Aldrich, 99%), malononitrile (Aldrich, 99%), 2-nitro-9H-fluorene (Aldrich, 98%), Pd/C (Aldrich, 10%), methacryloyl chloride (Fluka, 97%), 2-(2-aminoethoxyethanol) (Aldrich, 98%), fluorenone (Aldrich, 98%), ethylene glycol dimethacrylate (Aldrich, 98%), DMSO (Merck, 99%), acetone (Aldrich, 99%), ethanol (Aldrich, 99%), dichloromethane (Aldrich, 99%), DMF (Aldrich, 99%), hexanes (Aldrich, 99%), and ethyl acetate (Aldrich, 99%). Pyridine was dried under reflux over sodium hydroxide for 24 h and was distilled over 4 Å molecular sieves. Azo-bis-isobutyronitrile (AIBN, Aldrich, 99%) was recrystallized twice from methanol.

S2. Synthesis of intermediates, monomers and model

The overall monomer synthetic steps are shown in Schemes S1 to S4. The structure of the intermediates and monomers were confirmed by ¹H and ¹³C NMR (nuclear magnetic resonance) and by FT-IR (infrared spectroscopy). The spectra showed that the products were high purity chemicals.



Scheme S1. Synthesis of the monomer 2-(3-(9-(dicyanomethylene)-9H-fluoren-7-yl)ureido)ethyl methacrylate

**Scheme S3.** Synthesis of the monomer N-[2-(2-hydroxyethoxy)ethyl]methacrylamide**Scheme S4.**
Synthesis of the model 9-(dicyanomethyl)-9H-fluorene-9-carbonitrile

Synthesis of 1-(9H-fluoren-7-yl)-3-(2-hydroxyethyl)urea (1)

To a 500 mL flask fitted with a mechanical stirrer was added 25 mmol of 2-isocyanato-9H-fluorene and 50 mL of dichloromethane. Subsequently, 25 mmol of ethanolamine was added dropwise, and the solution was stirred at 0 °C for 30 min and then at rt for 6 h. Finally, the product 1-(9H-fluoren-7-yl)-3-(2-hydroxyethyl)urea was filtered off and washed with dichloromethane. Yield: 96%.

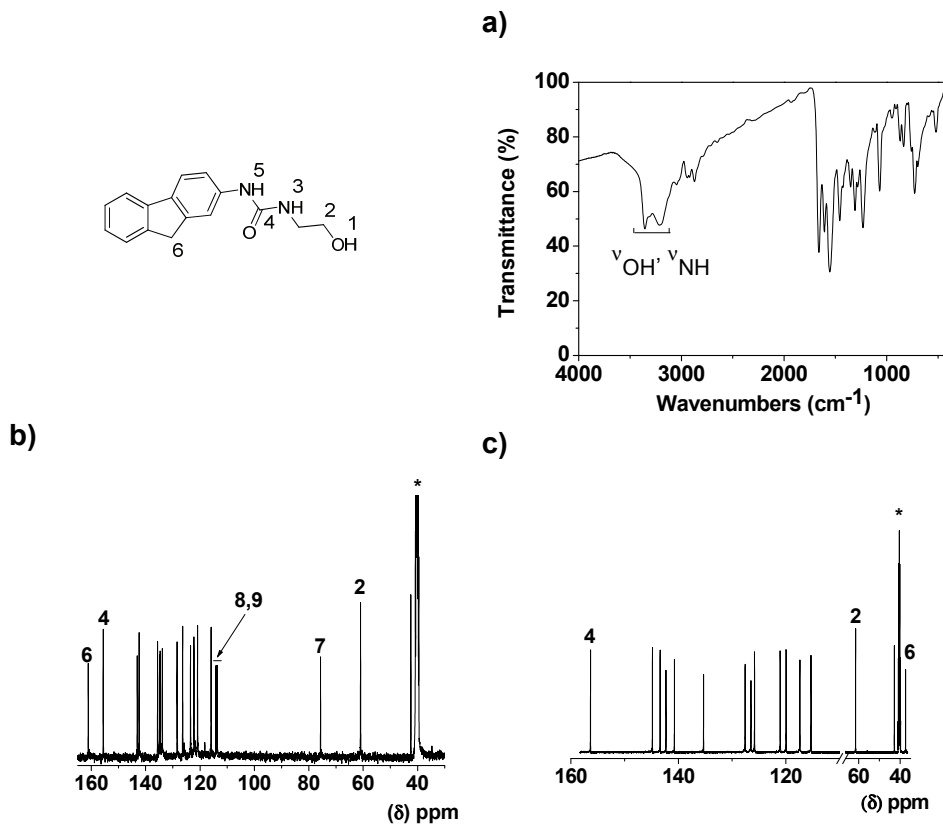


Figure S1. Characterization of (**1**) by (a) FTIR, (b) ¹H RMN, and (c) ¹³C RMN (* =solvent signal).

Synthesis of 1-(2-hydroxyethyl)-3-(9-oxo-9H-fluoren-7-yl)urea (2)

To a 125 mL flask equipped with a reflux condenser was added 13 mmol of 1-(9H-fluoren-7-yl)-3-(2-hydroxyethyl)urea dissolved in 50 mL of DMSO. To the reaction mixture was added 67 mmol of cesium carbonate, and the solution was stirred vigorously at rt for 5 d. Finally, the solution was precipitated in water to give the orange product 1-(2-hydroxyethyl)-3-(9-oxo-9H-fluoren-7-yl)urea. Yield: 98%.

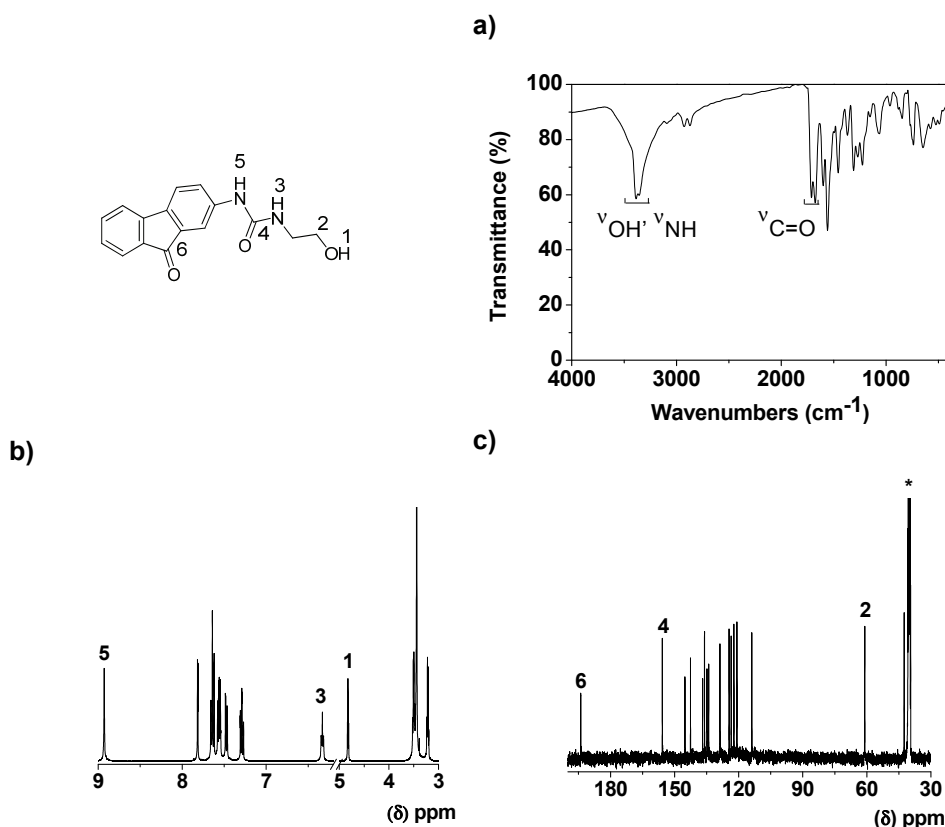
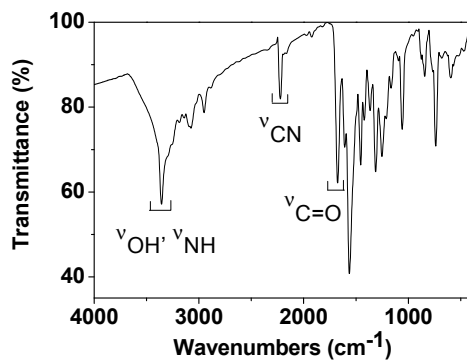
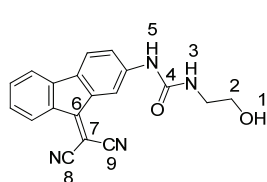


Figure S2. Characterization of (2) by (a) FTIR, (b) ^1H RMN, and (c) ^{13}C RMN (* =solvent signal).

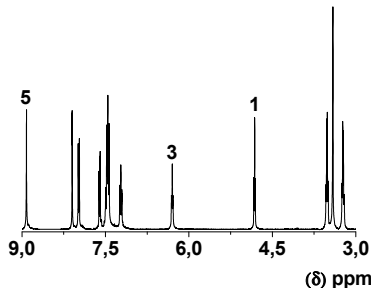
Synthesis of 1-(9-(dicyanomethylene)-9H-fluoren-7-yl)-3-(2-hydroxyethyl)-urea (3)

To a round-bottomed flask fitted with a mechanical stirrer and a reflux condenser was added 16 mmol of 1-(2-hydroxyethyl)-3-(9-oxo-9H-fluoren-7-yl)urea in 50 mL of dimethylformamide (DMF). Subsequently, 30 mmol of malononitrile was added, and the solution was stirred at reflux for 5 d, yielding a precipitate. The precipitate was filtered off and washed with acetone at reflux for 5 min. The product 1-(9-(dicyanomethylene)-9H-fluoren-7-yl)-3-(2-hydroxyethyl)urea was dried thoroughly in a vacuum oven at 60 °C. Yield: 40%.

a)



b)



c)

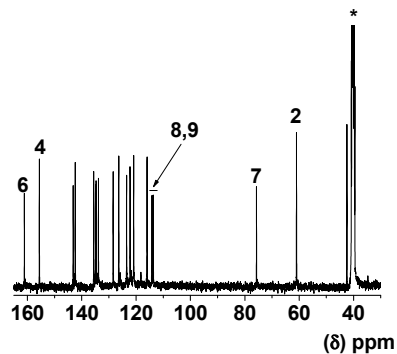


Figure S3. Characterization of (3) by (a) FTIR, (b) ¹H RMN, and (c) ¹³C RMN (* =solvent signal).

Synthesis of 9H-fluoren-2-amine (4)

To a hydrogenation flask was added 48 mmol of 2-nitro-9H-fluorene was mixed with in 20 mL of ethanol and 5 g of Pd/C (10% Pd), and the system was purged and pressured with hydrogen to 75 psi. The mixture was stirred at 60 °C for 3 h, and the hydrogen consumed was replaced every 15 min. The solid was filtered off and dried. Yield: 62%.

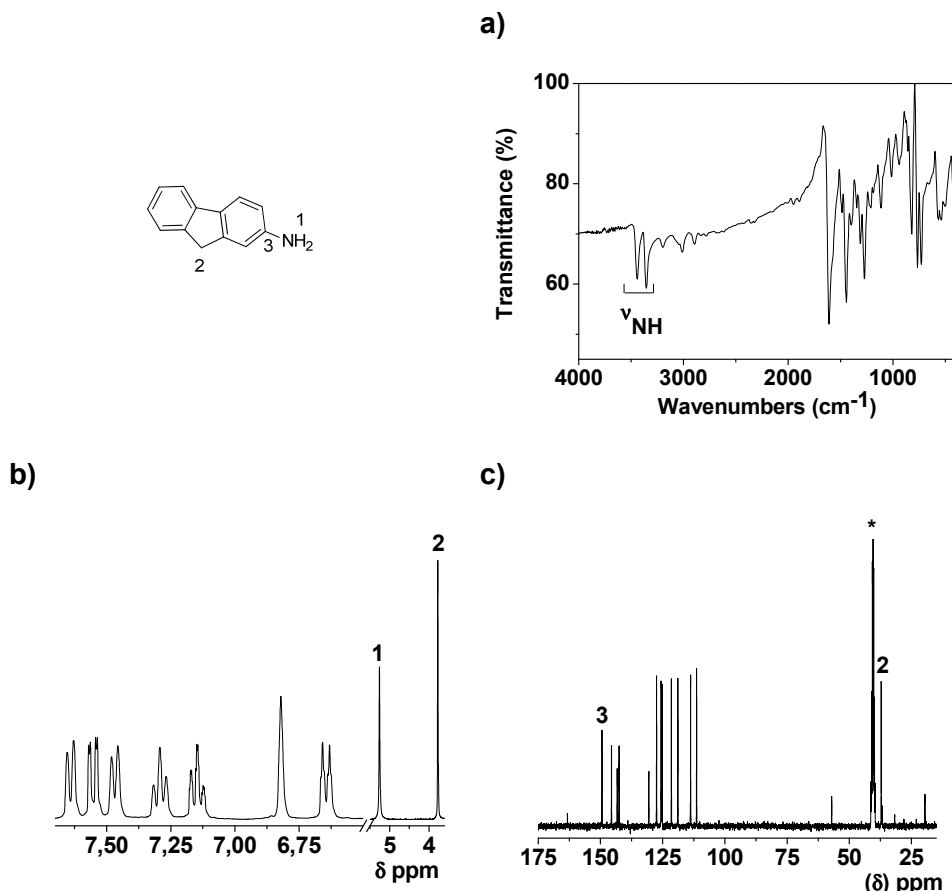


Figure S4. Characterization of (4) by (a) FTIR, (b) ¹H RMN, and (c) ¹³C RMN (* =solvent signal).

Synthesis of 2-amino-9H-fluoren-9-one (5)

To a flask equipped with a reflux condenser was added 30 mmol of 9H-fluoren-2-amine dissolved in 50 mL of DMSO. Subsequently, 89 mmol of cesium carbonate was added, and the solution was vigorously stirred for 5 d at rt. Finally, the solution was precipitated in water, and the garnet product 2-amino-9H-fluoren-9-one was thoroughly washed with water. Yield: 93%.

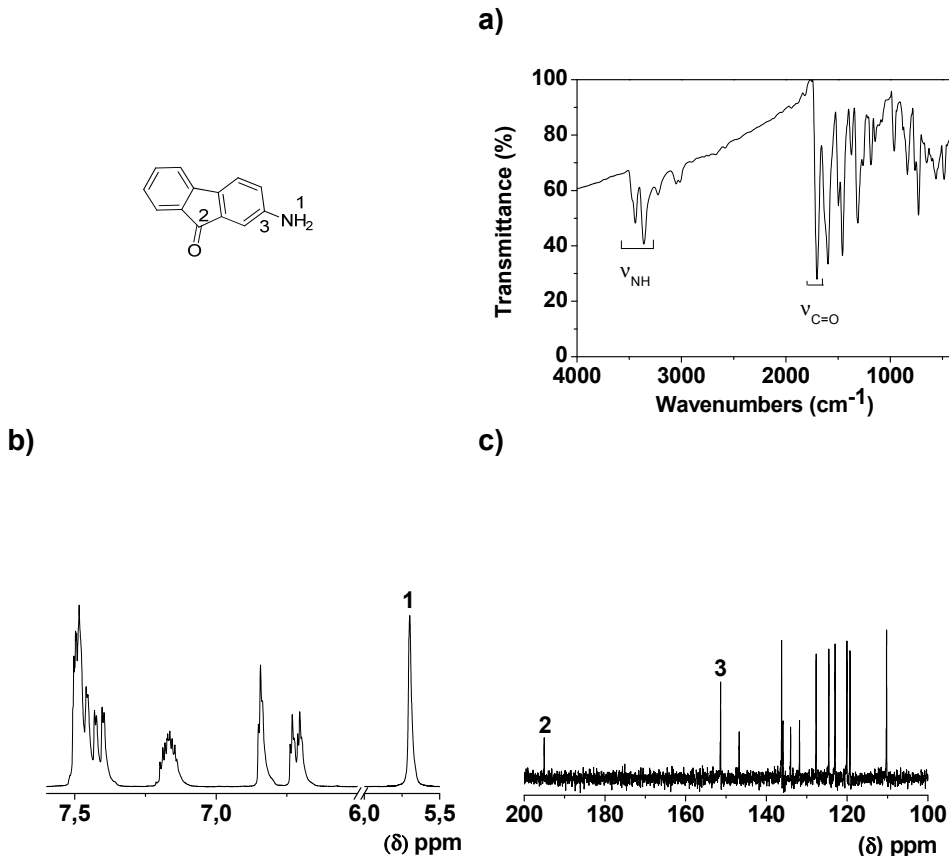


Figure S5. Characterization of (**5**) by (a) FTIR, (b) ^1H RMN, and (c) ^{13}C RMN.

Synthesis of 2-(2-amino-9H-fluoren-9-ylidene)malononitrile (**6**)

To a flask equipped with a reflux condenser was added 8 mmol of 2-amino-9H-fluoren-9-one dissolved in 20 mL of DMF. Afterward, 10 mmol of malononitrile was added portion-wise, and the solution was stirred at reflux for 5 d. The product 2-(2-amino-9H-fluoren-9-ylidene)malononitrile was filtered off and purified by column chromatography with a mixture of hexanes:ethyl acetate (1:1). Yield before purification: 80%. Yield after purification: 25%.

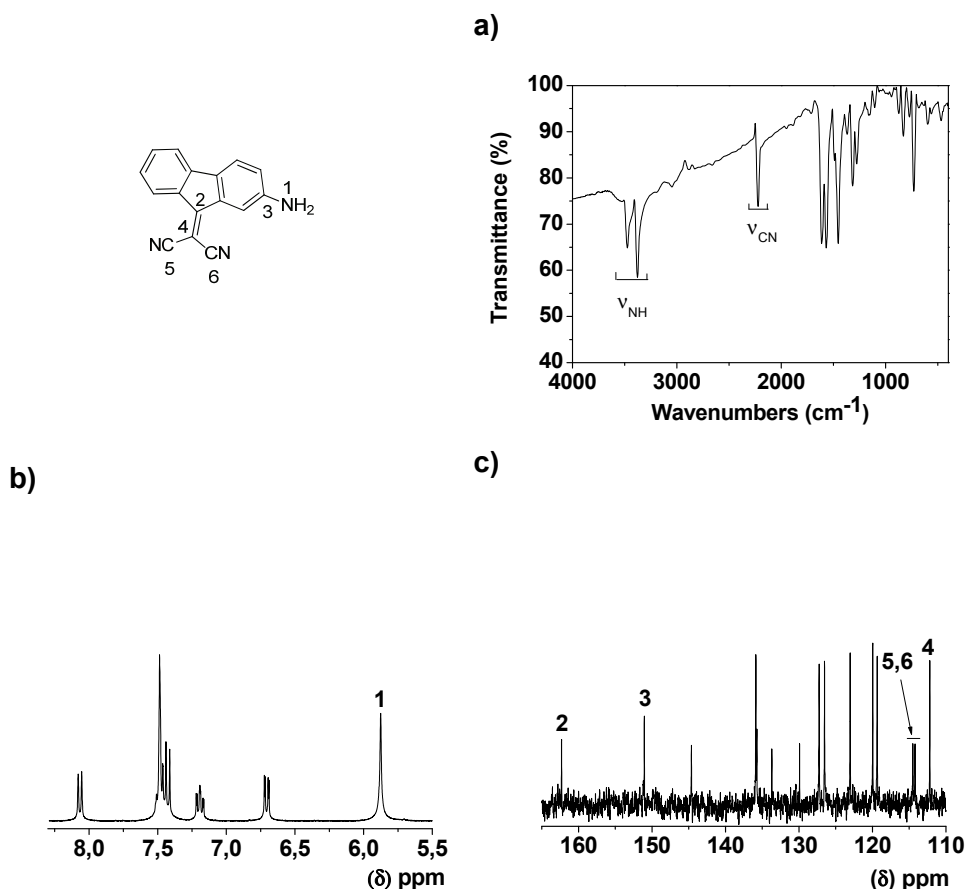


Figure S6. Characterization of (**6**) by (a) FTIR, (b) ¹H RMN, and (c) ¹³C RMN.

Synthesis of 2-(3-(9-(dicyanomethylene)-9H-fluoren-7-yl)ureido)ethyl methacrylate (7)

1.3 mmol of 1-(9-(dicyanomethylene)-9H-fluoren-7-yl)-3-(2-hydroxyethyl)urea was dissolved in 15 mL of pyridine in a round-bottomed flask. Afterward, 1.7 mmol of methacryloyl chloride was added drop-wise, and the solution was stirred at room temperature for 3 h. After that, the solution was precipitated in slightly acidified water at 0 °C. The product 2-(3-(9-(dicyanomethylene)-9H-fluoren-7-yl)ureido)ethyl methacrylate was extracted from the crude residue using a Soxhlet apparatus using acetone. The acetone was then removed by distillation, and the product was purified by column chromatography in a mixture of hexane:ethyl acetate (3:1). Yield: 83%.

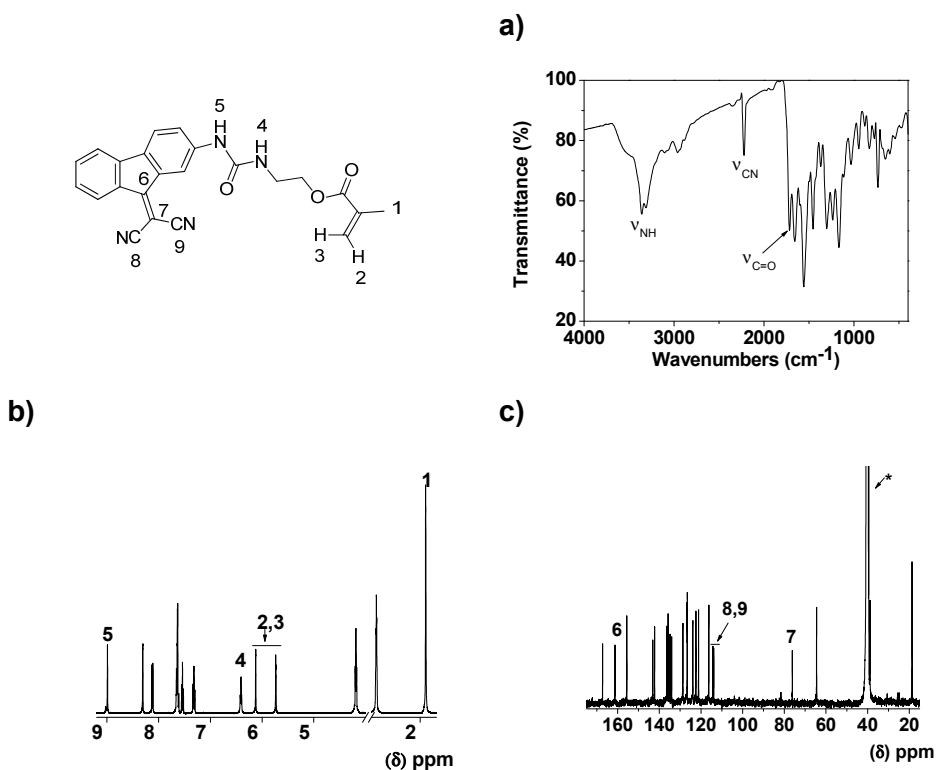


Figure S7. Characterization of (7) by (a) FTIR, (b) ¹H RMN, and (c) ¹³C RMN (* =solvent signal).

Synthesis of N-(9-(dicyanomethylene)-9H-fluoren-7-yl)methacrylamide (8)

2.1 mmol of 2-(2-amino-9H-fluoren-9-ylidene)malononitrile was dissolved in 8 mL of pyridine in a round-bottomed flask. Afterward, 2.7 mmol of methacryloyl chloride was added dropwise to the solution, and it was stirred at rt for 3 h. The product N-(9-(dicyanomethylene)-9H-fluoren-7-yl)methacrylamide was purified by column chromatography using a mixture of hexane:ethyl acetate (2:1) and was washed in a Soxhlet assembly with ethanol. Yield before purification: 87%. Yield after purification: 20%.

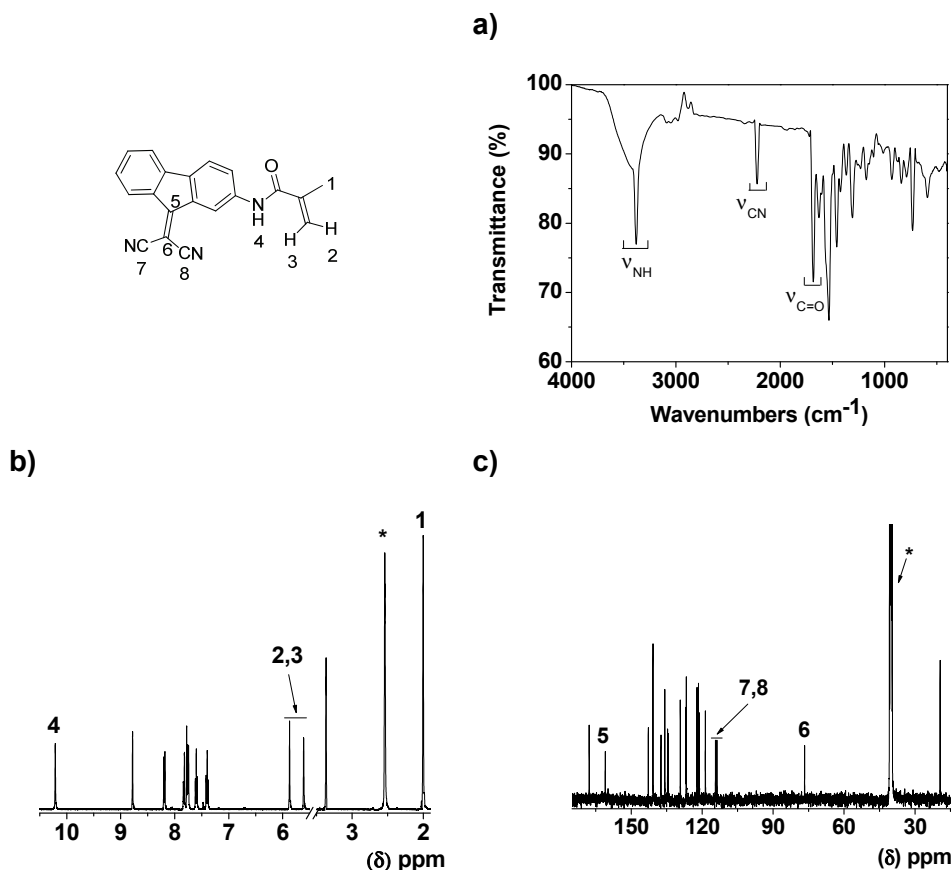


Figure S8. Characterization of (8) by (a) FTIR, (b) ^1H RMN, and (c) ^{13}C RMN (* =solvent signal).

Synthesis of 2-(2-aminoethoxyethanol) methacrylamide (9)

To 20 mL of an ice-cold, methanolic solution of 2-(2-aminoethoxyethanol) (2.4 mL, 24 mmol) was slowly added 2.4 mL (25 mmol) of methacryloyl chloride diluted in 20 mL of THF under a nitrogen blanket. Potassium hydroxide (1 M, aqueous) was added to maintain a pH of 8-9 throughout the reaction. The mixture was warmed to rt over 4 h. Afterwards, it was quenched by addition of hydrochloric acid to a final pH of 5, and the product was concentrated. Finally, to the crude residue was added sodium chloride, and it was extracted with dichloromethane. Yield: 97%.

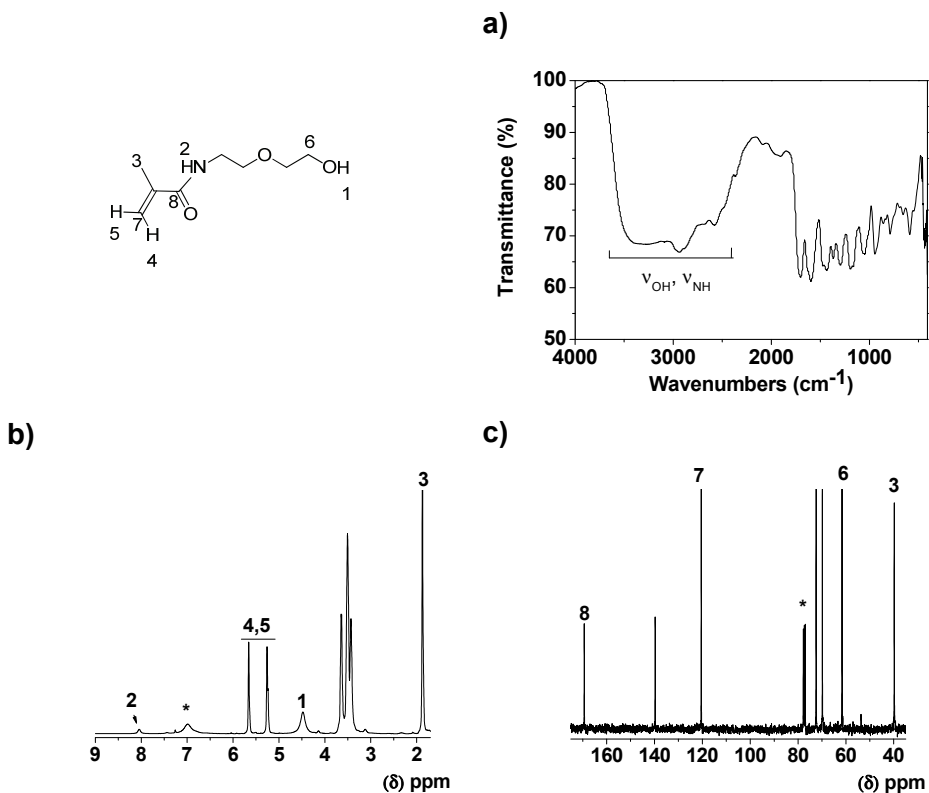


Figure S9. Characterization of (9) by (a) FTIR, (b) ^1H RMN, and (c) ^{13}C RMN. (* =solvent signal).

Synthesis of 2-(9H-fluoren-9-ylidene)malononitrile (**10**)

11 mmol of 9H-fluoren-9-one was dissolved in 25 mL of DMF. Afterward, 16.5 mmol of malononitrile was added, and the solution was stirred at reflux for 5 d. The solution was precipitated in water, and the solid was recrystallized from acetone.

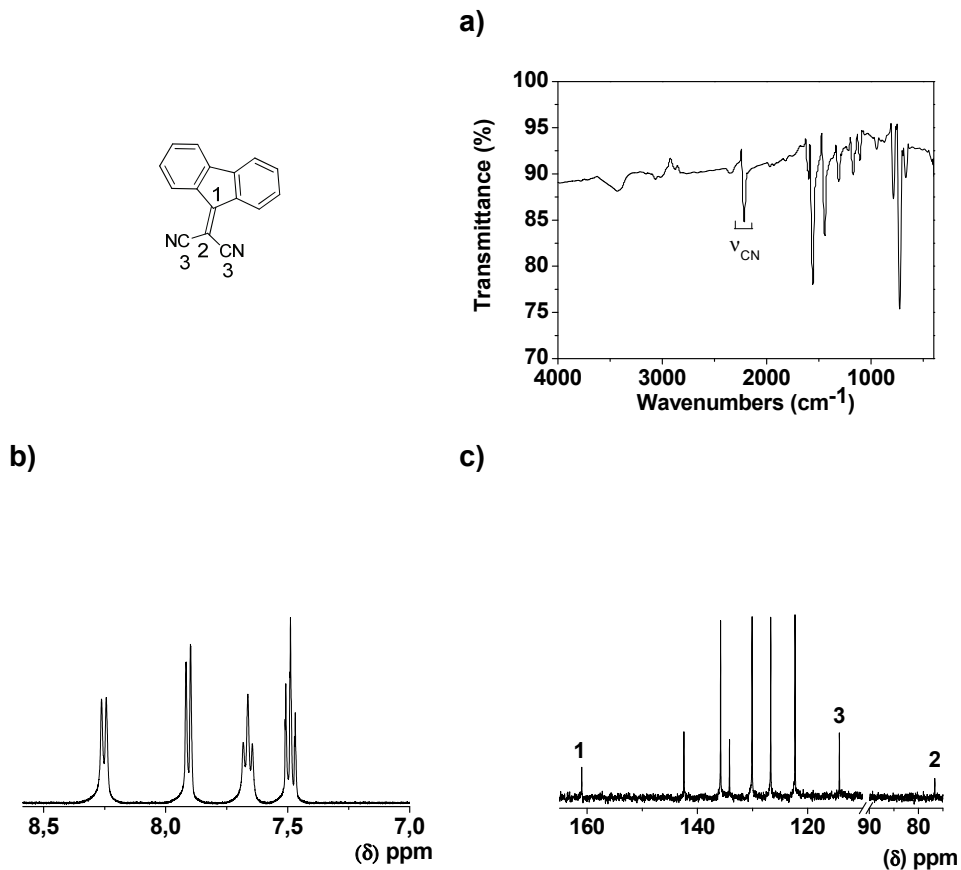


Figure S10. Characterization of (**10**) by (a) FTIR, (b) ^1H RMN, and (c) ^{13}C RMN.

Synthesis of 9-(dicyanomethyl)-9H-fluorene-9-carbonitrile (11)

8.8 mmol of 2-(9H-fluoren-9-ylidene)malononitrile was dissolved in 15 mL of DMSO. Afterward, 17.6 mmol of sodium cyanide was added, and the solution was stirred at rt for 2 h. The solution was precipitated in water, and the solid was filtered off and washed with water. The product 9-(dicyanomethyl)-9H-fluorene-9-carbonitrile was dried in a vacuum oven at 60 °C.

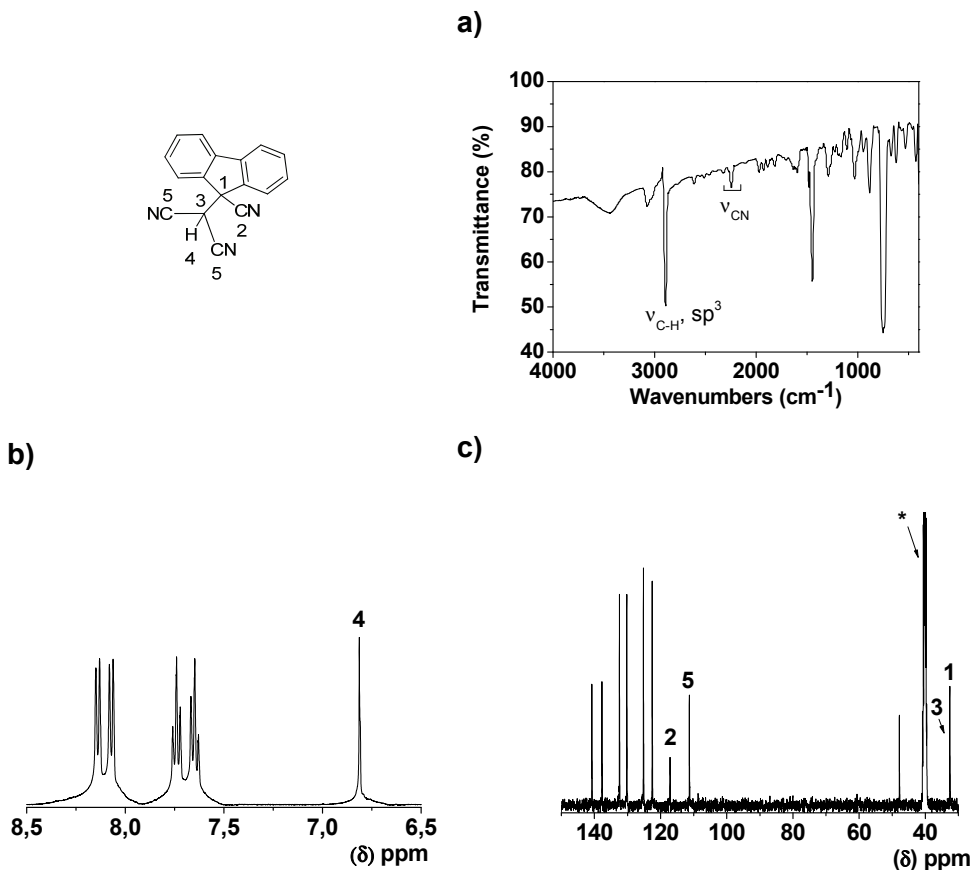
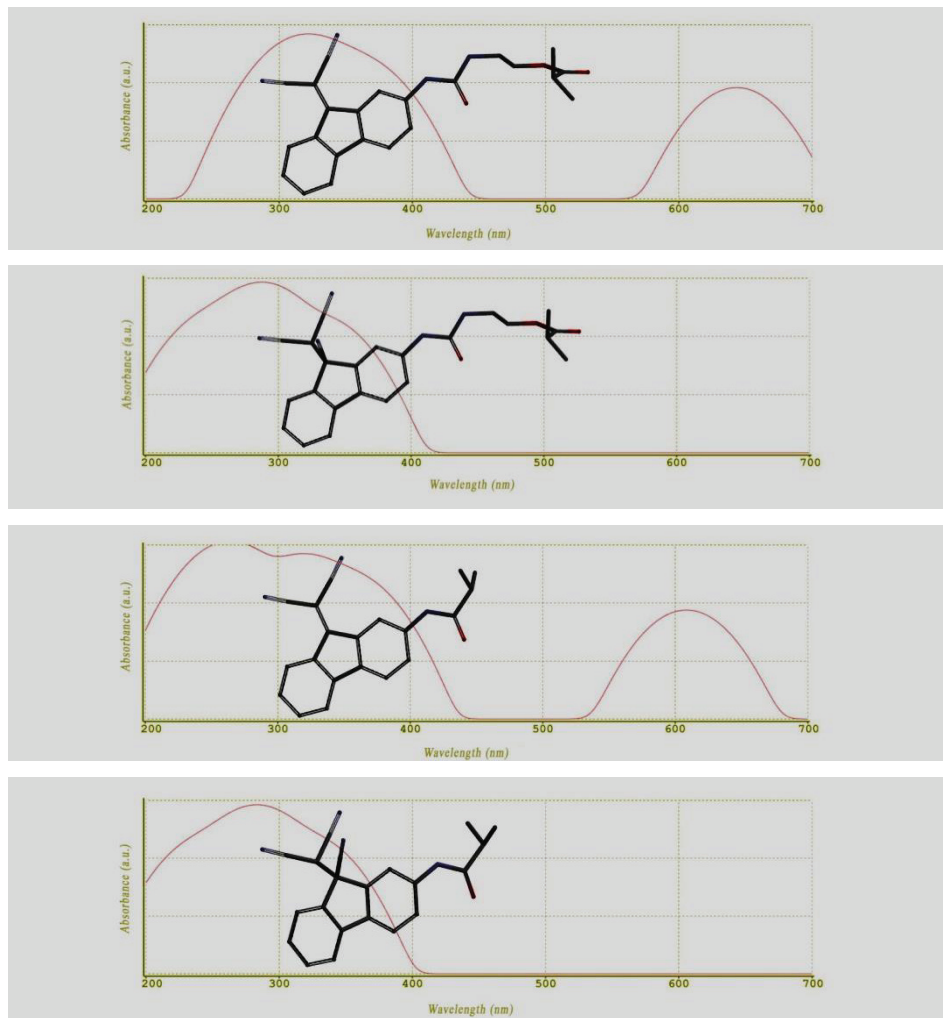


Figure S11. Characterization of (11) by (a) FTIR, (b) ¹H RMN, and (c) ¹³C RMN (* =solvent signal).

S3. Theoretical calculation of UV/Vis spectra of model molecules (UV-Vis DFT calculations at B3LYP/6-31G*)

S4. Membrane preparation

The membranes were prepared by radical polymerization of mixtures of the 4 different co-monomers using ethylene glycol dimethacrylate as cross-linking agent (1%) and AIBN (1 wt %) as a thermal radical initiator. Eight different polymer films were prepared in this fashion by varying the molar concentration of monomers. The reactions were carried out in silanized glass molds of 100 mm thickness in an oxygen-free atmosphere at 65 °C for 5 h.

S5. Measurements and instrumentation

The ^1H and ^{13}C NMR spectra were recorded using a Varian Inova 400 spectrometer operating at 399.92 and 100.57 MHz, respectively, using DMSO-d₆ as the solvent.

Infrared spectra (FT-IR) were recorded using a Nicolet Impact spectrometer.

The UV–Vis spectra were recorded using a Varian Cary3-Bio UV–Vis spectrophotometer.

The apparent response time was recorded using a digital stopwatch. The different polymeric films were dipped in a water solution of sodium cyanide (3 M), and the time was taken when the color of the film turned colorless to the naked eye. Each experiment was repeated three times, and the results were averaged.

A petición de la revista *Polymer chemistry*, se realizó un artículo completo de la comunicación publicada en *Chemical Communication*, titulada “Working with water insoluble organic molecules in aqueous media fluorene derivate-containing polymers as sensory materials for the colorimetric sensing of cyanide in water” (*Chem. Commun.* **2010**, 46, 7951–7953). La portada de dicho artículo se muestra a continuación (Figura 2.6).

Working with water insoluble organic molecules in aqueous media fluorene derivate-containing polymers as sensory materials for the colorimetric sensing of cyanide in water

Cite this: *Polym. Chem.*, 2011, **2**, 1129

www.rsc.org/polymers

PAPER

Working with water insoluble organic molecules in aqueous media: fluorene derivative-containing polymers as sensory materials for the colorimetric sensing of cyanide in water[†]

Saúl Vallejos, Hamid El Kaoutit, Pedro Estévez, Félix Clemente García, José Luis de la Peña, Felipe Serna and José Miguel García*

Received 13th January 2011, Accepted 13th February 2011

DOI: 10.1039/c1py00013f

This paper describes a strategy followed to achieve a sensing phenomenon in aqueous media using water-insoluble organic molecules. We have prepared a methacrylamide and a methacrylate with pendant cyanide chemosensors based on a fluorene-derivative motif, and we have fabricated highly hydrophilic membranes by means of copolymerising these hydrophobic monomers with others. Therefore, upon absorption of water in the membranes, solvated ions enter the membrane by a simple diffusion mechanism, reaching the hydrophobic chemosensor motif and giving rise to a macroscopic sensing phenomenon. In this way, we have prepared solid materials (dense membranes or films) capable of selectively detecting cyanide, with an extremely low detection threshold, in aqueous solution by means of colour changes (naked-eye sensing) (13 ppb). Nevertheless, the key point of this research is the description of the possibilities of anchoring organic insoluble molecules (*i.e.*, drugs, fungicides, bactericides, sensing probes, *etc.*) to stabilise them in water, or to prepare hydrogels, permitting the use of these molecules in aqueous media or in biological media for medical, biological or biochemical purposes.

Introduction

Molecular recognition is a widespread, naturally occurring key event in nature. The recognition between two or more molecules occurs when they are chemically and geometrically, or structurally, complementary. Thus, the “fit together” takes place spatially, and the binding to each other arises from intermolecular feeble interactions, including hydrogen bonds, electrostatic interactions, hydrophobic interactions and weak metal coordination.^{1,2} In nature, the processes take place in aqueous environments and are usually implicated in natural macromolecules or even in complex and organised systems, such as cells. Examples of the recognition process include the binding of an enzyme to a substrate,³ a drug to a biological target,^{4,5} antigen/antibody recognition in the immune system,^{6,7} the formation of messenger RNA from DNA templates,⁸ *etc.* In this context, the development of chemosensors for the detection of target chemicals is a field of current interest.⁹

Naturally, recognition in biological systems takes place in aqueous environments. The active sites, for example in an enzyme, have the shape needed to fit the *guest* molecule, or a part of the *guest* molecule, and the interaction relies on feeble bonds that take place due to the hydrophobic microdomain in a hydrophilic general domain provided by the chemical and by the quaternary structure of a protein. In a very simplified manner, the competitiveness of the water molecules to establish these weak integrations is locally diminished or altered by the active site microsurroundings.

Mimicking nature, water insoluble receptors may be chemically anchored to a linear or crosslinked hydrophilic polymer, giving rise to water-soluble sensing polymers or to water-swelled sensing networks. The latter approach permits easy control of swelling by means of increasing the crosslinking ratio. That is, the hydrophilic character of a polymer, derived from the chemical composition of the monomers, may be controlled not only by the monomer nature, but also by increasing the crosslinking monomer content of the network; thus, mechanically impairing the water uptake. Thus, an induced partially hydrophobic character may be addressed with an overall hydrophilic polymer associated with the mechanical stretching of the network upon swelling with water, as we have previously described.^{10,11} Moreover, the polymers usually have good thermal and mechanical properties, can be easily transformed into end materials, *e.g.*, into films or coatings obtained by casting, to produce cheap sensing

Departamento de Química, Facultad de Ciencias, Universidad de Burgos, Plaza de Míssel 39, 09001 Burgos, Spain. E-mail: jmiguel@ubu.es; Web: <http://www2.ubu.es/quimicaorganica/polimeros/polimeros.htm>; Fax: +34 947 25 88 31; Tel: +34 947 25 80 85

[†] Electronic supplementary information (ESI) available: Intermediates and monomer NMR and IR-FT spectra, a TGA curve, as well as a movie showing the colorimetric response of a film (**d**) toward cyanide. See DOI: 10.1039/c1py00013f

Figura 2.6. Portada del artículo S. Vallejos, H. El Kaoutit, P. Estévez, F. C. García, J. L. de la Peña, F. Serna, J. M. García, *Polym. Chem.* **2011**, *2*, 1129.

CAPÍTULO 3

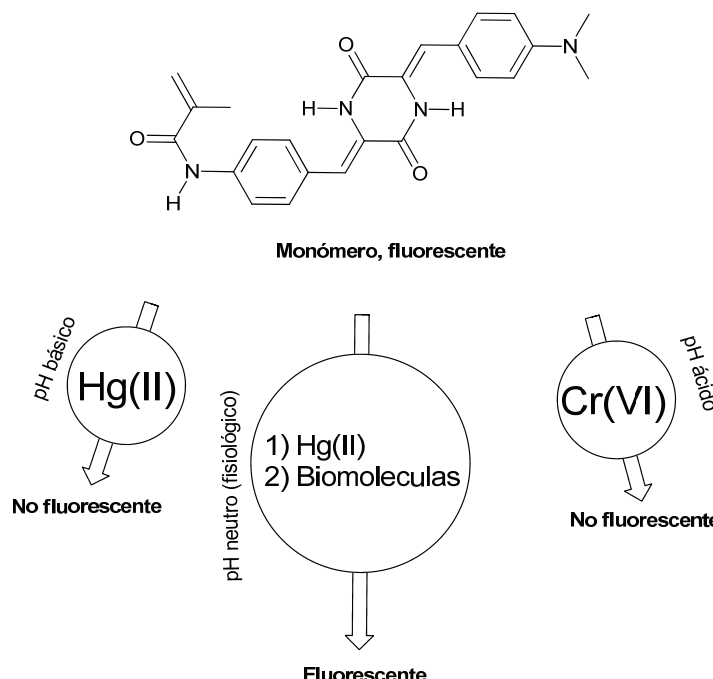
Polímeros con derivados de 2,5-dicetopiperazina en su estructura

Los derivados de la 2,5-dicetopiperazina son fáciles de sintetizar a partir de compuestos baratos de origen biológico, son rígidos, y permiten preparar compuestos con conjugación extendida. Dichas propiedades, combinadas con la versatilidad de los monómeros vinílicos, entre los que se incluyen los acrílicos, se han explotado a la hora de diseñar materiales poliméricos sensores en forma de membranas fluorogénicas con comportamiento tipo gel. Estas membranas presentan una notable fluorescencia, y se han empleado para la detección específica por cambios de fluorescencia de Hg(II), de Cr(VI) y de varias moléculas presentes en procesos biológicos, como CoA, GSH y Cys.

3.1 2,5-Dicetopiperazina y sus derivados

En este capítulo se describe la preparación de monómeros acrílicos con subunidades receptoras derivadas de 2,5-dicetopiperazina (Esquema 3.1), junto con el estudio de su capacidad sensora hacia diversas especies

químicas en disolución acuosa, y más específicamente hacia cationes [Hg(II) y Cr(VI)] y biomoléculas [Coenzima A (CoA), glutatión (GSH) y (Cys)]. Del mismo modo, se comentan aspectos generales de los polímeros vinílicos utilizados como soporte, así como las características y reactividad del receptor anclado a esta matriz, derivado de 2,5-dicetopiperazina.



Esquema 3.1. Estructura química del monómero con subestructura de 2,5-dicetopiperazina y cambios detectados en su fluorescencia en presencia de distintos analitos y a diferentes pH.

La dicetopiperazina, conocida también como dioxopiperazina o piperazinodiona,^{63,64} es una amida cíclica que tiene tres regioisómeros posibles (Esquema 3.2). Comúnmente se les denomina DKPs, y cada uno de ellos se obtiene por rutas sintéticas muy diferentes. Así, la 2,3-DKP se puede obtener a

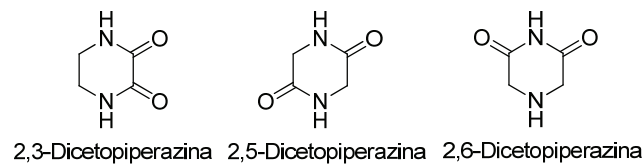
⁶³ E. Benedetti, P. Corradini, C. Pedone, *The Crystal and Molecular Structure of trans-3,6-Dimethyl-2,5-piperazinedione*, en *Polymer Research Institute of the Polytechnic Institute of Brooklyn*, New York, 1969.

⁶⁴ B. R. Davis, I. Bernal, *Proc. Nat. Acad. Sci.* **1973**, 70, 279.

partir de dimetiloxalato y etilendiamina. Los derivados 2,3-DKPs se utilizan en química médica, y además se pueden encontrar en antibióticos naturales como la piperacilina, la cefoperazona y la bioclomicina.

El derivado que tiene los grupos carbonilo en las posiciones 2 y 6 se puede sintetizar a través de la reacción entre la 2-cloroacetamida y el éster metílico de la glicina. Por último, la 2,5-DKP, que es el derivado que se ha utilizado en este estudio, se obtiene sencillamente a partir de la condensación de dos moléculas de glicina. En general las DKPs son importantes en el diseño de nuevas drogas dado su parecido estructural con los péptidos. Además, su estructura química da lugar a una disminución tanto de la reactividad de los enlaces amida como de la movilidad conformacional, hecho positivo de cara al diseño de fármacos.⁶⁵

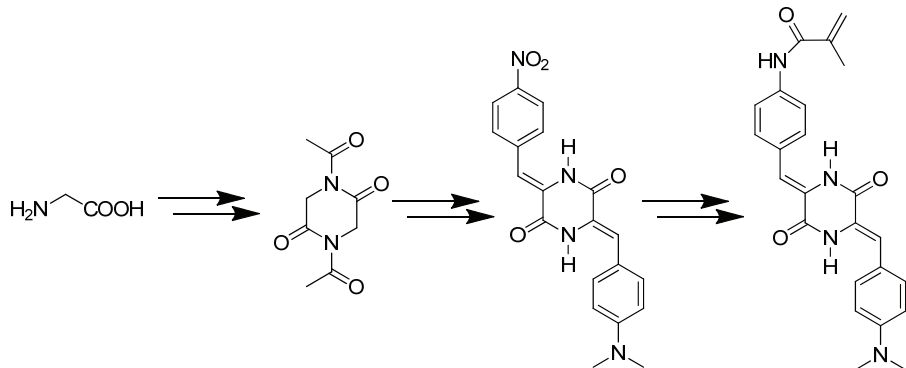
A la hora de plantear este trabajo se pensó en la estructura de 2,5-DKP por un doble motivo. El primero fue la fácil funcionalización del anillo, procedente además de un compuesto natural y barato, mientras que el segundo se debió a la rigidez ya comentada del propio anillo, que permite el diseño de estructuras planas y conjugadas (Esquema 3.3) especialmente útiles para aplicaciones relacionadas con la fluorescencia. Así, la condensación de la 2,5-DKP con aldehídos permitió la extensión de la conjugación, además de la introducción en la estructura de un grupo donador de electrones [-N(CH₃)₂], que dio como resultado final un monómero fluorescente.



Esquema 3.2. Estructura química de los regiosómeros de la dicetopiperazina.

⁶⁵ C. Dinsmore, D. Deshore, *Tetrahedron* **2002**, 58, 3297.

En los materiales preparados con este monómero, la interacción tanto del grupo dador como del propio anillo de 2,5-DKP con cationes, aniones y moléculas neutras dio lugar a la modificación de la densidad electrónica de la estructura, con la consiguiente variación en la fluorescencia de los polímeros, comportándose, por tanto, como sensores fluorogénicos hacia estas especies.



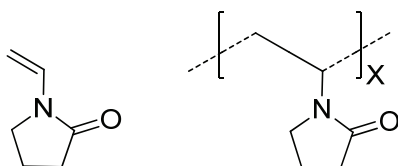
Esquema 3.3. Ruta sintética utilizada para la síntesis de monómero *N*-(4-((*Z*)-((*Z*)-5-(4-(dimetilamino)benziliden)-3,6-dioxopiperazin-2-ilidene)metil)fenyl)metacrilamida.

3.2 Polímeros con derivados de 2,5-dicetopiperazina en la cadena lateral

La preparación de las redes entrecruzadas con subgrupos receptores derivados de 2,5-dicetopiperazina se llevó a cabo siguiendo los procedimientos descritos en el Capítulo 2. De este modo, se obtuvieron membranas densas compuestas por la matriz inerte y los subgrupos receptores que se describen a continuación.

La matriz inerte se preparó empleando *N*-vinilpirrolidona (VP) como monómero principal (Esquema 3.4). Esta decisión vino determinada fundamentalmente por la gran solubilidad del derivado de 2,5-dicetopiperazina en *N*-vinilpirrolidona, que por otra parte es un excelente disolvente. En este sentido, hay que tener en cuenta que en la polimerización en bloque el conjunto de comonómeros, reticulante e iniciador han de dar lugar a una disolución. La elevada hidrofilia que la VP induce en los polímeros preparados con este monómero hizo necesario el empleo de un mayor porcentaje de entrecruzante

para disminuir físicamente el hinchamiento de las membranas, con el objetivo de mantener su manejabilidad en agua. Además, cabe mencionar que la VP presenta características adicionales interesantes de cara a las propiedades químicas y a la biocompatibilidad de los polímeros que de ella se derivaran. Así, la polivinilpirrolidona (PVP) lineal es soluble en agua y en un gran número de disolventes orgánicos, posee una elevada estabilidad química, buena capacidad para formar películas delgadas, adherencia a diversos substratos, y a su vez una baja toxicidad y capacidad de complejación. Desde un punto de vista biomédico, tanto como polímero lineal como reticulado, se aplica como expansor del plasma sanguíneo en accidentados, aglutinante en muchos comprimidos farmacéuticos, en gotas para los ojos y como una molécula portadora de yodo en desinfectantes yodados, por nombrar algunos ejemplos. También se utiliza en productos de cuidado personal, tales como champús y pastas de dientes, y en la industria cosmética como un agente dispersante y como un lubricante en pomadas.⁶⁶⁻⁶⁹ Como aditivo alimentario, la PVP es un estabilizante (E1201).



Esquema 3.4. *N*-Vinilpirrolidona (izquierda) y polivinilpirrolidona (derecha).

En cuanto a al subgrupo receptor, como se ha comentado es un derivado de 2,5-DKP (Esquema 3.1). Los polímeros sensores se prepararon copolimerizando con VP un pequeño porcentaje en moles de la metacrilamida que porta dicho subgrupo. Tras varios ensayos, se consiguió la mejor

⁶⁶ H. Folttmann, A. Quadir, *Drug Delivery Technol.* **2008**, 8, 22.

⁶⁷ F. Haaf, A. Sanner, F. Straub, *Polym. J.* **1985**, 17, 143.

⁶⁸ A. C. Rönnau, W. Wulferink, E. Unver, T. Ruzicka, J. Krutmann, M. Grewe, *Br. J. Dermatol.* **2000**, 143, 1055.

⁶⁹ A. Adachi, A. Fukunaga, K. Hayashi, M. Kunisada, T. Horikawa, *Contact Dermatitis*, **2003**, 48, 133.

combinación en relación a la solubilidad de los monómeros, y a la manejabilidad, hinchamiento en agua (entorno a un 200%) y respuesta fluorogénicas del material sensor, cuya constitución se muestra en el Esquema 3.5. El material fue troquelado en tiras sensoras de pequeño tamaño similares a las que se utilizan para la medida de pH. La proporción molar de monómero sensor fue realmente pequeña, un 0.25%, ya que cantidades más altas de monómero provocaban la saturación en el espectrofotómetro de fluorescencia.

En relación con la respuesta fluorogénica de las membranas sensoras, tras realizar los análisis habituales con una batería de especies se observó que en medio ácido el catión Cr(VI) provocaba la disminución de la fluorescencia (proceso denominado amortiguamiento, *quenching*, apagado, u “ON-OFF”), mientras que en medio básico era el catión Hg(II) el que daba lugar este fenómeno.⁷⁰

Una vez analizada la interacción de la membrana con Hg(II) se diseñaron con apoyo bibliográfico una serie de experimentos con tioles con el objeto de captar el mercurio (II) de la red polimérica trás la interacción,⁷¹ dando lugar al proceso de fluorescencia inverso, es decir encendido u “OFF-ON”. Para ello, se utilizaron tioles comerciales y convencionales como el 1,2-bis(2-mercptoetoxi)etano, y tioles con gran interés desde el punto de vista biológico como el Coenzima A (CoA), el glutatión (GSH) o la cisteína (Cys),⁷² lo que permitió el estudio de las membranas híbridas, cargadas con Hg(II), como sensores fluorogénicos diseñados por la aproximación por ensayos de desplazamiento.

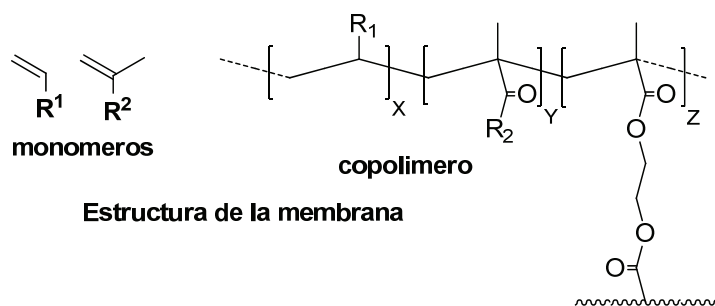
Como comentario final a este apartado, indicar que la detección mediante fases sólidas, específicamente mediante membranas con comportamiento tipo gel, tiene la ventaja de ofrecer un material con el que se

⁷⁰ H. A. Kim, Z. Guo, W. Zhu, J. Yoon, H. Tian, *Chem. Soc. Rev.* **2011**, *40*, 79.

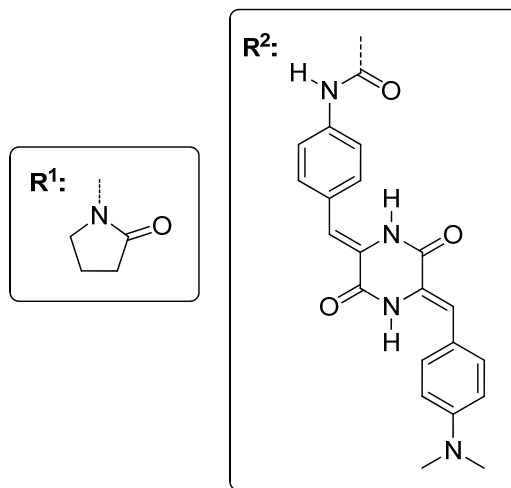
⁷¹ W. Lin, X. Cao, Y. Ding, L. Yuan, Q. Yu, *Org. Biomol. Chem.* **2010**, *8*, 3618.

⁷² J. Du, J. Fan, X. Peng, P. Sun, J. Wang, H. Li, S. Sun, *Org. Lett.* **2010**, *12*, 476.

pueden elaborar tiras sensoras para su uso *in situ*, por personal no especializado. Así, por ejemplo, la presencia o ausencia de mercurio [Hg(II)] o de cromo [Cr(VI)] en un vertido, o en un efluente acuoso, se puede seguir visualmente por inmersión de una tira de membrana en el propio medio. Además, el material reticulado se puede preparar directamente como recubrimiento en el extremo de una fibra óptica para la elaboración de sondas cromogénicas o fluorogénicas de aplicación industrial.



Relación molar de los monómeros: X/Y/Z = 99.75/0.25/7



Esquema 3.5. Estructura de la membrana sensora sintetizada.

3.3 Resultados

A continuación se describen los resultados obtenidos a través de la transcripción íntegra de los tres trabajos publicados, clasificados a su vez por las especies detectadas [Hg(II), biomoléculas y Cr(VI)].

- ❖ *A selective and highly sensitive fluorescent probe of Hg²⁺ in organic and aqueous media: the role of a polymer network in extending the sensing phenomena to water environments.*
 - ❖ *An organic/inorganic hybrid membrane as a solid “turn-on” fluorescent chemosensor for coenzyme a (CoA), cysteine (Cys), and glutathione (GSH) in aqueous media*
 - ❖ *Methacrylate copolymers with pendant piperazinedione-sensing motifs as fluorescent chemosensory materials for the detection of Cr(VI) in aqueous media*
-

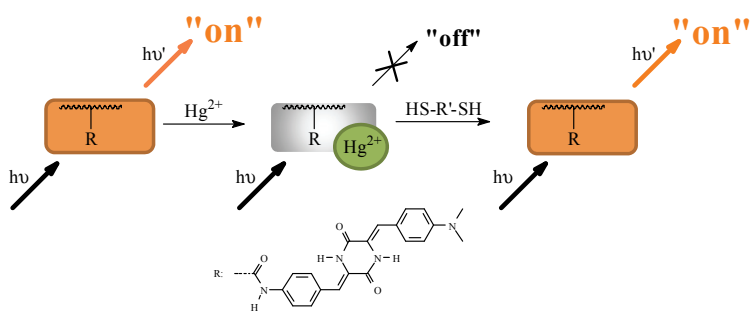
A selective and highly sensitive fluorescent probe of Hg²⁺ in organic and aqueous media: the role of a polymer network in extending the sensing phenomena to water environments.

A selective and highly sensitive fluorescent probe of Hg^{2+} in organic and aqueous media: the role of a polymer network in extending the sensing phenomena to water environments.

Saúl Vallejos, Pedro Estévez, Saturnino Ibáñez, Asunción Muñoz, Félix C. García, Felipe Serna, José M. García.*

Departamento de Química, Facultad de Ciencias, Universidad de Burgos. Plaza de Misael Banuelos s/n, E-09001 Burgos, Spain. Fax: +34947258831; Tel: +34947258085; E-mail: jmiquel@ubu.es.

Graphical abstract



Abstract

This paper describes the preparation of a hydrophilic copolymer membrane with two comonomers: *N*-vinylpyrrolidone (commercial) and a new water insoluble piperazinedione derivative, which is a fluorogenic mercury sensing motif. The dense membrane permitted the fluorogenic detection of Hg^{2+} in aqueous media. The sensitivity of the membrane this cation was significantly high, with a detection limit of 10 ppt. This limit of detection is much lower than that of DMSO/water solutions of the sensing monomer, which is 10 ppb, and significantly lower than the maximum contaminant level (EPA) in drinking water, 2 ppb.

Sensors and Actuators, B: Chemical 2011, 157, 2, 686– 690.

1. Introduction

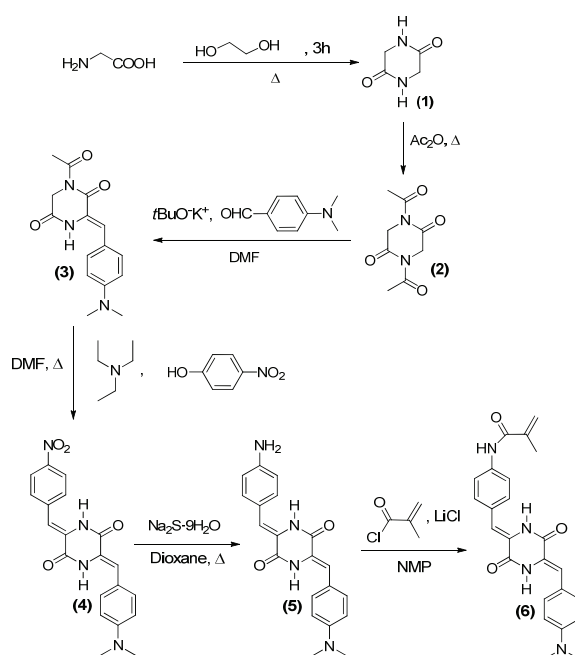
Mercury contamination in water sources is ubiquitous due to the erosion of natural deposits, discharge from refineries and factories, as well as runoff from landfills and croplands. Mercury is very toxic; bioaccumulation within the brain and kidneys causes serious problems to human health and ultimately leads to neurological diseases. In this regard, the United States Environmental Protection Agency (EPA) has set the maximum contaminant level (MCL) in drinking water, and also the goal to ensure public health, to be 2 ppb, rendering its detection important for health and environmental safety and also from an industrial viewpoint.¹ Chemical probes are useful for the fast detection of mercury contamination. They operate by complexation of the guest Hg²⁺ with a fluorogenic or chromogenic host, giving rise to a macroscopically detectable colour change or change in fluorescent parameters. Fluorescent chemosensors for Hg²⁺ ion are especially of interest because fluorescence is a highly sensitive, simple and readily available technique in most scientific laboratories.² Thus, hundreds of articles regarding fluorescence detection of Hg²⁺ have been published in the last few years. Previous work has focused on improving the selectivity and sensitivity of the probes. Many of the published articles describing chemosensors are based on rhodamine derivatives,²⁻⁹ although crown, criptand or calixarene derivatives;¹⁰⁻¹⁴ compounds with nitrogen containing heterocycles, azo groups, or with schiff bases;¹⁵⁻¹⁹ urea, thiourea or amide;^{20,21} amine or thioether;^{22,23} coumarin motif- containing molecules,²⁴⁻²⁶ silver or gold nanoclusters or nanoparticles^{27,28} DNA or oligonucleotide bases;^{29,30} or conjugated polymers^{31,32} among others, have been exploited intensively.

Bearing this in mind, we followed our previous strategy by preparing polymerizable sensing organic molecules that are water insoluble. We polymerized them with hydrophilic co-monomers to yield hydrophilic membranes that exhibit their sensing characteristics in aqueous

media.³³⁻⁴⁰ Therefore, we have prepared solid systems, or practical kits, for water “dip-in” fluorogenic Hg^{2+} detection by means of host-guest interactions. The chemical anchoring of a sensing, or host, motif to a hydrophilic polymer chain provides a water-rich environment to the sensing moiety upon polymer swelling in water, therefore permitting the solvated hosts, or analytes, to reach the guest, or transducer cores, giving rise to the sensing phenomenon and resulting in detection of Hg^{2+} .

2. Experimental

The Hg^{2+} sensing monomer (**6**) was prepared following the synthetic strategy described in Scheme 1. The materials used, intermediates and monomer were prepared and characterized as shown in the Supplementary Data (SD).



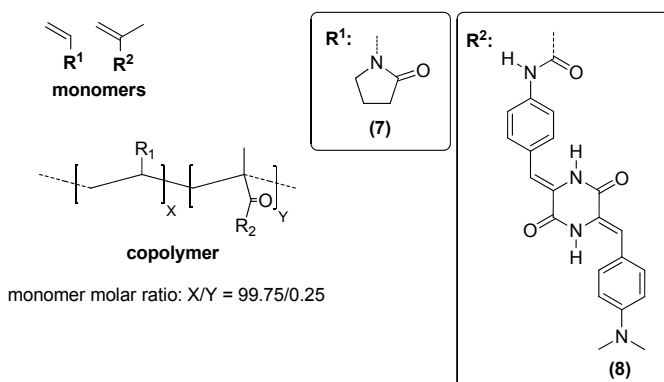
Scheme 1. Synthesis of the monomer *N*-(4-((1*Z*)-(Z)-5-(4-(dimethylamino)benzylidene)-3,6-dioxopiperazin-2-ylidene)methyl)phenyl)methacrylamide.

The sensory membrane was prepared by radical polymerization of a mixture of *N*-vinylpyrrolidone with (**6**), with a molar ratio of 99.75:0.25,

respectively. Ethylene glycol dimethacrylate was used as the cross-linking agent (7%, mol percentage regarding the overall co-monomer molar content) and AIBN (1 wt. %) as a thermal radical initiator. The reactions were carried out in silanized glass molds, 100 mm thick, in an oxygen-free atmosphere at 65 °C for 5 h.

3. Results and discussion

Thus, we prepared a methacrylamide monomer containing a piperazinedione derivative as the fluorogenic mercury sensing motif (**6**) and copolymerized them with a hydrophilic monomer [*N*-vinylpyrrolidone, (**7**)] (SD1, SD2, Scheme 2). The cross-linking agent, 1,2-ethanedioldimethacrylate, was used to obtain the dense, 100 mm thick polymer film or membrane (Scheme 2), with a water swelling percentage of 200%. This membrane is optically transparent and tractable, demonstrating good mechanical properties (see a digital picture in SD3), even after water or DMSO swelling. The thermal resistance, measured thermogravimetrically, was also good, showing a decomposition temperature (T_d , onset) close to 400 °C (see figure and data in SD3).



Scheme 2. Chemical structure of monomers and copolymer

Due to the insolubility of (**6**) in water, the fluorescent sensing behaviour of (**6**) toward cations and anions was tested in DMSO/water (90/10, v/v). Upon adding increasing quantities of Hg^{2+} to a buffered

organic/inorganic solution of (**6**), fluorescent quenching was observed in basic conditions ($\text{pH} = 9.7$), but not in physiological or acidic conditions ($\text{pH} = 7, 2.9$) (see SD1, SD5). Figure 1 depicts the quenching processes relating the fluorescence intensity to the mercury concentration, as well as the relationship between the fluorescence intensity maxima (F) at 591 nm and the molar ratio of Hg^{2+} to (**6**). The detection limit of Hg^{2+} was 110 ppb, above the MCL. Interestingly, after completely quenching the system with the addition of mercury equal to ten times the concentration of (**7**), fluorescence could be fully recovered with an equal concentration of 2-[2-(2-mercaptoethoxy)ethoxy]ethanethiol (MEEET), providing a fluorescent ON-OFF-ON system (see SD1, SD6).

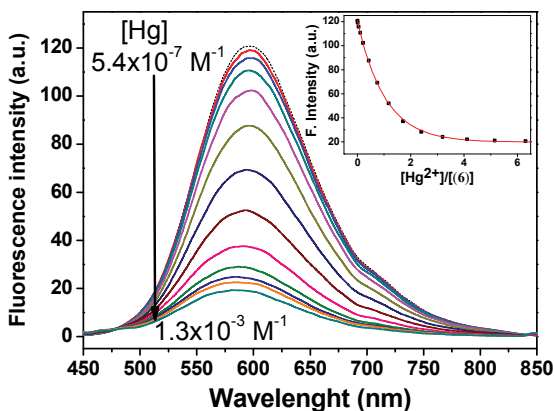


Figure 1. Titration curve of (**6**) with mercury cations in DMSO/water (90/10, v/v) at $\text{pH} = 9.7$ (TRIS) [excitation wavelength: 425 nm; inset: fluorescence intensity at 591 nm vs. Hg^{2+} to (**6**) molar ratio].

The molar composition ratio (MCR) of the monomers used for preparation of the film was adjusted to 99.75:0.25 [(**7**):(**6**), Scheme 2] in order to give a good fluorescence response. The observed colour was yellow, both when dry and when swelled by water or DMSO. Upon soaking in buffered DMSO/water aqueous solutions ($\text{pH} = 9.7$), the fluorescence of the films remained unaltered until successive additions of mercury caused fluorescence quenching. The time in-between measurements were 5 minutes, higher than the time needed to achieve the maximum quenching,

which represents a low response time. The system showed a detection limit of 400 ppt, much lower than the value obtained with (**6**) (see SD1, SD7, for intensity/mercury concentration relationships). Moreover, upon soaking the film in aqueous solutions at physiological pH (pH= 7.4), the film exhibited fluorescence quenching behaviour with increasing mercury concentration, achieving a detection limit of 10 ppt, well below the MCL (Fig. 2). Thus, the membrane exhibit a sensory behaviour toward Hg²⁺ with a dramatic increase in selectivity compared with the solution system previously described. This may tentatively be attributed to the isolation and immobilization of the sensing motifs within the membrane, thus inhibiting the inter-motif interactions, behaving as naked sensory subgroups. Regarding this point, we have previously demonstrated that the lowering of the molar content ratio of the sensing molecule in the copolymer structure conforming a membrane causes an increase in the sensing sensitivity [33,34]. The accuracy of the mercury concentration determination was verified by measuring the cation concentration of a sample prepared with tap water from our laboratory, thus emulating a real sample. The Hg²⁺ concentration added to the tap water was 1.01x10⁻⁸ M, and the concentrarion determined with the titration curve depicted in Fig. 2 was 1.55x10⁻⁸ M, in good accordance with the real concentration of the sample (the total concentrarion of Hg²⁺ in tap water was 0.34 ppb), whereas the concentration obtained using MQ water was 1.07x10⁻⁸ M. Moreover, the membrane was fully recovered upon treatment with MEEET, and could be reused to measure the mercury concentration of this sample with similar results.

The stoichiometry of the (**6**):Hg²⁺ complexes in the DMSO/water solution has been mathematically determined by studying the fluorescence quenching process, the intensity maxima variations versus the Hg²⁺ concentration, and their corresponding Job's plot (Fig. 3). The Job's plot has a maxima appearing at $X_{(6)} = 0.5$, clearly indicating the formation of complexes with a 1:1 stoichiometry. The stability constant, K , was significantly high, $100,000 \pm 10,000 \text{ M}^{-1}$, and was averaged with the results

obtained using two different models (see SD1, SD8).

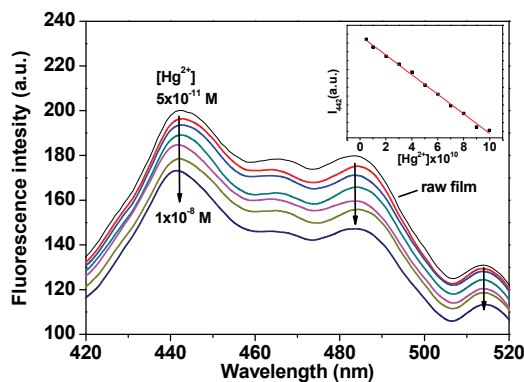


Figure 2. Selected titration curves of copolymer film with mercury cations in water at physiological pH (7.4) (excitation wavelength: 380 nm; inset: Hg^{2+} concentration vs. fluorescence intensity at 442 nm, F442).

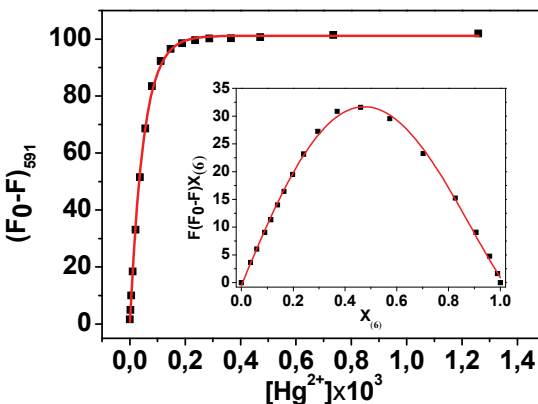


Figure 3. Plot of the observed fluorescence quenching ($F_0 - F$) at 591 nm vs. titration curve of (6) with mercury cations in DMSO/water (90/10, v/v) at $\text{pH} = 9.7$ (TRIS) (excitation wavelength: 425 nm; inset: the corresponding Job's plot. Solid line is the result of fitting and applying the corresponding equations, see SD1, SD8).

The mechanism of the fluorogenic response of (6) in solution, and within the membrane, to Hg^{2+} has been ascribed to the interaction of the *N,N*-dimethylamino-terminal group with the cation. The proposed sensing mechanism is supported by the following: a) the interaction is at equilibrium and can be reverted by adding a mercury chelating agent; b) after

fluorescence quenching of a DMSO/water solution of (**6**) by means of adding Hg(II), the fluorescence was recovered by acidifying the system (see SD1, SD9); c) ^1H NMR experiments support an interaction with the N-terminal of (**6**), as shown by the splitting of the signals of the methyl groups at approximately 3 ppm (see SD1, SD10); d) Uv/Vis experiments show a hypsochromic shift of the spectral band around 410 nm, up to 10 nm, upon interaction of (**6**) with Hg^{2+} . It could be attributed to the partial inhibition of the pumping of electrons from this group to the piperazine ring through the benzene ring.

To test the fluorogenic anion and cation sensing selectivity of (**6**), different anions and cations were added to a quartz fluorescence cell containing a DMSO/water solution of (**6**). This addition of Hg^{2+} resulted in a change in the gradual diminishing of the fluorescence intensity (F) of the 591 nm band. The fluorescent quenching was 8-fold when the relationship of (**6**) to Hg^{2+} was equimolar. In contrast, upon adding an equimolar amount of Cr(VI) and Fe(III), only a 1 and 0.5-fold fluorescence quenching was observed, respectively (Fig. 4).

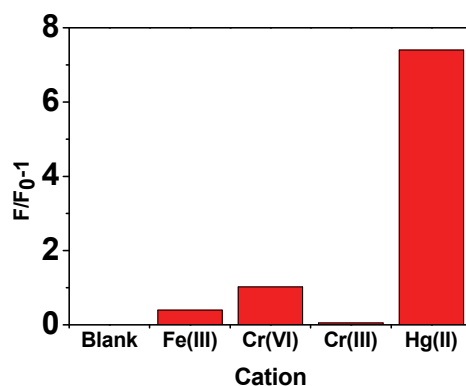


Figure 4. Fluorescence response profiles of (**6**) (5×10^{-5} M) upon addition of different cations in DMSO/water (90/10, v/v) at pH 9.7 (excitation wavelength: 335 nm; equimolar ratio of (**6**) to cation).

Interestingly, the fluorescence of the system remained unaltered upon adding Cr^{3+} . The quenching produced by Cr^{6+} and Fe^{3+} was not deeply pH

dependent, contrary to Hg^{2+} . The addition of other cations (Cu^{2+} , Co^{2+} , Zn^{2+} , Ba^{2+} , Ni^{2+} , Cd^{2+} , Pb^{2+} , Ag^+ , Sn^{2+} , Li^+ , Mg^{2+} , Ca^{2+} , Pd^{2+} , Mn^{2+}) and, a broad set of anions (sulfonate, chloroacetate, *p*-toluenesulfonate, oxalate, acetate, benzoate, cyanide, hydroxyl, nitrite, nitrate, carbonate, phosphate, fluoride, bromide, chloride), on the other hand, caused no effect.

3. Conclusion

In summary, the water-insoluble organic molecule (**6**), a methacrylamide monomer with fluorogenic chemosensing behaviour toward Hg^{2+} , was chemically incorporated into the lateral chain of a hydrophilic vinyl copolymer, providing a chemosensing dense membrane. The titration of organic solutions (DMSO/ H_2O , 90:10) of (**6**) could be followed by the fluorescent quenching of the initial solution of (**6**), with a detection limit of 110 ppb which is much lower than the MCL. The design of a hydrophilic membrane as a water swellable, transparent and solid material, permits the fluorogenic detection of Hg^{2+} in water at physiological pH, with a extremely low detection limit (10 ppt).⁴¹ Thus, through diffusion into the swelled polymer network, or membrane, the solvated cations reach the hydrophobic sensing organic motifs, giving rise to the recognition phenomenon.

Acknowledgment

We gratefully acknowledge financial support provided by the Spanish Ministerio de Educación y Ciencia – Feder (MAT2008-00946) and by the Junta de Castilla y León (BU001A10-2).

Supplementary data

Experimental procedures, intermediates, monomer characterization, further details of fluorescence data of (**6**) and of the membrane, mathematical models used to calculate the stability constants.

References

- 1 United States Environmental Protection Agency, National Primary Drinking Water Regulations MCL booklet, EPA 816-F-09-004 (2009). <http://water.epa.gov/drink/contaminants/upload/mcl.pdf>
- 2 J. Zhang, J. S. Kim, Small-molecule fluorescent chemosensors for Hg(II) ion, *Anal. Sci.* 25 (2009) 1271-1281.
- 3 A. Jana, J. S. Kim, H. S. Jung, P. K. Bharadwaj, A cryptand based chemodosimetric probe for naked-eye detection of mercury(II) ion in aqueous medium and its application in live cell imaging, *Chem. Commun.* (2009) 4417-4419.
- 4 W. Lin, X. Cao, Y. Ding, L. Yuan, Q. Yu, A reversible fluorescent Hg²⁺ chemosensor based on a receptor composed of a thiol atom and an alkene moiety for living cell fluorescence imaging, *Org. Biomol. Chem.* 8 (2010) 3618-3620.
- 5 J. Du, J. Fan, X. Peng, P. Sun, J. Wang, H. Li, S. Sun, A New fluorescent chemodosimeter for Hg²⁺: Selectivity, sensitivity, and resistance to Cys and GSH, *Org. Lett.* 12 (2010) 476-479.
- 6 C. Song, X. Zhang, C. Jia, P. Zhou, X. Quan, C. Duan, Highly sensitive and selective fluorescence sensor based on functional SBA-15 for detection of Hg²⁺ in aqueous media, *Talanta* 81 (2010) 643-649
- 7 W. Shi, S. Sun, X. Li, H. Ma, Imaging different interactions of mercury and silver with live cells by a designed fluorescence probe rhodamine B selenolactone, *Inorg. Chem.* 49 (2010) 1206-1210.
- 8 V. Bhalla, R. Tejpal, M. Kumar, Rhodamine appended terphenyl: A reversible "off-on" fluorescent chemosensor for mercury ions, *Sens. Actuators B: Chem.* 151 (2010) 180-185.
- 9 X. Zeng, L. Dong, C. Wu, L. Mu, S. F. Xue, Z. Tao, Highly sensitive chemosensor for Cu(II) and Hg(II) based on the tripodal rhodamine receptor, *Sens. Actuators B: Chem.* 141 (2009) 506-510.
- 10 A. Jana, J. S. Kim, H. S. Jung, P. K. Bharadwaj, A cryptand based chemodosimetric probe for naked-eye detection of mercury(II) ion in aqueous medium and its application in live cell imaging, *Chem. Commun.* (2009) 4417-4419.
- 11 M. Tian, H. Ihmels, Selective ratiometric detection of mercury(II) ions in water with an acridizinium-based fluorescent probe, *Chem. Commun.* (2009) 3175-3177.
- 12 S. Pandey, A. Azam, S. Pandey, H. M. Chawla, Novel dansyl-appended calix[4]arene frameworks: fluorescence properties and mercury sensing, *Org. Biomol. Chem.* 7 (2009) 269-279.
- 13 V. Bhalla, R. Tejpal, M. Kumar, A. Sethi, Terphenyl derivatives as "turn on" fluorescent sensors for mercury, *Inorg. Chem.* 48 (2009) 11677-11684.
- 14 R. K. Mahajan, R. Kaur, V. Bhalla, M. Kumara, T. Hattori, S. Miyano, Mercury(II) sensors based on calix[4]arene derivatives as receptor molecules, *Sens. Actuators B: Chem.* 130 (2008) 290-294.
- 15 H. Lu, L. Xiong, H. Liu, M. Yu, Z. Shen, F. Li, X. You, A highly selective and sensitive fluorescent turn-on sensor for Hg²⁺ and its application in live cell imaging, *Org. Biomol. Chem.* 7 (2009) 2554-2558.
- 16 Y. Zhou, C. Y. Zhu, X. S. Gao, X. Y. You, C. Yao, Hg²⁺ Selective ratiometric and "off-on" chemosensor based on the azadiene-pyrene derivative, *Org. Lett.* 12 (2010) 2566-2569.
- 17 Y. Xu, M. J. Panzer, X. Li, W. L. Youngs, Y. Pang, Host-guest assembly of squaraine dye in cucurbit[8]uril: its implication in fluorescent probe for mercury ions, *Chem. Commun.* 46 (2010) 4073-4075.
- 18 D. M. Nguyen, A. Frazer, L. Rodriguez, K. D. Belfield, fluorescence sensing of zinc and mercury ions with hydrophilic 1,2,3-triazolyl fluorene probes, *Chem. Mater.* 22 (2010) 3472-3481.
- 19 C. C. Cheng, Z. S. Chen, C. Y. Wu, C. C. Lin, C. R. Yang, Y. P. Yen, Azo dyes featuring a pyrene unit: New selective chromogenic and fluorogenic chemodosimeters for Hg(II), *Sens. Actuators B: Chem.* 142 (2009) 280-287.

- 20 F. Y. Wu, Y. Q. Zhao, Z. J. Ji, Y. M. Wu, A Highly Sensitive and selective fluorescent chemodosimeter for Hg²⁺ in neutral aqueous solution, *J. Fluoresc.* 17 (2007) 460-465.
- 21 M. H. Lee, S. W. Lee, S. H. Kim, C. Kang, J. S. Kim, Nanomolar Hg(II) detection using nile blue chemodosimeter in biological media, *Org. Lett.* 11 (2009) 2101-2104.
- 22 E. M. Nolan, S. J. Lippard, MS4, a seminaphthofluorescein-based chemosensor for the ratiometric detection of Hg(II), *J. Mater. Chem.* 15 (2005) 2778-2783.
- 23 Q. Zou, H. Tian, Chemodosimeters for mercury(II) and methylmercury(I) based on 2,1,3-benzothiadiazole, *Sens. Actuators B: Chem.* 149 (2010) 20-27.
- 24 M. G. Choi, Y. H. Kim, J. E. Namgoong, S. K. Chang, Hg²⁺-selective chromogenic and fluorogenic chemodosimeter based on thiocoumarins, *Chem. Commun.* (2009) 3560-3562.
- 25 W. Jiang, W. Wang, A selective and sensitive "turn-on" fluorescent chemodosimeter for Hg²⁺ in aqueous media viaHg²⁺ promoted facile desulfurization-lactonization reaction, *Chem. Commun.* (2009) 3913-3915.
- 26 D. N. Lee, G. J. Kim, H. J. Kim, A Fluorescent coumarinylalkyne probe for the selective detection of mercury(II) ion in water, *Tetrahedron Lett.* 50 (2009) 4766-4768.
- 27 (b) J. Xie, Y. Zheng, J. Y. Ying, Highly selective and ultrasensitive detection of Hg²⁺ based on fluorescence quenching of Au nanoclusters by Hg²⁺-Au⁺ interactions, *Chem. Commun.* 46 (2010) 961-963.
- 28 X. Su, J. Wang, K. Jiao, X. Yang, Colorimetric detection of mercury ion (Hg²⁺) based on DNA oligonucleotides and unmodified gold nanoparticles sensing system with a tunable detection range, *Biosens. Bioelectron.* 24 (2009) 3153-3158.
- 29 R. Yang, J. Jin, L. Long, Y. Wang, H. Wang, Reversible molecular switching of molecular beacon: controlling DNA hybridization kinetics and thermodynamics using mercury(II) ions, *Chem. Commun.* (2009) 322-324.
- 30 Y. Wang, Y. F. Li, J. Wang, Y. Sang, C. Z. Huang, End-to-end assembly of gold nanorods by means of oligonucleotide-mercury(II) molecular recognition, *Chem. Commun.* 46 (2010) 1332-1334.
- 31 M. Wan, Y. Zou, S. Tan, Y. Li, Two thieno[3,4b]pyrazine-containing copolymers: synthesis, characterization, and application in mercury ions detection, *Polym. Adv. Technol.* 21 (2010) 256-262.
- 32 B. Bao, L. Yuwen, X. Zhan, L. Wang, Water-soluble hyperbranched polyelectrolytes with high fluorescence quantum yield: Facile synthesis and selective chemosensor for Hg²⁺ and Cu²⁺ ions, *J. Polym. Sci. Part A: Polym. Chem.* 48 (2010) 3431-3439.
- 33 S. Vallejos, P. Estévez, F. C. García, F. Serna, J. L. de la Peña, J. M. García, Putting to work organic sensing molecules in aqueous media: fluorene derivative-containing polymers as sensory materials for the colorimetric sensing of cyanide in water, *Chem. Commun.* 46 (2010) 7951-7953.
- 34 S. Vallejos, H. El Kaoutit, P. Estévez, F. C. García, F. Serna, J. M. García, Working with water insoluble organic molecules in aqueous media: fluorene derivative-containing polymers as sensory materials for the colorimetric sensing of cyanide in water, *Polym. Chem.* 2 (2011) 1129-1138.
- 35 F. García, J. M. García, B. García-Acosta, R. Martínez-Máñez, F. Sancenón, J. Soto, Pyrylium-containing polymers as sensory materials for the colorimetric sensing of cyanide in water, *Chem. Commun.* (2005) 2790-2792.
- 36 B. García-Acosta, F. García, J. M. García, R. Martínez-Máñez, F. Sancenón, N. San-José, J. Soto, Chromogenic signaling of hydrogen carbonate anion with pyrylium-containing polymers, *Org. Lett.* 9 (2007) 2429-2432.
- 37 V. Calderón, F. Serna, F. García, J. L. de la Peña, J. M. García, Selective solid-liquid extraction of cations using solid-phase polyamides with crown ether moieties as cation host units, *J. Appl. Polym. Sci.* 106 (2007) 2875-2884.
- 38 N. San-José, A. Gómez-Valdemoro, F. C. García, V. Calderón, J. M. García, Novel aliphatic-aromatic poly(amide ureas): Synthesis, characterization and application to the elimination of environmentally toxic heavy metal ions, *React. Func. Polym.* 68 (2008) 1337-1345.

- 39 A. Gómez-Valdemoro, V. Calderón, N. San-José, F. C. García, J. L. de la Peña, J. M. García, The extraction of environmentally polluting cations from aqueous media with novel polyamides containing cation- and anion-selective host units, *J. Polym. Sci. Part A: Polym. Chem.* 47 (2009) 670-681.
- 40 A. Gómez-Valdemoro, N. San-José, F. C. García, J. L. de la Peña, F. Serna, J. M. García, Novel aromatic polyamides with main chain and pendant 1,2,4-triazole moieties and their application to the extraction/elimination of mercury cations from aqueous media, *Polym. Chem.* 1 (2010) 1291-1301.
- 41 P. D. Slid, H. Xu, E. M. Collins, M. S. Face-Collins, J. X. Zhao, Sensing mercury for biomedical and environmental monitoring, *Sensors* 9 (2009) 5446-5459.

SUPPLEMENTARY INFORMATION**A selective and highly sensitive fluorescent probe of Hg²⁺ in organic and aqueous media: the role of a polymer network in extending the sensing phenomena to water environments**

*Saúl Vallejos, Pedro Estévez, Saturnino Ibeas, Asunción Muñoz, Félix C. García, Felipe Serna, José M. García.**

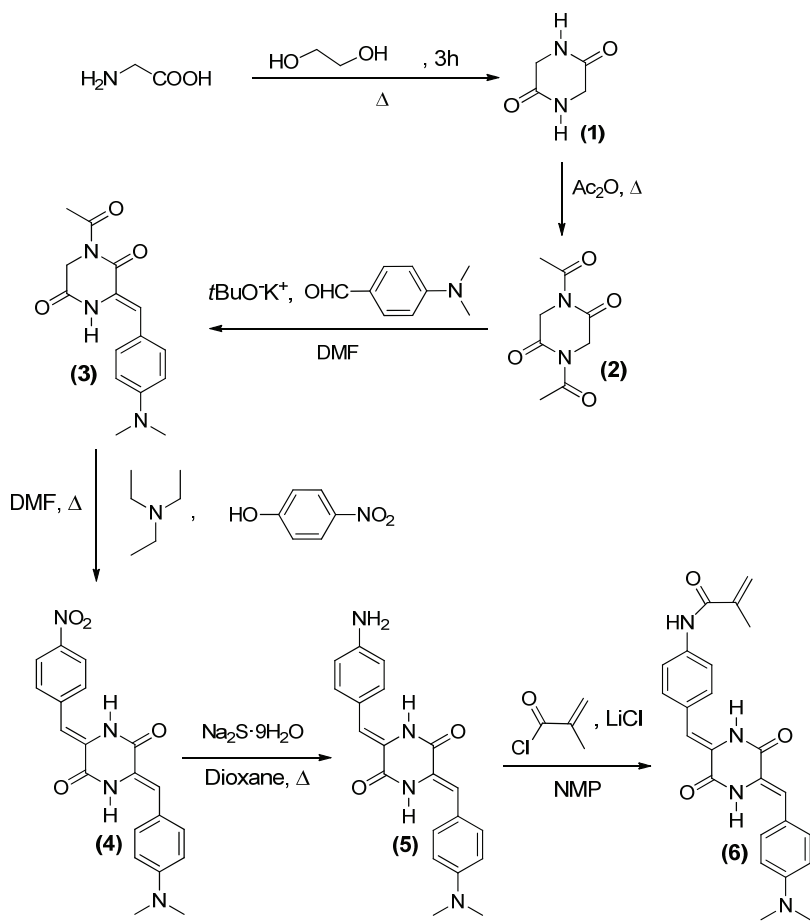
Departamento de Química, Facultad de Ciencias, Universidad de Burgos. Plaza de Misael Banuelos s/n, E-09001 Burgos, Spain

SD1. Materials

All the following materials and solvents are commercially available and were used as received, unless otherwise indicated: glycine (Sigma Aldrich, 99%), methacryloyl chloride (Fluka, 97%), ethylene glycol dimethacrylate (Aldrich, 98%), ethylene glycol (Fluka), acetic anhydride (Sigma Aldrich, puriss.), potassium-tertbutoxide (Sigma Aldrich, 99.99%), 4-(dimethylamino)-benzaldehyde (Sigma Aldrich, 98%), triethylamine (Fluka, 99.5%), lithium chloride (Sigma Aldrich, 99%), 4-nitrobenzaldehyde (Sigma Aldrich, 99%), sodium sulfide nonahydrate (Sigma Aldrich, 98%), dioxane (Probus, 99%), *N*-vinylpyrrolidone (Sigma Aldrich, 99%), *N*-methyl-2-pyrrolidone (Sigma Aldrich, 99.5%), diethyl ether (VWR, 99.99%), DMSO (Merck, 99%), acetone (Aldrich, 99%), ethanol (Aldrich, 99%), methanol (VWR, for HPLC), DMF (Aldrich, 99%). Azo-bis-isobutyronitrile (AIBN, Aldrich, 99%) was recrystallized twice from methanol.

SD2. Synthesis of intermediates and monomer

The overall monomer synthetic steps are shown in Scheme S1. The structure of the monomer and the intermediates were confirmed by ¹H and ¹³C NMR (nuclear magnetic resonance) and by FT-IR (infrared spectroscopy). The spectra showed that the products were high purity chemicals.



Scheme S1. Synthesis of the monomer *N*-(4-((1*Z*)-((*Z*)-5-(4-(dimethylamino)benzylidene)-3,6-dioxopiperazin-2-ylidene)methyl)phenyl) methacrylamide.

Synthesis of piperazine-2,5-dione (1)

One hundred grams of glycine were dissolved in 500 ml of ethylene glycol in a 1000 ml flask fitted with a mechanical stirrer. The mixture was stirred at 170°C for 3 hours and the solution was cooled at 5°C for 20 hours. The precipitate was filtered off and washed with 500 ml of methanol. Then, the solid was dissolved in boiling water, and the solution was cooled overnight. The white product was filtered off and washed with methanol. Yield: 70%.

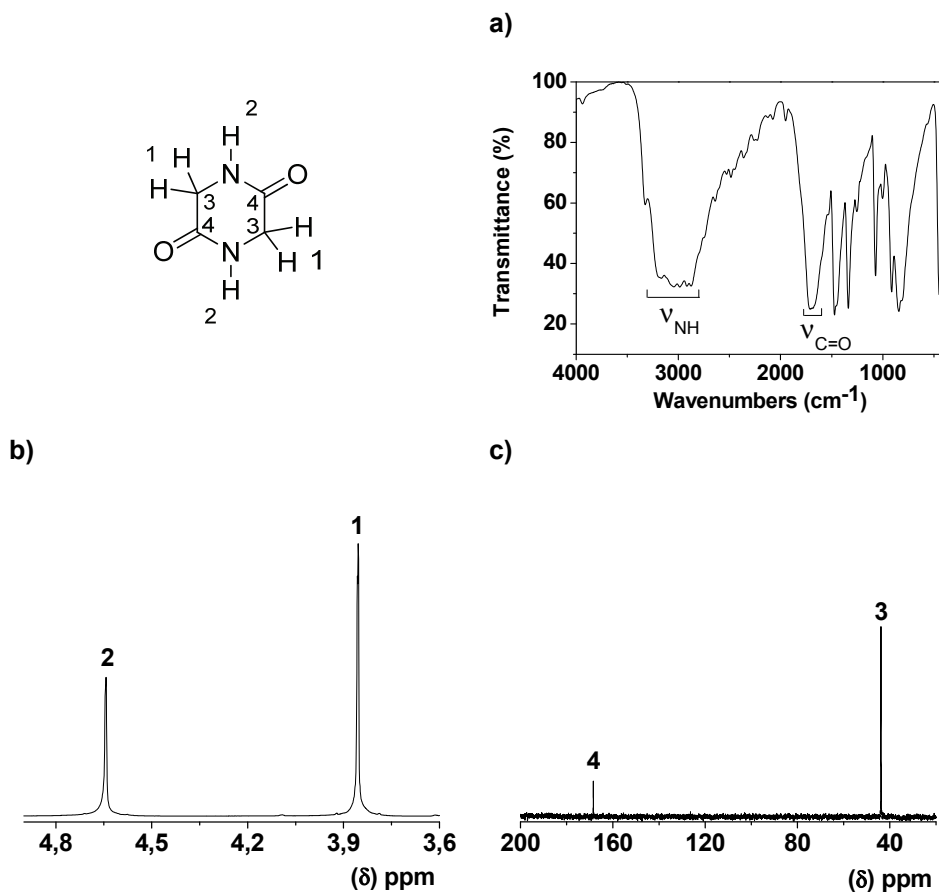


Figure S1. Characterization of (1) by (a) FTIR, (b) ¹H NMR, and (c) ¹³C NMR.

Synthesis of 1,4-diacetylpirazine-2,5-dione (2)

To a 250 ml flask equipped with a reflux condenser was added 0.164 mmol of the product (**1**) and 85 ml of acetic anhydride. The mixture was stirred at a reflux temperature for 7 hours. The solvent was then removed by distillation, and the product was washed with diethyl ether and filtered off. Yield: 90%.

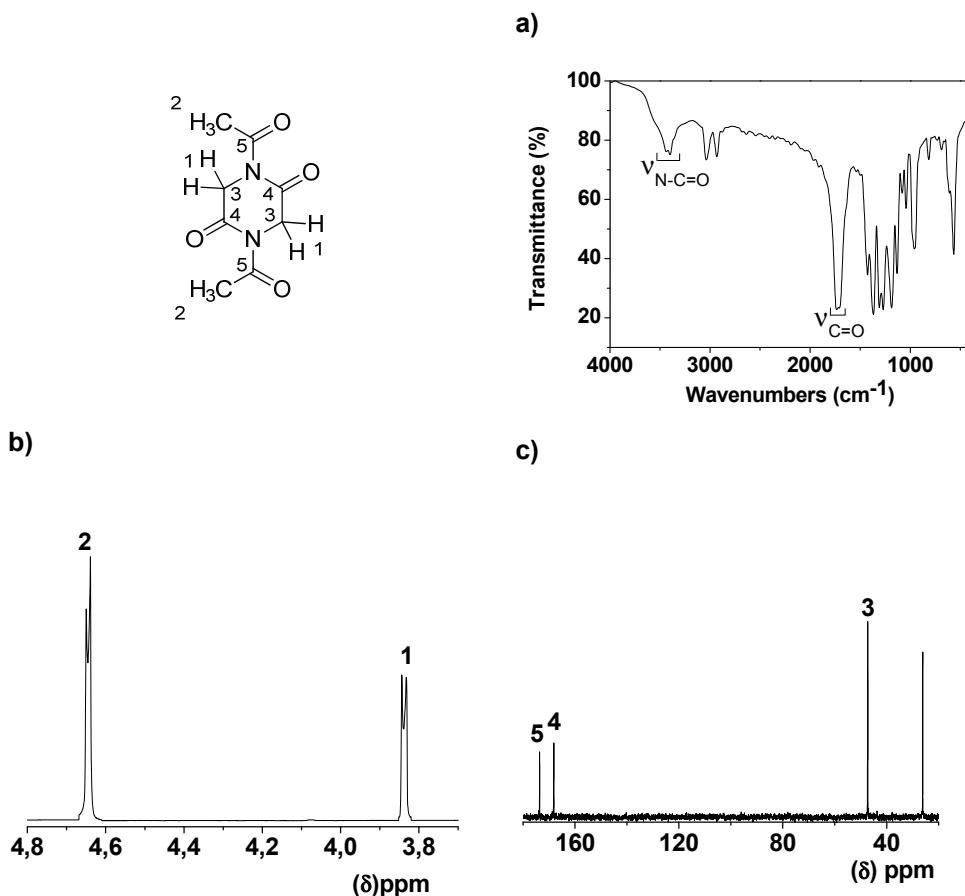


Figure S2. Characterization of (**2**) by (a) FTIR, (b) ^1H NMR, and (c) ^{13}C NMR.

Synthesis of (*Z*)-3-(4-(dimethylamino)benzylidene)-1-acetylpirperazine-2,5-dione (3)

In total, 25 mmol of the product (**2**) and 25 mmol of 4-(dimethylamino)benzaldehyde were dissolved in 70 ml of DMF in a flask equipped with a reflux condenser. Afterwards, 25 mmol of potassium *t*-butoxide was added and the mixture was stirred at room temperature for 12 hours. The product was precipitated in water and filtered off. Finally, the solid was washed with water and methanol. Yield: 50%.

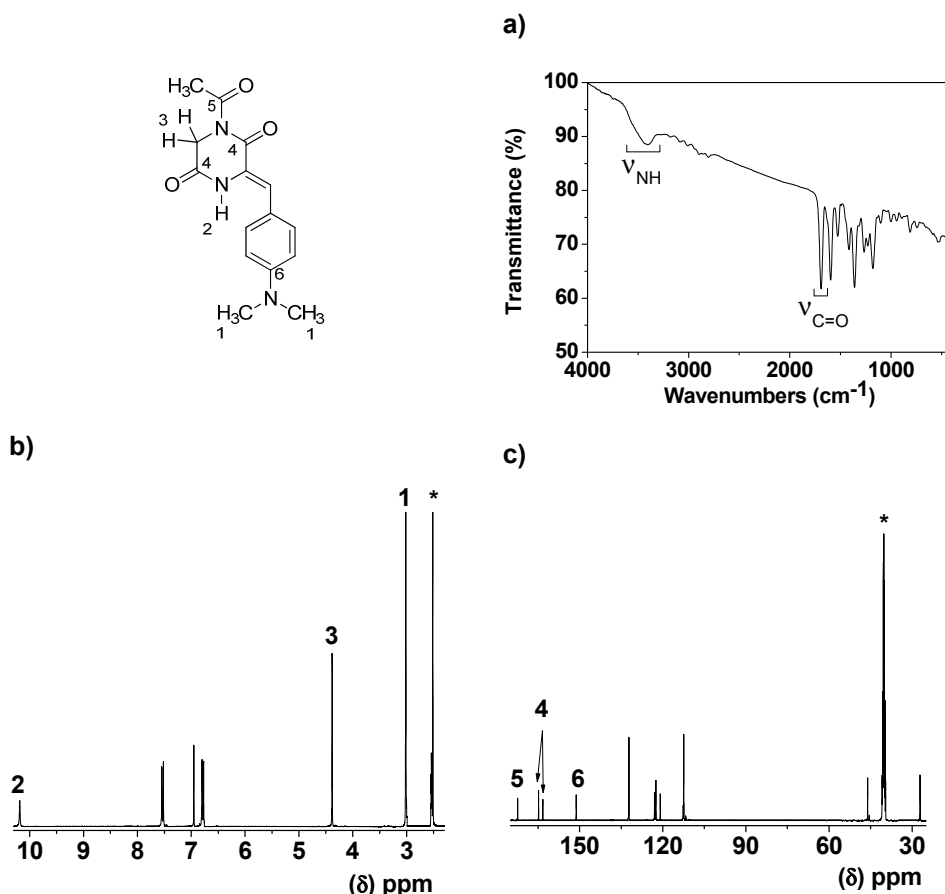


Figure S3. Characterization of (**3**) by (a) FTIR, (b) ^1H NMR, and (c) ^{13}C NMR (*=solvent signal).

Synthesis of (*3Z,6Z*)-3-(4-(dimethylamino)benzylidene)-6-(4-nitrobenzylidene) piperazine -2,5-dione (4)

In total, 9 mmol of the product (3) and 9 mmol of 4-nitrobenzaldehyde were dissolved in 135 ml of DMF in a flask equipped with a reflux condenser. Afterwards, 9 mmol of triethylamine was added and the mixture was stirred at 130°C for 12 hours. The solid was filtered off and washed with methanol. Finally, the solid was again washed with acetone at its reflux temperature in a flask equipped with a reflux condenser. Yield: 50%.

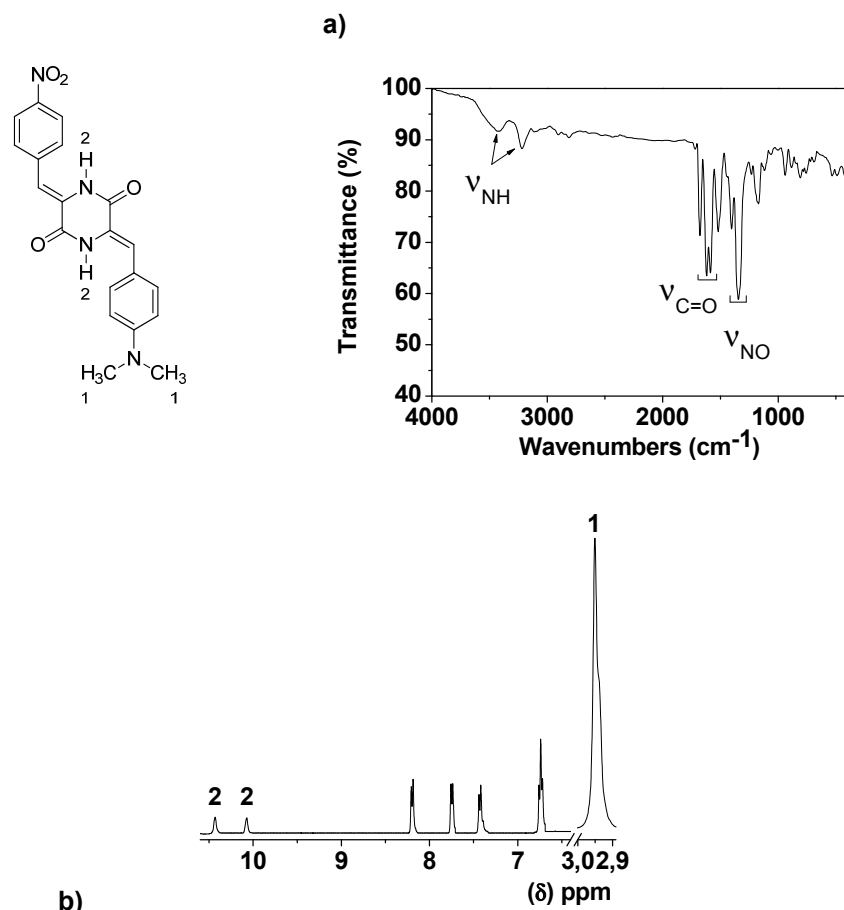


Figure S4. Characterization of (4) by (a) FTIR, and (b) ¹H NMR.

Synthesis of (*3Z,6Z*)-3-(4-(dimethylamino)benzylidene)-6-(4-aminobenzylidene) piperazine-2,5-dione (5)

In a 250 ml flask fitted with a reflux condenser, 4.75 mmol of compound (4) was dissolved in 100 ml of dioxane. After that, 14.25 mmol of sodium sulphide nonahydrate was added to the solution, and the mixture stirred at 80°C for 24 hours. The solution was filtered off and precipitated in 400 ml of water. The solid was filtered off and washed twice with methanol.

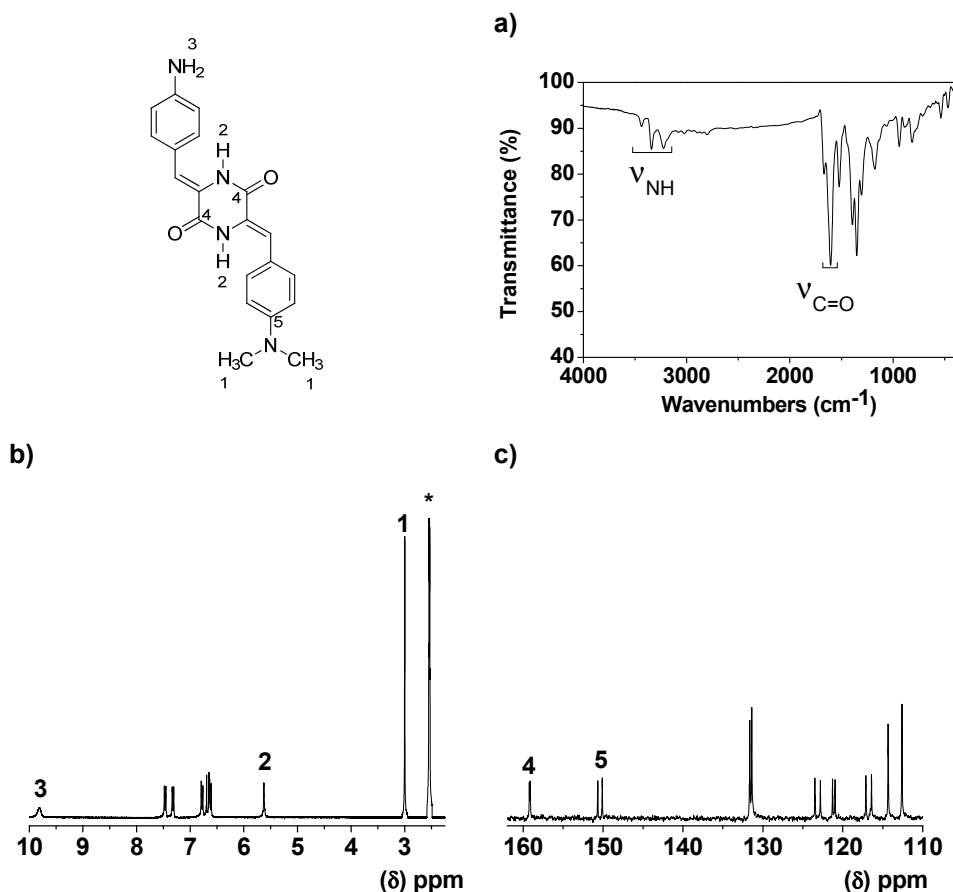


Figure S5. Characterization of (5) by (a) FTIR, (b) ^1H NMR, and (c) ^{13}C NMR (*=solvent signal).

Synthesis of *N*-(4-((1*Z*)-((*Z*)-5-(4-(dimethylamino)benzylidene)-3,6-dioxo-*p*-perazin-2-ylidene)methyl)phenyl)methacrylamide (6**)**

In a 25 ml flask fitted with a reflux condenser and under N₂ atmosphere, 3.45 mmol of compound (**5**) was dissolved in 7 ml of NMP. To this solution, 4.49 mmol of methacryloyl chloride and 400 mg of lithium chloride were added, and the mixture stirred at room temperature for 4 hours. The orange solid was filtered off and the product was purified from the crude residue using a Soxhlet apparatus with acetone. Yield: 80%.

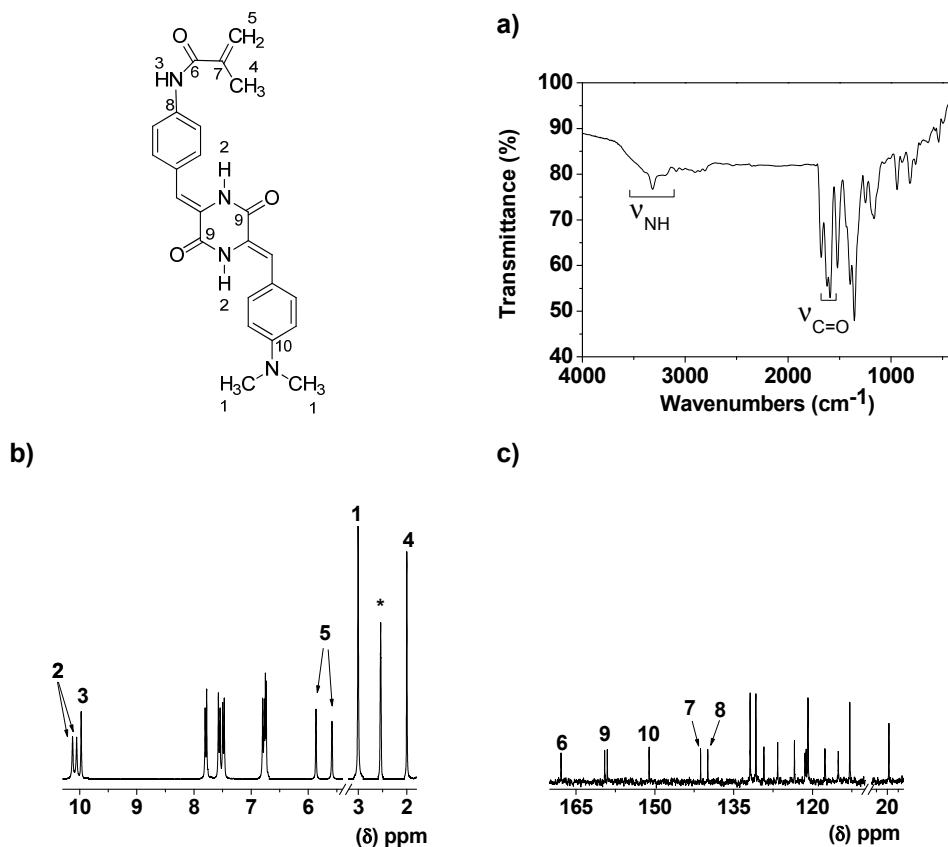
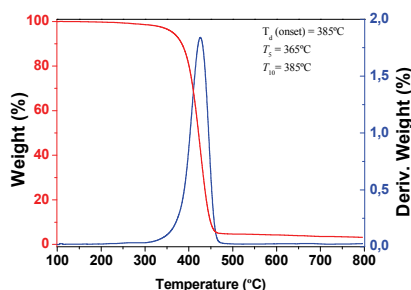


Figure S6. Characterization of (**6**) by (a) FTIR, (b) ¹H NMR, and (c) ¹³C NMR (*=solvent signal).

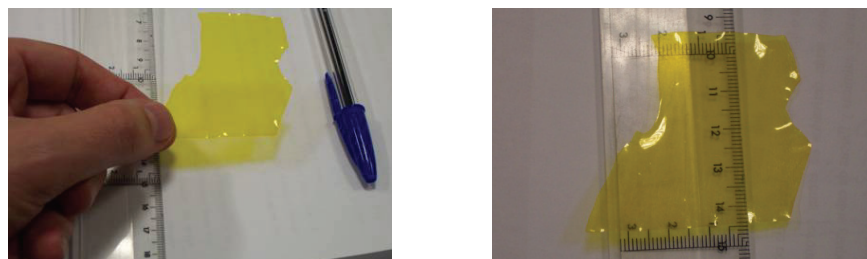
SD3. Membrane preparation and characterization

The membrane was prepared by radical polymerization of a mixture of *N*-vinylpyrrolidone (**7**) with (**6**), with a molar ratio of 99.75:0.25, respectively. Ethylene glycol dimethacrylate was used as the cross-linking agent (7%, mol percentage regarding the overall co-monomer molar content) and AIBN (1 wt. %) as a thermal radical initiator. The reactions were carried out in silanized glass molds, 100 µm thick, in an oxygen-free atmosphere at 65 °C for 5 h.

Thermal resistance is a key parameter of the suitability of organic materials for technological applications. The thermal resistance of the membrane was evaluated by thermogravimetry (TGA), and the decomposition temperatures that resulted in 5% and 10% weight loss, T_5 and T_{10} , 365 and 385°C, indicate that the material has good thermal stability.



The sensory material is a tractable film, as shown in the digital pictures.

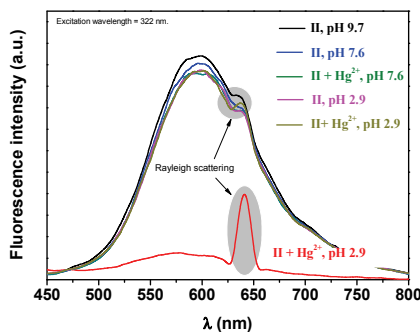


SD4. Measurements and instrumentation

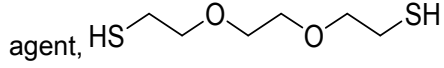
The ^1H and ^{13}C NMR spectra were recorded using a Varian Inova 400 spectrometer operating at 399.92 and 100.57 MHz, respectively, using DMSO- d_6 as the solvent. Infrared spectra (FT-IR) were recorded using a Nicolet Impact spectrometer. Millipore-Q water was used to prepare solutions, unless otherwise indicated. The concentration of Hg^{2+} in tap water was determined by means of inductively coupled plasma mass spectrometry (ICP, Agilent 7500 i) by the Analytical Service of the Scientific Park at the University of Burgos. Ultraviolet/Visible spectra (UV/Vis) were recorded using a Varian Cary3-Bio UV-Vis spectrophotometer. The fluorescence spectra were recorded using a Varian Cary Eclipse fluorometer. The time in-between measurements in the titration curves of Hg^{2+} were 5 minutes. Thermogravimetric analysis (TGA) of a 5 mg sample was performed under a nitrogen atmosphere on a TA Instrument Q50 TGA analyzer at a scan rate of 10 °C/min.

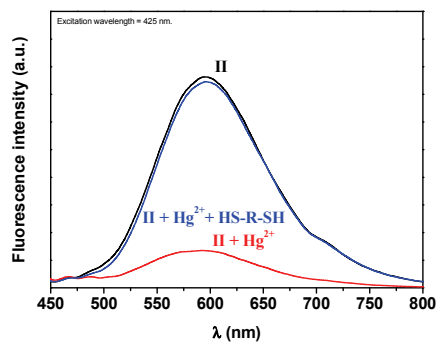
SD5. Fluorescence behaviour of DMSO/ H_2O solutions of (**6**) at different pH and upon adding Hg^{2+} [equimolar concentration of (**6**): Hg^{2+}]

The addition of Hg^{2+} to DMSO/ H_2O buffered (TRIS) solutions of (**6**) gave rise to the fluorescence quenching at basic pH, but not at physiological or acidic conditions.

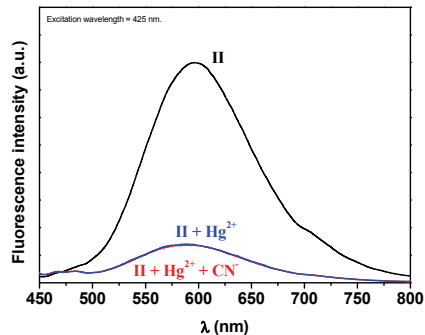


SD6. ON-OFF-ON fluorescence behaviour of the system

The addition of Hg^{2+} to DMSO/H₂O buffered (TRIS, pH 9.7) solutions of (**6**) gave rise to fluorescence quenching. The addition of a mercury chelating agent, HS-SH, gave rise to fluorescence recovery, thus behaving the system as an ON-OFF-ON fluorescence switch.

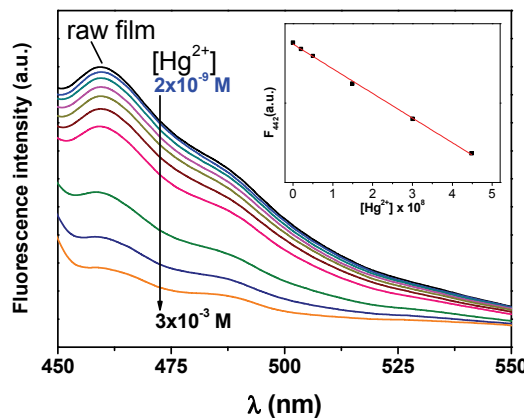


On the other hand, the addition of CN^- to the fluorescence quenched Hg^{2+} to DMSO/H₂O buffered (TRIS, pH 9.7) solutions of (**6**): Hg^{2+} caused no effect, and the fluorescence was not recovered.



SD7. Titration of mercury cation in buffered DMSO/water solution (90/10), pH = 9.7, with the membrane

Selected titration curves of copolymer film with mercury cations in buffered DMSO/water solution (90/10, v/v) of (**6**) (pH = 9.7) (inset: Hg^{2+} concentration vs. fluorescence intensity at 442 nm, F_{442}). Excitation wavelength = 425 nm.



SD8. Analysing the host:guest interactions: stability constants

The strength of the interaction of (6) with Hg^{2+} in buffered DMSO/water (90/10) solution ($\text{pH} = 9.7$) in terms of the stability constant of the host-guest complexes, has been analyzed by fluorescence spectroscopy using two methods:

a) Method I

Once the stoichiometry 1:1 of the (6): Hg^{2+} complexes is known, by means of the Job's plot,



Or



It is worth estimating the dimensionless stability constant given by

$$K_1 = \frac{[LM]}{[L][M]} \quad (2)$$

Where $[L]$, $[M]$, and $[ML]$ is the equilibrium concentration of (6), of Hg^{2+} and of the complex (6): Hg^{2+} , respectively. From the mass balance and fluorescence, the following equations can be deduced,

$$C_L = [L] + [ML] \quad (3)$$

$$C_M = [M] + [ML] \quad (4)$$

$$F = f_L [L] + f_{ML} [ML] \quad (5)$$

where C_L , C_M , F , f_L y f_{ML} are the total concentration of (6), of Hg^{2+} , the fluorescence intensity, and the fluorescence proportional factors of (6), of Hg^{2+} , respectively.

Solving the equilibrium concentration of (6), $[L]$, from Eq. (3) and substituting it in Eq. (5), we obtain the following expression

$$I_F = f_L C_L + [ML](f_{ML} - f_L) \quad (6)$$

where $f_L C_L$ is the fluorescence intensity of (6) upon absence of complex. Thus, given $\Delta F = F - f_L C_L$ and $\Delta f = f_{ML} - f_L$, Eq (6) is transformed into the expression

$$[ML] = \frac{\Delta F}{\Delta f} \quad (7)$$

From Eq. (1), and considering Eq. (3) to (7), Ea. (8) can be deduced

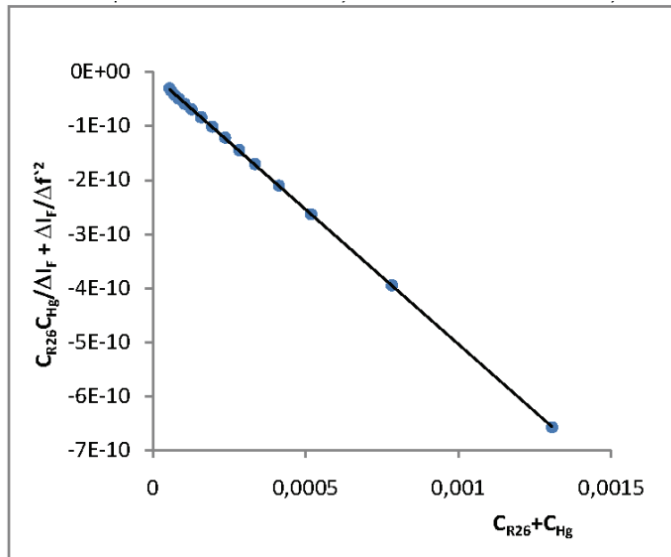
$$K_1 = \frac{[II:\text{Hg}^{2+}]}{[II][\text{Hg}^{2+}]} = \frac{\frac{\Delta F}{\Delta f}}{(C_L - \frac{\Delta F}{\Delta f})(C_M - \frac{\Delta F}{\Delta f})} \quad (8)$$

From Eq. (6) is deduced

$$\frac{C_L C_M}{\Delta I_F} + \frac{\Delta I_F}{\Delta f^2} = \frac{1}{K_1 \Delta f} + \frac{1}{\Delta f} (C_L + C_M) \quad (9)$$

Thus, the experimental data can be fitted using an interactive process starting with a tentative value of Δf , representing the left term of Eq. (9) vs. the sum of the concentration of (6) and Hg^{2+} , $[L] + [M]$. The value of Δf is calculated from the slope of the straight line obtained, and the process repeated until the tentative and the calculated Δf values are equal enough. The fitting of the

experimental data with Eq. (8) gave the following results: $K_1 = 110000 \pm 10000$, $\Delta f = -2000000 \pm 4000$, $R = 0.9999$.



a) Method II

An alternative way of obtaining the stability constant is reproducing the experimental data with an analytic expression, through a nonlinear least-squares algorithm, to obtain the constant K_1 .

The fluorescence intensity (F_0) of the initial solution of (6) in buffered DMSO/water (90/10), pH = 9.7, is proportional to the concentration of (6) (Eq. (10)),

$$F_o = f_L C_L \quad (10)$$

while the fluorescence intensity when there is no free (6), and all the initial (6) is bound to mercury cations [(6):Hg²⁺], F_{final} , is

$$F_{\text{final}} = f_{ML} C_L \quad (11)$$

From Eq. (3) y (4) the Eq. (12) can be deduced,

$$F = F_o + (f_{ML} - f_M)[ML] \quad (12)$$

Combining Eq. (10) and (11), Eq. (13) is obtained,

$$F_{final} - F_o = (f_{ML} - f_M)C_L \quad (13)$$

and Eq. (14) is obtained from Eq. (12) and (13).

$$F = F_o + \frac{F_{final} - F_o}{C_L} [ML] \quad (14)$$

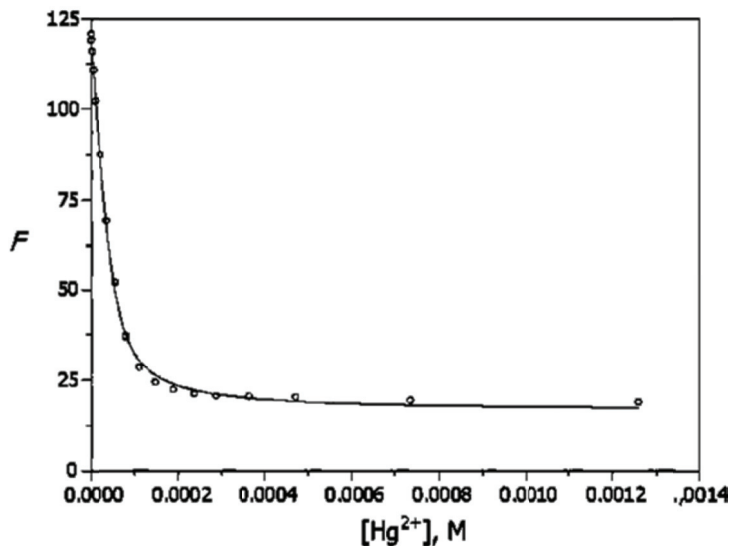
If we consider now the definition of the stability constant, Eq. (2), the following expression is obtained

$$K_I = \frac{[II:Hg^{2+}]}{[II][Hg^{2+}]} = \frac{[ML]}{(C_L - [ML])(C_M - [ML])} \quad (15)$$

Solving from this equation the concentration of (6):Hg²⁺, [ML], Eq. (14) can be transformed into

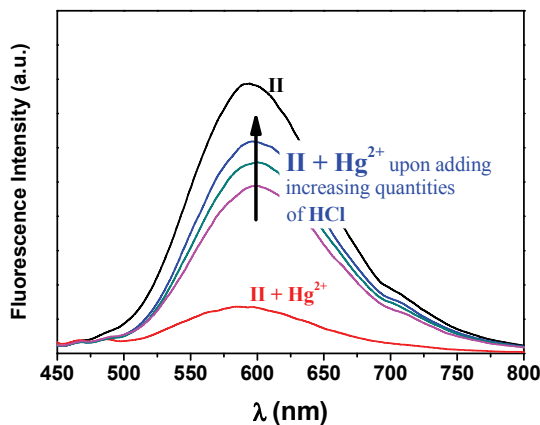
$$F = F_o + \frac{F_{final} - F_o}{C_L} \left[C_L + C_M + \frac{1}{K_I} - \sqrt{\left(C_L + C_M + \frac{1}{K_I} \right)^2 - 4C_L C_M} \right] \quad (16)$$

Thus, the experimental data can be fitted using a nonlinear least-squared algorithm, from an initial guess values of K_1 , F_o y F_{final} , giving rise to the following results: $K_1 = 90000 \pm 6000$, $F_o = 120.1 \pm 0.6$, $F_{final} = 16.3 \pm 0.7$



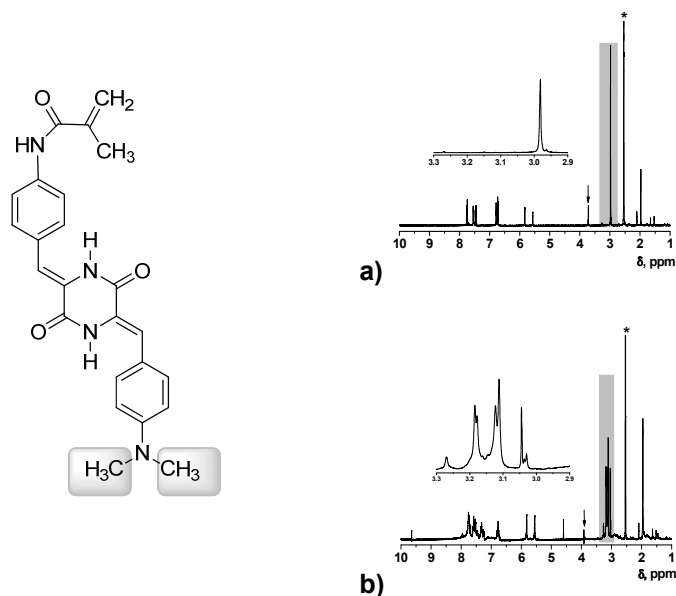
SD9. Recovery of the fluorescence of equimolar (6):Hg²⁺ DMSO/water (90/10) solution by means of acidifying the system.

The fluorescent quenching of a (6) DMSO/water (90/10) solution could be reverted by means of acidifying the initially buffered (TRIS, pH 9.7) solution, probably because of the protonation of the terminal dimethylamino group of (6), which lead to the decomplexation of Hg²⁺.



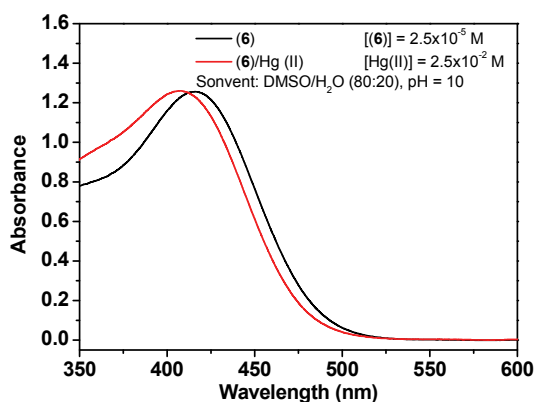
SD10. NMR data supporting the reversible association of Hg²⁺ with the dimethylamino-terminal group of (6)

¹H NMR spectra of (6) in DMSO/water (90/10, v/v) without (a) and with (b) Hg²⁺ (*=solvent signal –deuterated DMSO-; the water signal was eliminated upon irradiation –arrow–). The singlet corresponding to the protons of the dimethylamino group observed close to 3 ppm was shifted to a lower field upon interaction with the cation, and the sharp signal were transformed into a complex multiplet.



SD11. UV/Vis data of the reversible association of Hg²⁺ with (6)

Uv/Vis spectra of (6) in DMSO/water (90/20, v/v) without and with Hg²⁺.



An organic/inorganic hybrid membrane as a solid “turn-on” fluorescent chemosensor for coenzyme a (CoA), cysteine (Cys), and glutathione (GSH) in aqueous media

**An organic/inorganic hybrid membrane as a solid “turn-on”
fluorescent chemosensor for coenzyme a (CoA), cysteine (Cys), and
glutathione (GSH) in aqueous media**

*Saúl Vallejos, Pedro Estévez, Saturnino Ibeas, Félix C. García, Felipe
Serna and José M. García **

Departamento de Química, Facultad de Ciencias, Universidad de Burgos, Plaza de Misael Bañuelos s/n, E-09001 Burgos, Spain; E-Mails: svallejos@ubu.es (S.V.); paeb14@gmail.com (P.E.); sibeas@ubu.es (S.I.); fegarcia@ubu.es (F.C.G.); fserna@ubu.es (F.S.)

Abstract

The preparation of a fluorogenic sensory material for the detection of biomolecules is described. Strategic functionalization and copolymerization of a water insoluble organic sensory molecule with hydrophilic comonomers yielded a crosslinked, water-swellable, easy-to-manipulate solid system for water “dip-in” fluorogenic coenzyme A, cysteine, and glutathione detection by means of host-guest interactions. The sensory material was a membrane with gel-like behaviour, which exhibits a change in fluorescence behaviour upon swelling with a water solution of the target molecules. The membrane follows a “turn-on” pattern, which permits the titration of the abovementioned biomolecules. In this way, the water insoluble sensing motif can be exploited in aqueous media. The sensory motif within the membrane is a chemically anchored piperazinedione-derivative with a weakly bound Hg(II). The response is caused by the displacement of the cation from the membrane due to a stronger complexation with the biomolecules, thus releasing the fluorescent sensory moieties within the membrane.

Keywords: sensory materials; chemosensor; fluorogenic sensor; biomolecules; sensing biomolecules

Sensors 2012, 12, 2969-2982

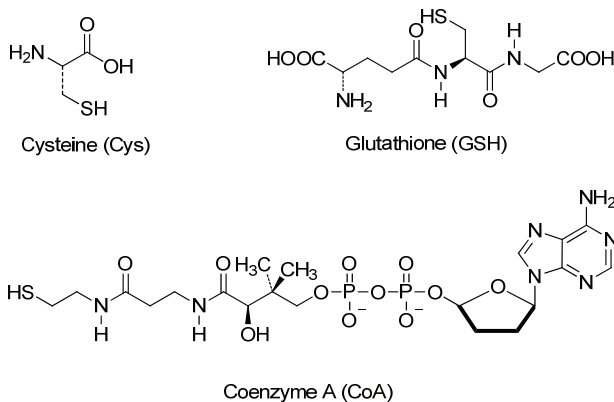
1. Introduction

The development of sensing molecules for the detection of chemicals is a topic of current interest.¹⁻⁶ The recognition of target molecules based on the variation of a macroscopic property of a sensing molecule associated with the specific interactions of the target with the receptor motifs of the sensor can be used to prepare sensory solutions for the easy, cheap and rapid quantification of chemicals by means of a widely used analytical technique (e.g., UV/Vis and/or spectrofluorometry). Moreover, if the receptor and the transducing motifs are chemically bound to a polymer network structure, then the organic material can be described as a solid system, which can potentially be used as a solid kit for the “dip-in” detection of analytes³.

For medical, biomedical and environmental reasons, biological molecules are among the most important target analytes.⁷ Biomolecules containing a thiol group, such as coenzyme A (CoA), L-cysteine (Cys), and glutathione (GSH), play important roles in biological processes including acyl group carrier capability or oxidation/reduction facility (*i.e.*, intramolecular reduction-oxidation metabolic cycles), which occur in hundreds of biochemical reactions.⁸⁻¹² The determination of the biomolecule concentration has been undertaken with various methodologies. One of the most interesting is the sensing methodology based on the host-guest supramolecular approach. The supramolecular approach has recently been applied to the determination of Cys,¹³⁻²⁷ CoA,⁸⁻¹⁰ and GSH to a lesser extent.²⁸

Herein, we describe a sensory organic/inorganic hybrid membrane for the fluorogenic detection of three important biomolecules: CoA, Cys, and GSH (the chemical structures are shown in Scheme 1). The membrane was a dense film consisting of a hydrophilic acrylic network that contained a small amount of piperazinedione-derivative/Hg(II) moieties as the sensory motif toward the biomolecules mentioned above. The piperazinedione-derivative was chemically anchored to the copolymer backbone. The water-swelled membrane responded to the presence of the targets in an aqueous environment at physiological pH

with an increase in the fluorescence intensity (*i.e.*, a fluorescence “turn-on” pattern), which permitted the titration of the biomolecules.



Scheme 1. Structure of Cys, GSH, and CoA.

2. Experimental Section

2.1. Materials

The following commercially available materials and solvents were used as received, unless otherwise indicated: mercury(II) acetate (Sigma Aldrich, 98%), glycine (Sigma Aldrich, 99%), methacryloyl chloride (Fluka, 97%), ethylene glycol dimethacrylate (Aldrich, 98%), ethylene glycol (Fluka), acetic anhydride (Sigma Aldrich, puriss.), potassium *t*-butoxide (Sigma Aldrich, 99.99%), 4-(dimethylamino)benzaldehyde (Sigma Aldrich, 98%), triethylamine (Fluka, 99.5%), lithium chloride (Sigma Aldrich, 99%), 4-nitrobenzaldehyde (Sigma Aldrich, 99%), sodium sulphide nonahydrate (Sigma Aldrich, 98%), dioxane (Probus, 99%), *N*-vinylpyrrolidone (Sigma Aldrich, 99%), *N*-methyl-2-pyrrolidone (Sigma Aldrich, 99.5%), diethyl ether (VWR, 99.99%), DMSO (Merck, 99%), acetone (Aldrich, 99%), ethanol (Aldrich, 99%), methanol (VWR, for HPLC), DMF (Aldrich, 99%), coenzyme A trolithium salt (Calbiochem, 99.9%), L-glutathione reduced (Alfa Aesar, 97%), and L-cysteine hydrochloride monohydrate (VWR). Azo-bis-isobutyronitrile (AIBN, Fluka, 98%) was recrystallised twice from methanol.

2.2. Measurements

¹H and ¹³C-NMR spectra were recorded in deuterated dimethyl sulphoxide (DMSO-d₆) as the solvent using a Varian Inova 400 spectrometer operating at 399.92 and 100.57 MHz, respectively. Infrared spectra (FTIR) were recorded with a Nicolet Impact spectrometer or with a JASCO FT/IT-4100 fitted with a PIKE TECH “Miracle” ATR. Thermogravimetric analysis (TGA) data were recorded using 5 mg of sample under a nitrogen or oxygen atmosphere on a TA Instrument Q50 TGA analyzer at a scan rate of 10 °C min⁻¹. UV-Vis spectra were recorded using a Varian Cary3-Bio UV-Vis spectrophotometer. The fluorescence spectra were recorded using a Varian Cary Eclipse fluorometer. Millipore-Q water was used to prepare the solutions. To determine the tensile properties of the membranes, strips (5 mm in width, 30 mm in length, and 30–45 µm thick) were cut from the polymer films and measured using a Hounsfield H10KM Universal Testing Dynamometer at 20 °C. Mechanical clamps held the sample, and an extension rate of 5 mm min⁻¹ was applied using a gauge length of 10 mm. At least six samples were tested for each polymer, and the data were averaged.

2.3. Intermediates and Monomer Synthesis

The overall synthetic steps for the monomer are shown in Scheme 2.

Synthesis of 1,4-diacetyl. Glycine (a total of 100 g, 1.33 mol) was dissolved in ethylene glycol (500 mL) in a 1,000 mL flask fitted with a mechanical stirrer. The mixture was stirred at 170 °C for 3 h, and the solution was cooled at 5 °C for 20 h. The precipitate, piperazine-2,5-dione, was collected by filtration and washed with methanol (500 mL). Then, the solid was dissolved in boiling water, and the solution was cooled overnight. The white product was filtered off and washed with methanol. Yield: 30%. M.p.: 330 °C. ¹H-NMR δ_H (399.9 MHz, DMSO-d₆, Me₄Si): 4.64 (2H, s, NH); 3.85 (4H, s, CH₂). ¹³C-NMR, δ_C (100.6 MHz, DMSO-d₆, Me₄Si): 168.46, 43.83. EI-LRMS m/z: 114 (M⁺•, 100),

86 (8), 72 (2), 58 (5), 56 (7). FTIR [wavenumbers (cm^{-1})]: $\nu_{\text{N-H}}$: broadband (3,250, 2,750); $\nu_{\text{C=O}}$: 1,696.

Piperazine-2,5-dione (18.7 g, 0.164 mmol) and acetic anhydride (85 mL) were added to a 250 mL flask equipped with a reflux condenser. The mixture was stirred at reflux for 7 h. The solvent was removed by distillation. The product **1** was washed with diethyl ether and collected by filtration. Yield: 90%. M.p.: 96 °C. $^1\text{H-NMR}$ δ_{H} (399.9 MHz, DMSO-d₆, Me₄Si): 4.64 (6H, s, CH₃); 3.84 (4H, s, CH₂). $^{13}\text{C-NMR}$, δ_{C} (100.6 MHz, DMSO-d₆, Me₄Si): 173.61, 168.17, 43.32, 26.12. EI-LRMS m/z: 198 (M⁺, 30), 156 (41), 114 (47), 86 (3), 71 (30), 43 (12). FTIR [wavenumbers (cm^{-1})]: $\nu_{\text{N-C=O}}$: broadband (3,452, 3,365); $\nu_{\text{C=O}}$: 1,718.

Synthesis of (3Z,6Z)-3-(4-(dimethylamino)benzylidene)-6-(4-nitrobenzylidene)piperazine-2,5-dione (2). A flask equipped with a reflux condenser was charged with 1,4-diacetyl piperazine-2,5-dione (**1**, 4.94 g, 25 mmol) and 4-(dimethylamino)benzaldehyde (3.72 g, 25 mmol) which were dissolved in DMF (70 mL). Potassium *t*-butoxide (2.8 g, 25 mmol) was added, and the mixture was stirred at room temperature for 12 h. The product, (Z)-3-(4-(dimethylamino)benzylidene)-1-acetyl piperazine-2,5-dione, was precipitated in water and collected by filtration. Finally, the solid was washed with water and methanol. Yield: 50%. M.p.: 210 °C. $^1\text{H-NMR}$ δ_{H} (399.9 MHz, DMSO-d₆, Me₄Si): 10.19 (1H, s, NH); 7.53 (2H, d, *J* 8.7, ArH); 6.95 (1H, s, CH); 6.79 (2H, d, *J* 9.0, ArH); 4.39 (2H, s, CH₂); 3.02 (6H, s, CH₃); 2.51 (3H, s, CH₃). $^{13}\text{C-NMR}$, δ_{C} (100.6 MHz, DMSO-d₆, Me₄Si): 172.31, 165.00, 163.19, 151.28, 132.07, 122.99, 122.45, 120.86, 112.39, 46.08, 26.96. EI-LRMS m/z: 287 (M⁺, 90), 245 (100), 160 (52), 115 (3), 78 (11), 62 (14). FTIR [wavenumbers (cm^{-1})]: $\nu_{\text{N-H}}$: broadband (3,661, 3,310); $\nu_{\text{C=O}}$: 1,696, 1,597 and 1,521.

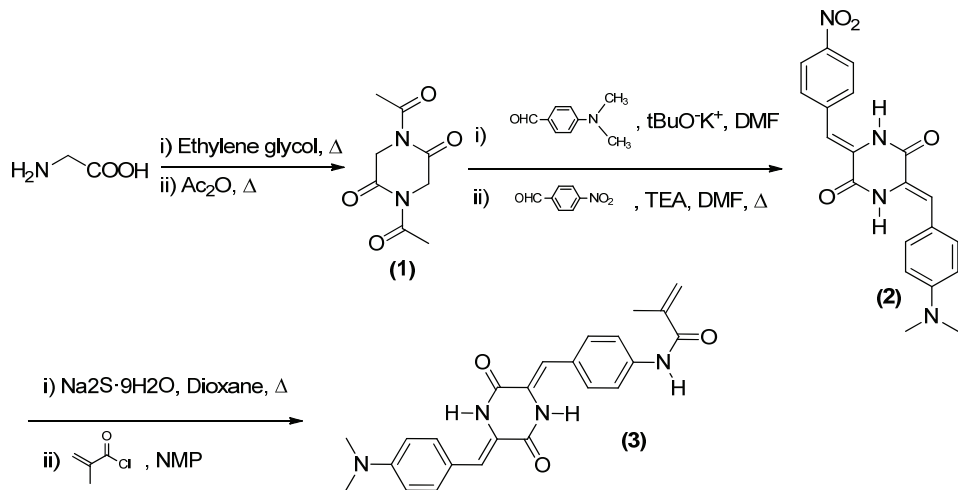
(Z)-3-(4-(dimethylamino)benzylidene)-1-acetyl piperazine-2,5-dione (2.6 g, 9 mmol) and 4-nitro-benzaldehyde (1.36 g, 9 mmol) were dissolved in DMF (135 mL) in a flask equipped with a reflux condenser. Triethylamine (0.9 g, 9

mmol) was added, and the mixture was stirred at 130 °C for 12 h. A solid was collected by filtration and washed with methanol. Finally, the solid was washed with acetone at its reflux temperature in a flask equipped with a reflux condenser. Yield: 50%. M.p.: not observed (the compound was amorphous; however, an exothermic crystallisation peak was observed at 353 °C). ¹H-NMR δ_H (399.9 MHz, DMSO-d₆, Me₄Si): 10.43 (1H, s, NH); 10.09 (1H, s, NH); 8.20 (2H, d, J 6.42, ArH); 7.75 (2H, d, J 7.35, ArH); 7.43 (2H, d, J 6.42, ArH); 6.74 (4H, t, J 5.93, ArH); 2.95 (6H, s, CH₃). EI-LRMS m/z: 378 (M⁺, 100), 332 (3), 287 (1), 215 (1), 159 (37), 117 (5), 89 (4), 77 (1). FTIR [wavenumbers (cm⁻¹)]: ν_{N-H}: broadband (3,628, 3,331), ν_{N-H}: 3,211; ν_{C=O}: 1,674 and 1,626; ν_{NO}: 1,578 (asymmetric) and 1,339 (symmetric).

Synthesis of N-(4-((1Z)-((Z)-5-(4-(dimethylamino)benzylidene)-3,6-dioxopiperazine-2-ylidene)methyl) phenyl)methacrylamide (3). In a 250 mL flask fitted with a reflux condenser, compound **2** (1.8 g, 4.75 mmol) was dissolved in dioxane (100 mL). Sodium sulphide nonahydrate (3.43 g, 14.25 mmol) was added to the solution, and the mixture was stirred at 80 °C for 24 h. The solution was filtered, and water (400 mL) was added. The resultant precipitate, (3Z,6Z)-3-(4-(dimethylamino) benzylidene)-6-(4-aminobenzylidene) piperazine-2,5-dione, was filtered off and washed twice with methanol. Yield: 72%. M.p.: 307 °C. ¹H-NMR δ_H (399.9 MHz, DMSO-d₆, Me₄Si): 9.81 (2H, s, NH₂); 7.47 (2H, d, J 9.03, ArH); 7.32 (2H, d, J 9.03, ArH); 6.78 (2H, d, J 10.08, ArH); 6.69-6.61 (4H, m, ArH); 5.63 (2H, s, NH); 3.00 (6H, s, CH₃). ¹³C-NMR, δ_C (100.6 MHz, DMSO-d₆, Me₄Si): 159.26, 159.12, 150.66, 150.08, 131.66, 131.43, 123.50, 122.82, 121.29, 120.99, 117.10, 116.41, 114.36, 112.60. EI-LRMS m/z: 348 (M⁺, 100), 334 (2), 306 (1), 218 (1), 161 (17), 159 (22), 133 (24), 131 (10). FTIR [wavenumbers (cm⁻¹)]: ν_{N-H}: 3,432, 3,340 and 3,229; ν_{C=O}: 1,672 and 1,598.

In a 25 mL flask fitted with a reflux condenser and under N₂ atmosphere, (3Z,6Z)-3-(4-(dimethylamino)benzylidene)-6-(4-aminobenzylidene) piperazine-2,5-dione (1.2 g, 3.45 mmol) was dissolved in NMP (7 mL). Methacryloyl chloride (0.47 g, 4.5 mmol) was added to the solution, and the

mixture was stirred at room temperature for 4 h. An orange solid (monomer **3**) was collected by filtration and purified from the crude residue by washing with hot acetone using a Soxhlet apparatus. Yield: 80%. M.p.: 330 °C. $^1\text{H-NMR}$ δ_{H} (399.9 MHz, DMSO-d₆, Me₄Si): 10.08 (2H, s, NH); 9.97 (1H, s, NH); 7.79 (2H, d, *J* 8.7, ArH); 7.56 (2H, d, *J* 8.7, ArH); 7.48 (2H, d, *J* 8.7, ArH); 6.77 (4H, m, ArH); 5.86 (1H, s, CH₂); 5.58 (1H, s, CH₂); 3.01 (6H, s, CH₃); 1.99 (3H, s, CH₃). $^{13}\text{C-NMR}$, δ_{C} (100.6 MHz, DMSO-d₆, Me₄Si): 167.77, 159.55, 159.02, 151.09, 141.26, 139.89, 131.89, 130.74, 129.22, 126.63, 123.43, 121.44, 121.14, 120.91, 117.64, 115.12, 112.91, 19.80. EI-LRMS *m/z*: 416 ($\text{M}^{+}\bullet$, 100), 376 (16), 347 (4), 159 (62), 131 (9), 117 (5), 77 (3). FTIR [wavenumbers (cm⁻¹)]: $\nu_{\text{N-H}}$: broadband (3,709, 3,100); $\nu_{\text{C=O}}$: 1,676, 1,624 and 1,595.



Scheme 2. Synthesis of the monomer *N*-(4-((1*Z*)-((*Z*)-5-(4-(dimethylamino)benzylidene)-3,6-dioxopiperazin-2-ylidene)methylphenyl)methacrylamide.

2.4. Membrane Preparation

Membrane **M1** was prepared by the radical polymerisation of a mixture of *N*-vinylpyrrolidone and (3) with a molar ratio of 99.75:0.25. Ethylene glycol dimethacrylate was used as the cross-linking agent (7% mol percentage regarding the overall comonomer molar content), and AIBN (1 wt%) was used as a thermal radical initiator. Membrane **M2** was prepared following the same procedure described for the preparation of **M1**; however, 0.25% molar content of mercury(II) acetate was added (the same concentration of (3)), which resulted in a hybrid organic-inorganic material. The thermal polymerisation was performed in 100 µm thick silanised glass moulds in an oxygen-free atmosphere at 65 °C for 5 h. The structure and the physical appearance are depicted in Figure 1.

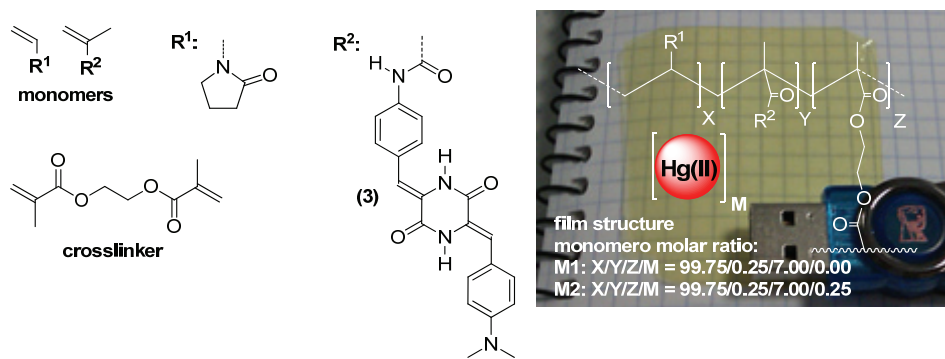


Figure 1. Chemical structures of the monomers and the copolymer. The copolymer is shown over a digital picture of the sensory film.

3. Results and Discussion

3.1. Material Characterisation

Mechanical and thermal resistance are key parameters to determine the suitability of an organic material for technological applications. From a mechanical point of view, **M1**, a dense membrane, showed good performance. The Young's modulus was 490 MPa and the elongation at break was 160% at room temperature with a relative humidity of 65%. The hydrophilic membranes were dried at 103 °C for 20 minutes, which resulted in an increase in the

Young's modulus to 1.1 GPa and a decrease in the elongation at break to 12%. The membrane recovered the initial values upon exposure to the ambient atmosphere. The hydrophilic character of the material resulted in a water uptake of 150% upon immersing the membrane in pure water. A comparison between the FTIR spectra of dry **M1** and **M1** stored in air overnight (under the abovementioned conditions) was performed. The band corresponding to the amide I of the hydrophilic *N*-vinylpyrrolidone moieties exhibited a band shift toward lower energy of 18 cm^{-1} (1,668 to $1,648\text{ cm}^{-1}$), while the shoulder at $1,727\text{ cm}^{-1}$ that corresponds to the hydrophobic ester residue of the crosslinker remained unchanged. These observations probably indicate that hydrophilic and hydrophobic microdomains were present in the water-swelled membrane after immersing the membrane in aqueous media for sensing purposes.

The polymerisation of the comonomers without and with low molar content mercury (II) acetate (0.25%) (**M1** and **M2**, respectively) resulted in materials with fairly different FTIR spectra (Figure 2). Comparing the spectra of dry samples of **M1** and **M2** resulted in the observation of an intense band that developed at $1,722\text{ cm}^{-1}$ for **M2**, with a concomitant shift of the amide I band to higher energies, from 1,668 to $1,675\text{ cm}^{-1}$, probably due to the acetate group.

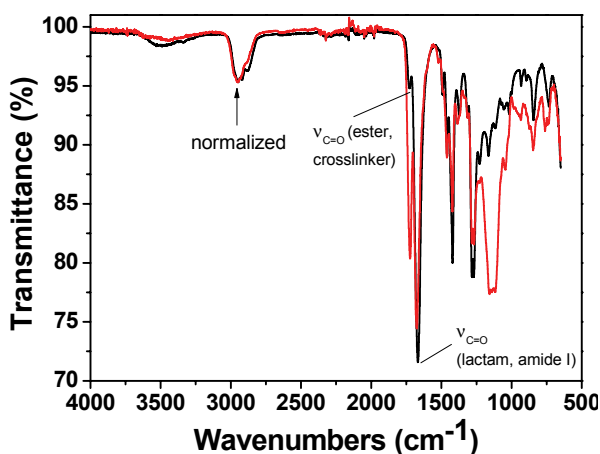


Figure 2. FTIR spectra of the dried membranes **M1** (black line) and **M2** (red line).

The thermal resistance of the membranes was evaluated using TGA. The decomposition temperatures that resulted in 5% and 10% weight loss under a nitrogen atmosphere (T_5 and T_{10} , respectively) were approximately 360 and 385 °C, which indicates the material had reasonably good thermal stability. **M1** and **M2** had a first weight loss at 200°C, which was attributed to the non-reticulated chain ends.²⁹ The TGA curves of the membranes are shown in Figure 3. The residue remaining after reaching 800°C was negligible for **M1** and approximately 8% for **M2**, which confirms the influence of the mercury content in the thermal behaviour. The mercury was first oxidised to HgO, which indicates the hybrid nature of the membrane. The immersion of membrane **M2** in water resulted in an insignificant loss of bound Hg(II), as determined by comparing the amount of residue that remained at 800°C under a nitrogen atmosphere for two samples of **M2** that were soaked in pure water for 3 and 24 h and subsequently dried. Both samples resulted in a residue of 8%. Nevertheless, the analysis of the role of the Hg(II) by TGA is cumbersome, because of the behaviour of the mercury salts upon heating. Initially, mercury oxides formed, and then, metallic mercury was formed with concomitant sublimation.³⁰ Changing the atmosphere from nitrogen to air yielded the complete loss of mass at 800 °C for **M1** and **M2**, which gave rise to a zero char yield.

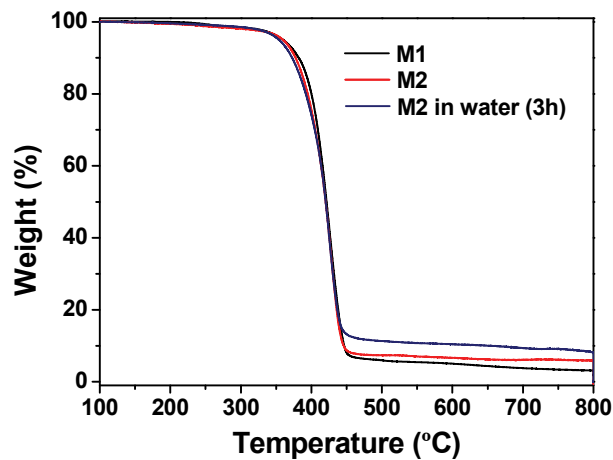


Figure 3. TGA curves of membranes **M1** and **M2**. The degradation pattern of **M2** after a cycle of soaking in pure water for 3 h with subsequent drying at rt is also included.

3.2. The Membranes as Sensory Materials

The membrane **M1** behaves as a sensory material for the fluorogenic detection of Hg(II) in aqueous media. Upon the addition of Hg(II), the fluorescence of the membrane at 548 nm was quenched, which demonstrated that the membrane had “turn-off” fluorescence behaviour in the presence of the cation. This observation was attributed to the interaction of the Hg(II) with the N-terminus of the sensory motif (**3**) within the membrane at a 1:1 stoichiometry.³¹ The integral preparation of a membrane containing equal molar quantities of (**3**) and Hg(II) (*i.e.*, **M2**), led to a material with a partially quenched fluorescence. Moreover, fluorescence recovery was observed for **M2** upon adding different biomolecules, *e.g.*, CoA, Cys and GSH (see Figure 4). The stronger interaction of these biomolecules with Hg(II) led to a fluorescent chemosensor with fluorescence “turn-on” behaviour, based on the displacement approach.^{1,2} A titration curve of the biomolecules was obtained by plotting the fluorescence maxima *versus* the biomolecule concentration. An illustrative example is shown for CoA in Figure 4. The limit of detection (LOD) was approximately 2×10^{-10} M.

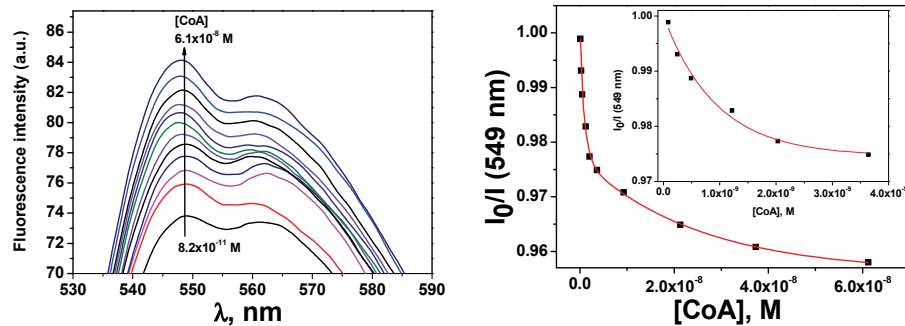


Figure 4. Selected fluorescence spectra (left) and titration curve (right) of **M2** upon adding increasing quantities of CoA in water at physiological pH (pH = 7.4, TRIS) at an excitation wavelength of 400 nm. The inset for the figure on the right is an expansion of the lower concentrations of the titration curve.

3.3. Copolymer Network/Hg(II) Interaction

Prior to the preparation of the membrane **M2**, the interaction of the monomer containing the sensing motif (**3**) with Hg(II) was studied in solution. The stoichiometry of the (**3**):Hg(II) complexes in a DMSO/water solution (90:10) was

mathematically determined by analysing the fluorescence quenching process, the intensity maxima variations versus the Hg(II) concentration, and the corresponding Job's plots. The Job's plot showed a maximum that appeared at a mole fraction for (3) ($\chi_{(3)}$) of 0.5, which clearly indicated the formation of complexes with a 1:1 stoichiometry, as shown in Table 1 and Figure 5.

Table 1. Stability constants corresponding to the complex (3):X [X = Hg(II), CoA, Cys and GSH], and CoA:Hg(II).

Complex	Complex stoichiometry	$K_1 \text{ (M}^{-1}\text{)}$	$K_2 \text{ (M}^{-1}\text{)}$
(3):Hg(II)	1:1	$110,000 \pm 10,000$	—
(3):CoA	1:1	$22,000 \pm 2,000$	—
(3):Cys	1:1	$20,000 \pm 8,000$	—
(3):GSH	1:1	$20,000 \pm 7,000$	—
CoA:Hg(II)	1:2	$8,400 \pm 900$	$6,000 \pm 3,000$

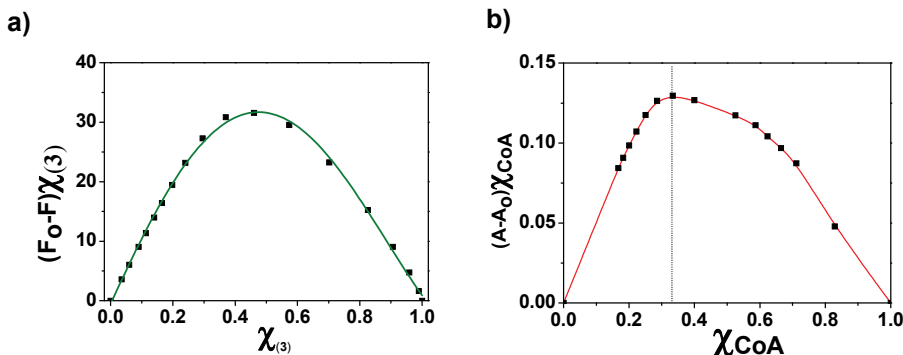


Figure 5. Job's plots corresponding to the following interaction studies: (a) (3) with Hg(II), obtained from fluorescence spectroscopy (591 nm) data corresponding to the titration curve of (3) with mercury cations in DMSO/water (90/10, v/v) at pH = 9.7 (TRIS); and (b) CoA with Hg(II), from UV/Vis spectroscopy (300 nm) data corresponding to the titration of CoA with mercury cations in DMSO/water (90/10, v/v) at pH = 7.4 (TRIS).

The strength of the interaction of (3) with Hg(II) in buffered DMSO/water (90/10) solution (pH = 7.4) in terms of the stability constant, K_1 , corresponding to the host-guest complexes, was analysed by fluorescence spectroscopy. The determination of the 1:1 stoichiometry of the (3):Hg(II) complexes allowed the following equilibrium to be stated:



which can also be written as the following:

$$K_1 = \frac{[ML]}{[L][M]} \quad (2)$$

where $[L]$, $[M]$, and $[ML]$ is the equilibrium concentration of (3), Hg(II), and the (3):Hg(II) complex, respectively. From the mass balance and fluorescence data, the following equations can be deduced:

$$C_L = [L] + [ML] \quad (3)$$

$$C_M = [M] + [ML] \quad (4)$$

$$I_F = f_L [L] + f_{ML} [ML] \quad (5)$$

where C_L , C_M , I_F , f_L , and f_{ML} are the total concentration of (3), total concentration of Hg(II), fluorescence intensity, and the fluorescence proportional factors of (3) and (3):Hg(II), respectively.

By solving the equilibrium concentration of (3) ($[L]$) from Equation (3) and substituting the value in Equation (5), the following expression was obtained:

$$I_F = f_L C_L + [ML] (f_{ML} - f_L) \quad (6)$$

where $f_L C_L$ is the fluorescence intensity of (3) upon absence of complex. Thus, given that $\Delta F = I_F - f_L C_L$ and $\Delta f = f_{ML} - f_L$, Equation (6) can be transformed into the following expression:

$$[ML] = \frac{\Delta F}{\Delta f} \quad (7)$$

From Equation (1), and considering Equation (3) to (7), Equation (8) can be deduced:

$$K_1 = \frac{[ML]}{[L][M]} = \frac{\frac{\Delta F}{\Delta f}}{\left(C_L - \frac{\Delta F}{\Delta f}\right)\left(C_M - \frac{\Delta F}{\Delta f}\right)} \quad (8)$$

Equation (9) can be deduced from Equation (8), which is the following:

$$\frac{C_L C_M}{\Delta I_F} + \frac{\Delta I_F}{\Delta f^2} = \frac{1}{K_1 \Delta f} + \frac{1}{\Delta f} (C_L + C_M) \quad (9)$$

Thus, the experimental data could be fitted using an iterative process starting with a tentative value of Δf , representing the left term of Equation (9) versus the sum of the concentration of (3) and Hg(II), $C_L + C_M$. The value of Δf was calculated from the slope of the straight line obtained, and the process was repeated until the tentative and the calculated Δf values were approximately equal. The fitting of the experimental data with Equation (8) yielded the following results: $K_1 = 110,000 \text{ M}^{-1} \pm 10,000$, $\Delta f = -2,000,000 \pm 4,000$, and $R^2 = 0.9999$.

3.4. Interaction of CoA, Cys, and GSH with Hg(II)

The interaction of CoA with Hg(II) was studied by UV/Vis spectroscopy, because CoA is not fluorescent. As depicted in the Job's plot shown in Figure 5, the results indicate that the complex stoichiometry was 1:2 [CoA:Hg(II)]. The stoichiometry could be clearly observed in the UV/Vis spectra, where two equilibria could be estimated (Figure 6). The equilibrium constants were determined using the following equations, where $[M]$, $[L]$, $[ML]$ and, $[M_2L]$ are the equilibrium concentration of Hg(II), CoA, the Hg(II):CoA complex, and Hg(II)₂:CoA complex, respectively.



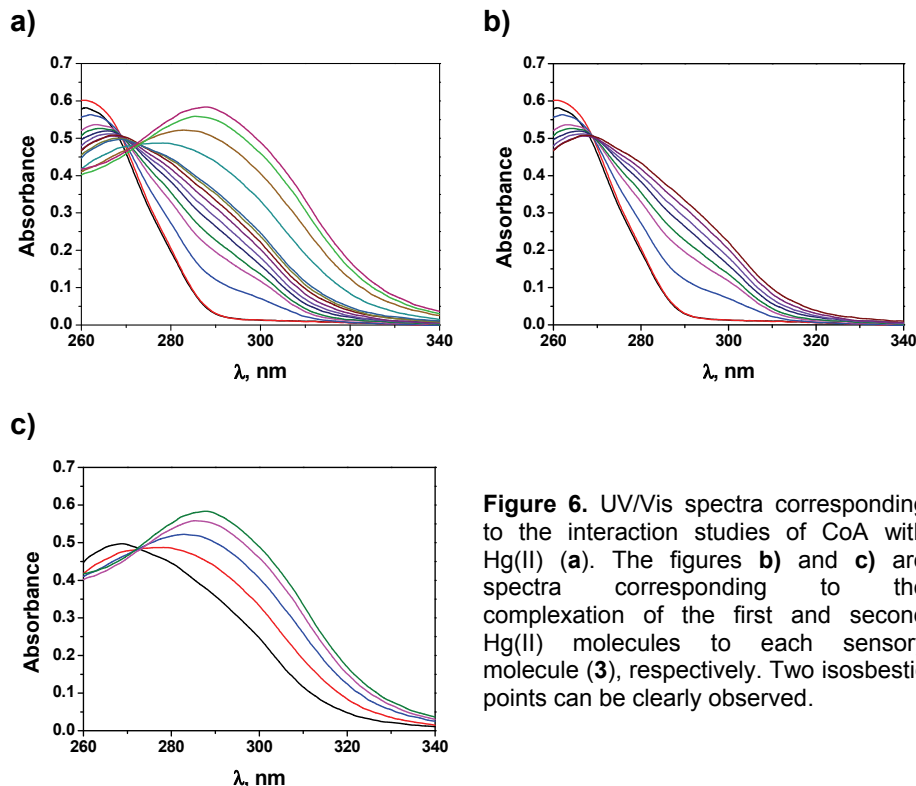


Figure 6. UV/Vis spectra corresponding to the interaction studies of CoA with Hg(II) (a). The figures b) and c) are spectra corresponding to the complexation of the first and second Hg(II) molecules to each sensory molecule (**3**), respectively. Two isosbestic points can be clearly observed.

The absorbance was measured at a wavelength where L did not absorb, and an absorbance balance was accounted for to obtain the following expression:

$$A = \varepsilon_L[L] + \varepsilon_{ML}[ML] + \varepsilon_{M_2L}[M_2L] \quad (12)$$

and considering Equations (10) and (11):

$$[ML] = K_1[M][L] \quad (13)$$

$$[M_2L] = K_1K_2[M]^2[L] \quad (14)$$

Then, combining Equations (12) to (14), Equation (15) was deduced:

$$A = \varepsilon_L[L] + \varepsilon_{ML}K_1[M][L] + \varepsilon_{M_2L}K_1K_2[M]^2[L] \quad (15)$$

Using a mass balance, where C_L is the total concentration of the ligand (CoA) and C_M is the total metal concentration (Hg), results in the following equations:

$$C_L = [L] + [ML] + [M_2L] \quad (16)$$

$$C_M = [M] + [ML] + 2[M_2L] \quad (17)$$

Combining Equations (15)–(17) results in Equation (18):

$$A = \frac{C_L}{1 + K_1[M] + K_1K_2[M]^2} (\varepsilon_L + \varepsilon_{ML}K_1[M] + \varepsilon_{M_2L}K_1K_2[M]^2) \quad (18)$$

The values of ε_L and ε_{M_2L} were estimated as $\varepsilon_L = A_0/C_L$ and $\varepsilon_{M_2L} = A_{\text{final}}/C_L$. The concentration of [M] was not known; however, C_M was used as an approximation. With these considerations, a nonlinear least-squares regression was conducted on the data, as depicted in Table 1 ($\varepsilon_{ML} = 16,000 \pm 700$).

Unfortunately, the study of the interaction of Cys, and GSH with Hg(II) could not be performed because the overlap of the absorbance of the biological molecules and the mercury salt in the UV/Vis spectra. Nevertheless, a similar behaviour as the CoA:Hg(II) complex would be expected.

3.5. Interaction of the Membrane **M2** with CoA, Cys and GSH

Following the previously described procedure for the study of the interaction of **3** with Hg(II), the complex stoichiometry of **(3):X** (X = CoA, Cys and GSH) and the stability constants were determined following the fluorescence quenching of **3** in solution. The results are shown in Table 1 and have an equimolar complex stoichiometry in all cases. These results show that the biomolecules also interact with the sensory motif **3** within the membrane causing the fluorescence quenching; however, the interaction was significantly weaker than the interaction between Hg(II) and **3**. The following complex behaviour of the sensory material **M2** was observed upon adding the biomolecules to the measurement media: (a) an initial recovery of the fluorescence was observed until a maxima was reached, which corresponded to the displacement of the Hg(II) bound to the sensory motif in **M2** due to the interaction of Hg(II) and the biomolecule; and (b) the quenching of the fluorescence upon increasing the concentration of the biomolecule passed the maxima due to the interaction between the sensory moieties of **M2** and the biomolecule. This phenomenon was also observed studying the system in solution, as depicted in Figure 7. As

pointed out in Section 3.1 and shown in Figure 4, a titration curve to measure CoA, Cys and GSH at nanomolar concentrations could be drawn. The upper concentration detection limit depended on the amount of the sensing monomer within the membrane bound to Hg(II), which could easily be modified by varying the monomer feed ratio in the membrane synthesis. The ratio of the monomer to Hg(II) was preferably 1:1, so the concentration window that the sensory material could measure was tunable. The interaction strengths between the three target molecules and the sensory motif were similar, as was estimated in solution by the stability constants (see Table 1), which permits a similar sensing behaviour of the hybrid film **M2** in relation to the fluorescence “turn-on” pattern for detecting the biomolecules.

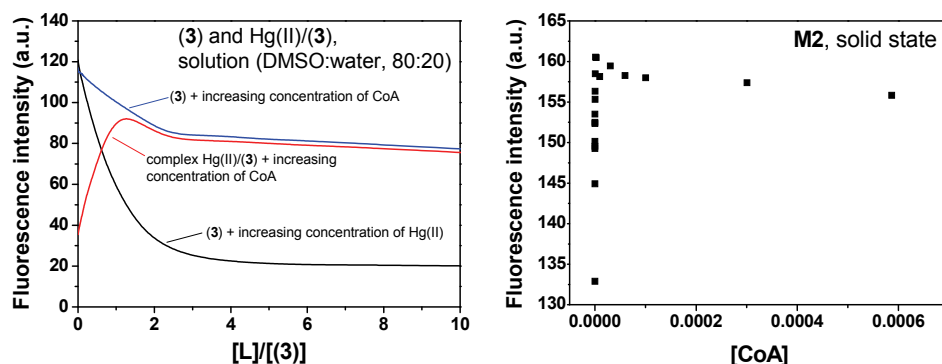


Figure 7. Cross interaction CoA, Hg(II) and (3) in DMSO:H₂O (80:20) solution (left), and interaction of the hybrid membrane **M2** with CoA in water (pH = 7.4, TRIS) (right).

4. Conclusions

This work describes the preparation of a fluorogenic sensory material for the detection of biomolecules such as CoA, Cys, and GSH, in water under physiological conditions. The material is a hybrid membrane with gel-like behaviour, which upon interaction with the target molecules showed a turn “on” fluorescence pattern that permitted the molecules to be titrated. The receptor sensory motif within the membrane was a chemically anchored piperazinedione-derivative with bound Hg(II). The response arose from the displacement of the Hg(II) from the membrane due to a stronger complexation

of Hg(II) with the biomolecules, thus releasing the fluorescent sensory moieties. The material recovered the fluorescence behaviour characteristic of the chemical structure of the receptors.

Acknowledgments

We gratefully acknowledge financial support provided by the Spanish Ministerio de Ciencia e Innovación—Feder (MAT2011-22544) and by the Junta de Castilla y León (BU001A10-2).

References

- 1 García, J.M.; García, F.C.; Serna, F.; de la Peña, J.L. Fluorogenic and chromogenic polymer chemosensors. *Polym. Rev.* 2011, 51, 341-390.
- 2 Martínez-Máñez, R.; Sancenón, F. Fluorogenic and chromogenic chemosensors and reagents for anions. *Chem. Rev.* 2003, 103, 4419-4476.
- 3 Kim, H.N.; Guo, Z.; Zhu, W.; Yoon, J.; Tian, H. Recent progress on polymer-based fluorescent and colorimetric chemosensors. *Chem. Soc. Rev.* 2011, 40, 79-93.
- 4 Jeong, Y.; Yoon, J. Recent progress on fluorescent chemosensors for metal ions. *Inorg. Chim. Acta* 2011, doi:10.1016/j.ica.2011.09.011
- 5 Gale, P.A. Anion receptor chemistry. *Chem. Commun.* 2011, 47, 82-86.
- 6 Descalzo, A.B.; Máñez Martínez-Máñez, R.; Sancenón Hoffmann, K.; Rurack, K. The supramolecular chemistry of organic-inorganic hybrid materials. *Angew. Chem. Int. Ed.* 2006, 45, 5924-5948.
- 7 Zhou, Y.; Xu, Z.; Yoon, J. Fluorescent and colorimetric chemosensors for detection of nucleotides, FAD and NADH: Highlighted research during 2004–2010. *Chem. Soc. Rev.* 2011, 40, 2222–2235
- 8 Li, J.; Ge, X.; Jiang, C. Spectrofluorometric determination of trace amounts of coenzyme A using terbium ion-ciprofloxacin complex probe in the presence of periodic acid. *Anal. Bioanal. Chem.* 2007, 387, 2083-2089.
- 9 Peng, Q.; Ge, X.; Jiang, C. A new spectrofluorometric probe for the determination of trace amounts of CoA in injection, human serum and pig livers. *Anal. Sci.* 2007, 23, 557-561.
- 10 Yu, F.; Xi, C.; Li, Z.; Cui, M.; Chen, F.; Gao, Y.; Chen, L. Enoxacin-Tb³⁺ complex as an environmentally friendly fluorescence probe for Coenzyme A and its applications. *Anal. Lett.* 2009, 42, 631-645.
- 11 Raoof, J.B.; Ojani, R.; Kolbadinezhad, M. Voltammetric sensor for glutathione determination based on ferrocene-modified carbon paste electrode. *J. Solid State Electrochem.* 2009, 13, 1411-1413.
- 12 Wood, Z.A.; Schröder, E.; Harris, J.R.; Poole, L.B. Structure, mechanism and regulation of peroxiredoxins. *Trends Biochem. Sci.* 2003, 28, 34-40.
- 13 Xu, H.; Gao, S.; Liu, Q.; Pan, D.; Wang, L.; Ren, S.; Ding, M.; Chen, J.; Liu, G. A highly sensitive and selective competition assay for the detection of cysteine using mercury-specific DNA, Hg²⁺ and SYBR green I. *Sensors* 2011, 11, 10187-10196.
- 14 Zhang, D.; Zhang, M.; Liu, Z.; Yu, M.; Li, F.; Yi, T.; Huang, C. Highly selective colorimetric sensor for cysteine and homocysteine based on azo derivatives. *Tetrahedron Lett.* 2006, 47, 7093-7096.

- 15 Wei, X.; Qi, L.; Tan, J.; Liu, R.; Wang, F. A colorimetric sensor for determination of cysteine by carboxymethyl cellulose-functionalized gold nanoparticles. *Anal. Chim. Acta* 2010, 671, 80-84.
- 16 Zhang, M.; Yu, M.; Li, F.; Zhu, M.; Li, M.; Gao, Y.; Li, L.; Liu, Z.; Zhang, J.; Zhang, D.; Yi, T.; Huang, C. A Highly selective fluorescence turn-on sensor for cysteine/homocysteine and its application in bioimaging. *J. Am. Chem. Soc.* 2007, 129, 10322-10323.
- 17 Kim, T.K.; Lee, D.N.; Kim, H.J. Highly selective fluorescent sensor for homocysteine and cysteine. *Tetrahedron Lett.* 2008, 49, 4879-4881.
- 18 Duan, L.; Xu, Y.; Qian, X.; Wang, F.; Liu, J.; Cheng, T. Highly selective fluorescent chemosensor with red shift for cysteine in buffer solution and its bioimage: Symmetrical naphthalimide aldehyde. *Tetrahedron Lett.* 2008, 49, 6624-6627.
- 19 Wang, Y.; Xiao, J.; Wang, S.; Yang, B.; Ba, X. Tunable fluorescent sensing of cysteine and homocysteine by intramolecular charge transfer. *Supramol. Chem.* 2010, 22, 380-386.
- 20 Yang, X.F.; Liu, P.; Wang, L.; Zhao, M. A chemosensing ensemble for the detection of cysteine based on the inner filter effect using a rhodamine B spirolactam. *J. Fluoresc.* 2008, 18, 453-459.
- 21 Jung, H.S.; Han, J.H.; Pradhan, T.; Kim, S.; Lee, S.W.; Sessler, J.L.; Kim, T.W.; Kang, C.; Kim, J.S. A cysteine-selective fluorescent probe for the cellular detection of cysteine. *Biomaterials* 2012, 33, 945-953.
- 22 Zhou, X.-B.; Chan, W.H.; Lee, A.W.M.; Yeung, C.C. Ratiometric fluorescent probe for enantioselective detection of D-cysteine in aqueous solution. *Beilstein J. Organic Chem.* 2011, 7, 1508-1515.
- 23 Lim, S.Y.; Kim, H.J. Ratiometric detection of cysteine by a ferrocenyl Michael acceptor. *Tetrahedron Lett.* 2011, 52, 3189-3190.
- 24 Yao, Z.; Bai, H.; Li, C.; Shi, G. Colorimetric and fluorescent dual probe based on a polythiophene derivative for the detection of cysteine and homocysteine. *Chem. Commun.* 2011, 47, 7431-7433.
- 25 Ravindran, A.; Mani, V.; Chandrasekaran, N.; Mukherjee, A. Selective colorimetric sensing of cysteine in aqueous solutions using silver nanoparticles in the presence of Cr³⁺. *Talanta* 2011, 85, 533-540.
- 26 Xu, Z.; Yoon, J.; Spring, D.R. Fluorescent chemosensors for Zn²⁺. *Chem. Soc. Rev.* 2010, 39, 2120-2135.
- 27 Chen, X.; Ko, S.K.; Kim, M.J.; Shin, I.; Yoon, J. A thiol-specific fluorescent probe and its application for bioimaging. *Chem. Commun.* 2010, 46, 2751-2753.
- 28 Zeng, X.; Zhang, X.; Zhu, B.; Jia, H.; Yang, W.; Li, Y.; Xue, J. A colorimetric and ratiometric fluorescent probe for quantitative detection of GSH at physiologically relevant levels. *Sens. Actuat. B Chem.* 2011, 159, 142-147.
- 29 Jablonski, A.E.; Lang, A.J.; Vyazovkin, S. Isoconversional kinetics of degradation of polyvinylpyrrolidone used as a matrix for ammonium nitrate stabilization. *Thermochim. Acta* 2008, 474, 78-80.
- 30 Tariq, S.A.; Hill, J.O. Thermal analysis of mercury(I) sulfate and mercury(II) sulfate. *J. Thermal Anal.* 1981, 21, 277-281.
- 31 Vallejos, S.; Estévez, P.; Ibeas, S.; Muñoz, A.; García, F.C.; Serna, F.; García, J.M. A selective and highly sensitive fluorescent probe of Hg²⁺ in organic and aqueous media: the role of a polymer network in extending the sensing phenomena to water environments. *Sens. Actuat. B Chem.* 2011, 157, 686-690.

Methacrylate copolymers with pendant piperazinedione-sensing motifs as fluorescent chemosensory materials for the detection of Cr(VI) in aqueous media

Methacrylate copolymers with pendant piperazinedione-sensing motifs as fluorescent chemosensory materials for the detection of Cr(VI) in aqueous media

Saúl Vallejos, Asunción Muñoz, Félix C. García, Felipe Serna, Saturnino Ibeas, José M. García*

Departamento de Química, Facultad de Ciencias, Universidad de Burgos. Plaza de Misael Bañuelos s/n, E-09001 Burgos, Spain. Corresponding author: J.M. García (e-mail: jmiguel@ubu.es; Phone: +34 947 258 085; Fax: +34 947 258 831).

Abstract

A fluorogenic sensory film, or dense membrane, capable of detecting Cr(VI), Fe(III), and Hg(II) in water was prepared. The film was prepared by a bulk radical polymerization of different comonomers, one of which contained a piperazinedione motif as sensory fluorophore. The film exhibited gel-like behavior and was highly tractable, even after being swollen in water. The sensing conditions were chosen to overcome interference from iron and mercury cations, giving rise to a material with a detection limit of 1 ppb for Cr(VI).

Keywords: Polymer membranes, polymer chemosensors, sensory materials, sensing hexavalent chromium, hexavalent/trivalent chromium discrimination

Journal of Hazardous Materials **2012**, 227-228, 480-483

1. Introduction

Chromium is ubiquitous in nature, ranking 21st among the elements in crustal abundance, and is found in biota, soil, air, and water. In naturally occurring chromium, hexavalent chromium [Cr(VI)] compounds are usually rare because they are readily reduced by organic matter to trivalent chromium [Cr(III)]. However, anthropogenic hexavalent chromium compounds, derived from processes associated with leather tanning, the pigment and dye industry, metal-related industries, and wood preservative production, are persistent contaminants in low organic matter-containing media. Although hexavalent chromium has long been considered a potent carcinogen when inhaled, studies in rats and mice, performed by the USA National Toxicology Program (NTP, 2008), showed evidence of carcinogenic properties of this ion when ingested. Unlike trivalent chromium, hexavalent chromium can easily permeate a cell membrane by using the existing, nonspecific phosphate and sulphate anion transport mechanisms. Once it is within a cell, Cr(VI) undergoes intracellular reduction, both enzymatic and non-enzymatic, yielding reactive intermediates, such as Cr(V), Cr(IV), and oxygen radicals that can damage DNA indirectly. The final product of this reduction is a trivalent chromium cation that can form complexes with different macromolecules, including DNA. In 2008, the NTP established the maximum contaminant load for Cr(VI) in the drinking water of children, based on noncancer endpoints, to be approximately 2.6 ppb.¹

Quantification of the total chromium content in an environmental sample is typically performed by atomic absorption or inductively coupled plasma spectrometry. The total Cr(VI) content can be measured calorimetrically, with a limit of detection (LOD) of 50 ppb, by complexing the cation with diphenylcarbazide² and by using high-performance liquid chromatography.^{3,4}

From the information discussed above, it follows that a quick, simple and inexpensive method for detecting hexavalent chromium could be of significant value,^{5,6} especially considering the challenge of distinguishing

between Cr(VI) and its less toxic analogue, Cr(III), as addressed by Gochfeld.^{2,7,8}

Herein, we describe the preparation of a polymer chemosensor for the detection and quantification of heavy metal cations.⁹ A highly hydrophilic sensory dense membrane, or film, has been prepared by copolymerization of hydrophobic sensory monomer, a piperazinedione-derived methacrylate monomer,^{10,11} with commercial hydrophilic monomers. Upon swelling of the membrane in the analyte solution, solvated target ions could enter the material by a simple diffusion mechanism, reaching the hydrophobic chemosensor motifs and giving rise to a macroscopic sensing phenomenon. Thus, fluorescent “dip-in” solid kits comprised of strips of this membrane allows for the selective detection of Cr(VI), Hg(II) and Fe(III) in aqueous solution due to the fluorescence quenching of the solid sensory material in contact with these cations. Moreover, a selective response for Cr(VI) in water media could be achieved by means of adjusting the pH of this media.

2. Experimental section

2.1. Membrane preparation

The membrane (**4**) was prepared by radical polymerization of a 99.75:0.25 mixture of *N*-vinylpyrrolidone (**1**) (Sigma Aldrich, >99%) and *N*-(4-((1 Z)-((Z)-5-(4-(dimethylamino)benzylidene)-3,6-dioxopiperazin-2-ylidene)methyl)phenyl)methacrylamide (**2**) according to a known procedure.¹² Ethylene glycol dimethacrylate (**3**) (Sigma Aldrich, 98%) was used as a cross-linking agent (7 mol % with respect to the overall comonomer molar content), and azobisisobutyronitrile (AIBN, Fluka, 98%, recrystallized twice from methanol, 1 wt %) was used as a thermal radical initiator. The thermal polymerization was carried out in silanized glass molds (100 μm thick) in an oxygen-free atmosphere at 65 °C for 5 h. The structure and physical appearance are depicted in Scheme 1.

2.2. Measurements

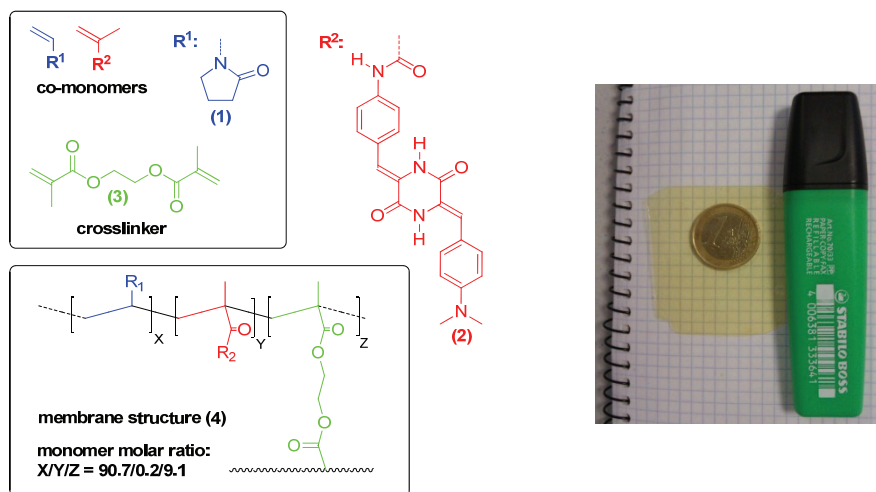
The fluorescence spectra were recorded using a Varian Cary Eclipse fluorometer. Millipore-Q water was used to prepare solutions. The fluorescence spectra of the sensory membrane, or film, were recorded soaking sensory film strips in 3 mL of water containing the target molecules, at controlled pH (buffer = Tris-HCl), in a fluorescence quartz cuvette. The angle between the membrane strips and both the incident light beam and the detector was 45° (incident light and detector at 90°), assuring that the reflected light due to the membrane surface was in opposite direction to the detector. The sensing, or response, time was 5 min. The sensing measurements were carried out using Fe(III), and Hg(II) as the nitrate salt, and Cr(VI) as potassium dichromate. To determine the tensile properties of the film, or dense membrane, strips (5 mm in width and 30 mm in length) were cut from polymer films (30–45 µm thick) on a Hounsfield H10KM Universal Testing Dynamometer at 20 °C. Mechanical clamps were used, and an extension rate of 5 mm min⁻¹ was applied using a gauge length of 10 mm. At least six samples were tested for each polymer, and the data were averaged. ¹H and ¹³C NMR spectra were recorded with a Varian Inova 400 spectrometer operating at 399.92 and 100.57 MHz, respectively, with deuterated dimethyl sulfoxide (DMSO-d₆) as solvent.

3. Results and discussion

We have prepared fluorogenic sensory materials using the bulk radical copolymerization of a sensing, piperazinedione ring-containing monomer, a hydrophilic vinyl monomer and a crosslinker (see inset in Figure 1).¹¹

The polymerization was performed in molds to produce a 100 µm thick hydrophilic film that exhibits gel-like behavior, with water uptake of 150% upon hindering the membrane in pure water. From a mechanical point of view, the dense membrane material yielded good performance with a Young's modulus of 490 MPa and a 160% elongation at break at room temperature and 65% relative humidity. The membrane has a hydrophilic character, and after drying

the material at 103°C for 20 minutes, the Young's modulus increased to 1.1 GPa while the elongation at break decreased to 12%. The membrane's initial performance data were recovered after returning to ambient temperature and humidity. These properties make the material ideal for performing measurements in water.



Scheme 1. Left: chemical structures of the copolymer membrane. Right: a digital picture of the yellow sensory membrane (notebook paper for contrast, one euro coin and highlighter for scale).

The film is fluorescent and demonstrates fluorescence quenching in the presence of Fe(III), Cr(VI) and Hg(II) in both basic and neutral aqueous solutions. Under acidic conditions, the quenching response is selective for Cr(VI); the 22-fold increase in fluorescence quenching virtually eliminates interference from the other two cations, as shown in Figure 1.

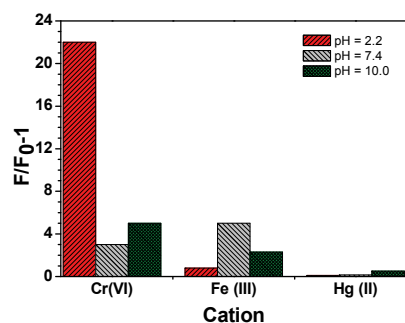


Figure 1. Fluorescence response profiles of the sensory film under acidic, neutral and basic conditions (cation concentration = 6×10^{-4} M; excitation wavelength = 335 nm; fluorescence intensity measured at 460 nm;).

This material does not exhibit fluorescence quenching in the presence of broad set of other cations, including Cr(III), and anions. An acidic titration of hexavalent chromium was performed using the membrane as fluorogenic material, as depicted in Figure 2, allowing the concentration of Cr(VI) to be determined with an LOD of 1 ppb.

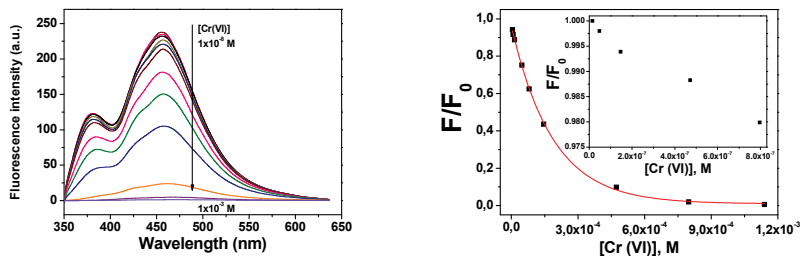


Figure 2. Left: selected fluorescence spectra of the film immersed in water at pH = 2.2, following the addition of increasing quantities of Cr(VI). Right: fluorescence titration curve of Cr(VI) (the fluorescence intensity data were taken at 456 nm - excitation wavelength = 335 nm-, inset: expansion at low hexavalent chromium concentration).

The real-world accuracy of our chromium (VI) detector was verified by measuring the cation concentration of a sample prepared with tap water from our laboratory (the concentration of chromium species was 1.3 ppb, determined by inductively coupled plasma mass spectrometry by the Analytical Service of the Scientific Park at the University of Burgos), at which we added a Cr(VI) concentration of 7.1×10^{-5} M, which was consistent with that predicted by the titration curve depicted in Figure 2 using the sensory membrane ($7.2 \pm 0.1 \times 10^{-5}$ M).

This detection phenomenon can be attributed to the interaction between the NH group on the piperazinedione ring and the aqueous Cr(VI) anions (CrO_4^{2-} or $\text{Cr}_2\text{O}_7^{2-}$), as shown in the NMR spectrum (see Figure 3). As a result, the ¹H NMR signals corresponding to the two NH groups of the piperazinedione ring are shifted significantly upfield upon interaction with the Cr(VI) species, as depicted in Figure 3. In contrast, the ¹H NMR signal of the acrylamide NH group shifted only a small amount, and the other signals remained unchanged. The NMR signals were assigned using 2D NMR experiments (COSY). Although the

detection of Cr(VI) by sensory membrane was performed in aqueous media, the NMR studies were carried out in DMSO-d₆ because the monomer (**2**) is insoluble in water. Taking this incongruity into account, an analysis of the amidic proton NMR shifts was performed using a corresponding Job's plot (see Figure 4) and indicated that two Cr(VI) species interact with each receptor molecule (**2**), regardless of the hexavalent chromium species present in the medium being measured (e.g. chromate, dichromate, hydrogen chromate, hydrogen dichromate, trichromate or tetrachromate).¹³ Considering that the dichromate is an anion and is the dominant specie at pH=2.2, and taking into account the ¹H NMR results, the interactions could tentatively ascribed to a double hydrogen bond between the two amides of the piperazinedione ring and two oxygens of the dichromate dianion, as depicted in the solid state structure of a relatively related complex obtained by single-crystal X-ray diffraction technique.¹⁴

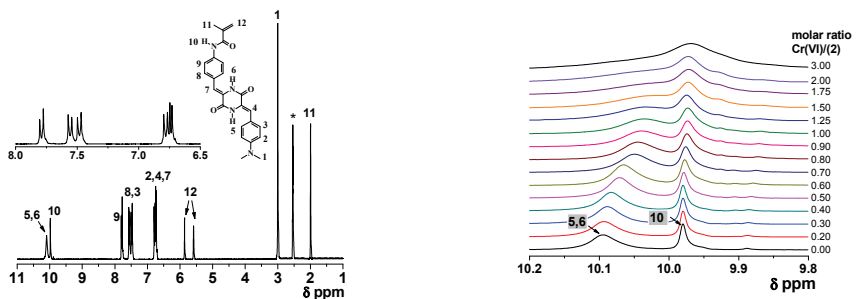


Figure 3. Left: ¹H NMR data of monomer **2** in DMSO-d₆ solution (* = solvent signal). Right: ¹H NMR data of monomer **2** in DMSO-d₆ solution upon increasing concentration of Cr(VI) of amidic protons 5,6, and 10 (see nuclei labels on left figure).

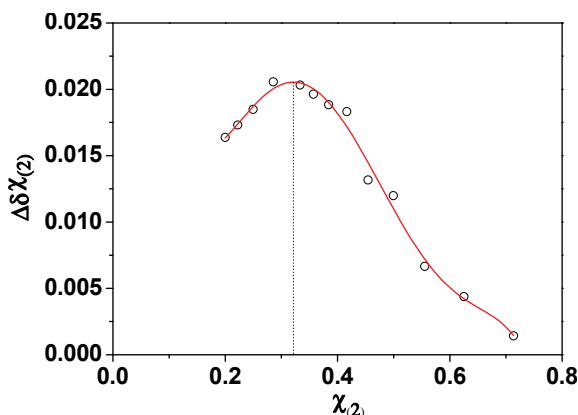


Figure 4. Job's plot corresponding to the interaction of Cr(VI) with the receptor monomer (**2**) in DMSO-d₆ solution derived from the ¹H NMR chemical shifts of the amidic protons on the piperazinedione ring.

4. Conclusions

In short, we describe a solid system with the potential for use as a solid kit for “dip-in” Cr(VI) detection that is capable of differentiating between Cr(VI) and less harmful Cr(III). Moreover, the material exhibited selective fluorescence quenching for Cr(VI) in the presence of a broad set of cations, allowing for the fluorometric quantification of Cr(VI) concentration with a detection limit of 1 ppb.

Acknowledgements

We gratefully acknowledge the financial support provided by the Spanish Ministerio de Ciencia e Innovación – FEDER (MAT2011-22544) and by the Junta de Castilla y León (BU001A10-2).

References

- 1 OEHHA, Draft for public comment and scientific review, Public Health Goal for Hexavalent Chromium in Drinking Water, January 25, 2011.
 - 2 M. Gochfeld, Panel discussion: analysis of chromium: methodologies and detection levels and behavior of chromium in environmental media, *Environ. Health Perspect.* 92(1991) 41-43.
 - 3 M. J. Marqués, A. Salvador, A. E. Morales-Rubio, M. de la Guardia, Analytical methodologies for chromium speciation in solid matrices: a survey of literature, *Fresenius J. Anal. Chem.* 632 (1998) 239-248.
 - 4 M.E. Losi, C. Amrhein, W.T. Frankenberger Jr, Environmental biochemistry of chromium, *Rev. Environ. Contam. Toxicol.* 136 (1994), 91-121.
 - 5 M.S. Hosseini, M. Asadi, Speciation determination of chromium using 1,4-diaminoanthraquinone with spectrophotometric and spectrofluorometric methods, *Anal. Sci.* 25 (2009), 807-812.
 - 6 T. Inui, K. Fujita, M. Kitano, T. Nakamura, Determination of Cr(III) and Cr(VI) at sub-ppb levels in water with solid-phase extraction/metal furnace atomic absorption spectrometry, *Anal. Sci.* 26 (2010) 1093-1098.
 - 7 Y. Xiang, L. Mei, N. Li, A. Tong, Sensitive and selective spectrofluorimetric determination of chromium (VI) in water by fluorescence enhancement, *Anal. Chim. Acta* 581 (2007) 132-136.
 - 8 A. Yari, H. Bagheri, Determination of Cr(VI) with selective sensing of Cr(VI) anions by a PVC-membrane electrode based on quinaldine red, *J. Chin. Chem. Soc.* 56 (2009) 289-295.
 - 9 J.M. Garcia, F.C. Garcia, F. Serna, J.L. de la Peña, Fluorogenic and Chromogenic Polymer Chemosensors. *Polym. Rev.* 51 (2011) 341-390.
 - 10 S. Vallejos, P. Estévez, S. Ibáñez, A. Muñoz, F.C. García, F. Serna, J.M. García, A selective and highly sensitive fluorescent probe of Hg²⁺ in organic and aqueous media: the role of a polymer network in extending the sensing phenomena to water environments. *Sens. Actuators B: Chem.* 157 (2011) 686-690.
 - 11 S. Vallejos, P. Estévez, S. Ibáñez, F.C. García, F. Serna, J.M. García, An organic/inorganic hybrid membrane as a solid “turn-on” fluorescent chemosensor for coenzyme A (CoA), cysteine (Cys), and glutathione (GSH) in aqueous media. *Sensors* 12 (2012) 2969-2982.
-

- 12 S. Vallejos, P. Estévez, S. Ibáñez, A. Muñoz, F.C. García, F. Serna, J.M. García, A selective and highly sensitive fluorescent probe of Hg²⁺ in organic and aqueous media: the role of a polymer network in extending the sensing phenomena to water environments, *Sens. Actuators B: Chem.* 157 (2011) 686–690
 - 13 S.S.M. Hassan, M.S. El-Shahawi, A.M. Othman, M.A. Mosaad, A potentiometric rhodamine-B based membrane sensor for the selective determination of chromium ions in wastewater, *Anal. Sci.* 21 (2005) 673-678.
 - 14 S. Ghosh, B. Roehm, R.A. Begum, J. Kut, M.A. Hossain, V.W. Day, K. Bowman-James, Versatile Host for Metallo Anions and Cations. *Inorg. Chem.* 46 (2007) 9519-9521
-

CAPÍTULO 4

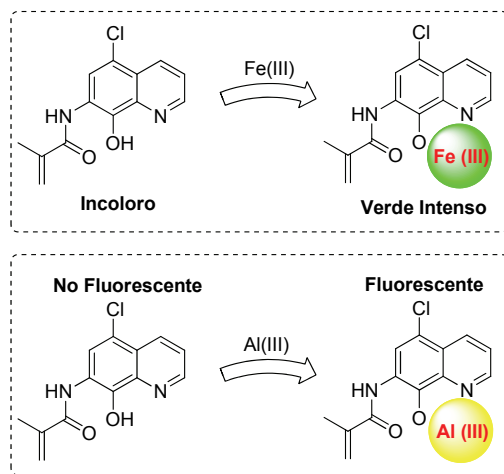
Polímeros con derivados de 8-hidroxiquinolina en su estructura

La 8-hidroxiquinolina, comúnmente conocida como oxina, es uno de los agentes quelantes más utilizados para varios cationes metálicos, como por ejemplo el Fe(III), con el que da lugar a complejos coloreados con alto coeficiente de extinción molar. Además, forma complejos muy fluorescentes con metales como el Al(III) o el Zr(IV). Por ello se ha derivatizado y utilizado tanto para la elaboración de polímeros solubles en agua como de membranas como materiales sensores cromogénicos hacia Fe(III) y fluorogénicos hacia Al(III).

4.1 8-Hidroxiquinolina y sus derivados

Este capítulo se describe la preparación de monómeros acrílicos basados en la estructura de la 8-hidroxiquinolina (Esquema 4.1), la síntesis de copolímeros lineales solubles en agua y de membranas densas que presentan una

excelente manejabilidad, así como el estudio del comportamiento como sensores colorimétricos y fluorimétricos de estos polímeros en presencia de Fe(III)¹⁴ y Al(III),¹⁵ respectivamente (Esquema 4.1).



Esquema 4.1. Estructura química del monómero con subestructura de 8-hidroxiquinolina y representación del proceso de detección de Fe(III) (arriba) y Al(III) (abajo).

La 8-hidroxiquinolina es un compuesto orgánico heterocíclico derivado de la quinoléina. Es de color amarillo pálido, se emplea en la industria en diversos ámbitos, y por lo general se prepara a partir del ácido quinolin-8-sulfónico, o de la anilina, mediante la síntesis de Skraup.⁷³ Los complejos con distintos metales, así como el propio heterociclo son inhibidores de la transcripción del ADN, y presentan propiedades antisépticas, desinfectantes y pesticidas.⁷⁴

Se trata de un agente quelante monoprótico bidentado que a pH neutro presenta el grupo hidroxilo en su forma protonada ($pK_a = 9.89$) y el anillo de piridina desprotonado ($pK_a = 5.13$).⁷⁵ El uso de este compuesto como agente precipitante de hierro y de otros metales en medidas gravimétricas está documentado desde hace más de 50 años.⁷⁶

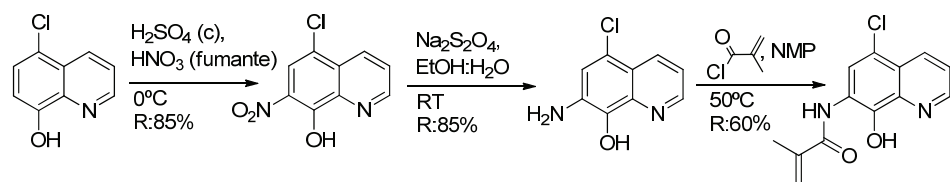
⁷³ G. Collin, H. Höke, *Ullmann's Encyclopedia of Industrial Chemistry*, Wiley VCH Weinheim, 2005.

⁷⁴ A. Y. Shen, S. N. Wu, C. T. Chiu, *J. Pharm. Pharmacol.* **1999**, *51*, 543.

⁷⁵ A. Albert; J. N. Phillips, *J. Chem. Soc.* **1956**, 1294.

⁷⁶ J. P. Phillips, *Chem. Rev.* **1956**, *56*, 271.

La elección de este subgrupo receptor vino determinada por las numerosas referencias bibliográficas existentes, relacionadas con análisis gravimétricos para metales como el Cr (VI).⁷⁷ A partir de ese punto, se valoró de forma positiva la versatilidad y la facilidad con la que se introducen modificaciones químicas en la 8-hidroxiquinolina (Esquema 4.2), ya que convierte a esta molécula en una materia prima ideal para los estudios realizados en esta memoria. Curiosamente, los mejores resultados se obtuvieron en la detección de Fe(III) y Al(III), tal como se comenta a continuación.



Esquema 4.2. Ruta sintética utilizada para la síntesis de monómero N-(5-cloro-8-hidroxiquinolin-7-il)metacrilamida.

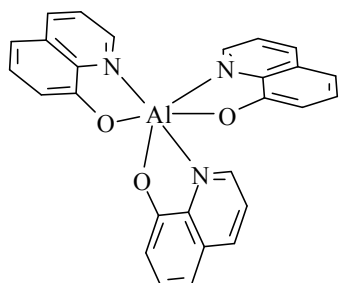
De la reacción de la 8-hidroxiquinolina con sales de aluminio en estado de oxidación (III) se obtiene el complejo con estequiometría ligando:metal 3:1 llamado Al(8-hidroxiquinolínato)₃,⁷⁸ y más conocido como Alq₃ (Esquema 4.2). Este complejo se utiliza de forma habitual como componente de los diodos orgánicos emisores de luz (OLED). En el caso del hierro (III), la 8-hidroxiquinolina forma complejos similares al que se muestra en el Esquema 4.3, esta vez coloreados.⁷⁶

La detección y cuantificación de estos dos cationes en disolución acuosa es de gran interés biomédico, alimentario y ambiental. Así, el control de la concentración de hierro es importante para evitar sabores y olores no deseados en agua potable, para controlar los vertidos de industrias que trabajan con derivados de hierro, para mantener las propiedades organolépticas en vinos, en el análisis clínico de hierro en la sangre para el

⁷⁷ N. N. Greenwood, A. Earnshaw, *Chromium, Molybdenum and Tungsten*, en *Chemistry of the Elements*, Elsevier, Madrid, 1997.

⁷⁸ R. Katakura, Y. Koide, *Inorg. Chem.* **2006**, 45, 5730.

control de anemias o en el control de Legionella en torres de refrigeración.⁷⁹ En cuanto al aluminio, su amplio uso provoca la acidificación de suelos y medios acuosos, y es potencialmente fitotóxico y tóxico para los seres vivos acuáticos.⁸⁰ En forma iónica es también una preocupación importante para la salud humana, ya que se cree que puede dañar el sistema nervioso, los tejidos y las células, y parece estar relacionado con el Alzheimer y otras enfermedades, como la demencia, la encefalopatía, el Parkinson y varios tipos de cáncer.⁸¹



Esquema 4.3. Representación de la estructura del $\text{Al}(8\text{-hidroxiquinolinato})_3$ ($\text{Alq}3$).

4.2 Polímeros con derivados de 8-hidroxiquinolina en la cadena lateral

Como se ha comentado en la sección anterior, el desarrollo de moléculas que actúan como sensores cromogénicos o fluorogénicos de Fe(III) y Al(III) es un tema de interés científico y tecnológico,^{14,82} por lo que tras el diseño y síntesis de un monómero acrílico (Esquema 4.2) capaz de establecer complejos estables con estos cationes, se pensó en una doble aproximación desde el punto de vista macromolecular:

- ❖ Polímero lineal sensor soluble en agua.
- ❖ Polímero reticulado sensor como membrana densa con comportamiento gel.

⁷⁹ RD 861/2003.

⁸⁰ N. E. W. Alstad, B. M. Kjelsberg, L. A. Vøllestad, E. Lydersen, A. B. S. Poléo, *Environ. Pollut.* **2005**, 133, 333.

⁸¹ P. Nayak, *Chem. Rev.* **1996**, 149, 125.

⁸² K. Kisoo, H. Kihyon, K. Sungjun, L. Jong-Lam, *J. Phys. Chem.* **2012**, 116, 9158.

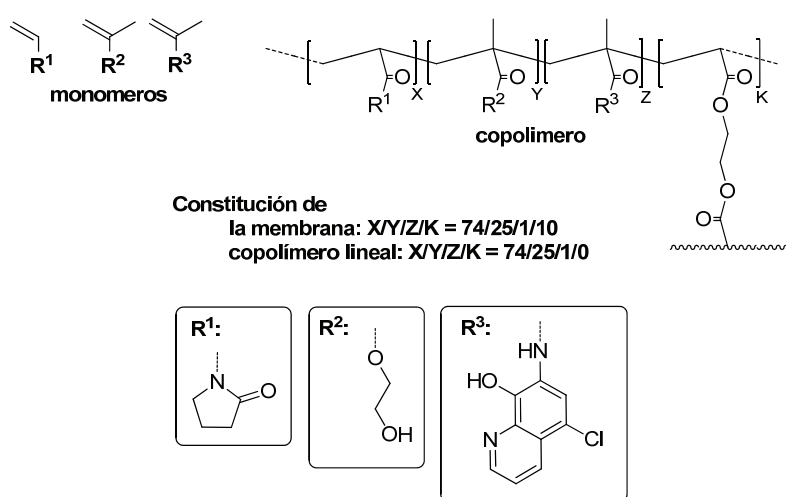
La síntesis de las redes entrecruzadas con derivados de 8-hidroxiquinolina en su estructura se llevó a cabo según los procedimientos descritos en el Capítulo 2. Por su parte, la síntesis de los polímeros lineales se llevó a cabo por polimerización radical en disolución de los comonómeros, utilizando tanto iniciación térmica (AIBN, azobisisobutironitrilo) como fotoquímica (2,2-dimetoxi-2-fenilacetofenona).

En el diseño de la matriz inerte de las membranas densas se tuvieron en cuenta no solo los requisitos descritos los capítulos precedentes para otros materiales sensores similares, sino que además se consideró la comercialización de éstos, por lo que se prestó más atención, si cabe, al aspecto externo de las membranas, y a su manejabilidad. Las membranas obtenidas como films tienen no solo la ventaja de ofrecer un material manejable para la detección de los cationes, sino también un sistema de producción versátil que permite distintos formatos del material dependiendo del uso que se le vaya a dar. Por ejemplo, el empleo como tiras sensoras en forma de película requiere formatos finos, manipulables, de respuesta rápida y con comportamiento de gel. Sin embargo, si el producto estuviera orientado, por ejemplo, al control de *Legionella* en torres de refrigeración, se necesitarían formatos de mayor tamaño, con mayor resistencia mecánica y velocidad de respuesta apropiada para su utilización en continuo.

En relación a estos comentarios, la matriz de los polímeros de este estudio se elaboró con *N*-vinilpirrolidona (VP) y acrilato de 2-hidroxietilo (A2HE). Ambos monómeros proporcionan hidrofilia a la membrana, aportando el primero rigidez y el segundo flexibilidad. Las propiedades mecánicas en hinchado se aseguraron incrementando el porcentaje de entrecruzante, al igual que en el caso de los materiales con derivados de 2,5-dicetopiperazina (ver Capítulo 3).

La composición de la cadena principal de los polímeros lineales fue la misma que la de la membrana densa, a excepción del entrecruzante.

En relación con los subgrupos receptores, el monómero metacrílico derivado de la 8-hidroxiquinolina fue compatible al 100% con la matriz inerte, además de ser altamente soluble, lo que facilitó el proceso de polimerización y permite proporciones de subgrupos receptores más altos para otras aplicaciones. Al igual que con el resto de materiales, se sintetizaron varias estructuras poliméricas variando parámetros como la relación de comonomeros, el porcentaje de entrecruzante, y el sistema de iniciación, de las cuales surgió la mejor combinación de propiedades en términos de manejabilidad e hinchamiento en agua (entorno a un 60%) de las membranas, solubilidad en agua de los polímeros lineales y respuesta cromogénica y fluorogénica ante las especies objetivo. La constitución del material se muestra en el Esquema 4.4.



Esquema 4.4. Estructura de los monómeros acrílicos utilizados en la síntesis de las membranas sensoras y constitución de los materiales.

Como es habitual, se realizaron los análisis con una batería de especies, observando que el material sensor sufría un cambio de color en presencia de Fe(III), y que su fluorescencia aumentaba en con Al(III) en el medio. Sin embargo, no se vieron cambios de color con cationes como el Cr(VI), aunque si se observó la precipitación de varios compuestos, tal y como se describe en la bibliografía.⁷⁷ El fenómeno sensor se analizó por técnicas de

determinación estructural, como la resonancia magnética nuclear, empleando para ello el polímero lineal soluble en agua.

En relación con la posible explotación comercial, cabe resaltar que la magnitud de la señal detectable se puede modular de forma muy sencilla mediante una variación de la concentración del quimiosensor en el material.

4.3 Resultados

A continuación se describen los resultados obtenidos a través de la transcripción íntegra de los trabajos publicados.

- ❖ *Solid sensory polymer substrates for the quantification of iron in blood, wine and water by a scalable RGB technique*
 - ❖ *Selective and sensitive detection of aluminium ions in water via fluorescence “turn-on” with both solid and water soluble sensory polymer substrates*
-

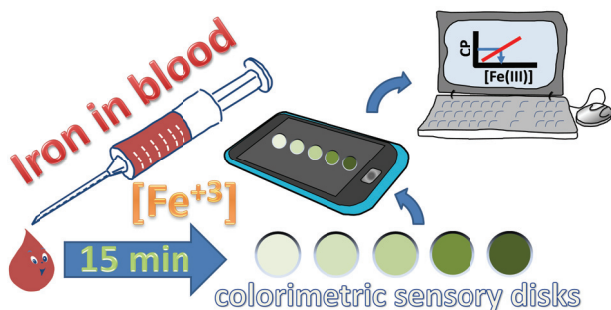
Solid sensory polymer substrates for the quantification of iron in blood, wine and water by a scalable RGB technique

Solid sensory polymer substrates for the quantification of iron in blood, wine and water by a scalable RGB technique

Saúl Vallejos, Asunción Muñoz, Saturnino Ibeas, Felipe Serna, Félix Clemente García and José Miguel García.*

Departamento de Química, Facultad de Ciencias, Universidad de Burgos. Plaza de Misael Banuelos s/n, E-09001 Burgos, Spain. Fax: +34947258831; Tel: +34947258085; E-mail: jmiguel@ubu.es.

Graphical abstract



Abstract

Iron in blood serum, wine and water has been visually detected and quantified quickly by processing photographs of an iron colorimetric sensory polymer substrate. The photographs may be taken with a conventional digital camera or Smartphone. The sensory materials were designed following a straightforward strategy. A proven iron organic chelator was easily transformed into an acrylic monomer and further copolymerized with hydrophilic co-monomers to render a membrane comprised of a hydrophilic, gel-like, polymer network. The film-like membrane generated was cut into small-diameter sensory discs. Thus, upon immersion of the sensory disks in blood serum, wine, and water, a colour development was rapidly observed which could be easily correlated with the iron concentration of the samples.

Journal of Materials Chemistry A 2013, 1, 15435-15441

RGB digital parameters obtained from photographs of the sensors were processed statistically using principal component analysis (PCA) and used to elaborate titration curves and quantify iron concentrations. The response time of the sensory films was short, 15 min, and the concentrations measured in water ranged from 56 ppb to 56 ppm. This broad range covers the U.S. Environmental Protection Agency (EPA) and European Union (EU) drinking water standards for iron in drinking water (<300 and 200 ppm, respectively), the typical iron content of wines (1 to 10 ppm) and the normal range of iron in the blood serum in men (0.8-1.8 ppm). This methodology for detecting and quantifying chemical species avoids the time-consuming sample preparation, expensive laboratory techniques, and specialized personnel needed to carry out conventional analytical methods.

Introduction

Iron is ubiquitous throughout the universe and is found from the Earth's core to its crust, as well as within our water resources, in reservoirs and in living organisms, including mammalian cells.^{1,2} This element plays an essential role in many biological functions and its control is important to biological systems because both deficiencies and overloads cause pathological conditions.³ Regarding its industrial use, iron and its derivatives have varied and important applications, which also make its control essential. Because an overdose of iron causes serious problems, it is also an environmental concern. The U.S. Environmental Protection Agency (EPA)⁴ and the European Union (EU)⁵ have established limits of 0.3 mg/L (300 ppb) and 0.2 mg/L (200 ppb), respectively, for iron in drinking water. In foods, intake doses and the development of an undesirable flavour, odour or colour are of particular concern, especially in beverages. As the body can regulate iron uptake, overdose is rare and generally occurs only when supplements are taken. The development of chemosensors and chemodosimeters for iron cations, and specifically for Fe(III), usually begins with harnessing the strong Lewis acidic character of the cation ($pK_a = 2.2$).⁶ Therefore, this species can easily promote chemical

reactions, such as hydrolysis and oxidative processes, and can form coordination compounds; Fe(III)'s proclivity for forming coordination compounds permits it to be sensed using a variety of techniques.^{1,7}

Iron is essential for human beings; concentrations that are lower or higher than the normal level may lead to anemia or other health hazards, such as liver and kidney damage.⁸ Routine blood analysis usually determines the amount of iron in blood serum using ultraviolet-visible spectroscopy. This method requires an iron-complexing reagent to form differentially coloured compounds. The necessary reagents include reductants (e.g., ascorbic acid, hydroxylamine, thioglycolic acid), complexing agents (ferrozine, ferene, chromeazurol S), precipitating agents (trichloroacetic acid), buffer solutions, etc.⁹

Additionally, cations play an important role in winemaking. The small quantity of iron present in wines is significant as it causes instability, i.e., ferric casse; therefore, its concentration must be measured and controlled. Ferric casse occurs in both red and white wines. In the former, this condition is caused by the reaction between ferric iron and phenols, which initially leads to colour darkness but may later lead to flocculation and precipitation. In white wines, ferric casse occurs because an unstable colloid forms, which subsequently flocculates and precipitates, due to a reaction between ferric ions, phosphoric acid and proteins. The iron content in wines comes from the grapes (2 - 5 ppm), soil on the grapes, metal winemaking machinery, handling and transportation equipment, etc.¹⁰ The usual methods for determining the iron concentration in wine are also colorimetric; potassium thiocyanate (KSCN) is usually used as the complexing agent. Similar to the analysis of blood serum, wine samples must also be digested with nitric acid and hydrogen peroxide before complexation with KSCN to form coloured compounds. Another accurate method is flame atomic absorption spectroscopy. However, this method also requires the digestion of the sample and the use of expensive equipment and must be performed by highly specialized personnel.

Therefore, we decided to prepare visual detection kits for iron cations in different aqueous environments, i.e., aqueous media of interest, such as food (e.g., drinking water and wine), as well as biological media of medical interest, such as blood. We followed our previously described strategy, which consisted of utilizing organic molecules in aqueous environments by chemically anchoring them to highly tractable polymeric membranes that exhibit gel behavior and may be obtained in the form of films.¹¹ Therefore, we chose a well-known ferric iron chelator, 8-hydroxyquinoline (**HOx**), modified it with a polymerizable methacrylamide group, and prepared a hydrophilic material that performed as a specific colorimetric chemosensor for iron cations. The basic structure of **HOx** was chosen because it forms a 3:1 complex with ferric ion ($\text{Fe}:\text{Ox}_3^{2+}$); this complex has an extremely high overall stability constant ($\log K_1K_2K_3 = 36.9$).¹² Moreover, the chemical composition of the sensory polymer membrane was engineered to fit the relevant detection requirements, e.g., determination of normal iron content in the blood serum, (1.3 ± 0.5 ppm for men) safe iron levels in drinking water (lower than 300 ppb) or wine (2-5 ppm coming from grapes) and iron concentrations low enough to avoid health or organoleptic problems. Furthermore, the colour of the small sensory discs, cut from the membrane or film, was related to the iron concentration of the samples by photographing the discs, obtaining the RGB digital parameters defining the colour of each disc, then processing these parameters statistically using the principal component analysis (PCA). Therefore, a procedure for just-in-time quantification of the iron content in beverages, water and biological samples through use of a sensory material, a digital camera or a Smartphone, and a computer has been described, thus avoiding the time-consuming sample preparation, expensive laboratory techniques, and need for specialized personnel required to carry out standard analytical methods.

Experimental

Materials

All of the materials and solvents were commercially available and used as received unless otherwise indicated. They included the following: 5-chloro-8-hydroxyquinoline (Aldrich, 95%), sulfuric acid (VWR, 98%), nitric acid (Merck, fuming), 2-butanone (Merck, 99.5%), sodium dithionite (VWR, 85%), *N*-methylpyrrolidone (NMP) (Aldrich, 99.5%), *N,N*-dimethylformamide (DMF) (Aldrich, 99.8%), methacryloyl chloride (Alfa Aesar, 97%), dimethyl sulfoxide (DMSO, Merck, 99%), ethanol (VWR, 99.9%), methanol (VWR, 99.8%), 2-hydroxyethyl acrylate (**2HEA**, Aldrich, 96%), 2,2-Dimethoxy-2-phenylacetophenone (Aldrich, 99%), diethyl ether (VWR, 99.9%). The lithium chloride (Aldrich, 99%) was dried thoroughly in a muffle furnace at 400°C for one day.

Instrumentation

The ¹H and ¹³C NMR spectra were recorded with a Varian Inova 400 spectrometer operating at 399.94 and 100.58 MHz, respectively, or on a Varian Mercury 300 spectrometer operating at 299.87 and 75.41 MHz, respectively. Deuterated dimethyl sulfoxide (DMSO-d₆) was used as a solvent. Infrared spectra (FT-IR) were recorded with a Nicolet Impact spectrometer. The UV-vis spectra were recorded with a Varian Cary3-Bio UV-vis spectrophotometer. Flame atomic absorption spectroscopy was performed with a Hitachi Z-8200 Polarized Zeeman atomic absorption spectrophotometer. High-resolution electron-impact mass spectrometry (EI-HRMS) was carried out on a Micromass AutoSpec Waters mass spectrometer (ionization energy: 70 eV; mass resolving power: >10000). The elemental analysis was carried out in a LECO CHNS-932 analyser. Pictures of vials or sensory disks were taken with the Samsung Galaxy Note II Smartphone digital camera. For simplicity, speed and convenience, the three R, G and B colour parameters for each vial or disc were obtained directly after taking the pictures with the Smartphone using the app

called ColorMeter automatically averaging the data of 11×11 (121) pixels.¹³ Principal component analysis (PCA) was carried out using the Statgraphics Centurion XVI software installed on a personal computer in a Windows 7 environment. The variable (principal component) values were standardized and accounted for >99% of the variance in all experiments.

Measurements

The water-swelling percentage (WSP) of the membrane was obtained from the weights of a dry (ω_d) and a water-swelled membrane (the membrane was immersed in pure water at 20°C until the swelled equilibrium was achieved) (ω_s) as follows: $100 \times [(\omega_s - \omega_d)/\omega_d]$.

The sensing measurements in water were performed at pH 2 (buffered with potassium chloride and hydrochloric acid. The sensing measurements in wine were performed using untreated samples. The measurements of the iron concentration in blood serum were performed with commercially available lyophilized blood serum standards (PreciControl ClinChem Multi 1 and 2, Cobas®, Roche), after reconstitution with Milli-Q water and without further treatment.

Digital photographs taken of: a) vials containing water solutions of the sensory linear copolymer **LCp** and different quantities of Fe(III), or b) sensory discs after immersing in iron containing aqueous media (water, wine, or blood serum), cut from membrane **Mem**, permitted quantification of the Fe(III) concentration using the RGB colour model. The RGB colour model is used to display images in electronic systems; it is related to human colour perception. The acronym RGB stands for the three additive primary colours, red (R), green (G) and blue (B). The three RGB values that define each pixel colour range from 0 to 255 and are device dependent; thus, a RGB value does not define the same colour across devices. The opposite phenomenon is also true: the same colour may be reproduced with different RGB values across different devices because the image sensors and colour management vary. Thus, the RGB

values of each vial or disc, were measured from the photograph. To determine the overall information pertaining to the three RGB values and their correlation with the Fe(III) concentration, these data were recorded and subjected to a principal component analysis (PCA). A relationship between the parameters was found that permitted the reduction of the three variables to yield only one principal component (PC), which was correlated with the Fe(III) concentration.

The fact that the RGB parameters are not absolute and depend on the photograph-taking device, light, software, etc., means that a picture of a single sensory disc in isolation cannot be used to directly obtain the Fe(III) concentration of a sample. This problem can be easily overcome by taking the picture of this disc alongside a calibration system, which entails capturing a picture that contains both the sample and reference discs (discs immersed in solutions containing known Fe(III) concentration), and processing the unknown and the reference discs concomitantly; the reference samples can be standards that were previously prepared and stored, because they remain valid for a long period of time. The colour perception of the human eye works in a similar manner, and different people usually see different hues. Therefore, a reference must also be utilized when the quantitative analysis is performed with the naked eye; for instance, pH measurements taken using litmus paper require colour bars provided with each litmus paper package that relate the observed color with the pH. For the sake of clarity, a workflow regarding the procedure followed to quantify Fe(III) in water media by a scalable RGB technique has been included in the supplementary information, Figure S6.

Synthesis of Intermediates

The methacrylamide monomer **HOxMMA** was synthesized by following the reaction sequence described in Scheme 1.

5-Chloro-7-nitroquinolin-8-ol (1).

To a 1 L flask, which was fitted with a mechanical stirrer and a thermometer, was added 111 mmol (20 g) of 5-chloro-8-hydroxyquinoline and 2.24 mol (110

mL) of concentrated sulfuric acid. Afterwards, the system was cooled to 0 °C with an ice bath and 133 mmol (5.7 mL) of fuming nitric acid was added dropwise to the solution, keeping the temperature during the addition lower than 2°C. The solution was stirred at 0 °C for 1 additional hour before being warmed to room temperature. It was cautiously poured into ice water, resulting in the precipitation of product. The heterogeneous system was stirred overnight and the orange solid was filtered off before being washed thoroughly with water and methanol. The product was recrystallized in 2-butanone. Yield: 21.2 g (85%).
¹H-NMR (399.94 MHz; DMSO-d₆): δ (ppm), 9.15 (d, 1H, 3.9 Hz); 8.67 (d, 1H, 8.4 Hz); 8.26 (s, 1H); 8.01 (dd, 1H, 8.4 and 4.4 Hz). ¹³C-NMR (100.58 MHz; DMSO-d₆): δ (ppm), 151.57; 150.98; 141.01; 134.59; 133.23; 129.53; 126.86; 122.99; 118.71. EI-HRMS, m/z: 224 (M⁺, 100), 150 (90), 194 (55), 115 (46), 166 (45), 226 (35), 114 (25), 152 (21). FT-IR (Wavenumbers, cm⁻¹): ν_{O-H}: 2808; ν_{Ar,C=C}: 1600; ν_{NO₂} (as, s): 1503, 1332; ν_{C-Cl}: 1018.

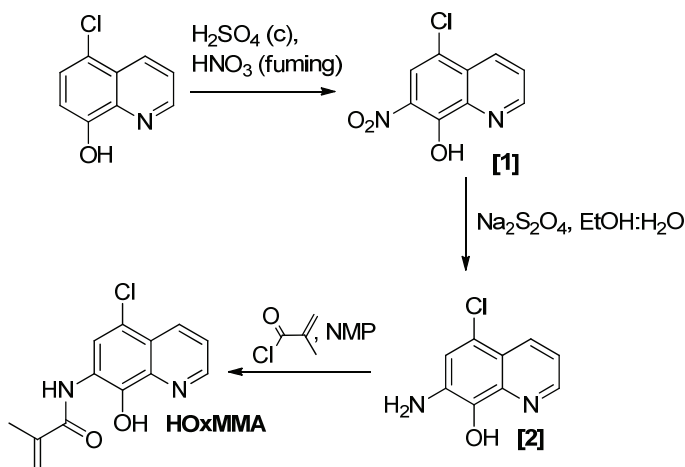
7-Amino-5-chloroquinolin-8-ol (2).

To 100 mL of 50% aqueous ethanol in a round-bottom flask was added 14.96 mmol (3.36 g) of 5-chloro-7-nitroquinolin-8-ol (**1**) and 78.69 mmol (13.70 g) of sodium dithionite. The mixture was stirred overnight under an atmosphere of nitrogen at room temperature. The yellow solid was filtered off and washed with water. The product was recrystallized in ethanol. Yield: 2.47 g (85%). ¹H-NMR (299.87 MHz; DMSO-d₆): δ (ppm), 9.42 (s, 1H); 8.78 (d, 1H, 3.9 Hz); 8.29 (d, 1H, 8.4 Hz); 7.35 (m, 1H); 7.34 (s, 1H); 5.36 (s, 2H). ¹³C-NMR (75.41 MHz; DMSO-d₆): δ (ppm), 149.82; 139.39; 136.02; 135.879; 133.13; 119.96; 119.24; 118.74; 118.695. EI-HRMS, m/z: 194 (M⁺, 100), 96 (33), 78 (22), 63 (21), 165 (15), 131 (10), 167 (9), 65 (8). FT-IR (Wavenumbers, cm⁻¹): ν_{C-NH₂}: 3320; ν_{O-H}: 3262; ν_{Ar,C=C}: 1588; ν_{C-Cl}: 1052.

N-(5-chloro-8-hydroxyquinolin-7-yl)methacrylamide (HOxMMA).

Together with 0.628 g of LiCl, 4.62 mmol (0.9 g) of 7-amino-5-chloroquinolin-8-ol (**2**) dissolved in 11 mL of NMP was added to a flask equipped with a reflux

condenser. Subsequently, 8.31 mmol (0.812 mL) of methacryloyl chloride was added and the solution was stirred for 12 hours at 50°C under an atmosphere of nitrogen. Finally, the product was precipitated in water. The solid was removed by filtration and treated with water at reflux. Yield: 0.73 g (60%). ¹H-NMR (299.87 MHz; DMSO-d₆): δ (ppm), 10.72 (s, 1H); 9.32 (s, 1H); 9.00 (d, 1H, 3.9 Hz); 8.53 (d, 1H, 8.4 Hz); 8.23 (s, 1H); 7.73 (dd, 1H, 8.4 and 4.4Hz); 5.99 (s, 1H); 5.61 (s, 1H); 2.05 (s, 3H). ¹³C-NMR (75.41 MHz; DMSO-d₆): δ (ppm), 167.30; 150.27; 144.60; 140.56; 139.62; 133.42; 124.66; 123.99; 123.78; 123.03; 122.02; 118.85; 19.48. EI-HRMS, m/z: 262 (M⁺, 100), 193 (88), 41 (86), 69 (55), 165 (63), 264 (37), 195 (32), 129 (29), 221 (27). FT-IR (Wavenumbers, cm⁻¹): ν_{N-H}: 3441; ν_{O-H}: 3930; ν_{C=O}: 1692; ν_{ArC=C}: 1585; ν_{C-Cl}: 1057. Anal. Calcd for C₁₃H₁₁ClN₂O₂: C, 59.44; H, 4.22; N, 10.66; found: C, 59.15; H, 4.36; N, 10.47.



Scheme 1. Monomer synthesis

Linear polymer synthesis

The linear copolymer (**LCp**) was prepared by radical polymerization of the hydrophilic monomer **2HEA** and the sensing monomer **HOxMMA** in a 99/1 molar ratio, respectively. A nitrogen gas inlet and a reflux condenser were added to a 100-mL three-necked flask equipped with a magnetic stirrer. Next, 0.4 mmol (105 mg) of **HOxMMA** and 40 mmol (4.60 g) of 2-hydroxyethyl

acrylate (**2HEA**) were dissolved in DMF (40 mL) and added to the flask. Subsequently, the radical thermal initiator AIBN (656.84 mg, 4 mmol) was added and the solution was heated to 60 °C. After stirring for 4 h under an atmosphere of nitrogen, the solution was allowed to cool before being added dropwise to diethyl ether (300 mL) with vigorous stirring to yield the product as a brown precipitate. The polymer was purified by performing two cycles of the solution/precipitation procedure with methanol (10 mL) as the solvent and diethyl ether (100 mL) as the non-solvent. The final product was dried overnight in a vacuum oven at 60 °C. Yield: 85% (4 g).

Membrane preparation

The membrane (**Mem**), film shaped, was prepared by the bulk radical polymerization of *N*-vinylpyrrolidone (**VP**), 2-hydroxyethylacrylate (**2HEA**), *N*-(5-chloro-8-hydroxyquinolin-7-yl)methacrylamide (**HOxMMA**) with ethylene glycol dimethacrylate (**EGDMA**) as cross-linking agent and a co-monomer molar ratio **VP/2HEA/HOxMMA/EGDMA** of 74/25/1/10. AIBN (1 wt%) was employed as thermal radical initiator. The bulk radical polymerization reaction was carried out in a silanized glass mould that was 200 µm thick in an oxygen-free atmosphere at 60 °C overnight.

The structures of **LCp** and **Mem** are depicted in Scheme 2.

Solid sensory substrates

The solid sensory substrates were manufactured from **Mem** films by using a conventional office paper punch to cut out sensory discs that were 5 mm in diameter (see Scheme 2 and the ESI, Figures S9 and S10, showing colourlessness and transparency of the materials).

Results and discussion

Strategy for detection and quantification

Most of the chemosensors described in the literature are organic molecules, insoluble in water, that work only in organic solutions. Our goal is to choose

one of these well-known, previously-described chromogenic organic chemosensors, easily modify its structure to introduce a polymerizable chemical group, and copolymerize it with highly hydrophilic co-monomers to render both water soluble sensory linear polymers and membranes with gel behaviour that are capable of detecting and quantifying target molecules in aqueous systems.

Choosing the colorimetric chemosensory motif for preparing the sensory materials for detecting Fe(III)

We have chosen one of the best-known chemosensory motifs for detecting Fe(III), 8-hydroxyquinoline (**HOx**), also known as 8-quinolinol or oxine, because it has been used extensively as a precipitating agent for the quantitative gravimetric analysis of a number of metal ions.¹⁴ The mechanism of its chelation is well known. With iron, $\text{Fe(III)}_n:\text{Ox}_m^-$ complexes are formed with stoichiometries (listed here as n:m) of 1:1, 1:2 and 1:3. The stability constants for these complexes are extremely high, and the structures of the complexes have already been determined by single crystal X ray crystallography (see ESI, section S2).^{12,15,16} This, together with the highly coloured nature of the complexes, point to the potential of molecules containing this motif to be used as colorimetric chemodosimeters.

Accordingly, an acrylic monomer (**HOxMMA**) was designed containing the 8-hydroxyquinoline sensory motif (Scheme 1).

Material preparation and characterization

The synthesis of the sensory monomer, **HOxMMA**, was straightforward and was achieved using widely available and inexpensive chemicals; additionally, good yield and purity were obtained. The ^1H and ^{13}C NMR and FTIR spectra of the intermediates and monomers can be found in the electronic supplementary information (ESI), Section S1. As expected, **HOxMMA** establishes strong complexes with Fe(III). Nevertheless, this organic compound cannot be used as a ferric ion probe for aqueous solutions because it is insoluble in water.

Therefore, the complexation study was initially performed in an EtOH:H₂O (1:1, v/v) medium using a UV/Vis technique. The phenomena that were observed were similar to those described for the Fe(III)_n:Ox⁻_m system,¹² depicted in the ESI, Figure S5: the gradual addition of Fe(III) to the ethanolic solution of **HOxMMA** caused a colour change that corresponded to a shift toward the lower energies of the band at $\lambda_{\text{max}} = 663$ nm with a concomitant and significant increase in the absorbance to reach a maximum at $\lambda_{\text{max}} = 678$ nm. This shift is attributed to the formation of 1:3 and 1:2 complexes. Successive additions of Fe(III) caused further shifts in the maxima to reach $\lambda_{\text{max}} = 725$ nm with a concomitant decrease in the absorbance.

Nevertheless, our goal is the detection of chemical species in fully aqueous environments. Therefore, a fully water-soluble, linear polymer, **LCp**, that contained a sensory motif with a 5-chloro-8-hydroxyquinole derivative (Scheme 2), was synthesized, and its sensory behaviour toward Fe(III) was observed to be similar to ethanolic solutions of **HOxMMA**, as observed in the ESI, Figure S6. In this regard, Figure 1a depicts the Fe(III) titration with a water solution of **LCp**. Upon increasing the Fe(III) concentration, the development of the absorption band at $\lambda_{\text{max}} = 637 - 651$ nm, which corresponds to the formation of complexes with stoichiometries of 1:3 and 1:2, was observed; the representation of the absorbance at 637 nm vs the Fe(III) concentration permitted construction of the titration curve (Figure 1b), with a limit of detection and of quantification¹⁷ of 142 and 431 ppb, respectively. Interestingly, the colour development could be followed visually (Figures 1c and 1d), and a titration of Fe(III) could be determined by using the RGB parameters of a digital photograph taken of the vials with a conventional digital camera or mobile phone. Principal component analysis was used to reduce the red, green and blue parameters to a single principal component (PC), as we have previously reported (see ESI, figure S11).¹⁸ Therefore, two titration curves were prepared with respect to the Fe(III) concentration, the first corresponding to a ferric ion concentration maximum of 5.6 ppm (Figure 1c) and the second corresponding

to 560 ppm (Figure 1d). The limits of detection and of quantification were 493 and 1494 ppb, respectively. After calculating the titration curves, three test samples that contained 1.7, 3.4 and 18.6 ppm of Fe(III) were measured, providing measured concentrations of 1.8, 3.5 and 17.5 ppm, respectively; these data agreed with the actual ferric ion concentrations. The test samples were prepared with tap water that was buffered at pH 2, and the Fe(III) concentrations corresponded to sum of the added and innate tap water ferric ion concentration; the concentrations of the test samples were measured with flame atomic absorption spectrometry. The calibration curves, RGB parameters, and principal component analysis are shown in the ESI, Figures S8.

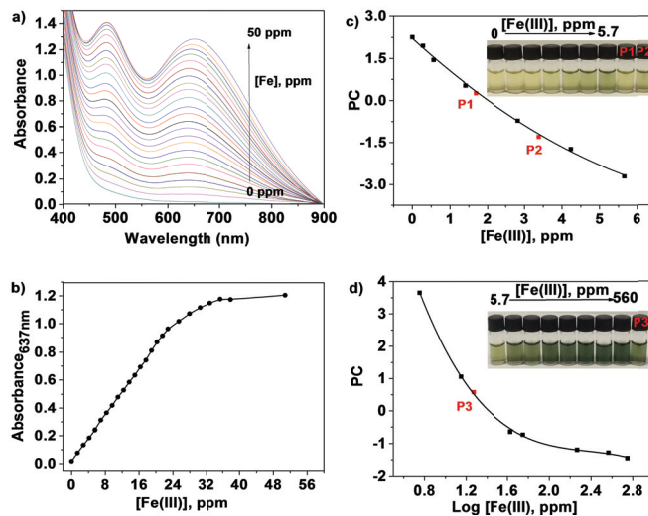


Figure 1. Titration of Fe(III) with a solution of linear copolymer LCp in water ($\text{pH} = 2$): Left [panels a) and b]): using the UV/Vis technique; right [panels c) and d]): using the RGB parameters from the digital pictures of the samples and reducing the three parameters (R, G, B) to one PC via principal component analysis. The samples labelled in red with the letter P correspond to the test samples; the concentration of the LCp was 17.64 g/L, which corresponded to 22.3 milliequivalents of the sensory motif (HOxMMA) per litre.

However, the development of practical visual detection systems for chemicals relies on the preparation of tractable solid kits for use by non-specialized personnel. For this purpose, the film Mem, which contained the Fe(III) probe HOxMMMA, was prepared as shown in Scheme 2. Mem is a

dense membrane with gel-like behaviour in aqueous environments and is fully tractable when dry or water-swollen. The target molecules enter the membrane, which is where the sensing event takes place, by diffusion into the water-rich membrane gel phase.^{11a} The film's structure is largely hydrophilic; it has a water-swelling percentage (WSP) of 65%. The membrane was cut to obtain the sensory disks.

Material testing in the presence of blood, wine and water

Ferric ions in blood serum, wine, and water have been visually detected using only the naked eye by immersing a sensory disc into the sample for a few minutes. Thus, the colourless discs were immersed in water that contained between 56 ppb and 56 ppm of Fe(III), white wines that contained between 1.0 and 2.3 ppm of Fe(III), and human blood serum that contained between 1.1 and 10.6 ppm of Fe(III). The disks turned green-brown when exposed to Fe(III) in all environments. The pictures of the disks, shown in Figure 2, depict the colour variations caused by differences in the concentrations of the ferric ions.

Moreover, digital photographs of the discs were used to quantify the Fe(III) content *in-situ*.¹⁸ After photographing the discs, the three RGB parameters of each disc were processed using principal component analysis; the three RGB values of each colour were reduced to one variable (principal component, PC), which permitted the elaboration of the titration curves (Figure 2; the principal component parameters are shown in the ESI, Figure S12 to S15).

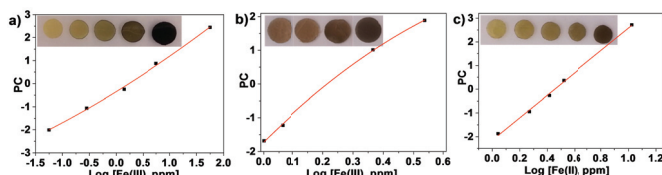
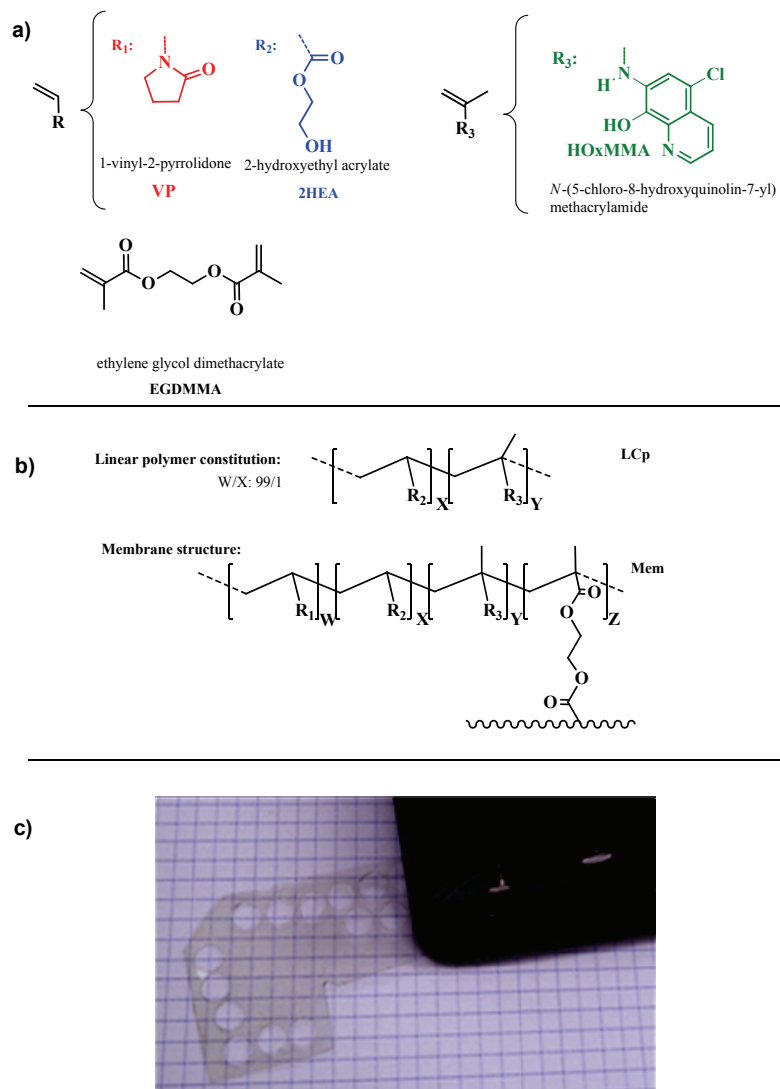


Figure 2. Titration of Fe(III) using the RGB parameters from digital photographs of the sensory discs immersed in: a) water, pH = 2, concentration of ferric ion from 56 ppb to 56 ppm; b) white wine, untreated samples with ferric ion content from 1.0 to 3.4 ppm; and c) blood serum, untreated samples, from 1.1 to 10.6 ppm. The three parameters (R, G, B) were reduced to one principal component (PC) via principal component analysis.



Scheme 2.
Constitution of a) the monomer structures and b) the linear polymer (**LCp**) and membrane (**Mem**)
c) digital picture of the sensory film and of the office paper punch that was used to obtain the solid sensory discs, 5 mm in diameter.

Response time

The solid sensory material showed a rapid response time of 15 to 30 min for the low ppm range of Fe(III) concentrations. These values were measured with a UV/vis technique and correspond to the time needed to achieve 90 and 98% absorbance, respectively (a 99.9% response was obtained after soaking the disk for 60 min).

A real-time video demonstrating the colorimetric response of the sensory discs in aqueous Fe(III) solution can be found in the ESI.

Substrate selectivity and interference study

As previously indicated, the 8-hydroxyquinoline sub-structure is an effective complexing agent for a number of metal ions. However, the tested cations [Li(I), Na(I), K(I), Rb(I), Cs(I), Ag(I), Mg(II), Sr(II), Ba(II), Mn(II), Co(II), Ni(II), Cu(II), Zn(II), Pb(II), Cd(II), Hg(II), Cr(III), Zr(III), La(III), Ce(III), Nd(III), Sm(III), Dy(III), Al(III), Cr(VI)] did not give rise to colour development for water solutions of both **LCp** and sensory discs.

Moreover, the extremely high stability constant of the $\text{Fe(III)}_n\text{-Ox}^-_m$ complexes lead to a colorimetric selective detection system, even in the presence of different neutral and ionic species. The reconstituted blood serum solutions contained a number of metals and biomolecules because they are used as standards to calibrate measurements of the serum blood components in medical applications (>25 components, see ESI, Table S2); however, none of these components caused any interference, although they were present in different weight ratios with respect to the iron ions. Furthermore, an interference study, which was carried out with **Mem** in water that contained a cocktail of cations, gave a similar result, as shown Figure 3.

With respect to Fe(II), the response of this system was exactly the same as for Fe(III), which means that the sensing system described here responds to iron ions in general. There is a simple explanation for this result. The standard reduction potential (E°) for the pair $[\text{Fe(III)}:\text{MeOx-3}]/[\text{Fe(II)}:\text{MeOx-2}] + \text{MeOx-}$, where MeOx- is 5-methylquinolin-8-olate, is -0.30 V, pointing to the oxidation of the Fe(II) to the Fe(III) complex in the presence of oxygen. If this is the case, measurements in similar aqueous systems, which are in the presence of oxygen, would detect both Fe(II) and Fe(III) as Fe(III), i.e., total iron content.

Substrate sensitivity

In water, a broad range of concentrations were measured, 56 ppb to 56 ppm, covering the EPA and the EU water recommendation ranges for Fe(III) content in drinking water (see ESI, Figure S12).

Examination of actual wine samples gave an iron concentration range of 1.0 to 3.4 ppm, thus showing the analytic potential of the sensory material (the concentration of iron in wines was previously measured by flame atomic absorption spectrometry, see ESI, Figure S14 for wine brand names).

In blood serum, the concentration of ferric ions ranged from 1 to 10 ppm, covering the normal range of iron in the blood serum of men, which is 0.8–1.8 ppm (see ESI, Figure S15).

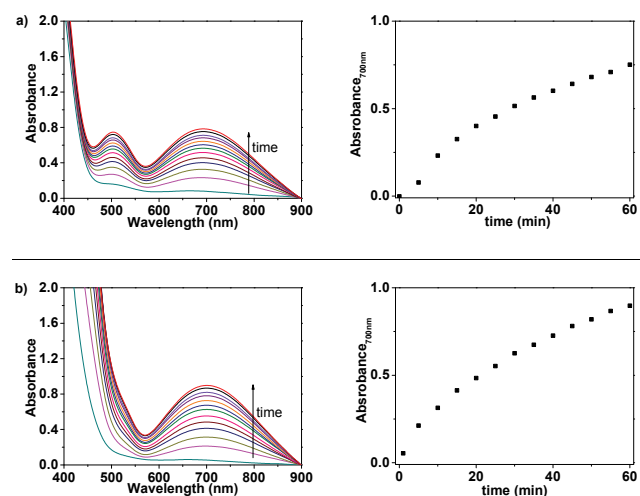


Figure 3. Interference study. UV/Vis response of **Mem** in water ($\text{pH} = 2$) containing: a) only Fe(III), 1.2×10^{-2} M; and b) a cocktail of cations: Fe(III), Zn(II), Ni(II), Cu(II), and Mn(II) [concentration of each cation, including Fe(III), was 1.2×10^{-2} M].

Conclusions

In short, we have prepared colorimetric sensory solid polymer substrates, shaped as discs that are 5 mm in diameter and 0.1 mm in thickness, for the

naked-eye detection of iron ions in aqueous environments of special interest in medical, industrial and environmental applications, e.g., in blood serum, wine and drinking water. The colourless and transparent discs turned green-brownish upon immersion in samples containing Fe(III). The colour development was proportional to the concentration of Fe(III), and a simple digital picture of the sensory discs was used to quantify the Fe(III) concentration. The digital definition of the colour of each disc, i.e., the RGB parameters, processed statistically using the principal component analysis (PCA), permitted construction of calibration curves and the measurement of unknowns. Our procedure for quantifying the iron content in beverages, water and biological media in a few minutes by means of a sensory material, a digital camera or a Smartphone, and a computer avoids the usual time-consuming sample preparation, expensive laboratory techniques, and use of specialized personnel required in conventional Fe(III) determination. The chemical composition of the sensory polymer membrane was engineered to give a short response time and to meet special detection requirements (e.g., determining whether the iron content of blood serum is within the normal limits for healthy individuals, or if water and wine have iron concentrations low enough to avoid health or organoleptic problems). Accordingly, the response time of the sensory films was short, 15 min, and the concentrations measured in water ranged from 56 ppb to 56 ppm. This broad range covers the U.S. Environmental Protection Agency (EPA and European Union's (EU) drinking water standards for iron (<300 and 200 ppm, respectively), the typical content of iron in wines (1 to 10 ppm) and the normal range of iron in the blood serum of men (0.8-1.8 ppm).

Acknowledgements

We wish to thank Ms. Evelia Malla and Mr. Jesús Fernández, specialists in Clinical Analysis of the Burgos University Hospital, for fruitful discussions regarding iron analysis in blood serum. We also gratefully acknowledge the financial support provided by the Spanish Ministerio de Economía y

Competitividad-Feder (MAT2011-22544) and by the Consejería de Educación - Junta de Castilla y León.

Notes and references

- 1 K. Kaur, R. Saini, A. Kumar, V. Luxami, N. Kaur, P. Singh and S. Kumar, *Coord. Chem. Rev.*, 2012, 256, 1992–2028.
- 2 J. B. Howard and D. C. Rees, *Adv. Protein Chem.*, 1991, 42, 199-280.
- 3 a) E. C. Theil and K. N. Raymond, *Bioinorganic Chemistry*, I. Bertini, H. Gray, S. Lippard, and J. Valentine Eds., University Science Books, Mill Valley, 1994, ch. 1; b) R. R. Crichton, D. T. Dexter and R. J. Ward, *Coord. Chem. Rev.*, 2008, 252, 1189-1199; c) R. B. Lauffer, *Iron and Human Disease*, R. B. Lauffer, Ed., CRC Press, Boca Raton, 1992, pp. 1-20.
- 4 U.S. Environmental Protection Agency (EPA). 2012 Edition of the Drinking Water Standards and Health Advisories, EPA 822-S-12-001, <http://water.epa.gov/action/advisories/drinking/upload/-dwstandards2012.pdf>. Accessed May 16, 2013.
- 5 European Union's (EU) drinking water standards. Council Directive 98/83/EC of 3 November 1998 on the quality of water intended for human consumption. <http://eur-lex.europa.eu/LexUriServ/LexUriServ.do?uri=OJ:L:1998:330:0032:0054:EN:PDF>. Accessed September 2, 2013.
- 6 J. A. Dean, *Lange's Handbook of Chemistry*, 15th ed., McGraw-Hill, New York, 1987, Table 8.7 (Section 8).
- 7 X. Chen, T. Pradhan, F. Wang, J. S. Kim and J. Yoon, *Chem. Rev.*, 2013, 112, 1910-1956.
- 8 H. A. Zamani, M. T. Hamed-Mosavian, E. Hamidfar, M. R. Ganjali and P. Norouzi, *Mat. Sci. Eng. C*, 2008, 28, 1551-1555.
- 9 D. C. Harris, *Quantitative Chemical Analysis*, 8th ed., W. H. Freeman and company, New York, 2010, ch 17.4.
- 10 P. Ribéreau-Gayon, Y. Glories, A. Maujean, D. Dubourdieu, *Handbook of Enology*, Vol. 2, The Chemistry of Wine. Stabilization and Treatments, 2nd Ed., John Wiley & Sons Ltd, Chichester, 2006, ch. 4.
- 11 a) J. M. Garcia, F. C. Garcia, F. Serna and J. L. de la Peña, *Polym. Rev.*, 2011, 51, 341-390; b) S. Vallejos, H. El Kaoutit, P. Estevez, F. C. Garcia, J. L. de la Peña, F. Serna and J. M. García, *Polym. Chem.*, 2011, 2, 1129-1138; c) S. Vallejos, P. Estevez, F. C. Garcia, F. Serna, J.L. de la Peña and J. M. Garcia, *Chem. Commun.*, 2010, 46, 7951-7953; d) S. Vallejos, P. Estevez, S. Ibeas, A. Muñoz, F. C. Garcia, F. Serna and J. M. Garcia, *Sens. Actuators B: Chem.*, 2011, 157, 686-690; e) S. Vallejos, A. Munoz, F. C. Garcia, F. Serna, S. Ibeas and J. M. Garcia, *J. Hazard. Mater.*, 2012, 227-228, 480-483; f) S. Vallejos, P. Estevez, S. Ibeas, F. Garcia, F. Serna and J. M. Garcia, *Sensors*, 2012, 12, 2969-2982.
- 12 T. D. Turnquist and E. B. Sandell, *Anal. Chim. Acta*, 1968, 42, 239-245.
- 13 App from the software engineering company VisTech.Projects was downloaded and installed into the smartphone from Google Play. App web page: <http://www.vistechprojects.com/app/colorimeter>
- 14 G. H. Jeffery, J. Bassett, J. Mendham and R. C. Denney, *Vogel's Textbook of Quantitative Chemical Analysis*, 5th Ed., Longman Scientific & Technical, Harlow, 1989, pp. 178 and 407-408.
- 15 L. Pech, Y. A. Bankovsky, A. Kemme and J. Lejejs, *Acta Cryst.*, 1997, C53, 1045-1047.
- 16 Data collected and selected by R.M. Smith, A.E. Martell, NIST Critically Selected Stability Constants of Metal Complexes, Reference Database 46, Version 8.0, US Department of

Commerce, National Institute of Standards and Technology, Gaithersburg, MD, USA, 2004.
<http://www.nist.gov/srd/nist46.cfm>

- 17 The limit of detection (LOD) and the limit of quantification (LOQ) were estimated by the following equation: $LOD = 3.3 \times SD/s$ and $LOQ = 10 \times SD/s$, where SD is the standard deviation of a blank sample and s is the slope of the calibration curve in a region of low Hg(II) content.
- 18 H. El Kaoutit, P. Estevez, F. C. Garcia, F. Serna and J. M. Garcia, Anal. Methods, 2013, 5, 54-58.

SUPPLEMENTARY INFORMATION**Solid sensory polymer substrates for the quantification of iron in blood, wine and water by a scalable RGB technique.**

*Saúl Vallejos, Asunción Muñoz, Saturnino Ibeas, Felipe Serna, Félix Clemente García, José Miguel García.**

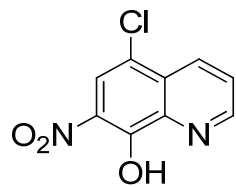
Departamento de Química, Facultad de Ciencias, Universidad de Burgos, Plaza de Misael Bañuelos s/n, 09001 Burgos, Spain. Email: jmiguel@ubu.es

Table of contents:

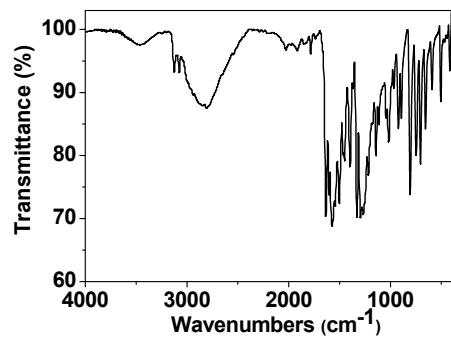
- S1.- NMR and FT-IR of intermediates and monomer HOxMMA**
- S2.- Structure and stability constants of Fe(III)-8-hydroxyquinoline complexes**
- S3.- Titration of Fe(III) with the monomer HOxMMA, copolymer LCp, and membrane Mem by means of UV/Vis spectroscopy**
- S4.- Titration of Fe(III) in water with copolymer LCp via the analysis of the RGB parameters from each vial using a digital picture**
- S5.- Sensory membrane or film Mem**
- S6.- Schematic procedure followed to quantify Fe(III) in water media by a scalable RGB technique**
- S7.- Titration of Fe(III) in water with the discs that were cut from sensory membrane Mem via the analysis of the RGB parameters for each vial within a digital picture**
- S8.- Titration of Fe(III) in wine with discs that were cut from sensory membrane Mem via the analysis of the RGB parameters for each vial within a digital picture**
- S9.- Titration of Fe(III) in blood serum with discs cut from sensory membrane Mem via the analysis of the RGB parameters for each vial within a digital picture.**

S1.- NMR and FT-IR of intermediates and monomer

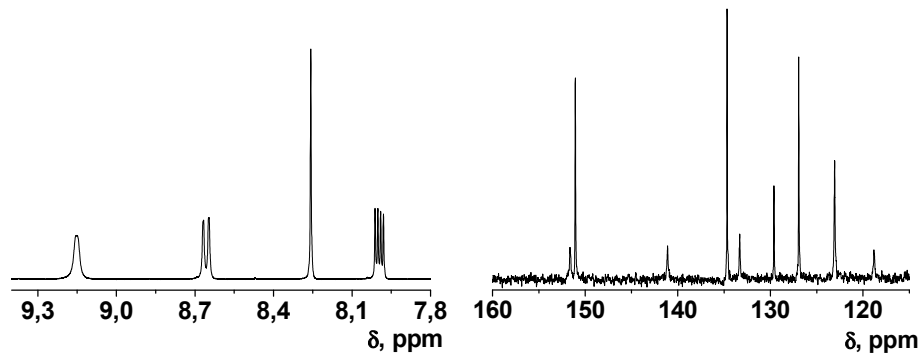
a)



b)



c)



d)

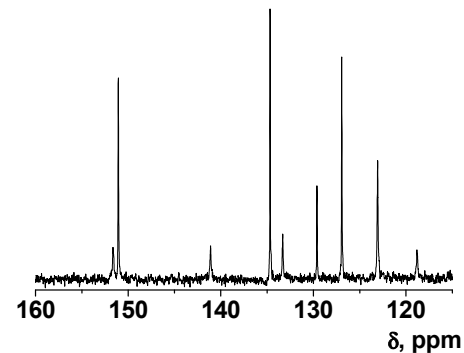


Figure S1. Characterization of 5-chloro-7-nitroquinolin-8-ol (1): (a) chemical structure; (b) FT-IR; (c) ^1H NMR; (d) ^{13}C NMR (NMR solvent: DMSO-d_6).

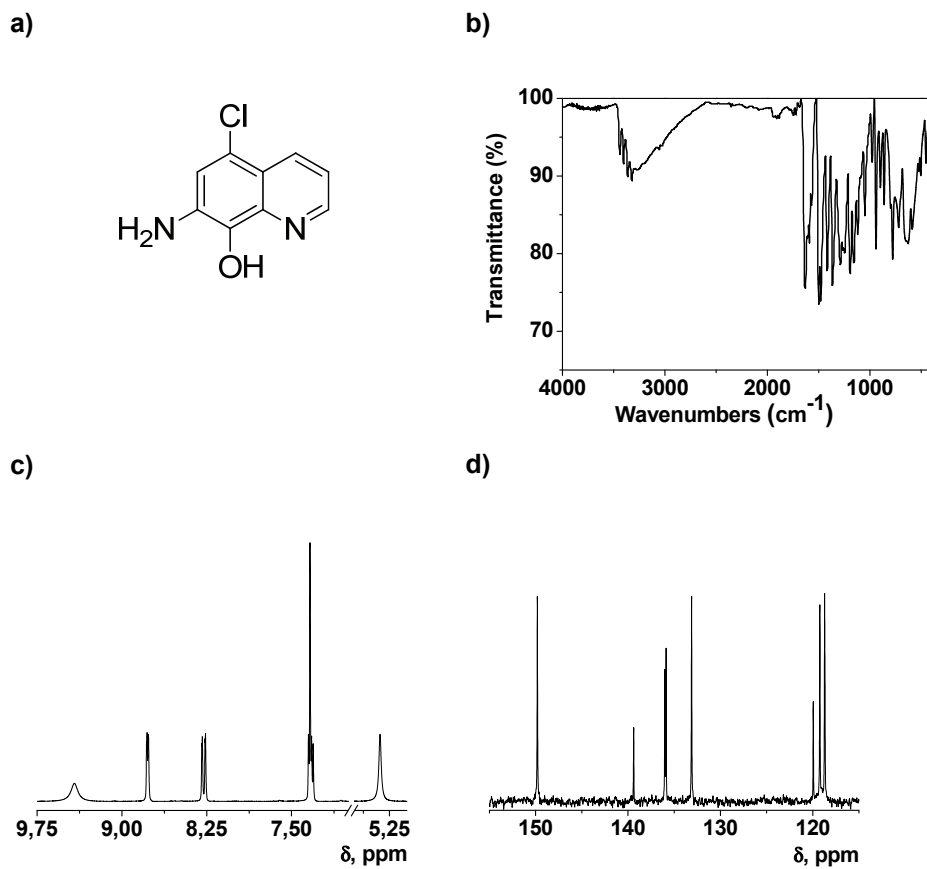


Figure S2. Characterization of 7-amino-5-chloroquinolin-8-ol (**2**): (a) chemical structure; (b) FT-IR; (c) ^1H NMR; (d) ^{13}C NMR (NMR solvent: DMSO-d_6).

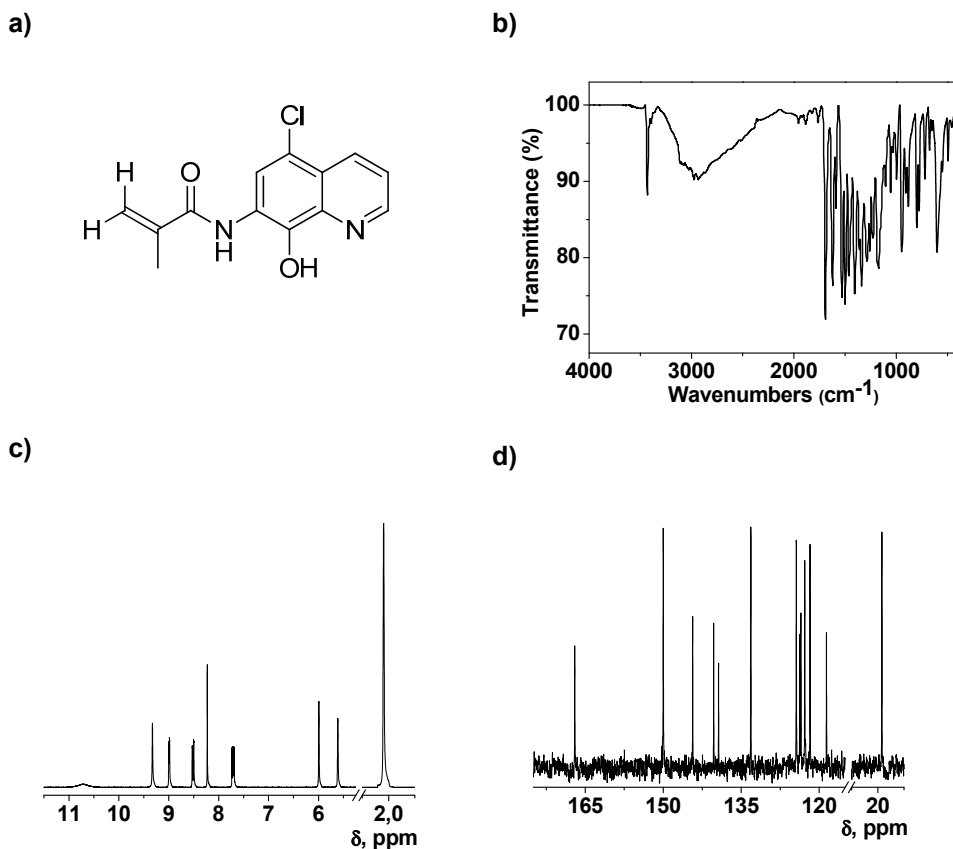
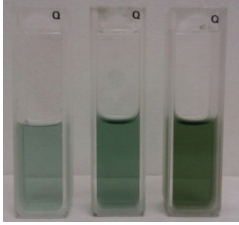


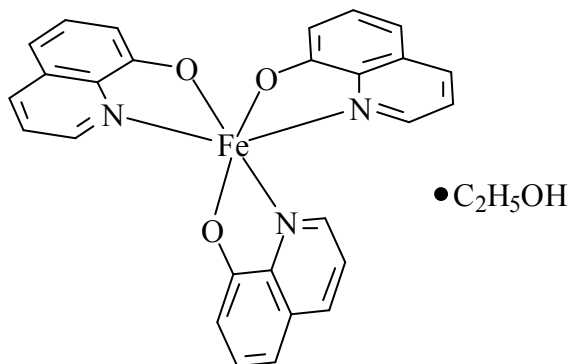
Figure S3. Characterization of *N*-(5-chloro-8-hydroxyquinolin-7-yl)methacrylamide (**HOxMMA**): (a) chemical structure; (b) FT-IR; (c) ^1H NMR; (d) ^{13}C NMR (NMR solvent: DMSO-d₆).

S2.- Structure and stability constants of Fe(III)-8-hydroxyquinoline complexes (Turnquist and Sandell),¹² as well as a crystal structure of Fe(8-hydroxyquinoline)3 (Pech et al.)¹⁵

Table S1 depicts the species corresponding to the interaction between the Fe(III) and 8-hydroxyquinoline complexes. The complex Fe(8-hydroxyquinoline)₃ was found to crystallize with an ethanol molecule, which was not included in the coordination sphere of the iron. The O and N atoms of the bidentate ligands form three five-membered chelated rings, as shown in Figure S4.

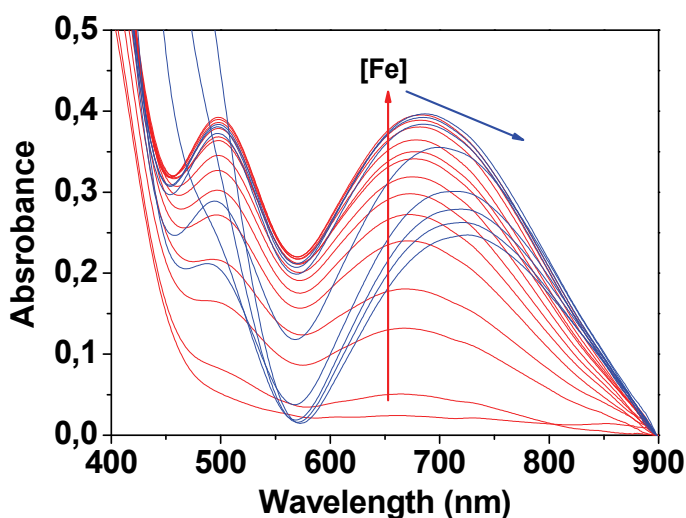
Table S1. Stability constants of Fe(III):8-hydroxyquinoline complexes (1:1, 1:2 and 1:3)

Complexes	Stability constants
$\text{Fe(III)} + \text{Ox}^- \rightleftharpoons \text{Fe Ox}^{2+}$	$K_1 = \frac{[\text{FeOx}^{2+}]}{[\text{Fe(III)}][\text{Ox}^-]} = 4.9 \times 10^{13}$
$\text{Fe Ox}^{2+} + \text{Ox}^- \rightleftharpoons \text{Fe Ox}_2^+$	$K_2 = \frac{[\text{FeOx}_2^+]}{[\text{FeOx}^{2+}][\text{Ox}^-]} = 4.2 \times 10^{12}$
$\text{Fe Ox}^+ + \text{Ox}^- \rightleftharpoons \text{Fe Ox}_3$	$K_3 = \frac{[\text{FeOx}_3]}{[\text{FeOx}_2^+][\text{Ox}^-]} = 3.9 \times 10^{10}$
 <p>Color development upon increase of the HOx concentration relative to a Fe(III) concentration of 2.5×10^{-4} M in EtOH:H₂O (1/1, v/v; pH = 2). From left to right, dominant species 1:1, 2:1, 3:1 (Fe:Ox).</p>	<p>Overall stability constant (K_s):</p> $\log K_s = \log K_1 K_2 K_3 = 36.9$

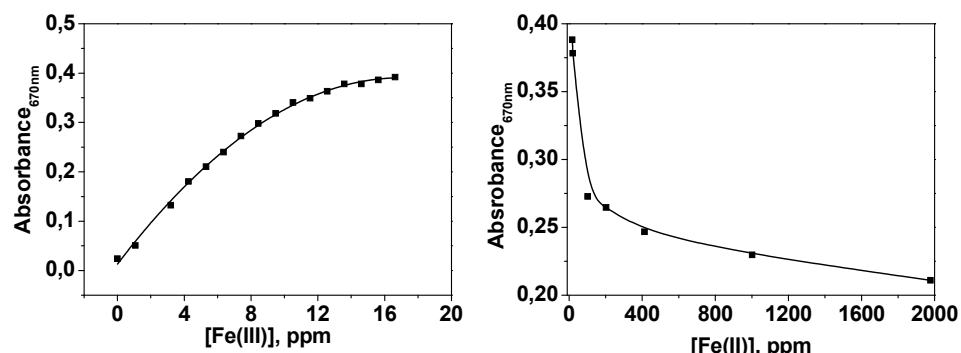
**Figure S4.** Representation of the crystal structure of the $\text{Fe(8-hydroxyquinoline)}_3$ complex, which was crystallized from $\text{CHCl}_3/\text{EtOH}$, as reported by Pech *et al.*¹⁵

S3.- Titration of Fe(III) with the monomer HOxMMA, copolymer LCp, and membrane Mem by means of UV/Vis spectroscopy

a)



b)



c)

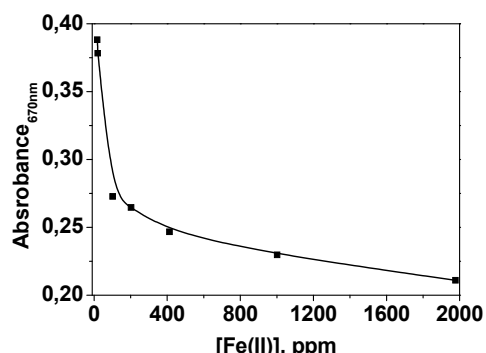
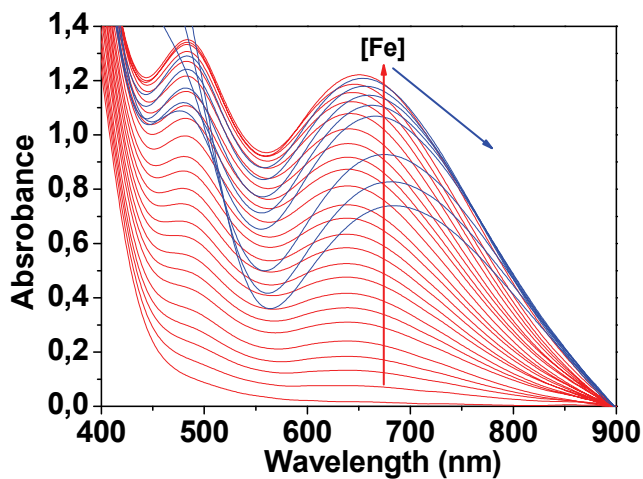
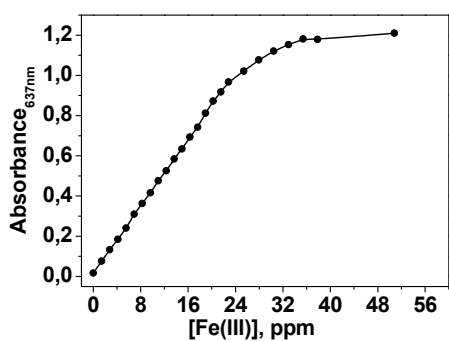


Figure S5. UV/Vis spectra taken during the titration of Fe(III) with HOxMMA, 3.82×10^{-4} M, with Fe(III) in ethanol:water (50/50 v/v) ($\text{pH} = 2$, KCl–HCl). The concentration of Fe(III) ranged from 1.91×10^{-5} to 3.53×10^{-2} M. a) UV/Vis spectra. Right: absorbance at 670 nm corresponding to lower -b-) and higher -c-) ferric iron concentrations (higher than 16 ppm). The top curve -b-) indicates the formation of ligand:metal 3:1 and 2:1 complexes, while the bottom curve -c-) indicates the displacement of the complex equilibrium toward the formation of a 1:1 complex. The titration was carried out in a quartz cuvette by adding increasing quantities of $\text{Fe}(\text{NO}_3)_3 \cdot 9\text{H}_2\text{O}$ in water solution.

a)



b)



c)

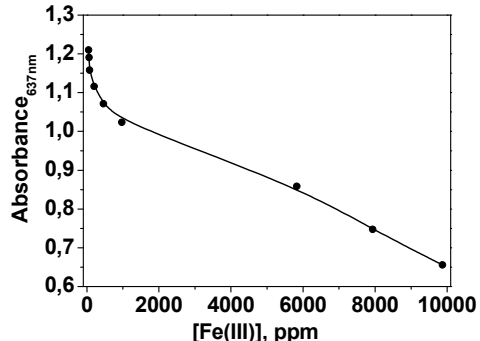
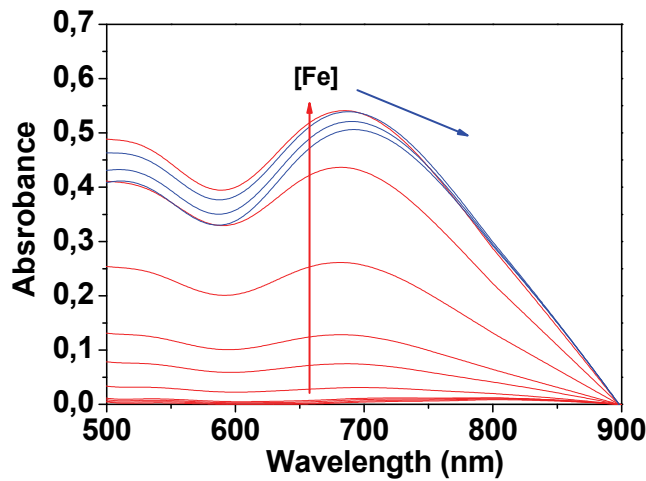
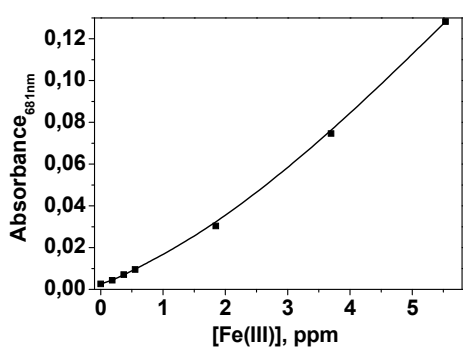


Figure S6. UV/Vis spectra taken during the titration of Fe(III) with **LCp** in water (pH = 2, KCl–HCl). The concentration of the **LCp** was 17.64 g/L, which corresponded to 22.3 milliequivalents of sensory motifs (HOx derivative) per liter. The concentration of Fe(III) ranged from 2.49×10^{-5} to 0.18 M. a): UV/Vis spectra. Right: absorbance at 637 nm corresponding to lower –b)- and higher –c)- ferric iron concentration (the former lower than 50 ppm and the later until 10000 ppm). The top curve -b)- indicates the formation of ligand:metal 3:1 and 2:1 complexes, while the bottom curve -c)- indicates the displacement of the complex equilibrium toward the formation of a 1:1 complex. The titration was performed in a quartz cuvette by adding increasing quantities of $\text{Fe}(\text{NO}_3)_3 \cdot 9\text{H}_2\text{O}$.

a)



b)



c)

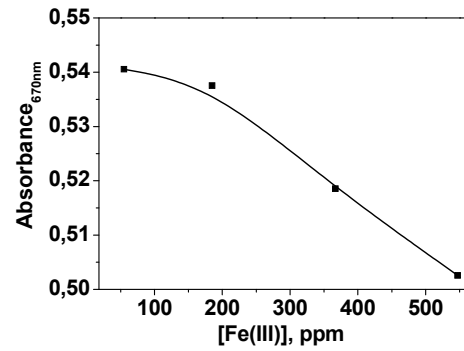


Figure S7. UV/Vis spectra taken during the titration of Fe(III) with **Mem** in water ($\text{pH} = 2$, KCl-HCl). The concentration of Fe(III) ranged from 3.30×10^{-6} to 9.77×10^{-3} M. a): UV/Vis spectra. Right: absorbance at 681 nm, which corresponded to lower -b-) and higher -c)- ferric iron concentrations (the former lower than 20 ppm and the later until 550 ppm). The top curve -b)- indicates the formation of ligand:metal 3:1 and 2:1 complexes, while the bottom curve -c)- indicates the displacement of the complex equilibrium toward the formation of 1:1 complex. The titration was performed by immersing the membrane in the water inside of the quartz cuvette and adding increasing quantities of $\text{Fe}(\text{NO}_3)_3 \cdot 9\text{H}_2\text{O}$.

S4.- Titration of Fe(III) in water with copolymer LCp via the analysis of the RGB parameters from each vial in a digital picture



[Fe (III)], ppm	R	G	B	PC
0.002	211	201	142	2.26
0.282	208	199	138	1.956
0.566	204	196	130	1.45
1.411	193	187	123	0.54
2.822	181	176	109	-0.72
4.234	169	165	102	-1.732
5.656	157	157	93	-2.71
P1	191	185	119	0.261
P2	175	169	105	-1.30

Standardized; eigenvalue = 2.99; % variance = 99.5%



[Fe (III)], ppm	R	G	B	PC
5.66	0.753	154	156	99
14.11	1.150	104	112	70
42.34	1.627	70	81	53
55.89	1.747	67	79	53
184.80	2.267	57	70	49
369.04	2.567	56	68	48
559.44	2.748	52	66	46
18.648 (P3)	1.271	95	105	64

Standardized; eigenvalue = 2.99; % variance = 99.8%

Figure S8. Principal component analysis (PCA) of the RGB data from the pictures of LCp solutions in water (pH = 2, KCl–HCl) that contained different quantities of Fe (III). The concentration of the LCp was 17.61 g/L, which corresponds to 22.3 milliequivalents of sensory motifs per litre. The titration was performed in the quartz cuvette by adding increasing quantities of $\text{Fe}(\text{NO}_3)_3 \cdot 9\text{H}_2\text{O}$. The test samples are labelled in red as P1, P2 and P3.

S5.- Sensory membrane or film Mem

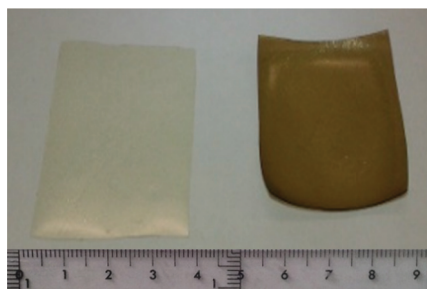


Figure S9. Dry sensory film, **Mem**, before (left) and after immersing into water containing 0.1 M of Fe(III).



Figure S10. Preparation of the sensory discs by cutting 5 mm diameter circles from the sensory membrane or film **Mem** with an office paper punch.

S6.- Schematic procedure followed to quantify Fe(III) in water media by a scalable RGB technique

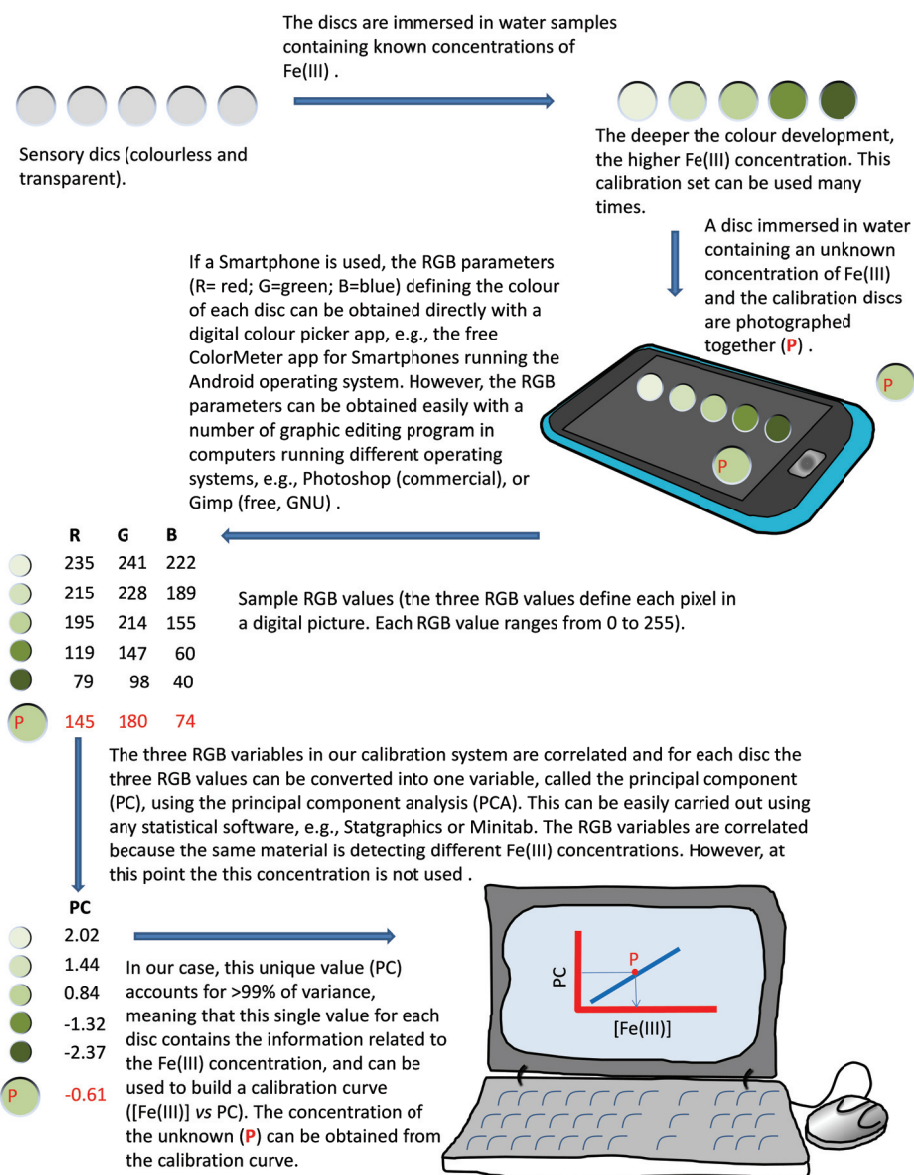


Figure S11. Schematic procedure followed to quantify Fe(III) in water media by a scalable RGB technique.

S7.- Titration of Fe(III) in water with the discs that were cut from sensory membrane Mem via the analysis of the RGB parameters for each vial within a digital picture



[Fe(III)], ppm	Log [Fe(III)]	R	G	B	PC
5.60x10 ⁻²	-1.252	36	48	70	-2.01
2.80x10 ⁻¹	-0.553	46	57	77	-1.06
1.40	0.146	58	66	81	-0.25
5.60	0.748	73	79	87	0.88
56.00	1.748	96	96	95	2.44

Standardized; eigenvalue = 2.99; % variance = 99.7%

Figure S12. Principal component analysis (PCA) of the RGB data from pictures of the Mem sensory discs that were treated with aqueous solutions (pH = 2, KCl-HCl) containing different quantities of Fe (III).

S8.- Titration of Fe(III) in wine with discs that were cut from sensory membrane Mem via the analysis of the RGB parameters for each vial within a digital picture



Brand name	Winery	Appellation of origin	Fe, ppm
Charquiño,2011	Albariño	Rías Baixas	1.002
Albarín, 2011	Pardevalles	Tierra de León	3.436
Viura, 2009	Faustino	Rioja	1.157
Don García Blanco	JGC	Plonk, no appellation	2.320

Figure S13. White wine used for the Fe(III) measurements. The iron content was measured with flame atomic absorption spectrometry.



[Fe(III)], ppm	Log [Fe(III)]	R	G	B	PC
1.002	0.001	57	70	78	-1.68
3.446	0.536	78	84	87	1.89
1.157	0.063	59	71	80	-1.22
2.320	0.366	71	80	86	1.01

Standardized; eigenvalue = 2.97; % variance = 99.0%

Figure S14. Principal component analysis (PCA) of the RGB data from pictures of the **Mem** sensory discs after being immersing in white wine without further treatment. The concentration of iron in wine was determined with flame atomic absorption spectroscopy.

S9.- Titration of Fe(III) in blood serum with discs cut from sensory membrane Mem via the analysis of the RGB parameters for each vial within a digital picture



[Fe(III)], ppm	Log [Fe(III)]	R	G	B	PC
1.10	0.041	42	51	72	-1.87
1.86	0.270	49	58	76	-0.94
2.60	0.415	54	63	79	-0.27
3.32	0.521	60	68	81	0.36
10.60	1.025	79	85	91	2.72

Standardized; eigenvalue = 3.00; % variance = 99.9%

Figure S15. Principal component analysis (PCA) of the RGB data from pictures of **Mem** sensory discs that were immersed in reconstituted human blood serum without further treatment. Commercial lyophilized human sera with constituents added as required to obtain desired component levels were used (PreciControl ClinChem Multi 1 and 2, Cobas®, Roche).

Table S2. Concentration of selected components of the PreciControl ClinChem Multi 1 and 2 (Cobas®, Productos Roche).[#]

Short name/Component	MULTI 1		MULTI 2	
	Value	Unit	Value	Unit
GLUH2/Glucose	1020	ppm	2340	ppm
GLDH/Glutamate dehydrogenase	260	U/L	443	U/L
GGT/Glutamyltransferase gamma	538	U/L	2370	U/L
HDLC3/HDL-Cholesterol	288	ppm	615	ppm
HGLOB/Haptoglobin	873	ppm	1240	ppm
HBDH/Hydroxybutyrate dehydrogenase alpha	1700	U/L	3320	U/L
IGA/Immunoglobulin A	1470	ppm	2290	ppm
IGG/Immunoglobulin G	7470	ppm	11900	ppm
IGM/Immunoglobulin M	729	ppm	1090	ppm
Fe/Iron	1.1	ppm	2.45	ppm
KAPPA/KAPPA	1840	ppm	3030	ppm
LDLC2/LDL-Cholesterol	557	ppm	963	ppm
LAC/Lactate	145	ppm	308	ppm
LDH/Lactate dehydrogenase	1740	U/L	3260	U/L
LAMBD/Lambda	1020	ppm	1690	ppm
LIP/Lipase	46.5	U/L	1030	U/L
MG/Magnesium	19.8	ppm	32.1	ppm
PHOS/Phosphate (inorganic)	38.1	ppm	64.5	ppm
K/Potassium	143	ppm	251	ppm
PALB2/Prealbumin	187	ppm	285	ppm
Na/Sodium	2620	ppm	3170	ppm
TP/Total protein	48800	ppm	75400	ppm
TRSF2/Transferrin	2020	ppm	3520	ppm
TG/Triglycerides	1090	ppm	2060	ppm
UREA/Urea	417	ppm	1210	ppm
UA/Uric acid	54.6	ppm	109	ppm

Food and Drug administration decision summary report - PreciControl ClinChem Multi 1 and 2, device description section:¹ "The PreciControl ClinChem Multi 1 and 2 consist of lyophilized human sera with constituents added as required to obtain desired component levels. Concentrations of the components in the controls have been adjusted to represent normal and pathological levels. The concentrations of the components in the controls are lot-specific.
All products derived from human blood are prepared exclusively from the blood of donors tested individually and shown to be free from HBsAg and antibodies to HCV and HIV. The testing methods applied were FDA-approved".

¹ FDA Decision on novel multi-analyte control device, document downloaded from FDA web page <http://www.accessdata.fda.gov/scripts/cdrh/devicesatfda/index.cfm?db=pmn&id=K102016>, document link: http://www.accessdata.fda.gov/cdrh_docs/reviews/K102016.pdf. Date prepared: July 16, 2010.

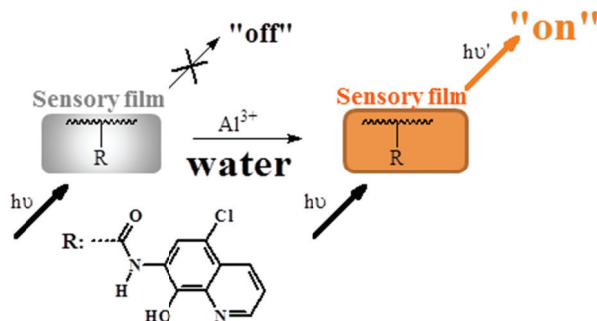
Selective and sensitive detection of aluminium ions in water via fluorescence “turn-on” with both solid and water soluble sensory polymer substrates

Selective and sensitive detection of aluminium ions in water via fluorescence “turn-on” with both solid and water soluble sensory polymer substrates

Saúl Vallejos, Asunción Muñoz, Saturnino Ibeas, Felipe Serna, Félix Clemente García and José Miguel García.*

Departamento de Química, Facultad de Ciencias, Universidad de Burgos, Plaza de Misael Bañuelos s/n, 09001 Burgos, Spain. Fax: (+) 34 947 258 831, Tel: (+) 34 947 258 085. E-mail: jmiguel@ubu.es

Graphical abstract



Abstract

A solid substrate comprised of a cross-linked polymer network is shaped as a film with gel-like behaviour and is used to detect aluminium ions in water; concurrently, a water soluble sensory polymer synthesised toward the same purpose is also discussed. The detection in both systems was achieved via fluorescence “turn-on”. The limits of detection for Al(III) were 1.6 and 25 ppb for the former and latter materials, respectively; these levels are significantly lower than the EPA recommendations for drinking water.

Keywords

Sensory polymer, aluminium sensing, fluorescence chemosensor, fluorescence turn-on

Journal of Hazardous materials. 2014, 276, 52-57

1. Introduction

Aluminium is the most abundant metallic element in the Earth's crust, accounting for more than 8% by weight; it is also the third most abundant element overall after oxygen and silicon.

Aluminium has had a tremendous impact on the socioeconomic development of humans, and it has been used as a pure metal, alloys, and trivalent ion derivatives, making it ubiquitous in industry, new technological devices, food and drug preservatives and additives, drugs, water treatment, housewares, personal hygiene products, and many others.

Due to its extensive use, aluminium also causes the acidification of soils and aqueous media; Al(III) is potentially phytotoxic and toxic toward aquatic biota.¹⁻³ This ionic form is also a major concern for human health because it is believed that it can damage the nervous system, tissues and cells, leading to its implication as a causative factor for Alzheimer's and other diseases, such as dementia, encephalopathy, Parkinson's, various types of cancer, and others.⁴⁻¹³

Within this context, fluorescence chemosensors that can facilitate the inexpensive, rapid and facile detection of Al(III) are important for use in the medical and environmental fields. However, the fluorescence detection and quantification of Al(III) in organic¹⁴⁻²¹ and aqueous/organic²²⁻²⁴ media have rarely been described; examples of this highly interesting sensing technique in fully aqueous media are even scarcer,²⁵ and polymer chemosensors have not been applied in Al(III) dip-in solid sensory kits.

Consequently, in this work we report the development of intelligent materials that exhibit a selective fluorescence "turn-on" response toward aluminium ions in pure water. Thus, the copolymerisation of an acrylic with a hydroxyquinoline moiety generated both a water soluble linear copolymer and a solid film-shaped polymer membrane with excellent sensing performance toward Al(III) aqueous media.

2. Experimental Section

2.1. Materials

All of the materials and solvents were commercially available and used as received unless otherwise indicated: 2-cyano-2-propyl dodecyl trithiocarbonate (RAFT agent, Aldrich, 97%), *N*-vinylpyrrolidone (**VP**, Aldrich, 99%), 2-hydroxyethylacrylate (**2HEA**, Aldrich, 96%), ethylene glycol dimethacrylate (**EGDMA**, Aldrich, 98%), aluminium nitrate nonahydrate (Aldrich, 98%), ammonium nitrate (Aldrich, 98%), barium chloride dehydrate (LabKem, 99%), cadmium nitrate tetrahydrate (Alfa Aesar, 98.5%), cerium(III) nitrate hexahydrate (Alfa Aesar, 99.5%), caesium nitrate (Fluka, 99%), cobalt(II) nitrate hexahydrate (LabKem, 98%), copper(II) nitrate trihydrate (Aldrich, 98%), dysprosium(III) nitrate hydrate (Alfa Aesar, 99.9%), iron(II) sulphate heptahydrate (Aldrich, 99%), iron(III) nitrate nonahydrate (Aldrich, 98%), lanthanum(III) nitrate hexahydrate (Alfa Aesar, 99.9%), lead(II) nitrate (Fluka, 99%), lithium chloride (Aldrich, 99%), magnesium nitrate hexahydrate (LabKem, 98%), manganese (II) nitrate hexahydrate (Alfa Aesar, 98%), mercury(II) nitrate monohydrate (Scharlab, 99%), neodymium(III) nitrate hexahydrate (Alfa Aesar, 99.9%), nickel(II) nitrate hexahydrate (VWR, 99%), platinum(II) chloride (Aldrich, 98%), chromium(III) nitrate nonahydrate (Alfa Aesar, 98.5%), potassium dichromate (Aldrich, 99.5%), potassium nitrate (Aldrich, 99%), rubidium nitrate (Aldrich, 99.7%), samarium(III) nitrate hexahydrate (Alfa Aesar, 99.9%), silver nitrate (LabKem, 99%), sodium nitrate (LabKem, 99%), strontium nitrate (Alfa Aesar, 98%), tin (II) chloride (Aldrich, 98%), zinc nitrate hexahydrate (Aldrich, 98%), and zirconium(IV) chloride (Alfa Aesar, 98%).

2.2. Measurements and instrumentation

The ^{27}Al NMR spectra were recorded with a Varian Inova 400 spectrometer operating at 104.21 MHz. Deuterium oxide (D_2O) was used as the solvent. The fluorescence spectra were recorded with an F-7000 Hitachi Fluorescence spectrophotometer. The thermogravimetric analysis (TGA) data were recorded

using a 4-5 mg sample under a synthetic air atmosphere with a TA Instrument Q50 TGA analyser at $10^{\circ}\text{C min}^{-1}$.

The Al(III) titration experiments with the linear copolymer (**LCp**) were carried out as follows: solutions **LCp** ($2.65 \cdot 10^{-2}$ mEq/L of sensory motifs) in Millipore-Q water (pH = 4.5, buffered with NaOH/AcOH) were prepared and transferred to the measuring cuvette. The concentration of Al(III) was progressively increased by adding cumulative volumes of 1.039 M aqueous stock (Millipore-Q, pH = 4.5) solutions of $\text{Al}(\text{NO}_3)_3 \cdot 9\text{H}_2\text{O}$. The fluorescence spectra were taken 5 min after each addition.

The Al(III) titration experiments with the sensory membrane (**Mem**) were carried out as follows: the membrane was dipped into Millipore-Q water (pH = 4.5, buffered with NaOH/AcOH) in the measuring cuvette. The concentration of Al(III) was then progressively increased by adding cumulative volumes of 1.039 M stock Millipore-Q water (pH = 4.5) solutions of $\text{Al}(\text{NO}_3)_3 \cdot 9\text{H}_2\text{O}$. The fluorescence spectra were taken 30 min after each addition to allow the system to reach equilibrium.

The quantum yield (F) of the monomer complex **HOxMMA-Al(III)**, prepared from a 3×10^{-5} M methanolic solution of **HOxMMA** after adding an equimolar concentration of Al(III), were measured in dimethylsulphoxide using quinine sulphate in sulphuric acid (0.05 M) as a reference standard.²⁶

2.3. Monomer synthesis

The methacrylamide monomer *N*-(5-chloro-8-hydroxyquinolin-7-yl)methacrylamide (**HOxMMA**) was synthesised from inexpensive and readily available chemicals, starting with 5-chloro-8-hydroxyquinoline (Aldrich, 95%), as described previously.²⁷

2.4. Polymer synthesis

The linear copolymer (**LCp**) was prepared using a radical polymerisation of the hydrophilic monomers **VP** and **2HEA** and the sensing monomer (**HOxMMA**) in a

74/25/1 molar ratio (**VP/2HEA/HOxMMA**). A 100-mL three-necked flask equipped with a magnetic stirrer, a nitrogen gas inlet, and a reflux condenser was charged with a solution of 0.4 mmol (105 mg) of **HOxMMA**, 9.9 mmol (1.15 g) of **2HEA** and 29.7 mmol (3.3 g) of **VP** in DMF (40 mL) under nitrogen blanket. Subsequently, AIBN (66 mg, 0.4 mmol) was added, and the solution was heated to 60°C. After stirring for 4 h under nitrogen, the solution was allowed to cool before being added dropwise to diethyl ether (300 mL) with vigorous stirring, yielding a brown precipitate. The polymer was purified using two cycles of a solution/precipitation procedure with methanol (10 mL) as the solvent and diethyl ether (100 mL) as the non-solvent. It was finally dried overnight in a vacuum oven at 60 °C. Yield: 85% (4 g).

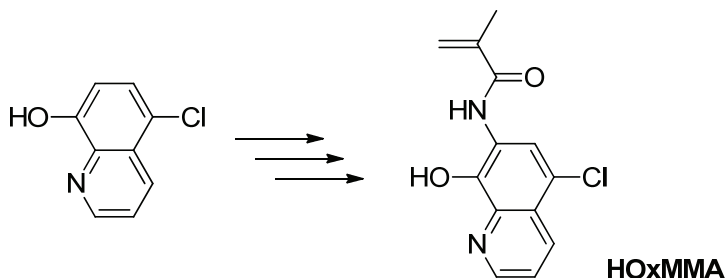
The cross-linked film or membrane (**Mem**) was prepared using atom-transfer radical polymerisation (ATRP) with **VP**, **2HEA**, **HOxMMA** and **EGDMA** as a cross-linking agent in a comonomer molar ratio of 74/25/1/10 (**VP/2HEA/HOxMMA/EGDMA**). AIBN (1 wt %) was used as the thermal radical initiator, and 2-cyano-2-propyl dodecyl trithiocarbonate was the RAFT agent (50 mg per 65.5 mmol of comonomers). Afterward, the bulk radical polymerisation reaction was carried out in a 200 mm thick silanised glass mould in an oxygen-free atmosphere at 60°C for 4 h.

A hybrid **Mem-Al(III)** membrane was prepared by treating a sensory disc cut from the membrane **Mem** (weight = 10 mg) with 10 mL of water (pH = 4.5) containing 0.1 M Al(III) overnight. Afterward, the disc was washed 5 times dipping the membrane each time for 12 h in 50 mL of MilliQ. Finally, the membrane was dried at rt for 24 h.

3. Results and discussion

In this work, we report on the design and preparation of intelligent materials that exhibit a selective fluorescence “turn-on” response toward aluminium ions in pure water. Consequently, the copolymerisation of an acrylic monomer called *N*-(5-chloro-8-hydroxyquinolin-7-yl)methacrylamide (**HOxMMA**) (Scheme 1) with

hydrophilic comonomers generated a water soluble linear copolymer (**LCp**) and a film-shaped polymer membrane (**Msen**) with gel-like behaviour.



Scheme 1. Monomer precursor and structure.

3.1. Sensory material preparation and characterization

The preparation of **HOxMMA** was achieved from commercially available 8-hydroxyquinoline (HOx); this compound is commonly known as oxine.²⁸ HOx is an excellent metal chelating agent for aluminium; the deprotonated form of this compound generates Al(III)/Ox⁻ complexes with 1:1, 1:2 and 1:3 stoichiometric ratios, as shown in the Supplementary Data (Table S1). The published logarithm of the overall stability constant ranges from 30.6 to 32.3²⁹ and tris-(8-hydroxyquinolinato)aluminium(III) was crystallised in a meridional conformation with the aluminium atom coordinated to the bidentate 8-quinolato ligands in a distorted octahedral configuration, as shown in Figure S1 (Supplementary Data).³⁰ The formation of complexes of oxine derivatives with Al(III) in solution is accompanied by a significant increment in the fluorescence intensity, a so called fluorescence “turn-on”. The nature of the lack of fluorescence in aqueous or organic solutions of oxine derivatives has been ascribed to a photoinduced tautomerization reaction followed by deexcitation of the tautomer which occurs mainly via a nonradiative route pathway.^{31,32} On the other hand, the interaction with different metals to render the complexes impairs this photoprocess giving rise to the observed fluorescence enhancement.

The interaction of **HOxMMA** with Al(III) followed the same pattern and the formation of the AlOxMMA₃ complex was derived from the Job's plot in

Figure S2 (Supplementary Data). The Job's plot showed a maximum that appeared at a mole fraction for HOxMMA (X_{HOxMMA}) of 0.75, clearly indicating the formation of complexes with a 1:3 stoichiometry. The formation of the complex could also be followed by ^{27}Al NMR (Figure S3, Supplementary Data).³³

Aqueous solutions of **LCp** are non-fluorescent but become fluorescent after adding aluminium ions, following an "off-on" pattern, as shown in Figure 1. The fluorescence intensity is proportional to the Al(III) concentration, enabling the generation of titration curves.

In addition, the 5 mm sensory discs cut from the non-fluorescent membrane (**Msen**) also exhibited sensory behaviour; this material becomes fluorescent upon immersion in water containing aluminium ions and can also generate titration curves for Al(III).

Furthermore, a hybrid organic-inorganic membrane (**Mem-Al(III)**) could be obtained after immersing **Msen** in water containing a relatively high concentration of Al(III). These types of materials are promising for luminescent conversion applications (LUCO), and the CIE chromaticity coordinates upon irradiation with a conventional 365 nm UV light were $x = 0.32$ and $y = 0.61$ (Supplementary Data, Section S5 and Figure S11). However, the quantum yield of the **HOxMMA-Al(III)** complex was low, $f_{HOxMMA-Al(III)} = 0.006$, and it must be improved for these applications. Because this material was obtained by immersing **Mem** in water containing a large excess of Al(III), the complexes formed on each chain pendant quinolato moiety with Al(III) corresponded to a 1:1 stoichiometry, as revealed by the weight percentage of Al_2O_3 (0.5%) obtained after heating the treated hybrid membrane to 800°C in air (see the thermogravimetric analysis, TGA, Supplementary Data, Figure S12). The TGA analysis also demonstrated the good thermal performance of the material, exhibiting 5% and 10% weight losses at 335 and 364°C, respectively.

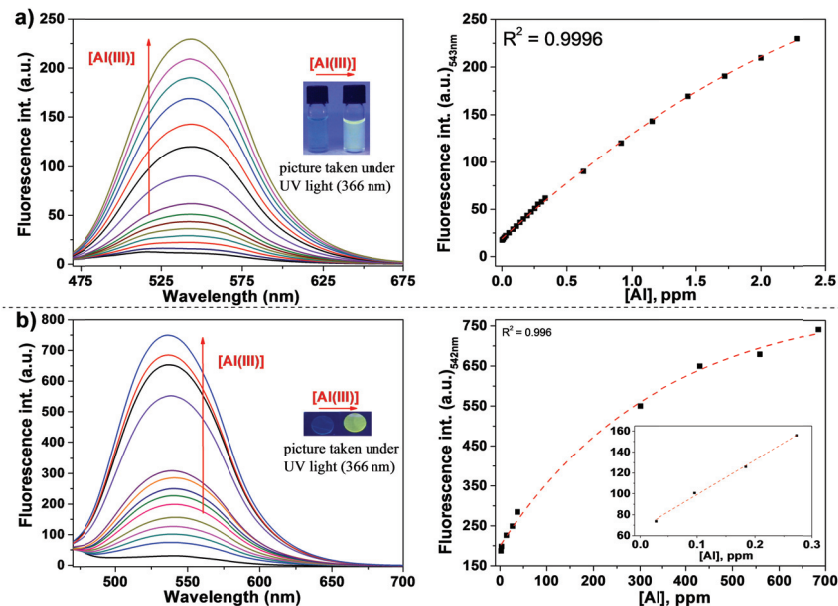
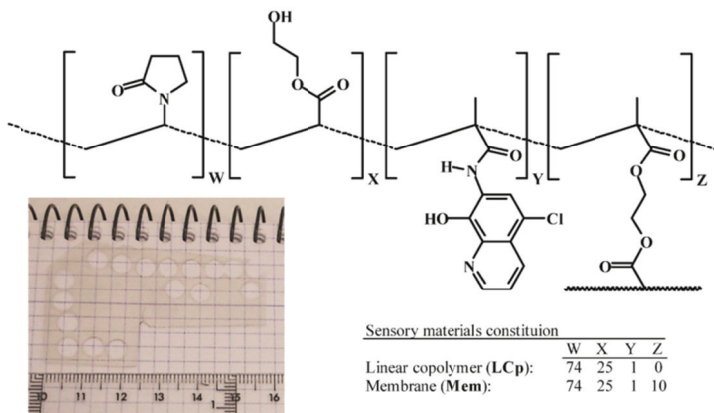


Figure 1. Titration of Al(III) in water using the fluorescence technique: a) with **LCp** in an aqueous solution (left: selected fluorescence spectra; right: titration curve Al(III) concentration vs. fluorescence intensity at 543 nm). The concentration of the **LCp** was 30.2 g/L, corresponding to 2.65 mEq/L of the sensory motif (**HOxMMA**); b) solid discs of **Mem** (left: selected fluorescence spectra; right: titration curve Al(III) concentration vs. fluorescence intensity at 542 nm, inset: expansion at the lower range of concentrations). Conditions: MilliQ water was buffered (NaOH/AcOH) at pH = 4.5; excitation slit = 10 nm; emission slit = 10 nm; excitation wavelength = 439 nm; scan speed = 12000 nm/min; the Al(III) concentration was increased every half hour.



Scheme 2. Linear copolymer (**LCp**) and membrane (**Mem**) structures. A picture of the membrane taken on a notebook that shows the aspect ratio and the transparency of the sensory material; the holes correspond to where the 5 mm discs were removed for the sensory kits.

Future applications of sensory systems in the real world depend on critical parameters, such as response times, selectivity and sensitivity discussed below.

3.2. Response time

The response times were 3 and 12 min for the aqueous **LCp** solution at the millimolar range for Al(III). These values were measured using the fluorescence technique and correspond to the time needed to achieve 90 and 99% fluorescence, respectively (see Figure S4). However, the response times were 15 and 25 min for **Mem** (see Supplementary Data, Figure S5). Unfortunately, these times are significantly increased at higher concentrations (see Supplementary Data, Figure S6). However, these times can be lowered by 90% after adding a drop with a known volume of the Al(III) sample directly to the membrane, avoiding the dipping process (Table S2).

3.3. Substrate selectivity and interference study

The selectivity of the sensory materials was tested with anions and cations. Aqueous solutions containing numerous anions caused no variations in the fluorescence behaviour of **LCp** in water at pH = 4.5 (see Supplementary Data, Figure S7). However, among a broad set of possible interfering cations [NH_4^+ , Ba(II), Cd(II), Ce(III), Cs(I), Co(II), Cu(II), Dy(III), La(III), Pb(II), Li(I), Mg(II), Mn(II), Hg(II), Nd(III), Ni(II), Pt(II), Cr(III), Cr(VI), K(I), Rb(I), Sm(III), Ag(I), Na(I), Sr(II), Sn(II), Zn(II) and Zr(IV)], only the individual addition of La(III), Zr(IV), Zn(II), Cd(II) and Pb(II) induced fluorescence, although the concomitant addition of these cations with Al(III) caused no interference (Figure S8), meaning that the stability constant of the aluminium complexes is much higher than that of other cations. This behaviour can also be observed during the 3D fluorescence experiments (Figure 2). The characteristic spectra of the aqueous **LCp** solutions with Al(III) are not distorted after adding a cocktail of the cations mentioned above. Interestingly, the individual interactions of **LCp** with the cations that induced fluorescence generate different 3D spectra that are characteristic of each cation (Supplementary Data, Figure S10).

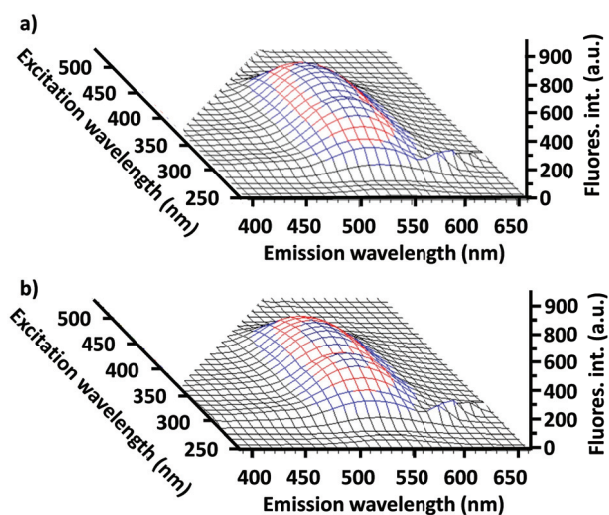


Figure 2. Interference study (excluding Fe(III)). 3D fluorescence plot of an aqueous **LCp** solution a) after adding $2.65 \cdot 10^{-4}$ M Al(III) and b) after adding a mixture of cations that caused individual enhancements to the fluorescence intensity (Al(III) + La(III) + Zr (IV) + Zn(II) + Cd(II) + Pb(II) at $2.65 \cdot 10^{-4}$ M for each species). The concentration of the **LCp** was 30.2 g/L, corresponding to 2.65 mEq/L of the sensory motif (**HOxMMA**). Measuring conditions: excitation slit = 10 nm; emission slit = 10 nm; scan speed = 30000 nm/min; the solutions of the **LCp** and the salts were prepared with MilliQ water buffered (NaOH/AcOH) at pH = 4.5. The cations were added as their nitrate, chloride or sulphate salts.

However, ferric iron provides true interference, as usually occurs in most Al(III) chemosensory systems. The interaction of Fe(III) with the oxime residue of **LCp** generates a complex with a similar structure to that of Al(III) and also with high stability constants. This complex is non-fluorescent. However, if Al(III) and Fe(III) are present together, both metal ions form complexes, producing a lower fluorescence intensity than that observed with a solution containing only Al(III) (Supplementary Data, Figure S9). Moreover, these materials have been described as sensory colorimetric substrates for the detection of Fe(III) [28] and the presence of this interfering cation can be visually observed and quantified using a UV/Vis technique. Once the concentration of Fe(III) is known, the concentration of Al(III) can be calculated using the titration curves for Al(III) with different quantities of Fe(III), overcoming the interference induced by the ferric ion (Figure 3).

3.4. Substrate sensitivity

Regarding the sensitivity of the systems, a broad range of concentrations of Al(III) in water were measured using **LCp** in water: 1.6 ppb to 2.3 ppm, covering the EPA³⁴ recommended ranges for the Al(III) content in drinking water (Figure 1). The limit of detection (LOD) and the limit of quantification (LOQ)³⁵ were 1.6 and 4.9 ppb, respectively. On the other hand, the sensory material **Mem** could detect Al(III) concentrations ranging from 27 ppb to 690 ppm, covering a broad concentration range with a LOD and a LOQ of 25 and 75 ppb, respectively.

Conclusions

In summary, we have prepared a water soluble sensory polymer for the “off-on” fluorogenic detection of Al(III) in water, specifically a hydrophilic polymer containing hydroxyquinoline sensory moieties on the pendant chain. The limit of Al(III) detection was 1.6 ppb. In addition, the same sensory substructures were used to prepare a gel-like film used as the sensory polymer in a solid kit for the “off-on” fluorogenic detection of Al(III); Al(III) was detected after immersing 5 mm discs cut from the membrane in watery solutions for a short time (i.e., 15 min) to detect millimolar concentrations of the cation.

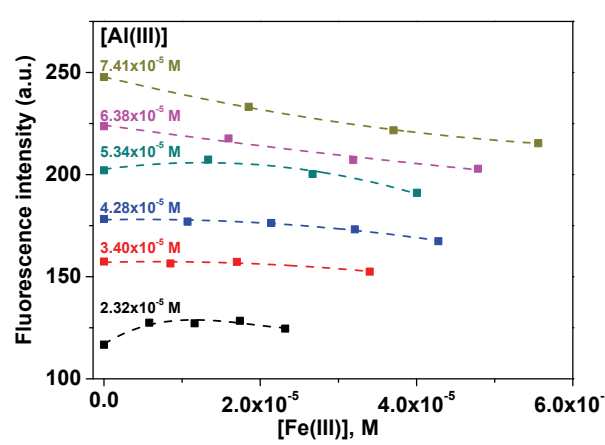


Figure 3. Titration of Al(III) in water using the fluorescence technique with an aqueous LCp solution containing different concentrations of Fe(III). The concentration of the LCp was 30.2 g/L, corresponding to 2.65 milliequivalents of the sensory motif (HOxMMA) per litre. Conditions: MilliQ water was buffered at pH = 4.5 (NaOH/AcOH); excitation slit = 10 nm; emission slit = 10 nm; excitation wavelength = 439 nm; scan speed = 12000 nm/min.

The limit of Al(III) detection was 25 ppb; this value is well below the EPA recommendations for drinking water. A unique interfering effect was found with Fe(III), and this obstacle could be circumvented by preparing titration curves of Al(III) in the presence of known quantities of Fe(III). Consequently, these systems allow for the colorimetric detection and quantification of ferric iron in addition to fluorogenic Al(III) detection.

Acknowledgments

We gratefully acknowledge the financial support provided by the Spanish Ministerio de Economía y Competitividad-Feder (MAT2011-22544) and by the Consejería de Educación - Junta de Castilla y León (BU232U13).

Appendix A. Supplementary data

Supplementary data available: experimental procedure, characterisation, response time, interaction with other cations, selectivity, interference, and CIE chromaticity coordinate graphs and data.

References

-
- 1 E. Álvarez, M. L. Fernández-Marcos, C. Monterroso, M. J. Fernández-Sanjurjo, Application of aluminium toxicity indices to soils under various forest species, *Forest Ecol. Manage.* 211 (2005) 227-239.
 - 2 J. Barceló, C. Poschenrieder, Fast root growth responses, root exudates, and internal detoxification as clues to the mechanisms of aluminium toxicity and resistance: a review, *Environ. Exp. Bot.* 48 (2002) 75-92.
 - 3 N. E. W. Alstad, B. M. Kjelsberg, L. A. Vøllestad, E. Lydersen, A. B. S. Poléo, The significance of water ionic strength on aluminium toxicity in brown trout (*Salmo trutta* L.), *Environ. Pollut.* 133 (2005) 333-342.
 - 4 C. S. Cronan, W. J. Walker, P. R. Bloom, Predicting aqueous aluminium concentrations in natural waters, *Nature* 324 (1986) 140-143.
 - 5 P. Nayak, *Environ. Res.*, 2002, 89, 101-115; G. D. Fasman, Aluminum and Alzheimer's disease: model studies, *Coord. Chem. Rev.* 149 (1996) 125-165.
 - 6 G. Berthon, Aluminium speciation in relation to aluminium bioavailability, metabolism and toxicity, *Coord. Chem. Rev.* 228 (2002) 319-341.

- 7 A. M. Pierides, W. G. Edwards Jr., U. X. Cullum Jr., J. T. McCall, H. A. Ellis, Hemodialysis encephalopathy with osteomalacic fractures and muscle weakness, *Kidney Int.* 18 (1980) 115-124.
- 8 A. C. Alfrey, Aluminum, *Adv. Clin. Chem.* 23 (1983) 69-91.
- 9 D. P. Perl, D. C. Gajdusek, R. M. Garruto, R. T. Yanagihara, C. J. Gibbs, *Science* 217 (1982) 1053-1055.
- 10 D. P. Perl, A. R. Brody, Alzheimer's disease: X-ray spectrometric evidence of aluminum accumulation in neurofibrillary tangle-bearing neurons, *Science* 208 (1980) 297-299.
- 11 W. M. El-Sayed, M. A. Al-Kahtani, A. M. Abdel-Moneim, Prophylactic and therapeutic effects of taurine against aluminum-induced acute hepatotoxicity in mice, *J. Hazard. Mater.* 192 (2011) 880-886.
- 12 A. Shokrollahi, M. Ghaedi, M. S. Niband, H.R. Rajabi, Selective and sensitive spectrophotometric method for determination of sub-micro-molar amounts of aluminium ion, *J. Hazard. Mater.* 151 (2008) 642-648.
- 13 K. P. Kepp, Bioinorganic chemistry of Alzheimer's disease, *Chem. Rev.* 112 (2012) 5193-5239.
- 14 H. M. Park, B. N. Oh, J. H. Kim, W. Qiong, I. H. Hwang, K.-D. Jung, C. Kim, J. Kim, Fluorescent chemosensor based-on naphthol-quinoline for selective detection of aluminum ions, *Tetrahedron Lett.* 52 (2011) 5581-5584.
- 15 S. H. Kim, H. S. Choi, J. Kim, S. Joong, D. T. Quang, J. S. Kim, Novel optical/electrochemical selective 1,2,3-triazole ring-appended chemosensor for the Al³⁺ ion, *Org. Lett.* 12 (2010) 560-563.
- 16 D. Maity, T. Govindaraju, Pyrrolidine constrained bipyridyl-dansyl click fluoroionophore as selective Al³⁺-sensor, *Chem. Commun.* 46 (2010) 4499-4501.
- 17 X.-Y. Cheng, M.-F. Wang, Z.-Y. Yang, Y. Li, T.-R. Li, C.-J. Liu, Q.-X. Zhou, A highly sensitive and selective Schiff base fluorescent chemodosimeter for aluminum(III), *J. Coord. Chem.* 66 (2013) 1847-1853.
- 18 J. Lee, H. Kim, S. Kim, J. Y. Noh, E. J. Song, C. Kim, J. Kim, Fluorescent dye containing phenol-pyridyl for selective detection of aluminum ions, *Dyes Pigm.* 96 (2013) 590-594.
- 19 Z.-C. Liao, Z.-Y. Yang, Y. Li, B.-D. Wang, Q.-X. Zhou, A simple structure fluorescent chemosensor for high selectivity and sensitivity of aluminum ions, *Dyes Pigm.* 97 (2013) 124-128.
- 20 D. Maity, T. Govindaraju, Conformationally Constrained (Coumarin-Triazolyl-Bipyridyl) Click Fluoroionophore as a Selective Al³⁺ Sensor, *Inorg. Chem.* 49 (2010) 7229-7231.
- 21 D. Maity, T. Govindaraju, Naphthaldehyde-Urea/Thiourea Conjugates as Turn-On Fluorescent Probes for Al³⁺ Based on Restricted C=N Isomerization, *Eur. J. Inorg. Chem.* (2011), 5479-5489.
- 22 Y.-W. Wang, M.-X. Yu, Y.-H. Yu, Z.-P. Bai, Z. Shen, F.-Y. Li, X.-Z. You, A colorimetric and fluorescent turn-on chemosensor for Al³⁺ and its application in bioimaging, *Tetrahedron Lett.* 50 (2009) 6169-6172.
- 23 S. B. Maity, P. K. Bharadwaj, A chemosensor built with rhodamine derivatives appended to an aromatic platform via 1,2,3-triazoles: dual detection of aluminum(III) and fluoride/acetate ions, *Inorg. Chem.* 52 (2013) 1161-1163.
- 24 T.-H. Ma, M. Dong, Y.-M. Dong, Y.-W. Wang, Y. Peng, A unique water-tuning dual-channel fluorescence-enhanced sensor for aluminum ions based on a hybrid ligand from a 1,1'-binaphthyl scaffold and an amino acid, *Chem. Eur. J.* 16 (2010) 10313-10318.
- 25 V. D. Suryawanshi, A. H. Gore, P. R. Dongare, P. V. Anbhule, S. R. Patil, G. B. Kolekar, A novel pyrimidine derivative as a fluorescent chemosensor for highly selective detection of aluminum (III) in aqueous media, *Spectrochim. Acta A* 114 (2013) 681-686;

- 26 A. M. Brouwer, Pure Appl. Chem., 2011, 83, 2213-2228.
 - 27 S. Vallejos, A. Muñoz, S. Ibeas, F. Serna, F. C. García, J. M. García, J. Mater. Chem. A, 2013, 1, 15435-15441.
 - 28 S. Vallejos, A. Muñoz, S. Ibeas, F. Serna, F. C. García, J. M. García, Solid sensory polymer substrates for the quantification of iron in blood, wine and water by a scalable RGB technique, J. Mater. Chem. A 1 (2013) 15435-15441.
 - 29 R. M. Smith, A. E. Martel, R. J. Motekaitis, NIST Standard Reference Database 46, NIST Critically Selected Stability Constants of Metal Complexes Database, Version 8.0; National Institute of Standards and Technology (NIST), Gaithersburg, MD, 2004.
 - 30 M. Ul-Haque, W. Horne, S. J. Lyle, Crystal and molecular structure of tris-(8-quinolinolato)aluminium(III) containing occluded acetonylacetone, J. Cryst. Spec. Res. 21 (1991) 411-417.
 - 31 B. Valeur, I. Leray, Design principles of fluorescent molecular sensors for cation recognition, Coord. Chem. Rev. 205 (2000) 3-40.
 - 32 Elisabeth Bardez,* Isabelle Devol, Bernadette Larrey, and Bernard Valeur, Excited-State Processes in 8-Hydroxyquinoline: Photoinduced Tautomerization and Solvation Effects, J. Phys. Chem. B 101 (1997) 7786-7793.
 - 33 M. Tashiro, K. Furihata, T. Fujimoto, T. Machinami, E. Yoshimura, Characterization of the malate-aluminum(III) complex using ^1H and ^{27}Al NMR spectroscopy, Magn. Reson. Chem. 45 (2007) 518-521.
 - 34 The U.S. Environmental Protection Agency (EPA) has established a limit of 50 to 200 ppb for iron in drinking water (non-enforceable guidelines regarding cosmetic or aesthetic effects). Source: 2012 Edition of the Drinking Water Standards and Health Advisories, EPA 822-S-12-001, <http://water.epa.gov/action/advisories/drinking/upload/dwstandards2012.pdf>, accessed November 21, 2013.
 - 35 The limit of detection (LOD) and the limit of quantification (LOQ) were calculated from the titration curves using the following equations: $\text{LOD} = 3.3 \times \text{SD}/s$ and $\text{LOQ} = 10 \times \text{SD}/s$, where SD is the standard deviation of the blank sample, and s is the slope of the calibration curve in a region with a low analyte content.
-

SUPPLEMENTARY INFORMATION**Selective and sensitive detection of aluminium ions in water via fluorescence “turn-on” with both solid and water soluble sensory polymer substrates**

*Saúl Vallejos, Asunción Muñoz, Saturnino Ibeas, Felipe Serna, Félix Clemente García, José Miguel García.**

Departamento de Química, Facultad de Ciencias, Universidad de Burgos, Plaza de Misael Bañuelos s/n, 09001 Burgos, Spain. Email: jmiguel@ubu.es

Table of contents:

S1.- Structure and stability constants of the Al(III)-8- hydroxyquinolinato complexes.....
S2.- Response time for the sensory linear copolymer LCp and the sensory membrane Mem.....
S3.- Selectivity and interference studies for the sensory materials
S4.- Individual interactions of the sensory materials with Al(III), La(III), Zr(IV), Zn(II), Cd(II) and Pb(II)
S5.- CIE chromaticity coordinates of the hybrid Mem-Al(III) material

S1.- Structure and stability constants of the Al(III)-8-hydroxyquinolinato complexes¹ as well as a crystal structure of tris-(8-hydroxyquinolinato)aluminium(III) (Ul-Haque *et al.*)²

Table S1 depicts the species corresponding to the interaction between the Al(III) and 8-hydroxyquinolinato (Ox^-) complexes.

Table S1. Stability constants of the Al(III):8-hydroxyquinoline complexes (1:1, 1:2 and 1:3)

Complexes	Stability constants
$Al(III) + Ox^- \rightleftharpoons AlOx^{2+}$	$K_1 = \frac{[AlOx^{2+}]}{[Al(III)][Ox^-]}$
$AlOx^{2+} + Ox^- \rightleftharpoons AlOx_2^+$	$K_2 = \frac{[AlOx_2^+]}{[AlOx^{2+}][Ox^-]}$
$AlOx^+ + Ox^- \rightleftharpoons AlOx_3$	$K_3 = \frac{[AlOx_3]}{[AlOx_2^+][Ox^-]}$

The published logarithm of the overall stability constant ($\log K_s$) ranged from 30.6 to 32.3 ($\log K_s = \log K_1 K_2 K_3$).¹

The tris-(8-hydroxyquinolinato)aluminium(III) complex was crystallised in a meridional conformation with the aluminium atom coordinated to the bidentate 8-quinolato ligands in a distorted octahedral configuration, as shown in Figure S4.

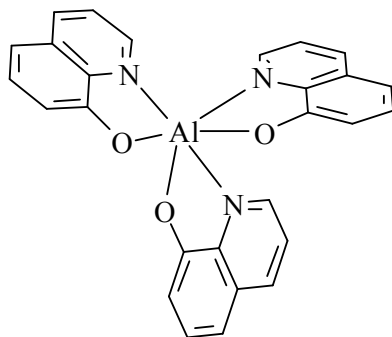


Figure S1 Representation of the $Al(8\text{-hydroxyquinolinato})_3$ crystal structure, which was crystallised from $CHCl_3/EtOH$, as reported by Ul-Haque *et al.*²

The stoichiometry of this complex was confirmed in our system with a Job's plot, as shown in Figure S2. The Job's plot showed a maximum that

¹ R. M. Smith, A. E. Martel and R. J. Motekaitis, NIST Standard Reference Database 46, NIST Critically Selected Stability Constants of Metal Complexes Database, Version 8.0; National Institute of Standards and Technology (NIST), Gaithersburg, MD, 2004.

² M. Ul-Haque, W. Horne and S. J. Lyle, *J. Cryst. Spec. Res.*, **1991**, 21, 411-417.

appeared at a mole fraction for **HOxMMA** (χ_{HOxMMA}) of 0.75, clearly indicating the formation of complexes with a 1:3 [Al(III):HOxMMA] stoichiometry.

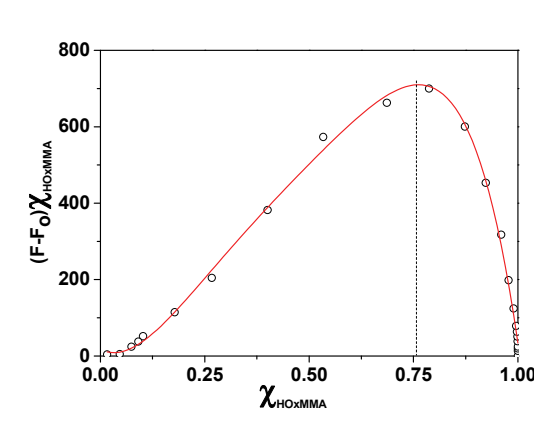


Figure S2. Job's plots corresponding to the interaction of **HOxMMA** with Al(III) obtained from the fluorescence spectroscopy data collected while determining a titration curve for Al(III) with **HOxMMA** in MeOH/water (80/20, v/v) at pH = 2.0 (NaOH/AcOH). The Job's plot represents the molar fraction of a species (□) vs. its product with a fluorescence intensity enhancement ($F - F_0$) at 549 nm. F_0 and F are the fluorescence intensities of the **HOxMMA** solution and the system containing different proportions of **HOxMMA** and Al(III), respectively.

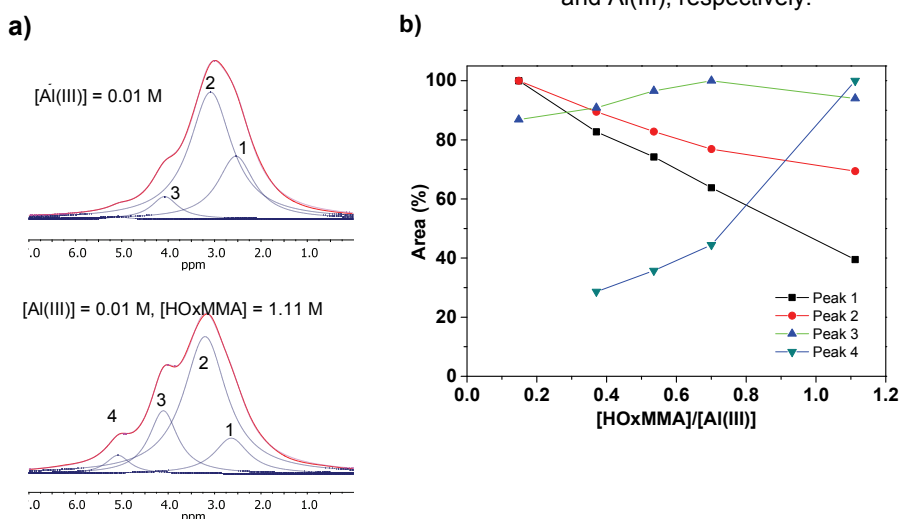


Figure S3. ^{27}Al NMR analysis of the Al(III) complex with **HOxMMA**: a) spectra (pink lines) of a sample containing Al(III) with and without **HOxMMA**. Peaks 1, 2 and 3 correspond to free Al(III) species and were obtained by curve fitting; b) evolution of the relative peak areas after increasing the concentration of **HOxMMA** in a sample containing 0.01 M Al(III) (the highest area of each peak is given a value of 100%). The Al(III) complex is observed during the evolution of Peak 4. Solvent: D_2O (**HOxMMA** was added in a DMSO-d_6 solution); reference $\text{Al}(\text{NO}_3)_3$.³

³ M. Tashiro, K. Furihata, T. Fujimoto, T. Machinami and E. Yoshimura, *Magn. Reson. Chem.*, 2007; 45, 518-521.

S2. Response time of the sensory linear copolymer (LCp) and the sensory membrane (Mem)

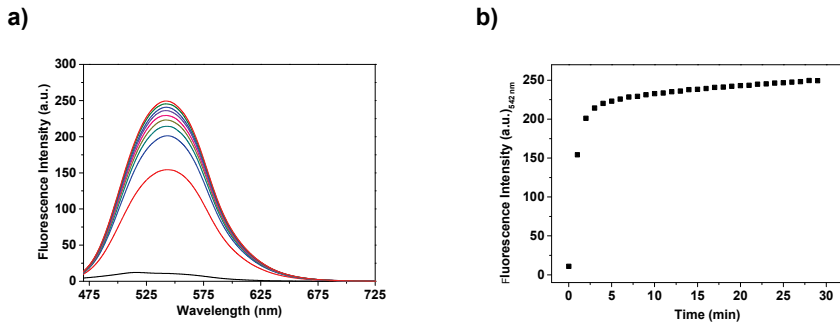


Figure S4. Response time experiment. Interaction of Al(III) (2.6×10^{-3} M) with an aqueous (pH = 4.5, buffered with sodium hydroxide and acetic acid) **LCp** (2.6 mEq/L of sensory oxine derivative motifs) solution over time: a) selected fluorescence spectra; b) response relative to the fluorescence intensity at 542 nm vs. time. Conditions: 1 mL of aqueous **LCp** solution (pH = 4.5) was placed in a quartz cuvette; afterward, Al(III) was added from an aqueous (pH = 4.5)/Al(III) stock solution. The fluoresce spectra were recorded once every min. Conditions: excitation slit = 10 nm; emission slit = 10 nm; excitation wavelength = 439 nm; scan speed = 12000 nm/min; [Al(III)] = 2.6×10^{-3} M.

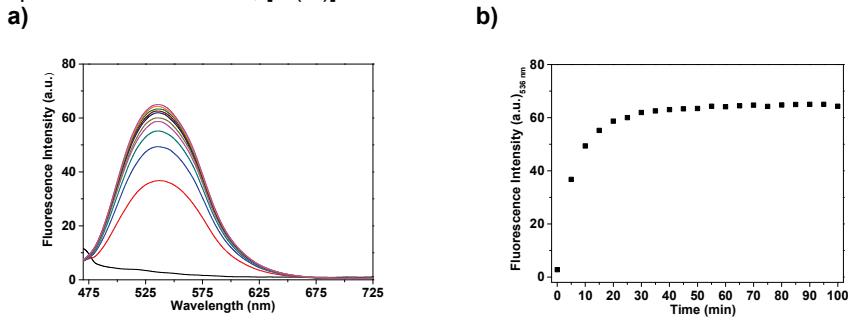


Figure S5. Response time experiment. Interaction of Al(III) in water (pH = 4.5, buffered with NaOH/AcOH) with **Mem** over time: a) selected fluorescence spectra; b) response in terms of the ratio of fluorescence intensity at 536 nm vs. time. **Mem** was immersed in water (pH = 4.5) in a quartz cuvette; afterward, Al(III) was added from an aqueous (pH = 4.5)/Al(III) stock solution. The fluoresce spectra were recorded once every 5 min. Conditions: water volume in cuvette = 3 mL; excitation slit = 5 nm; emission slit = 5 nm; excitation wavelength = 439 nm; scan speed = 2400 nm/min; [Al(III)] = 3.3×10^{-2} M.

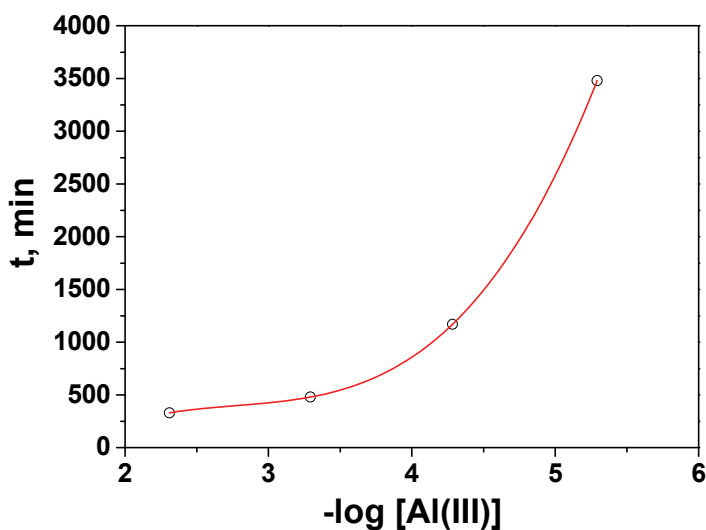


Figure S6. Al(III) concentration vs. response time using Mem as the sensory material. The response times were measured using the fluorescence technique and correspond to the time needed to achieve a 90% increase in fluorescence intensity.

Table S2. Response time for Mem with a water sample ($\text{pH} = 2.0$) containing 5.2×10^{-6} M Al(III).

Measuring method	Response time (min)
Dipping the sensory material in the measuring solution	3480
Dropping 10 μL of the measuring solution on the sensory material	400

S3. Sensory material selectivity and interference studies

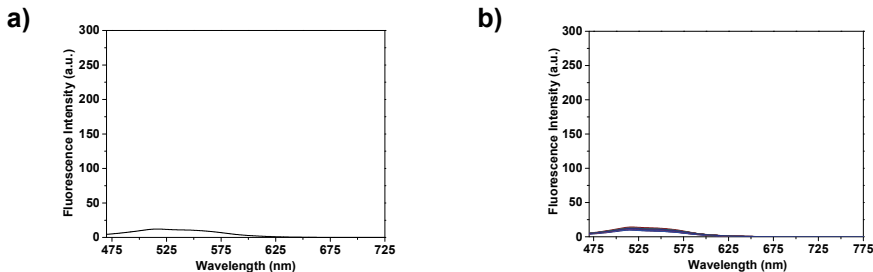


Figure S7. Interference study. The effect of adding different anions to a water solution of **LCp** on the fluorescence spectra: a) spectra of **LCp** in water; b) spectra of **LCp** in water after adding $2.65 \cdot 10^{-4}$ M of the following anions separately: cyanide, acetate, fluoride, perchlorate, dodecylsulphate, nitrite, hydrogenphthalate, pyrophosphate, persulphate, methanesulfonate, pyrophosphate dibasic, trifluoromethanesulfonate, *p*-toluenesulfonate, bromide, thiocyanate, oxalate, carbonate, benzoate, dihydrogenphosphate, sulphate, chloroacetate, trifluoroacetate and periodate. The concentration of the **LCp** was 30.2 g/L, corresponding to 2.65 mM of the sensory motif (**HOxMMA**). Measuring conditions: excitation slit = 10 nm; emission slit = 10 nm; excitation wavelength = 439 nm; scan speed = 12000 nm/min; the solutions of **LCp** and of the salts were prepared with MilliQ water buffered at pH = 4.5 with sodium hydroxide and acetic acid.

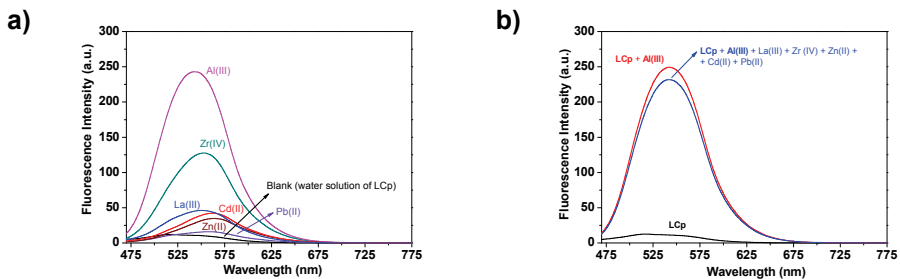


Figure S8. Interference study (excluding Fe(III)). The effect of adding different cations to a water solution of **LCp** on the fluorescence spectra: a) spectra of **LCp** in water after adding $2.65 \cdot 10^{-4}$ M of the cations that increased the fluorescence separately; the cations added were Al(III), NH₄(I), Ba(II), Cd(II), Ce(III), Cs(I), Co(II), Cu(II), Dy(III), La(III), Pb(II), Li(I), Mg(II), Mn(II), Hg(II), Nd(III), Ni(II), Pt(II), Cr(III), Cr(VI), K(I), Rb(I), Sm(III), Ag(I), Na(I), Sr(II), Sn(II), Zn(II) and Zr(IV); b) spectra of the **LCp** solution in water after adding at the same time a large set of cations that caused the fluorescence to increase when added separately. The concentration of the **LCp** was 30.2 g/L, corresponding to 2.65 mM of the sensory motif (**HOxMMA**). Measuring conditions: excitation slit = 10 nm; emission slit = 10 nm; excitation wavelength = 439 nm; scan speed = 12000 nm/min; the solutions of **LCp** and the salts were prepared in MilliQ water buffered at pH = 4.5 with sodium hydroxide and acetic acid. The cations were added as their nitrate or chloride salts.

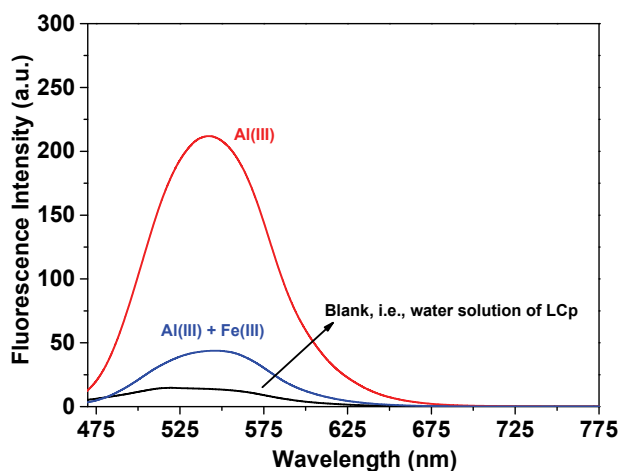


Figure S9. Interference study with Fe(III). The effect of adding $2.65 \cdot 10^{-4}$ M Al(III) and a mixture of Al(III) and Fe(III) ($2.65 \cdot 10^{-4}$ M for each species) to an aqueous LCp solution on the fluorescence spectra. The LCp concentration was 30.2 g/L, corresponding to 2.65 mEq/L of the sensory motif (HOxMMA). Measuring conditions: excitation slit = 10 nm; emission slit = 10 nm; excitation wavelength = 439 nm; scan speed = 12000 nm/min; the solutions of LCp and the salts were prepared with MilliQ water buffered at pH = 4.5 with NaOH/AcOH. The cations were added as their nitrate salts.

S4. Individual interaction of sensory materials with Al(III), La(III), Zn(II), Cd(II), Pb(II)

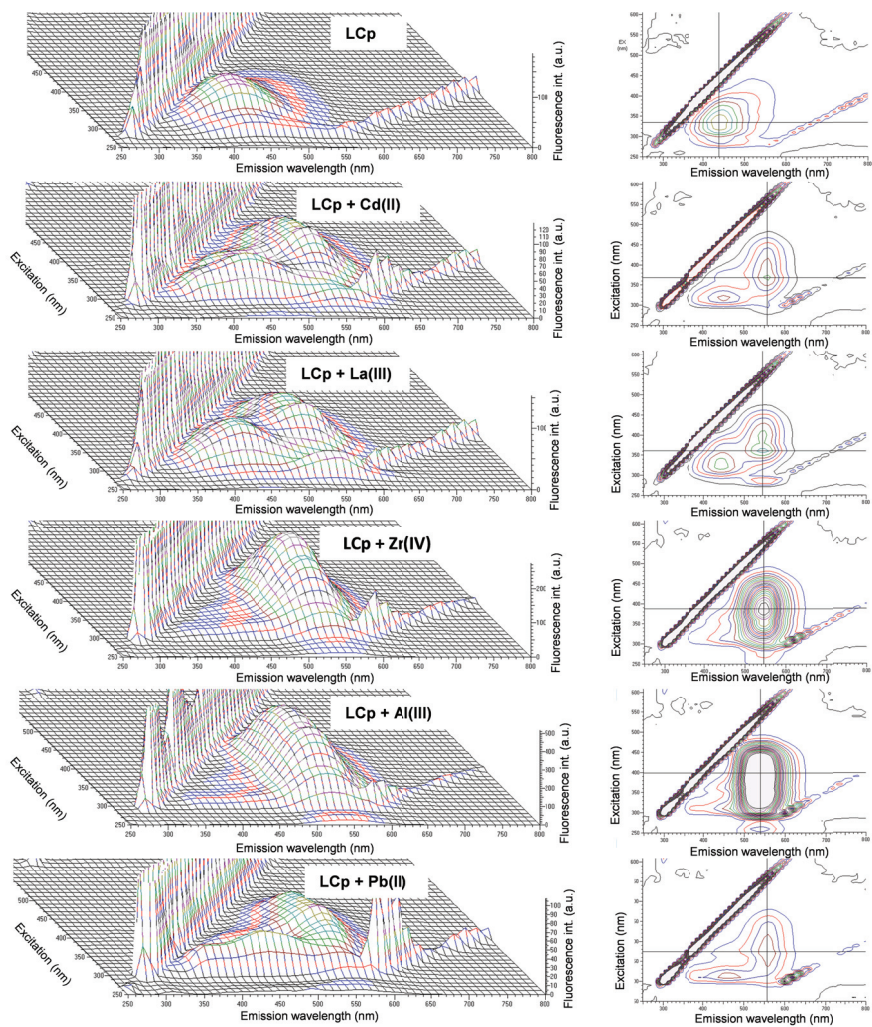


Figure S10. 3D (left) and 2D (right) fluorescence plots of an aqueous **LCp** solution after adding the cations that induced an increased fluorescence intensity ($\text{Al(III)} + \text{La(III)} + \text{Zr(IV)} + \text{Zn(II)} + \text{Cd(II)} + \text{Pb(II)}$) at 2.65×10^{-4} M. The **LCp** concentration was 30.2 g/L, corresponding to 2.65 mEq/L of the sensory motif (**HoxMMA**). Measuring conditions: excitation slit = 10 nm; emission slit = 10 nm; scan speed = 30000 nm/min; the solutions of **LCp** and the salts were prepared with MilliQ water buffered at pH = 4.5 with NaOH/AcOH. The cations were added as their nitrate, chloride or sulphate salts.

S5.- CIE chromaticity coordinates for the hybrid Mem-Al(III) material

The fluorescence spectra can be compared using a chromaticity diagram for luminescent converter (LUCO) materials with the naked eye. The perception of colours is culturally dependent and has been averaged and standardised. Human colour perception has been mapped in terms of two CIE⁴ chromaticity coordinates: x and y .

The CIE chromaticity coordinates (x and y) can be calculated from the fluorescence spectra using the following CIE 1931 colour matching functions:⁴

$$X = \int_{380}^{780} I(\lambda) \bar{x}(\lambda) d\lambda$$

$$Y = \int_{380}^{780} I(\lambda) \bar{y}(\lambda) d\lambda$$

$$Z = \int_{380}^{780} I(\lambda) \bar{z}(\lambda) d\lambda$$

Where $I(\lambda)$ is the spectral power distribution, λ is the wavelength of the equivalence monochromatic light in nm and $\bar{x}(\lambda)$, $\bar{y}(\lambda)$, and $\bar{z}(\lambda)$ are colour matching functions (i.e., the numerical representation of the chromatic response of the human eye),⁴ where $x = X/(X+Y+Z)$ and $y = Y/(X+Y+Z)$.

According to the CIE 1931 colour matching functions, the coordinates for the hybrid material (**Mem-Al(III)**) were $x = 0.32$ and $y = 0.61$, and the result is overlaid on the chromaticity diagram depicted in Figure S11; the observed colour is close to the green necessary for the R component of the RGB colour model for electronic devices. However, the quantum yield of the **HOxMMA-Al(III)** complex prepared from a 3×10^{-5} M methanolic solution of **HOxMMA** after adding an equimolar concentration of Al(III) was $\Phi_{\text{HOxMMA -Al(III)}} = 0.006$. This

⁴ International Commission on Illumination (<http://cie.co.at/>). The colour matching parameters were downloaded for free from the CIE web page (<http://files.cie.co.at/204.xls>). Access date: November 8, 2013.

result must be greatly improved for practical applications (i.e., using these materials as LUCO converters for the observed colour).

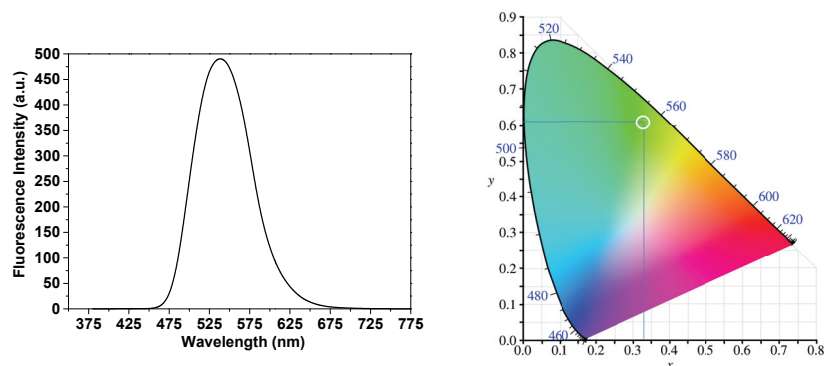


Figure S11. Fluorescence spectra (left) and the CIE chromaticity coordinates (x and y) drawn on the CIE 1931 xy chromaticity diagram (right, white circle) for the hybrid **Mem-Al(III)** material. Measuring conditions: excitation slit = 10 nm; emission slit = 10 nm; excitation wavelength = 365 nm; scan speed = 12000 nm/min; the CIE 1931 xy chromaticity diagram is a public domain image downloaded from Wikipedia (http://commons.wikimedia.org/wiki/File:CIE1931xy_blank.svg).

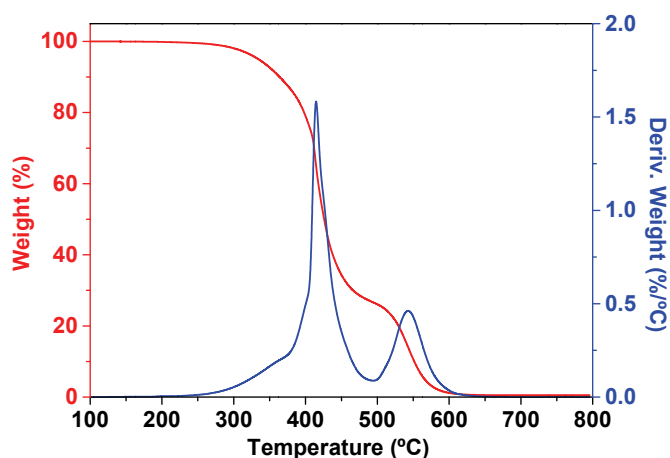


Figure S12. TGA of the hybrid membrane (Mem-Al(III)).

CAPÍTULO 5

Polímeros con derivados de acilhidrazona en su estructura

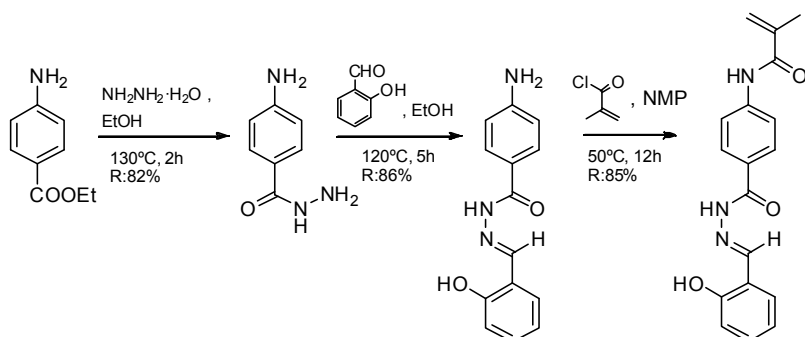
Las bases de Schiff forman una de las familias de compuestos orgánicos más utilizados en síntesis química, dentro de la cual se encuentran las acilhidrazonas. Estas moléculas se caracterizan por formar complejos fluorescentes con iones metálicos, como el Al(III), que habitualmente exhiben un rendimiento cuántico elevado. Por este motivo, se diseñó un monómero acrílico con esta funcionalidad en su constitución, se prepararon los polímeros, y se estudiaron como sensores fluorogénicos hacia esta catión.

5.1 Acilhidrazona y sus derivados

A lo largo de este capítulo se describe la síntesis de monómeros metacrílicos derivados de la acilhidrazona (Esquema 5.1), junto con su copolimerización y estudio de los materiales resultantes como sondas sólidas fluorescentes hacia Al(III). Las acilhidrazonas son compuestos con una gran variedad de

aplicaciones, entre las que destacan las farmacológicas,^{83,84} aunque también se utilizan en el ámbito de los sensores químicos, ya que forman complejos estables con cationes como el Al(III) y presentan procesos de “apagado” y “encendido” de fluorescencia con altos rendimientos cuánticos.^{85,86}

Una de las características inherentes a este tipo de compuestos es su preparación sencilla, eficiente y barata por reacción de una hidrazone y un aldehído, tal y como se muestra en el Esquema 5.1 en la preparación del monómero acrílico. El aldehído utilizado en la síntesis es el aldehído salicílico, clave para que la acilhidrazone sea un excelente sensor OFF-ON para cationes Al(III) (Esquema 5.2).



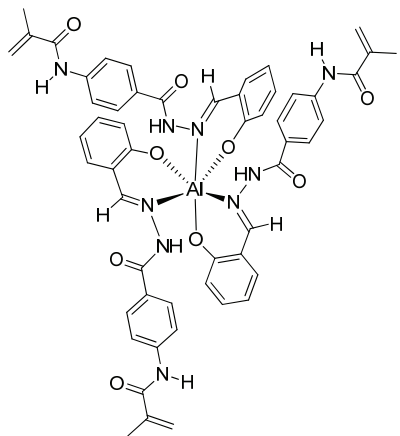
Esquema 5.1. Ruta sintética utilizada para la síntesis de monómero (*E*)-*N*-(4-(2-(2-hidroxibencilideno)hidrazinocarbonil)fenil)metacrilamida.

⁸³ P. Hernández, *Investigación y desarrollo de nuevas N-acilhidrazonas bioactivas*, Universidad de la República, Montevideo, 2011, “<http://riquim.fq.edu.uy/items/show/977>”, 22-06-2014.

⁸⁴ D. R. Ifa, C. R. Rodrigues, R.B. de Alencastro, C. A. M. Fraga, E.J. Barreiro, *J. Mol. Struc.* **2000**, 505, 11.

⁸⁵ K. Tiwari, M Mishra, V. Singh, *RSC Adv.* **2013**, 3, 12124.

⁸⁶ K. K. Chaturvedi, R. V. Singh, J. P. Tandon, *Polyhedron* **1987**, 6, 1101.



Esquema 5.2. Estructura química del complejo 3:1 formado por el monómero derivado de acilhidrona en presencia del catión Al(III).

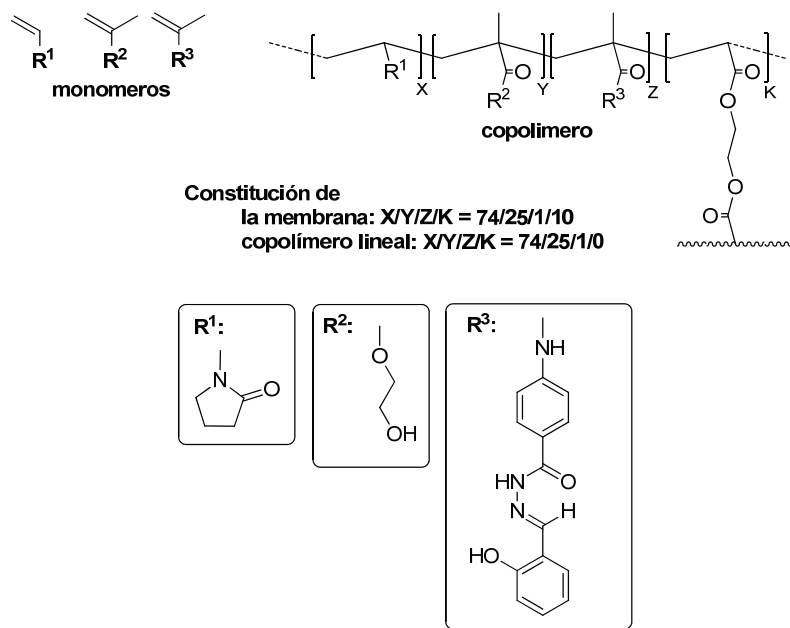
5.2 Polímeros con derivados de acilhidrona en la cadena lateral

Las nuevas tecnologías basadas en la luminiscencia se encuentran en pleno auge, y cada vez se reclaman más materiales con distintas luminiscencias y altos rendimientos cuánticos. En este sentido, se han desarrollado nuevos materiales poliméricos basados en un monómero con receptores pertenecientes a la familia de las acilhidronas, que en presencia de Al(III) sufre un proceso de “encendido” de fluorescencia (OFF-ON) y que tiene un rendimiento cuántico muy elevado. La preparación de este material utilizando dicho monómero (Esquema 5.1) se llevó a cabo de forma análoga a la descrita previamente (Capítulo 2), obteniéndose tanto polímeros lineales solubles en agua como reticulados en forma de membrana densa.

La matriz inerte fue la misma que la empleada en los materiales con subgrupos derivados de 8-hidroxiquinolina (Capítulo 4), es decir, está formada por *N*-vinilpirrolidona (VP) y acrilato de 2-hidroxietilo (A2HE). De igual forma, la estructura de los polímeros lineales fue la misma que la de esta matriz, a excepción del reticulante. En cuanto a los subgrupos receptores, derivados de acilhidrona, se incorporaron como monómeros en una proporción molar del

1%. La constitución de los materiales preparados se muestra en el Esquema 5.3.

Tras realizar los análisis habituales con una batería de especies, se observaron los cambios esperados con cationes Al (III), es decir, el aumento de fluorescencia en presencia de los mismos. Por otro lado, también se observaron procesos OFF-ON para otros cationes, tal y como se detalla en los resultados.



Esquema 5.3. Estructura de los monómeros acrílicos y constitución de las membranas sensoras.

5.3 Resultados

A continuación se describen los resultados obtenidos a través de la transcripción íntegra del trabajo publicado.

- ❖ *Forced solid-state interactions for the rapid, highly sensitive and selective “turn-on” fluorescence sensing of aluminium ions in water using a sensory polymer substrate.*

*Forced solid-state interactions for the rapid, highly sensitive and selective
“turn-on” fluorescence sensing of aluminium ions in water using a sensory
polymer substrate*

Forced solid-state interactions for the rapid, highly sensitive and selective “turn-on” fluorescence sensing of aluminium ions in water using a sensory polymer substrate.

*Saúl Vallejos, Asunción Muñoz, Saturnino Ibeas, Felipe Serna, Félix Clemente García and José Miguel García.**

Departamento de Química, Facultad de Ciencias, Universidad de Burgos, Plaza de Misael Bañuelos s/n, 09001 Burgos, Spain. Fax: (+) 34 947 258 831, Tel: (+) 34 947 258 085. E-mail: jmiguel@ubu.es

Abstract

Selective and highly sensitive solid sensory substrates for detecting Al(III) in pure water are reported. The material is a flexible polymer film that exhibits gel behavior and membrane performance. The film features a chemically anchored salicylaldehyde benzoylhydrazone derivative as an aluminum ion fluorescence sensor. A novel procedure for measuring Al(III) at the ppb level using a single solution drop for measurement in half an hour was developed. The procedure consisted in allowing a drop to enter the hydrophilic material for 30 minutes, followed by a 5-minute drying period, thus forcing the Al(III) to interact with the sensory motifs within the membrane, and then measuring the fluorescence of the system. The limit of detection of Al(III) was 22 ppm. Furthermore, a water-soluble sensory polymer containing the same sensory motifs was developed, with a limit of detection of Al(III) of 1.5 ppb, significantly lower than the EPA recommendations for drinking water.

Keywords

Sensory polymer, aluminium sensing, fluorescence chemosensor, fluorescence turn-on

Artículo enviado para su publicación.

Introduction

Aluminum is ubiquitous in nature as the most abundant metallic element in the Earth's crust, and occurs in our everyday lives in the form of its metallic, alloy, and trivalent ion derivatives. Indeed, aluminum's contribution to human welfare is evidenced by its use in food and drug preservatives and additives, personal hygiene products, housewares, and technological devices. However, in spite of aluminum's tremendous impact on the socioeconomic development of mankind, the extensive application of the metal also involves environmental hazards related to the acidification of soils and aqueous media, with its ions exhibiting toxicity toward aquatic biota.¹⁻³ With respect to humans, aluminum also presents a major health concern because it is believed to be a causative factor for Alzheimer's and other diseases, such as dementia, encephalopathy, Parkinson's, and different types of cancer.⁴⁻¹⁴ Accordingly, there is a distinct and environmental need for detection and quantification devices for Al(III), especially if they can allow for measurements to be performed inexpensively, *in-situ*, and in real time. In this respect, optical chemosensors play a vital role.

However, optical chemosensory systems based on the sensitive fluorescence technique have not been broadly reported,¹⁵⁻²⁷ and the most interesting sensing techniques that can be used in pure water are even scarcer.²⁸⁻³⁰

Within this context, we report herein a water-soluble polymer chemosensor that exhibits a fluorescence "turn-on" for Al(III). Moreover, we describe a chemosensing polymer film substrate for the fluorescence detection and quantification of Al(III) and a new methodology for quantifying Al(III) in minutes at the ppb level using only a few microliters of measuring solution; specifically, a drop of water containing Al(III) is absorbed by the solid hydrophilic sensory material, forcing solvated cations into the film, evaporating water by applying heat, and forcing bare cations to interact with the sensing motifs in the polymer structure, thereby increasing the sensitivity and dramatically diminishing the response time. The sensory materials were prepared by

copolymerization of an hydrophilic acrylic monomer with a novel methacrylic monomer featuring a salicylaldehyde benzoylhydrazone moiety as a sensing core for Al(III).

Experimental Section

Materials

All materials and solvents were commercially available and used as received unless otherwise indicated: 2,2-dimethoxy-2-phenylacetophenone (Aldrich, 99%), 2,2'-azobis(2-methylpropionitrile) (AIBN) (Aldrich, 98%) hydrazine monohydrate (Aldrich, 98%), 1-(4-aminophenyl)-1-propanone (Aldrich, 99%), ethanol absolute (VWR, 99.97%), salicylaldehyde (Merck, >99%), triethylamine (Aldrich, >99%), methacryloyl chloride (Alfa Aesar, 97%), 1-vinyl-2-pyrrolidone (VP) (Aldrich, 99%), 2-hydroxyethylacrylate (2HEA) (Aldrich, 96%), ethylene glycol dimethacrylate (EGDMA) (Aldrich, 98%), aluminum nitrate nonahydrate (Aldrich, 98%), ammonium nitrate (Aldrich, 98%), barium chloride dehydrate (LabKem, 99%), cadmium nitrate tetrahydrate (Alfa Aesar, 98.5%), cerium(III) nitrate hexahydrate (Alfa Aesar, 99.5%), cesium nitrate (Fluka, 99%), cobalt(II) nitrate hexahydrate (LabKem, 98%), copper(II) nitrate trihydrate (Aldrich, 98%), dysprosium(III) nitrate hydrate (Alfa Aesar, 99.9%), iron(II) sulfate heptahydrate (Aldrich, 99%), iron(III) nitrate nonahydrate (Aldrich, 98%), lanthanum(III) nitrate hexahydrate (Alfa Aesar, 99.9%), lead(II) nitrate (Fluka, 99%), lithium chloride (Aldrich, 99%), magnesium nitrate hexahydrate (LabKem, 98%), manganese (II) nitrate hexahydrate (Alfa Aesar, 98%), mercury(II) nitrate monohydrate (Scharlab, 99%), neodymium(III) nitrate hexahydrate (Alfa Aesar, 99.9%), nickel(II) nitrate hexahydrate (VWR, 99%), platinum(II) chloride (Aldrich, 98%), chromium(III) nitrate nonahydrate (Alfa Aesar, 98.5%), potassium dichromate (Aldrich, 99.5%), potassium nitrate (Aldrich, 99%), rubidium nitrate (Aldrich, 99.7%), samarium(III) nitrate hexahydrate (Alfa Aesar, 99.9%), silver nitrate (LabKem, 99%), sodium nitrate (LabKem, 99%), strontium nitrate (Alfa Aesar, 98%), tin (II) chloride (Aldrich, 98%), zinc nitrate hexahydrate (Aldrich, 98%),

zirconium(IV) chloride (Alfa Aesar, 98%), *N,N*-dimethylformamide (DMF) (Aldrich, 99.9%), and *N,N*-dimethylacetamide (DMA) (Merck, 99%).

Measurements and instrumentation

^{27}Al , ^1H and ^{13}C NMR spectra were recorded with a Varian Inova 400 spectrometer operating at 104.21, 399.92 and 100.57 MHz, respectively, with deuterated dimethylsulfoxide (DMSO-d₆), deuterium oxide (D₂O) or a 80:20 mixture of both, respectively, as the solvents.

The fluorescence spectra were recorded with an F-7000 Hitachi Fluorescence spectrophotometer.

Thermogravimetric analysis (TGA) data were recorded using a 4-5 mg sample under a synthetic air atmosphere with a TA Instruments Q50 TGA analyzer at 10°C min⁻¹.

IR-ATR infrared spectra (FTIR) were recorded with a JASCO FT/IR-4100 fitted with a PIKE TECH "Miracle" ATR accessory.

Al(III) titration experiments with the sensory monomer (3) and with the sensory linear polymer (**L_{Sen}**) were carried out as follows. Solutions of (3) ($2 \cdot 10^{-3}$ M in DMA/water, 50/50) and **L_{Sen}** (0.25 mEq/L of sensory motifs) in Millipore-Q water (pH = 4.5, buffered with NaOH/AcOH) were prepared and transferred to the cuvette used for measurement. The concentration of Al(III) was progressively increased by adding cumulative volumes of 1×10^{-10} to 1×10^{-1} M aqueous stock (Millipore-Q, pH = 4.5) solutions of Al(NO₃)₃•9H₂O. Fluorescence spectra were captured 5 min after each addition.

The Al(III) titration experiments with the sensory membrane (**M_{Sem}**) were carried out as follows. Five microliter Al(III) solutions in Millipore-Q water (pH = 4.5, buffered with NaOH/AcOH, Al(III) concentration ranging from 56 ppb to 5600 ppm) were deposited on the surface of the sensory discs and allowed to stand for 15 min, after which they were heated for 5 min at 100°C and then allowed to cooled to rt for 10 min. The fluorescence intensities were then

measured by positioning the membrane vertically in the spectrofluorometer, at 45° with respect to both the light source and the detector. Thus, the reflection of the source light on the film surface was prevented from reaching the detector by situating the discs in such a position that the source light hit the discs on one side and the other side emitted the detected light, with the reflected light going in the opposite direction.

HRMS spectra were obtained in an API QSTAR® XL Hybrid spectrometry system (Applied Biosystems) using ESI with a high resolution or FAB with a DMSO-like solvent.

The quantum yields, ϕ , were measured in DMA using quinine sulfate in sulfuric acid (0.05 M) as a reference standard.³¹

The water-swelling percentage (WSP), which is the weight percentage of water taken up by the films after soaking until equilibrium was reached, in pure water was calculated based on the weights of a dry sample film (w_d) and a water-swelled (the membranes were immersed in pure water at 20°C until the swelling equilibrium was achieved) sample film (w_s) as follows: $100 \times [(w_s - w_d)/w_d]$.

The mechanical properties of the membranes were measured on a Shimadzu EZ Test Compact Table-Top Universal Tester at 20°C.

Monomers synthesis

The methacrylamide monomer (*E*-*N*-(4-(2-(2-hydroxybenzylidene)hydrazine-carbonyl)phenyl) methacrylamide (**3**) was synthesized from inexpensive and readily available chemicals using proven and high-yield organic reactions, starting from ethyl 4-aminobenzoate, as described below and schematically depicted in Scheme 1.

Intermediate synthesis

4-Aminobenzohydrazide (1). To a 500 mL pressure tube fitted with a magnetic stirrer was added 72 ml (1.5 mol) of hydrazine monohydrate and 20 g (121

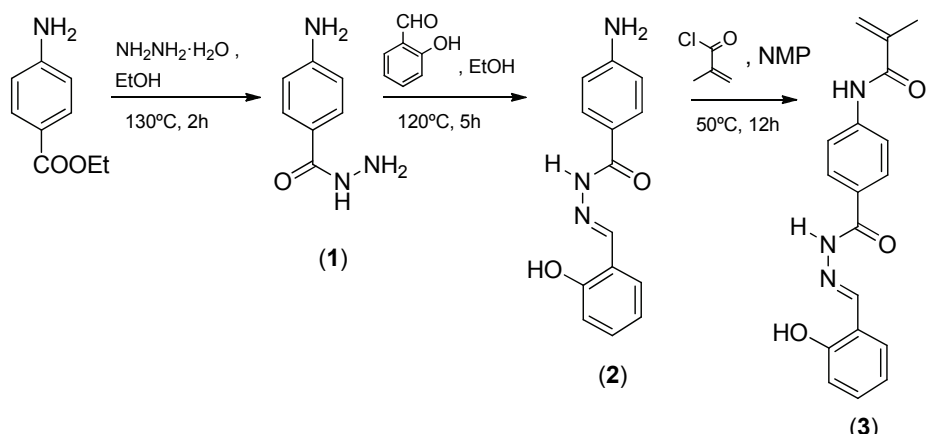
mmol) of ethyl 4-aminobenzoate. The solution was stirred at 130°C for 45 minutes and cooled to room temperature. One hundred thirty milliliters of absolute ethanol was added, and the solution was stirred at 100°C for 1 hour. Finally, the solution was cooled, filtered off and washed with water. The product could be recrystallized in ethanol. Yield after recrystallization: 12 g (65%). ¹H-NMR (399.94 MHz; DMSO-d₆): δ (ppm), 9.41 (s, 1H); 7.66 (d, 2H, 8.6Hz); 7.64 (d, 2H, 8.6Hz); 5.64 (s, 2H); 4.44 (s, 2H). ¹³C-NMR (100.58 MHz; DMSO-d₆): δ (ppm), 167.78; 152.61; 129.60; 121.07; 113.84. EI-MS, m/z: 151 (M⁺, 7), 121 (7), 120 (100), 93 (5), 92 (54), 91 (5), 78 (11), 69 (6), 65 (34), 63 (14). FTIR (wavenumber, cm⁻¹): ν_{NH}: 3427, 3345, 3300, 3236; ν_{C=O}: 1660. ESI-HRMS calcd for C₁₈H₁₇N₃O₃ 151.0746, found 151.0745.

(E)-4-amino-N'-(2-hydroxybenzylidene)benzohydrazide (2). One gram (6 mmol) of compound (1), 803 mg (6 mmol) of salicylaldehyde and 20 ml of ethanol were added to a 100 ml pressure tube. The mixture was stirred at 120°C for 5 hours. The reaction was then allowed to run at room temperature, and the pale-yellow precipitate was filtered off and washed with a small amount of cool ethanol. Yield: 1.32 g (86%). ¹H-NMR (399.94 MHz; DMSO-d₆): δ (ppm), 11.69 (S, 1H); 8.60 (s, 1H); 7.74 (d, 2H, 8.60 Hz); 7.51 (dd, 1H, 7.6 and 1.3 Hz); 7.34-7.28 (m, 1H); 6.99-6.91 (m, 2H); 6.66(d, 2H, 8.7 Hz); 5.88 (s, 1H). ¹³C-NMR (100.58 MHz; DMSO-d₆): δ (ppm), 163.58; 158.36; 153.48; 147.84; 131.82; 130.58; 130.34; 120.13; 119.69; 119.66; 117.31; 113.59. EI-MS, m/z: 255 (M⁺, 9.14), 151 (5), 136 (7), 121 (8), 120 (100), 92 (19), 78 (10), 65 (12), 63 (10). FTIR (wavenumber, cm⁻¹): ν_{OH, NH}: 3455, 3356, 3281; ν_{C=O}: 1664. ESI-HRMS calcd for C₁₈H₁₇N₃O₃ 255.1008, found 255.1008.

Monomer synthesis

(E)-N-(4-(2-(2-Hydroxybenzylidene)hydrazinecarbonyl)phenyl) methacrylamide (3). To a pressure tube, 1.55 mmol (0.5 g) of product (2), 2.32 mmol (0,324 ml) of triethylamine and 15 mL of NMP were added. Subsequently, 2.01 mmol (0,197 ml) of methacryloyl chloride was added, and the solution was stirred for 12 hours at 50°C under a nitrogen atmosphere. Finally, the solution was

precipitated in water, and the product (**3**) was filtered off and recrystallized in ethanol. Yield: 0.35 g (70%). ¹H-NMR (399.94 MHz; DMSO-d₆): δ (ppm), 12.08 (s, 1H); 11.40 (s, 1H); 10.11 (s, 1H); 8.68 (s, 1H); 7.97 (d, 2H, 8.3 Hz); 7.90 (d, 2H, 8.0 Hz); 7.57 (d, 1H, 7.6 Hz); 7.34 (t, 1H, 7.7 Hz); 7.02-6.92 (m, 2H); 5.90 (s, 1H); 5.62 (s, 1H); 2.01 (s, 3H). ¹³C-NMR (100.58 MHz; DMSO-d₆): δ (ppm), 168.03; 163.16; 158.39; 148.90; 143.39; 141.09; 132.20; 130.50; 129.33; 128.14; 121.51; 120.29; 120.25; 119.62; 117.34; 19.60. EI-MS, m/z: 323 (M⁺, 17), 204 (15), 189 (14), 188 (100), 121 (17), 120 (7), 69 (9). IR (wavenumber, cm⁻¹): ν_{OH}, ν_{NH}: 3450 (bb), 3320, 3251; ν_{C=O}: 166. ESI-HRMS calcd for C₁₈H₁₇N₃O₃ 323.1270, found 323.1267.



Scheme 1. Monomer (**3**) synthesis and structure.

Al(III)-((E)-N-(4-(2-Hydroxybenzylidene)hydrazinecarbonyl)phenyl)) complex (**C_{1:3}**)

Two hundred fifty-three milligrams (0.782 mmol) of monomer (**3**), 98 mg (0.261 mmol) of aluminum nitrate nonahydrate and 25 ml of ethanol were added to a 100 ml pressure tube. The mixture was stirred at 120°C for 5 hours and overnight at 50°C. The solvent was then removed under vacuum, and the yellow solid product was washed with water. Yield: 45%. ²⁷Al-NMR (104.23 MHz; DMSO-d₆): δ (ppm), 18.48, 11.75. HR-ESI-MS, m/z: 324.1367 [(3)+H]⁺ (calcd. For C₁₈H₁₈N₃O₃, 324.1348); 671.2243 [Al(3)₂]⁺ (calcd. For C₃₆H₃₂AlN₆O₆,

671.2199; 994.3458 $[C_{1:3} + H]^+$ (calcd. For $C_{54}H_{49}AlN_9O_9$, 994.3469); 1016.3298 $[C_{1:3} + Na]^+$ (calcd. For $C_{54}H_{48}AlN_9O_9Na$, 1016.3288). Anal. calcd. (found) for $C_{1:3}$: C 65.25 (65.16), H 4.87 (4.85), N 12.68 (12.83).

Material preparation

Linear copolymer synthesis (L_{Sen})

The linear copolymer (L_{Sen}) was prepared by the radical polymerization of the hydrophilic monomers **VP** and **2HEA** and the sensing monomer (**3**) in a **VP:2HEA:(3)** molar ratio of 74.5:24.5:1.0. A 100 mL three-neck flask equipped with a magnetic stirrer and a reflux condenser was blanketed with nitrogen through a gas inlet. Next, 0.37 mmol (120 mg) of (**3**), 27.32 mmol (3.04 g) of **VP**, and 9.10 mmol (1.06 g) of **2HEA** were dissolved in DMF (37 mL) and added to the flask. Subsequently, 2,2-dimethoxy-2-phenylacetophenone (948 mg, 3.70 mmol) was added, and the solution was irradiated for 12 hours at rt (250w UV mercury lamp, Philips HPL-N, emission band in the UV region at 304, 314, 335 and 366 nm, with maximum emission at 366 nm). The solution was then added dropwise to diethyl ether (300 mL) with vigorous stirring, yielding a brown precipitate. The polymer was purified using two cycles of a solution/precipitation procedure with methanol (10 mL) as the solvent and diethyl ether (100 mL) as the non-solvent. The solution was finally dried overnight in a vacuum oven at 60°C. Yield: 3.60 g (85%).

Membrane preparation (M_{Sen})

The cross-linked film or membrane was prepared by thermally initiated bulk radical polymerization with **VP**, **2HEA**, (**3**), and **EGDMA** as a cross-linking agent in a comonomer molar ratio of 74/25/1/10 (**VP:2HEA:(3):EGDMA**), using **AIBN** (1 wt %) as the thermal radical initiator. The homogeneous solution of comonomers was transferred to an ampoule, degassed by nitrogen bubbling for 15 min, injected into an oxygen-free atmosphere in a 200 μ m thick silanized glass hermetic mold, and heated to 60°C for 12 h. Then, the membrane was

demolded and conditioned by being allowed to stand for 24 h at room temperature. The chemical structure is depicted in Scheme 2.

*Hybrid membrane preparation (**Al-M_{Sen}**)*

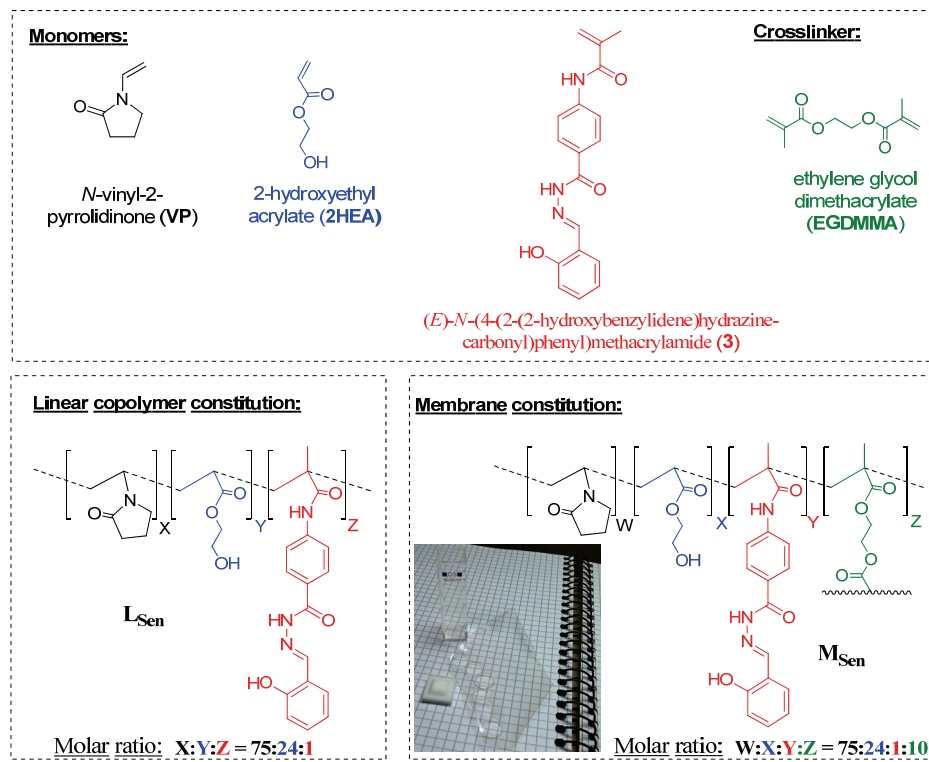
A hybrid aluminum(III)-**M_{Sen}** membrane (**Al-M_{Sen}**) was prepared by immersing **M_{Sen}** in a pH 2 solution of aluminum nitrate nonahydrate 0.1 M for 2 hours. The hybrid membrane (**Al-M_{Sen}**) was then thoroughly washed with water and acetone and finally dried under ambient conditions for 48 h.

Results and discussion

With the aim of improving the performance of chemosensors, we addressed the task of designing a material that is flexible and exhibits an improved fluorescence “off-on” sensing capability for Al(III). Thus, with these goals in mind, we synthesized a novel methacrylic monomer featuring a salicylaldehyde hydrazone moiety as the sensing core for Al(III), Scheme 1, from which solid sensory films were prepared (**M_{Sen}**). At the same time, a water-soluble sensory film was synthesized using this monomer (**L_{Sen}**)—thus fulfilling a secondary objective of this study—both as a sensing material and as a means for characterizing the interaction between Al(III) and the polymer structure (Scheme 2).

Preparation and characterization of the sensory materials

The monomer containing the salicylaldehyde benzoylhydrazone sensory motif (3) was prepared in a straightforward manner from widely available commercial chemicals, starting from hydrazine and ethyl 4-aminobenzoate, and followed by two further reaction steps, as shown in Scheme 1; the overall yield was 40%. The NMR spectrum of (3) gathered at rt is simple (Figure S3, SI), and the assignment of all peaks via conventional NOESY and COSY experiments was straightforward (Figures S4 and S5, SI).



Scheme 2. Monomer, linear copolymer (L_{Sen}) and membrane (M_{Sen}) structures. The photograph of the membrane on a notebook shows the aspect ratio and the transparency of the sensory material; the holes correspond to the areas where the 5 mm discs were removed for the sensory kits.

However, the heating of the NMR sample revealed the more complex nature of (3) in solution, and the splitting of signals at higher temperatures indicates equilibria between associated and non-associated species (Figure 1), with a clear domination of the associated species at rt, where unique ^{13}C NMR signals are observed for each nucleus; this feature was also observed in the ^1H NMR spectra (Figures S3, S4 and S5, SI).

The sensory core has demonstrated to be an excellent Al(III) chelator in different organic molecules, but always in organic or aqueous/organic solution, which is why we designed the monomer (3)^{24,27,29} and prepared the organic sensory materials to function in pure water. Conventional thermally initiated radical polymerization of (3) with inexpensive commercial comonomers **VP** and

2HEA yielded the water-soluble linear copolymer (**L_{Sen}**), and the addition of a crosslinker (**EGDMA**) yielded the membrane (**M_{sem}**) (Scheme 2). With respect to the envisioned application, it is worth mentioning that only approximately 1% of the synthetic sensory monomer (**3**) is needed for the preparation of **L_{Sen}** and **M_{sem}** as sensory materials. The ¹H NMR spectrum of **L_{Sen}** is in agreement with the feed monomer ratio of the polymerization reaction, including the small content of monomer (**3**), as depicted in Figure S11, SI.

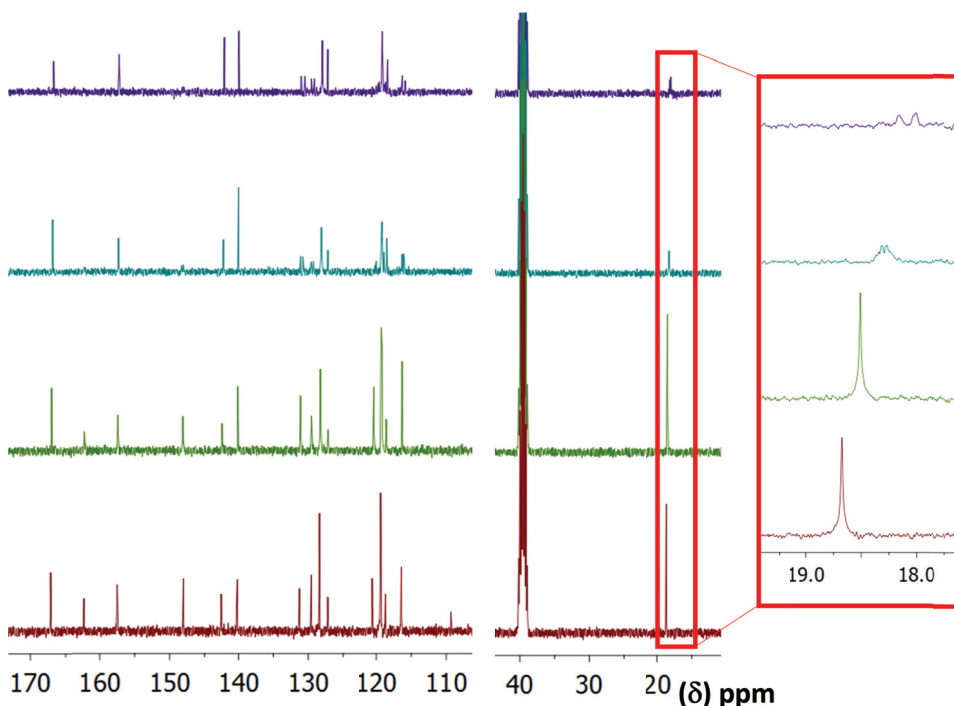


Figure 1. 100.58 MHz ¹³C NMR spectra of monomer (**3**) in DMSO-d₆ at different temperatures (from top to bottom: 80, 60, 40 and 25°C).

The dense polymer membrane, or film, was mechanically creasable and flexible, exhibiting a Young's modulus (MPa)/tensile strength (MPa)/elongation at break (%) under ambient conditions of 100/6/34. Drying the membranes at 60°C for 30 min gave rise to a significant increase in the Young's modulus and tensile strength, with a concomitant decrease in the elongation at break

(394/31/23), demonstrating the influence of the hydration of the membrane due to humidity in the air. Furthermore, the materials exhibited reasonably good thermal stability, as indicated by TGA analysis; the decomposition temperature associated with a 10% weight loss under a nitrogen atmosphere was approximately 350°C for both **L_{Sen}** and **M_{sem}**, whereas the char yield at 800°C was slightly higher for the crosslinked material, 9% for **M_{sem}** and 6% for **L_{Sen}**. The TGA curves and full data are shown in Figure S12, SI. The material's composition was designed to be hydrophilic to provide water solubility to the linear copolymer **L_{Sen}** and gel behavior to the membrane. The latter is a prerequisite because solvated Al(III) must enter the membrane to reach and interact with the receptor motifs. The water-swelling percentage (WSP) was 63%, between 40 and 100%, which is suitable for both the rapid diffusion of chemicals into the membrane and for maintaining the tractability, in terms of mechanical properties, of the water-swelled materials.

Depicting the sensory mechanism

Salicylaldehyde benzoylhydrazone derivatives form complexes with Al(III) with published Al(III):salicylaldehydate-derivative stoichiometries of 1:1 [24] and 1:3 [25-29]. Unlike similar organic compounds, these coordination complexes are highly fluorescent in solution. Thus, the interaction is either not clear or salicylaldehyde-derivative-dependent; therefore, we studied the complex stoichiometry to shed light on the sensory mechanism.

To this end, a complex (**C_{1:3}**) from the reaction of Al(NO₃)₃ with (**3**) in a molar ratio of 1:3 was prepared.

The complex **C_{1:3}** has a molecular weight of 994.00, and the analysis of its HR-ESI-MS spectrogram is coherent with the suggested stoichiometry 1:3 (Figures S6 and S7, SI).

In DMSO-d₆ solution, complex **C_{1:3}** reaches an equilibrium with complex **C_{1:2}** (or [Al(**3**)₂]⁺) and deprotonated (**3**) ([**(3)-H**]⁻), **C_{1:3}** ⇌ **C_{1:2}** + [**(3)-H**]⁻, as observed in COSY experiments (Figures S8 and S9).

This equilibrium was analyzed by ^1H NMR at different temperatures. At 30°C, four peaks corresponding to the methyl groups were observed: one signal for the symmetric complex **C_{1:3}**, another one for deprotonated [(3)-H]⁻ and two signals for the non-symmetric complex **C_{1:2}**. At 80°C, the two peaks corresponding to **C_{1:2}** merged into one (Figure 2).

Thus, the formation of the complex could also be monitored by ^{27}Al NMR (Figure 2),³² through which two main signals were obtained. The sharper signal, at approximately 19 ppm, corresponds to the symmetric species **C_{1:3}**, whereas the broader signal, centered at approximately 16 ppm, corresponds to the non-symmetric **C_{1:2}**. The small peak at approximately 5 ppm is derived from aluminum in the glass substrate of the reference.

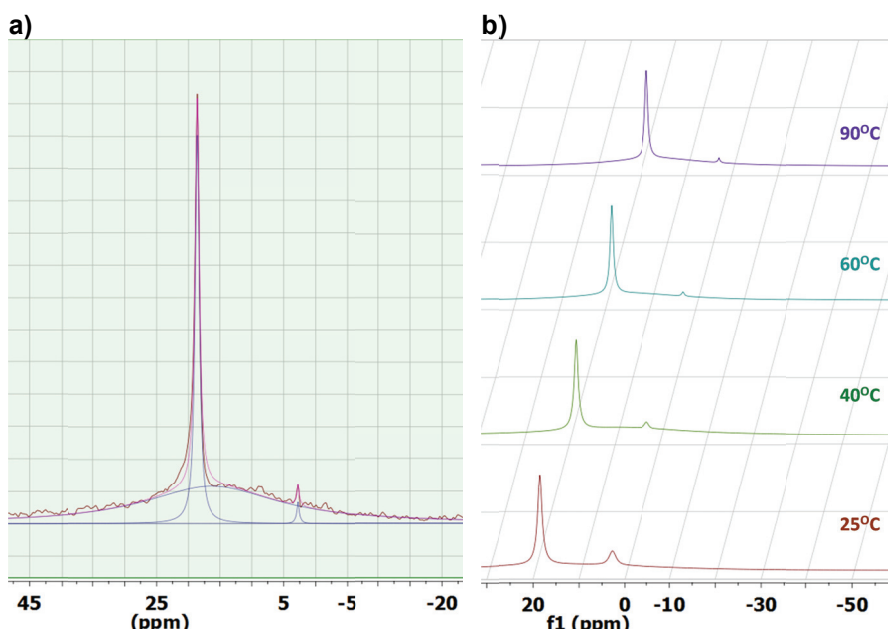


Figure 2. ^{27}Al NMR spectra of **C_{1:3}**: a) curve fitting of the spectrum at 90°C; b) spectra at different temperatures. Solvent: DMSO- $\text{d}_6/\text{D}_2\text{O}$ (80:20).

After analyzing the sensory mechanism ascribed to the formation of complexes with the monomer and Al(III), the same behavior would be expected to be responsible for the sensing characteristics of the sensory polymer materials. Accordingly, we found evidence of the formation of complexes with

an Al(III):salicylaldehyde-derivative stoichiometry of 1:3 in the Job's plot obtained from the fluorescence titration curves of Al(III) with solutions of L_{Sen} pure water; in this plot, a maximum was observed at a molar fraction of the salicylaldehyde derivative moieties of 0.75 (Figure S10, SI).

Sensing behavior of the sensory materials

As previously addressed, practically non-fluorescent pure aqueous solutions of L_{Sen} became highly fluorescent in presence of aluminum ions, i.e., following an "off-on" pattern, as shown in Figure 3, which enabled the drawing of a titration curve.

Following a similar "off-on" patterns, 5 mm discs cut from the M_{Sen} film showed a great increase in their fluorescence intensities upon immersion in water containing aluminum ions, as will be discussed in a later section. On the other hand, a manageable and highly fluorescent hybrid organic-inorganic film-shaped material (Al-M_{Sen}) was prepared after immersing M_{Sen} in a water solution of Al(III).

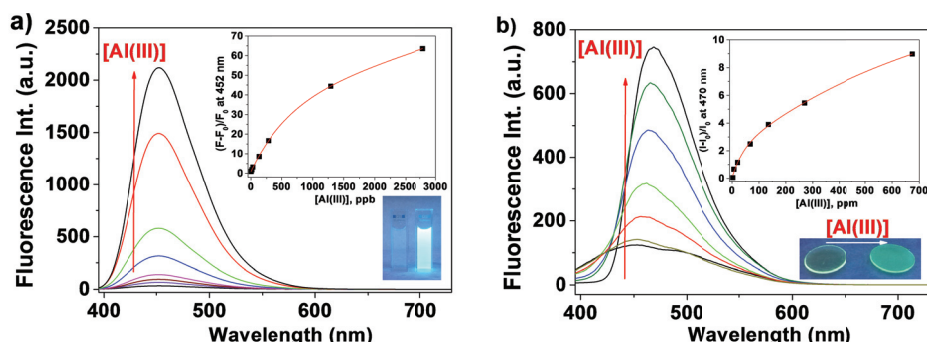


Figure 3. Titration of Al(III) in water using the fluorescence technique, a) Fluorescence spectra of L_{Sen} in aqueous solution (inset: Al(III) concentration vs. fluorescence enhancement; image captured under UV light, 364 nm). The concentration of the L_{Sen} was 2.81 g/L, corresponding to 0.25 mM of the sensory motif (3). b) Fluorescence spectra of solid discs cut from M_{Sen} after dropping 5 μL of water solutions of Al(III) (inset: Al(III) concentration vs. fluorescence enhancement; image of sensory disc captured under UV light, 364). Conditions: MilliQ water was buffered (NaOH/AcOH) at pH = 4.5; excitation slit = 5 nm; emission slit = 5 nm; excitation wavelength = 374 nm; scan speed = 12000 nm/min; the Al(III) concentration was increased every 5 minutes in the L_{Sen} measurements, and in solid systems, M_{Sen} , 5 μL of MilliQ water containing different concentrations of Al(III) was dropped on different discs, which were allowed to stand for 30 min, then heated to 100°C for another 5 min.

After preparing the sensory materials, critical parameters such as response times, interfering chemicals, selectivity and sensitivity were measured, as discussed below, and a short study of the performance of the hybrid film as a luminescent material was performed.

Response time

The response time was significantly short, approximately 5 min, for the sensory system composed of an aqueous L_{Sen} solution in the micromolar and millimolar Al(III) concentration ranges (Figure 4), and the response time was not dependent on the concentration of Al(III).

However, the most interesting sensory solid system, M_{Sen} , showed a much longer response time, especially at low Al(III) concentration. Moreover, this time was highly dependent on the concentration of Al(III). These trends were observed because the sensing phenomenon relies on two concomitant factors: the relatively slow physical diffusion of the target species, Al(III), into the membrane, and the rapid chemical interaction of the species with the sensory motifs chemically anchored to the membrane polymer network. Thus, for instance, the response time to a sub-millimolar concentration of Al(III) is approximately one day, as shown in Figure 4.

Nevertheless, the response time of the sensory solid material, M_{Sen} , could be reduced to only 20 min for every concentration of the target cation Al(III), achieving the goal of attaining a short measurement time (Figure 3). This reduction was accomplished by forcing the interaction in the solid state, i.e., a known quantity of the aqueous solution containing Al(III) was dropped on the surface of a dry membrane disc and allowed to stand for 15 min, during which the drop was immediately absorbed by the hydrophilic membrane structure, and the disc was then dried in an oven at 60°C for 5 min. From one side, the rapid absorption of the aqueous drop by the membrane drags the solvated Al(III) ions into the material, and from the other side, the simultaneous drying of the

material forces the interaction of previously hydrated Al(III) ions with the membrane sensory motifs (**3**).

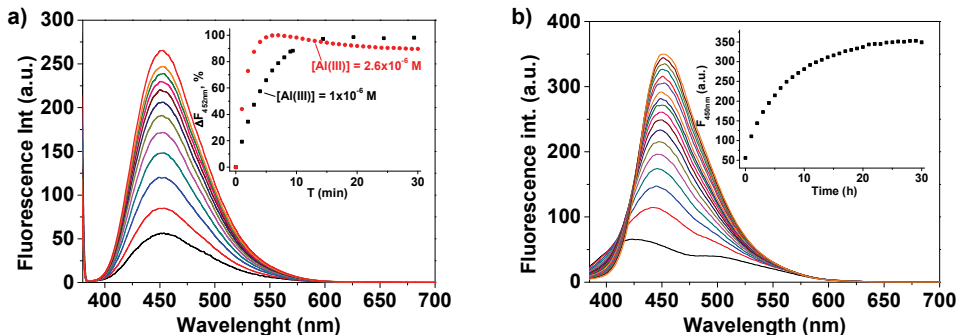


Figure 4. Response time experiments. Interaction of Al(III) in water (pH = 4.5, buffered with NaOH/AcOH) over time with. a) L_{Sen} in solution (the concentration of the L_{Sen} was 2.81 g/L, corresponding to 0.25 mEq/L of the sensory motif (**3**)), selected fluorescence spectra (inset: response in terms of fluorescence intensity increase at 452 nm vs. time. b) M_{Sen} immersed in a water solution containing Al(III) in a quartz cuvette (inset: response in terms of the fluorescence intensity at 450 nm vs. time. Fluorescence spectra were recorded periodically. Conditions: water volume in cuvette = 2 mL; excitation slit = 5 nm; emission slit = 5 nm; excitation wavelength = 374 nm; scan speed = 12000 nm/min; $[\text{Al(III)}] = 1 \times 10^{-6}$ M (26.7 ppb). The response at a higher Al(III) concentration, 2.6×10^{-4} M, was also measured for L_{Sen} (inset in a)) for comparative purposes.

Hybrid materials Al- M_{Sen}

The addition of Al(III) to DMA solutions of (**3**) caused fluorescence “turn on”, transforming the formerly weakly fluorescent solution into a highly fluorescent due to the formation of $\text{Al}(\mathbf{3})_n^{(3-n)+}$ complexes, with stoichiometries Al(III):(**3**) of 1:1, 1:2, and 1:3. The quantum yield of solutions of (**3**) in DMA, using quinine sulfate in sulfuric acid (0.05 M) as a reference standard,³³ was negligible, $\Phi = 0.02$. At the same time, the addition of Al(III) to this solution in molar ratios of 1:1, 1:2, and 1:3 with respect to (**3**) led to quantum yields of $\Phi = 0.59$, 0.53, and 0.59, respectively, indicating high fluorescence efficiency, as previously outlined.

After determining that the high quantum yield of the organometallic complexes arose from the interaction of (**3**) with Al(III), which was assessed in organic media because (**3**) is water-insoluble, and based on the potential of the materials derived from (**3**) as luminescent converters (LUCO), a hybrid

membrane, **Al-M_{Sen}**, was prepared. Furthermore, the color of the materials upon irradiation was analyzed in terms of the CIE chromaticity coordinates (x and y) calculated from the fluorescence spectra using the corresponding CIE 1931 color matching functions (Figures 5).³⁴ Figure S13, SI, shows an image of strips of the membrane **Al-M_{Sen}** captured under UV light. These types of materials are promising for luminescence conversion applications because of the high quantum yield and the blue emission observed upon irradiation under conventional 365 nm UV; the CIE chromaticity coordinates light were $x = 0.14$ and $y = 0.26$ for **Al-M_{Sen}**, whereas they were $x = 0.15$ and $y = 0.16$ for the monomer in organic solution; both systems showed blue emission.

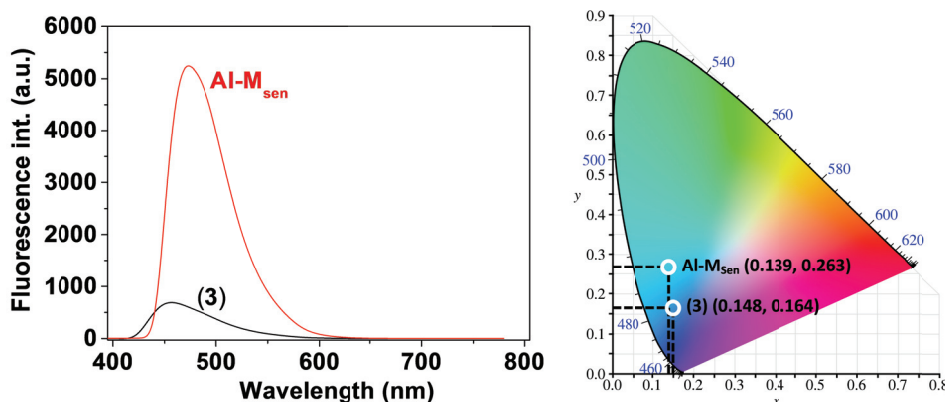


Figure 5. Fluorescence spectra (left) and the CIE chromaticity coordinates (x and y) drawn on the CIE 1931 xy chromaticity diagram (right, white circle) for the hybrid **Al-M_{Sen}** material. Measurement conditions: excitation slit = 5 nm; emission slit = 5 nm; excitation wavelength = 365 nm; scan speed = 12000 nm/min; the CIE 1931 xy chromaticity diagram is a public domain image downloaded from Wikipedia (http://commons.wikimedia.org/wiki/File:CIE1931xy_blank.svg).

Substrate selectivity and interference study

Preliminary interference studies concerning the sensory monomer (3) were carried out in organic/aqueous due to the lack of solubility of (3) in water. A broad set of cations were added to the sensing solutions at high concentration, 10 times the concentration of (3), and only five gave rise to an appreciable fluorescence enhancement, showing a 24-fold enhancement with Al(III) and between a 1- and 4-fold enhancement with Zr(IV), Cd(II), Zn(II), and La(III), as shown in Table S1, SI. The higher response toward Al(III) was also

accompanied by higher selectivity because both the emission and the excitation spectra are characteristic of this cations, as shown in the 2D and 3D spectra (Figures S14 to S19, SI). No fluorescence variations were observed upon adding a broad set of anions.

An image captured under UV light (366 nm) clearly depicts the fluorescence “turn on” of the aforementioned cations (Figure S20, SI).

An interference study of L_{Sen} in pure aqueous solution depicted a different scenario. From a practical viewpoint, Zr(IV) was considered a unique interferent. However, to test the performance of the sensory system, a competitive experiment was carried out (Figure 6). Thus, a cocktail of cations was added to the solution, and the results were compared with those obtained from an experiment in which only Al(III) was added. The cocktail comprised the cations that caused interference to (3), and no significant effect due to these cations was observed, neither in the fluorescence enhancement nor in the pattern of the fluorescence spectra, as shown in the inset of Figure 6. The same behavior was observed with the solid sensory substrate M_{Sen} , in which the spectral patterns of the membrane with and without Al(III) differ from that of the solutions of (3) and L_{Sen} due to solid swelled state, as illustrated in the 2D and 3D fluoresce spectra shown in Figures S21 and S22.

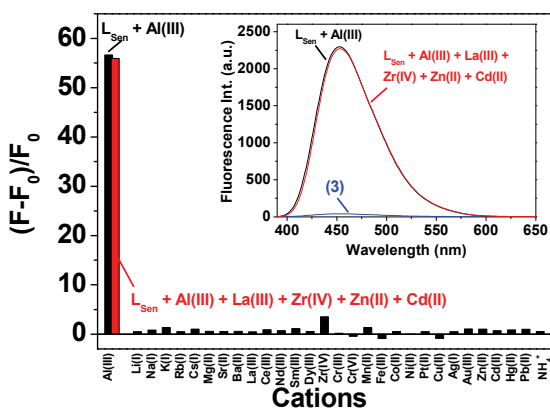


Figure 6. Fluorescence enhancement of an aqueous solution of L_{Sen} upon the addition of individual cations (black bars) and a cocktail of cations (red bar). Inset: fluorescence spectra. Conditions: the concentration of the L_{Sen} was 2.81 g/L, corresponding to 0.25 mEq/L of the sensory motif (3); the concentration of each cation, both in the individual an in cocktail experiments, was 2.6×10^{-4} M; the fluorescence intensity was measured at the maximum, 452 nm; excitation and emission slits = 5 nm; excitation wavelength = 374 nm; scan speed = 12000 nm/min.

Substrate sensitivity

Water solutions of \mathbf{L}_{Sen} were used as “off-on” fluorescence probes for detecting Al(III) at concentrations ranging from 0.3 ppb to 2.8 ppm (Figure 4). The limit of detection (LOD) and the limit of quantification (LOQ)³⁵ were 1.5 and 4.7 ppb, respectively, below the EPA Secondary Drinking Water Regulation (SDWR, 50 to 2000 ppb).³⁶ On the other hand, the LOD and LOQ achieved with the sensory disc cut from \mathbf{M}_{Sen} were much higher, 22 and 36 ppm, respectively. Thus, the solution system presented the advantage of sensitivity, whereas the solid system provided the benefit of a short response time and simplicity.

Conclusions

In summary, we designed both an innovative solid material for the fluorescence “off-on” detection of Al(III) and a new method for measuring the concentration of Al(III) using one drop of measuring solution within minutes at the ppb level, significantly lower than the EPA-recommended concentration for drinking water. The sensory material was a flexible polymer film exhibiting gel behavior. The film was prepared using a novel fluorescence aluminum ion sensory salicylaldehyde benzoylhydrazone derivative and other comonomers to impart hydrophilicity and good mechanical properties. The measurement method consisted in depositing a drop of the solution to be measured on the surface of the sensory film, allowing it to enter the hydrophilic material, followed by a drying period, thus forcing the Al(III) to interact with the sensory motifs within the membrane. The process required approximately half an hour to complete, after which the fluorescence of the system was measured using conventional methods. A water-soluble sensory polymer using the sensory monomer was also prepared, and its performance in detecting aluminum was characterized, yielding results similar to those obtained for the films; however, the measurements involving solutions were much less labor-intensive and time-consuming.

Acknowledgments

We gratefully acknowledge the financial support provided by the Spanish Ministerio de Economía y Competitividad-Feder (MAT2011-22544) and by the Consejería de Educación - Junta de Castilla y León (BU232U13).

Appendix A. Supplementary data

Supplementary data available: 1D and 2D NMR and mass spectra of monomer (**3**) and complexation studies of (**3**) with Al(III), 2D and 3D fluorescence spectra of (**3**) and **M_{sen}** with and without different cations in the media, and interference study.

References

- 1 Álvarez, E.; Fernández-Marcos, M. L.; Monterroso, C.; Fernández-Sanjurjo, M. J. *Ecol. Manage.* **2005**, *211*, 227-239.
 - 2 Barceló, J.; Poschenrieder, C. *Environ. Exp. Bot.* **2002**, *48*, 75-92.
 - 3 Alstad, N. E. W.; Kjelsberg, B. M.; Vøllestad, L. A.; Lydersen, E.; Poléo, A. B. S. *Environ. Pollut.* **2005**, *133*, 333-342.
 - 4 Cronan, C.S.; Walker, W. J.; Bloom, P. R. *Nature* **1986**, *324*, 140-143.
 - 5 Nayak, P. *Environ. Res.* **2002**, *89*, 101-115.
 - 6 Fasman, G. D. *Coord. Chem. Rev.* **1996**, *149*, 125-165.
 - 7 Berthon, G. *Coord. Chem. Rev.* **2002**, *228*, 319-341.
 - 8 Pierides, A. M.; Edwards Jr. W. G.; Cullum Jr. U. X; McCall, J. T.; Ellis, H. A. *Kidney Int.* **1980**, *18*, 115-124.
 - 9 Alfrey, A. C. *Adv. Clin. Chem.* **1983**, *23*, 69-91.
 - 10 Perl, D. P.; Gajdusek, D. C.; Garruto, R. M.; Yanagihara, R. T.; Gibbs, C. J. *Science* **1982**, *217*, 1053-1055.
 - 11 Perl, D. P.; Brody, A. R. *Science* **1980**, *208*, 297-299.
 - 12 El-Sayed, W. M.; Al-Kahtani, M. A.; Abdel-Moneim, A. M. *J. Hazard. Mater.* **2011**, *192*, 880-886.
 - 13 Shokrollahi, A.; Ghaedi, M.; Niband, M.S.; Rajabi, H. R. *J. Hazard. Mater.* **2008**, *151*, 642-648.
 - 14 Kepp, K. P. *Chem. Rev.* **2012**, *112*, 5193-5239.
 - 15 Park, H. M.; Oh, B. N.; Kim, J. H.; Qiong, W.; Hwang, I. H.; Jung, K.-D.; Kim, C.; Kim, J. *Tetrahedron Lett.* **2011**, *52*, 5581-5584.
 - 16 Kim, S. H.; Choi, H. S.; Kim, J.; Joong, S.; Quang, D. T.; Kim, J. S. *Org. Lett.* **2010**, *12*, 560-563.
 - 17 Maity, D.; Govindaraju, T. *Chem. Commun.* **2010**, *46*, 4499-4501.
 - 18 Cheng, X.-Y.; Wang, M.-F.; Yang, Z.-Y.; Li, Y.; Li, T.-R.; Liu, C.-J.; Zhou, Q.-X. *J. Coord. Chem.* **2013**, *66*, 1847-1853.
 - 19 Lee, J.; Kim, H.; Kim, S.; Noh, J. Y.; Song, E. J.; Kim, C.; Kim, J. *Dyes Pigm.* **2013**, *96*, 590-594.
 - 20 Liao, Z.-C.; Yang, Z.-Y.; Li, Y.; Wang, B.-D.; Zhou, Q.-X. *Dyes Pigm.* **2013**, *97*, 124-128.
-

- 21 Wang, Y.-W.; Yu, M.-X.; Yu, Y.-H.; Bai, Z.-P.; Shen, Z.; Li, F.-Y.; You, X.-Z. *Tetrahedron Let.* **2009**, *50*, 6169-6172.
- 22 Maity, S. B.; Bharadwaj, P. K. *Inorg. Chem.* **2013**, *52*, 1161-1163.
- 23 Ma, T.-H.; Dong, M.; Dong, Y.-M.; Wang, Y.-W.; Peng, Y. *Chem. Eur. J.* **2010**, *16*, 10313-10318.
- 24 Tiwari, K.; Mishra M.; Singh, V. P. *RSC Adv.* **2013**, *3*, 12124-12132.
- 25 Jiang, C.; Tang, B.; Wang, C.; Zhang, X. *Analyst* **1996**, *121*, 317-320.
- 26 Mánuel-Vez, M. P.; García-Vargas, M. *Talanta* **1994**, *41*, 1553-1559.
- 27 Jiang, C.; Tang, B.; Wang, R.; Cheng, J. *Talanta* **1997**, *44*, 197-202.
- 28 Suryawanshi, V. D.; Gore, A. H.; Dongare, P. R.; Anbhule, P. V.; Patil, S. R.; Kolekar, G. B. *Spectrochim. Acta A* **2013**, *114*, 681-686.
- 29 Guo, Y.-Y.; Yang, L.-Z.; Ru, J.-X.; Yao, X.; Wu, J.; Dou, W.; Qin, W.-W.; Zhang, G.-L.; Tang, X.-L.; Liu, W.-S. *Dyes Pigm.* **2013**, *99*, 693-698.
- 30 Vallejos, S.; Muñoz, A.; Ibeas, S.; Serna, F.; García, F. C.; García, J. M. *J. Hazard. Mater.* **2014**, *276*, 52-57.
- 31 Brouwer, A. M. *Pure Appl. Chem.* **2011**, *83*, 2213-2228.
- 32 Tashiro, M.; Furuhata, K.; Fujimoto, T.; Machinami, T.; Yoshimura, E. *Magn. Reson. Chem.* **2007**, *45*, 518-521.
- 33 Brouwer, A. M. *Pure Appl. Chem.* **2011**, *83*, 2213-2228.
- 34 International Commission on Illumination (<http://cie.co.at/>). The color matching parameters were downloaded for free from the CIE web page (<http://files.cie.co.at/204.xls>). Access date: November 8, 2013.
- 35 The limit of detection (LOD) and the limit of quantification (LOQ) were calculated from the titration curves using the following equations: LOD = $3.3 \times SD/s$ and LOQ = $10 \times SD/s$, where SD is the standard deviation of the blank sample, and s is the slope of the calibration curve in a region with low analyte content.
- 36 The U.S. Environmental Protection Agency (EPA) has established a limit of 50 to 200 ppb for aluminiumaluminum in drinking water (non-enforceable guidelines regarding cosmetic or aesthetic effects). Source: 2012 Edition of the Drinking Water Standards and Health Advisories, EPA 822-S-12-001, <http://water.epa.gov/action/advisories/drinking/upload/dwstandards-2012.pdf>, accessed October 20, 2014.

SUPPLEMENTARY INFORMATION

Forced solid-state interactions for the rapid, highly sensitive and selective “turn-on” fluorescence sensing of aluminium ions in water using a sensory polymer substrate.

*Saúl Vallejos, Asunción Muñoz, Saturnino Ibeas, Felipe Serna, Félix Clemente García and José Miguel García.**

Departamento de Química, Facultad de Ciencias, Universidad de Burgos, Plaza de Misael Bañuelos s/n, 09001 Burgos, Spain. Email: jmiguel@ubu.es

Table of contents:

S1.-	Experimental part. Intermediate characterization.....
S2.-	Experimental part. Monomer (3) characterization and study of its complexes with Al(III).....
S3.-	Material characterization.....
S4.-	Interference studies for the sensory materials.....

S1. Experimental. Intermediate and monomer characterization

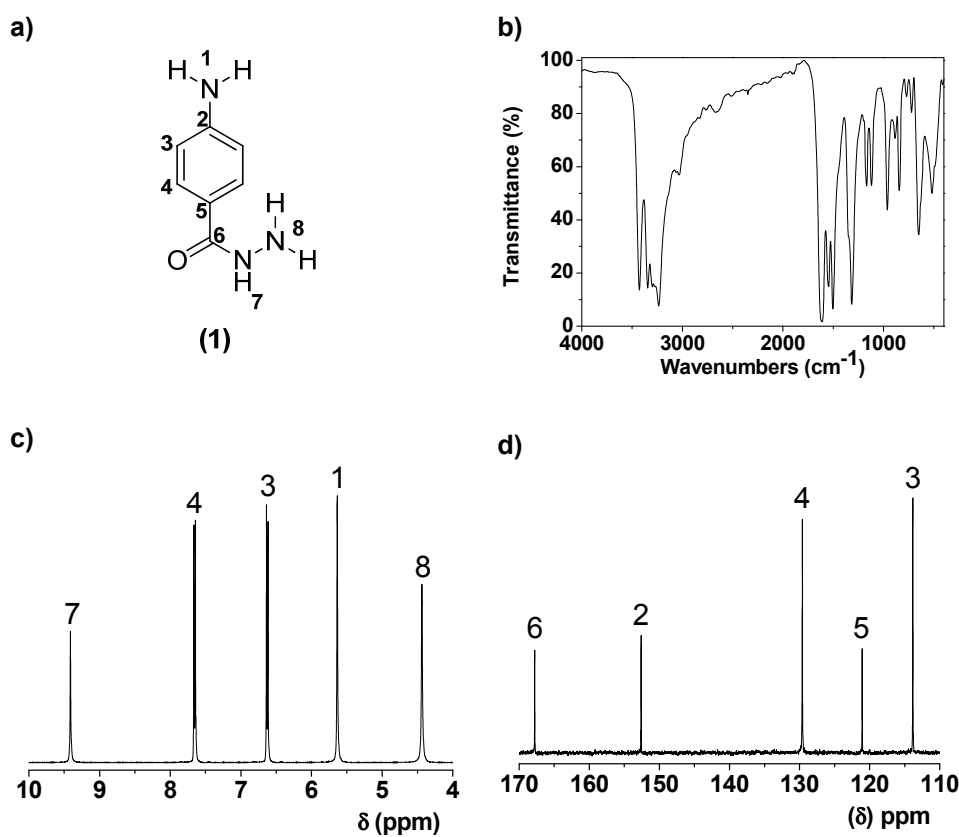


Figure S1. Characterization of 4-aminobenzohydrazide (1): a) chemical structure; b) FTIR; c) ^1H NMR; d) ^{13}C NMR (NMR solvent: DMSO- d_6).

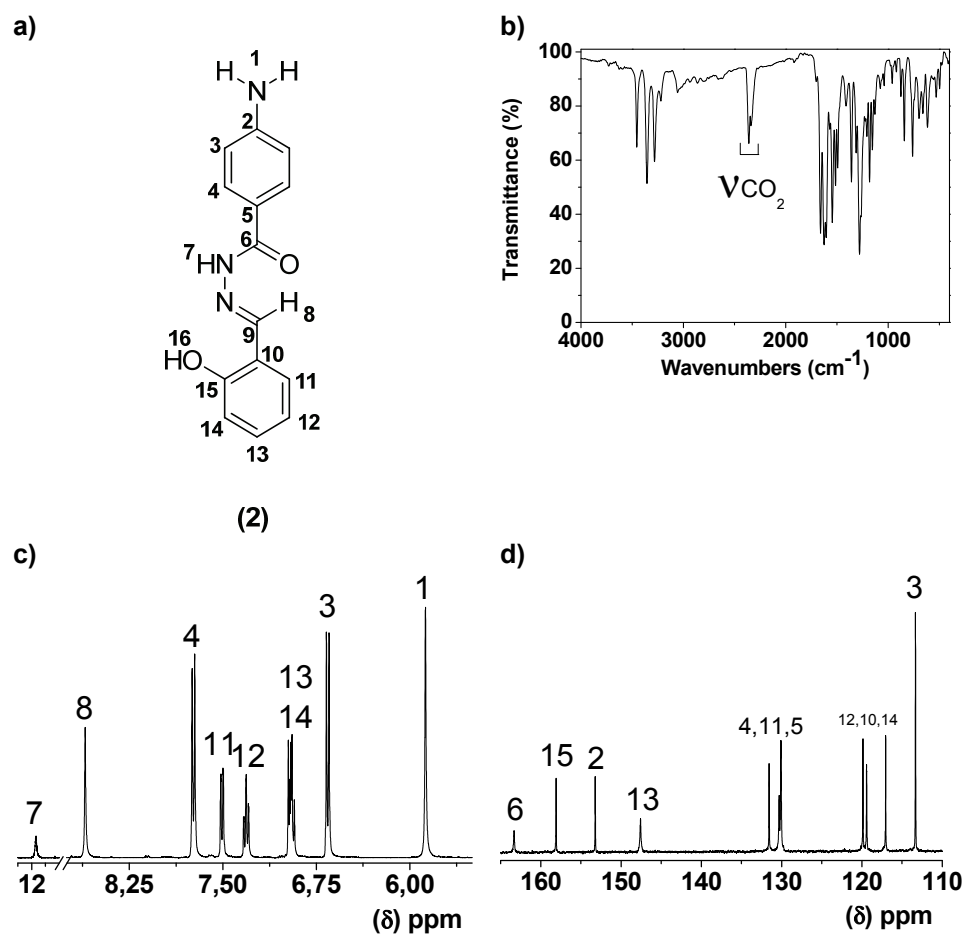


Figure S2. Characterization of (*E*)-4-amino-N'-(2-hydroxybenzylidene)benzohydrazide (2): a) chemical structure; b) FTIR; c) ¹H NMR; d) ¹³C NMR (NMR solvent: DMSO-d₆).

S2.- Experimental. Monomer (3) characterization and study of its complexes with Al(III)

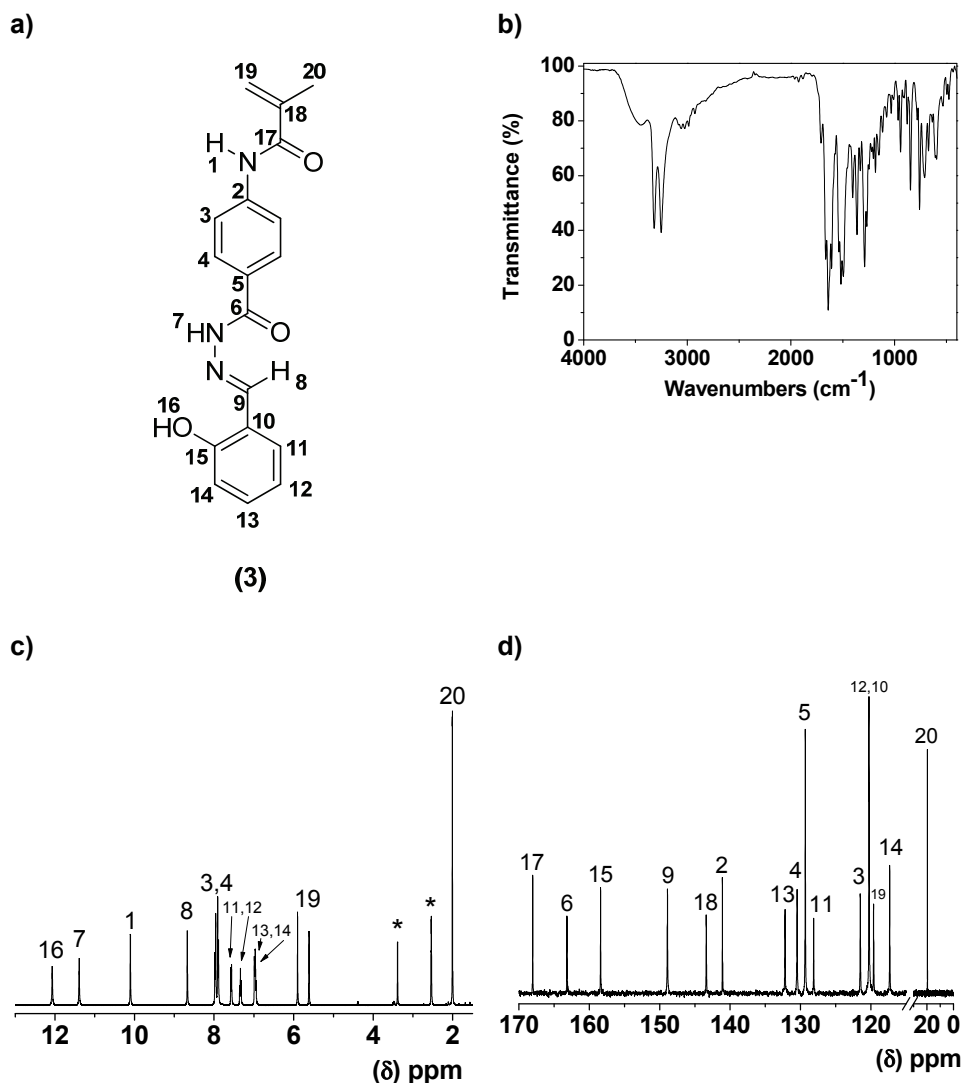


Figure S3. Characterization of (*E*)-*N*-(4-(2-(2-Hydroxybenzylidene)hydrazinecarbonyl)-phenyl) methacrylamide (3): a) chemical structure; b) FTIR; c) ^1H NMR; d) ^{13}C NMR (NMR solvent: DMSO- d_6).

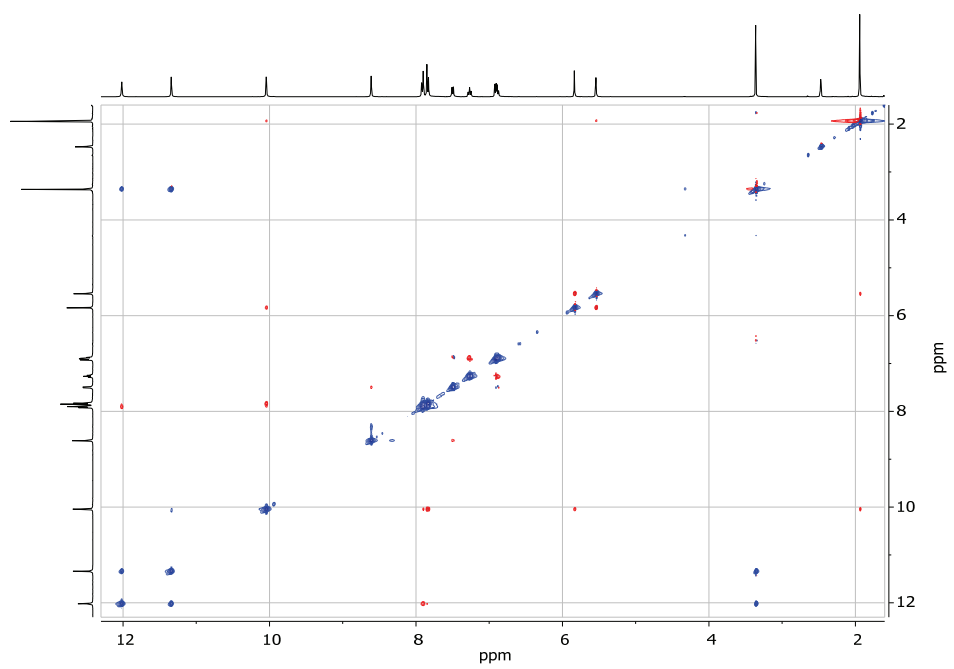


Figure S4. NOESY 2D spectra of (3) (NMR solvent: DMSO-d₆).

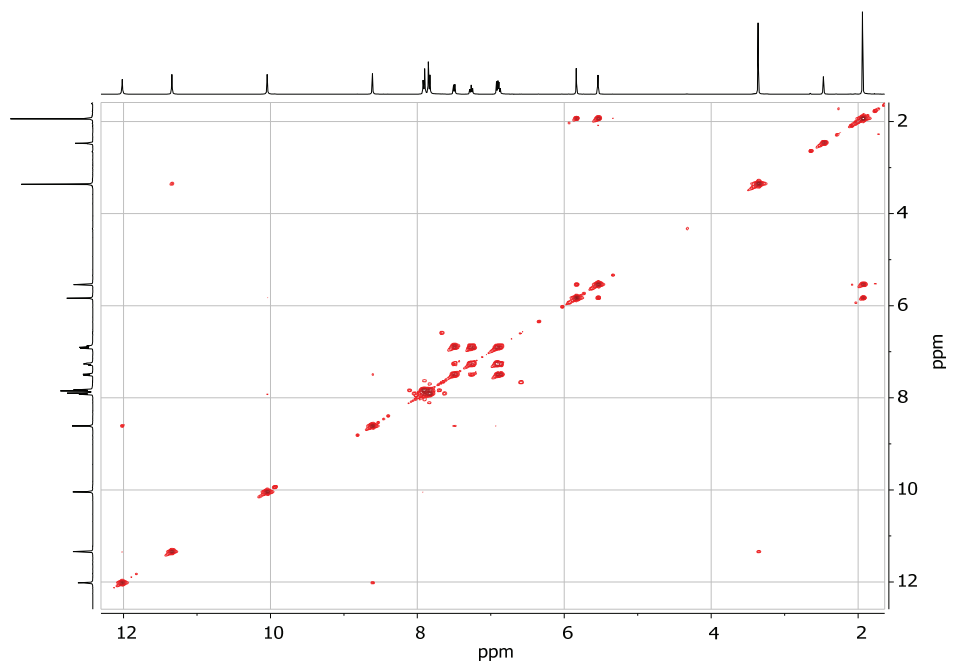
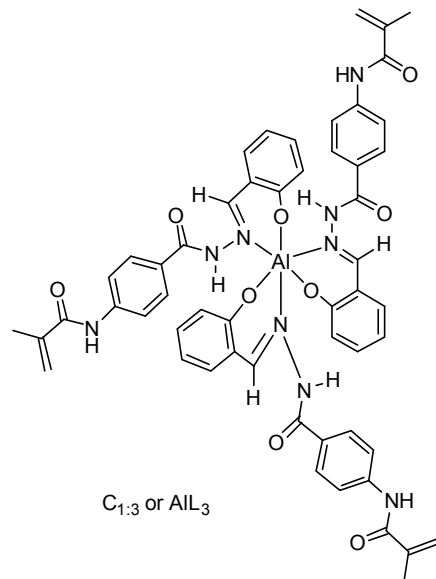


Figure S5. COSY 2D spectra of (3) (NMR solvent: DMSO-d₆).

a)



b)

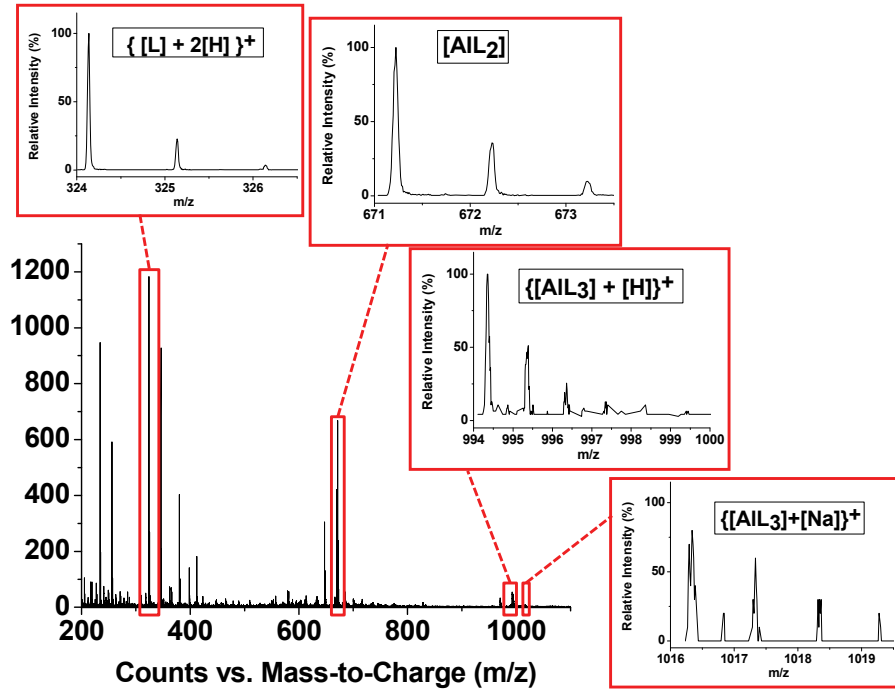


Figure S6. a) Proposed structure for the complex $C_{1:3}$. b) Positive-ion HR-ESI mass spectrum of $C_{1:3}$, emphasizing the heterometallic fragments.

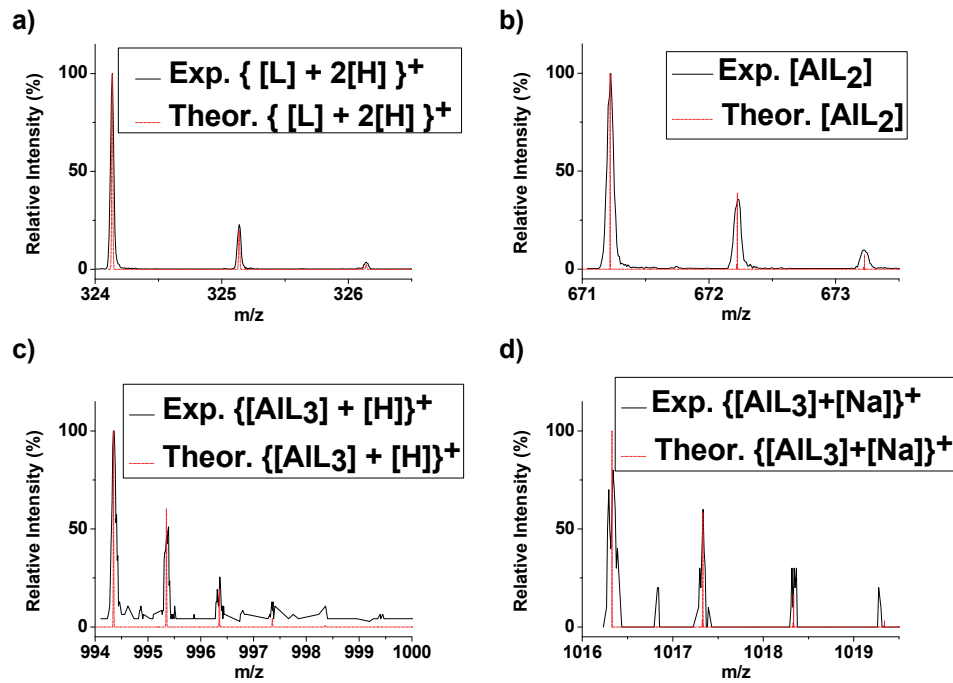


Figure S7. Comparison of four representative peaks from the positive-ion ESI mass spectrogram of a) $\{[L] + 2[H]\}^+$, b) $[AlL_2]$, c) $\{[AlL_3] + [H]\}^+$ and d) $\{[AlL_3] + [Na]\}^+$, with their simulated ones; the isotopic distribution has been taken into account.

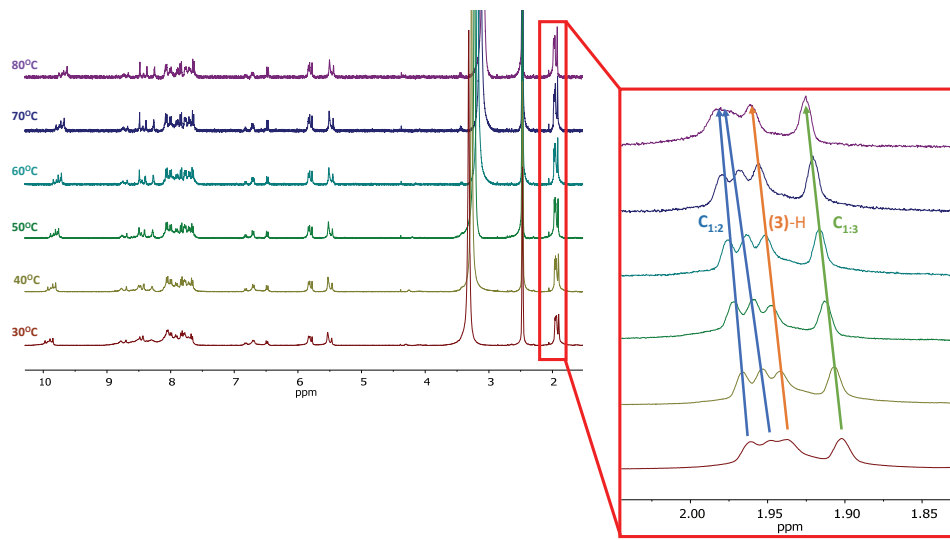


Figure 8. ^1H NMR spectra showing the equilibrium $[(3)_3:\text{Al(III)} \rightleftharpoons (3)_2:\text{Al(III)}^+ + (3)\text{-H}]$ at different temperatures (solvent = DMSO-d₆).

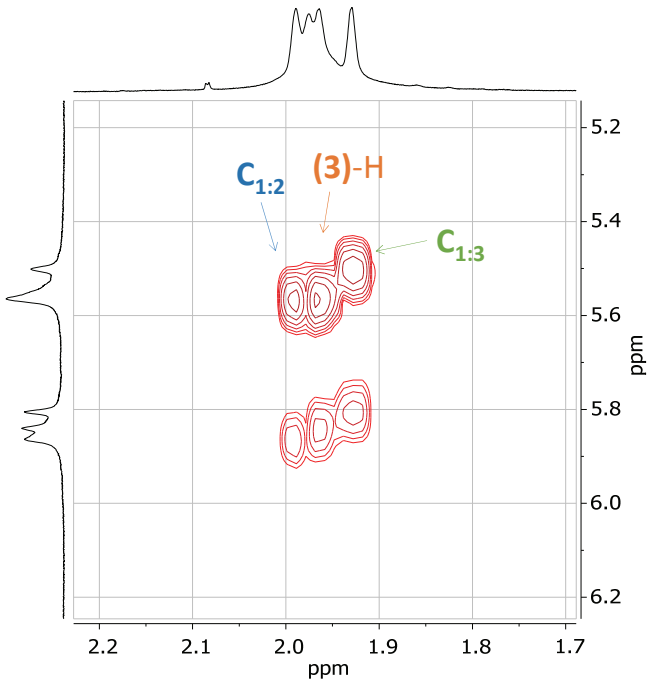


Figure 9. Expansion of the 400 MHz ^1H COSY spectrum for the equilibrium $[(3)_3:\text{Al(III)} \rightleftharpoons (3)_2:\text{Al(III)}^+ + ((3)\text{-H})]$ (25°C , solvent = DMSO-d₆).

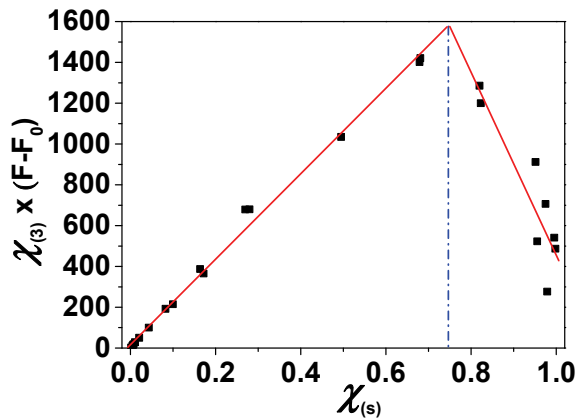


Figure S10. Job's plots corresponding to the interaction study of L_{Sen} in MilliQ water with Al(III). \square_s is the molar fraction of sensory motifs (salicylaldehyde-derivative moieties), and F and F_0 the fluorescence intensity at 452 nm at 0 and at a given concentration of Al(III), respectively. Conditions: the concentration of the L_{Sen} was 2.81 g/L, corresponding to 0.25 mEq/L of the sensory motif (3); MilliQ water was buffered (NaOH/AcOH) at pH = 4.5; excitation slit = 5 nm; emission slit = 5 nm; excitation wavelength = 374 nm; scan speed = 12000 nm/min; the Al(III) concentration was increased every 5 minutes. The fluorescence curves are depicted in Figure 3.

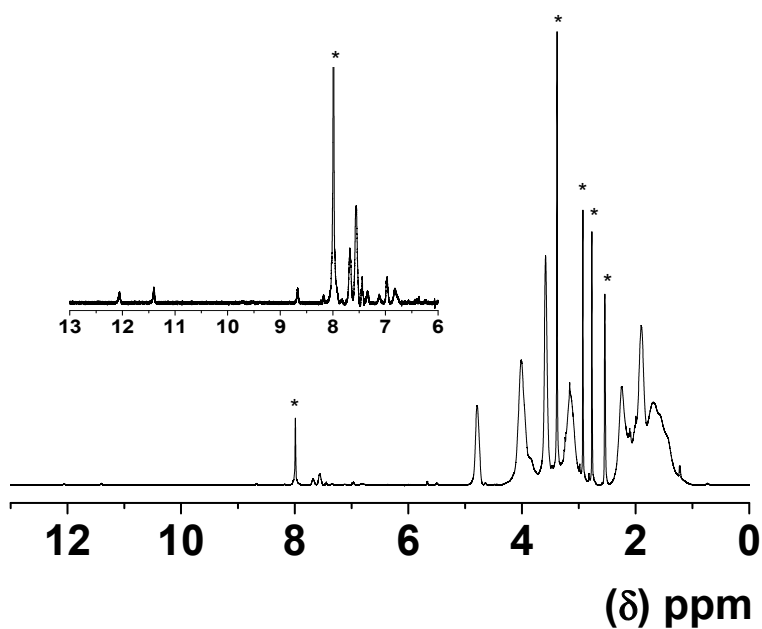
S3.- Material characterization

Figure S11. ^1H NMR spectrum of L_{Sen} . Inset shows an expansion of the aromatic regions corresponding to the signals of the sensory motifs derived from the copolymerization of (3) (*, NMR solvent: DMSO- d_6 ; signals corresponding to water and DMF are also observed).

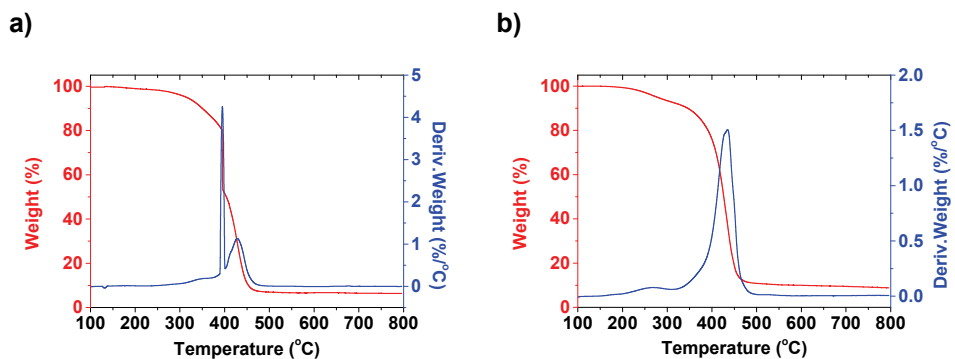


Figure S12. TGA of sensory materials under N_2 atmosphere: a) copolymer (L_{Sen}); b) membrane (M_{Sem}).



Figure S13. Photograph of film strips of membrane **Al-M_{sen}** captured under irradiation with UV light (364 nm).

S4.- Interference studies of sensory materials

Table S1. Fluorescence data of the cations that causes the fluorescene “turn on” of organic/aqueous solutions (DMA/H₂O, 50/50, v/v) of (3).

Cation	λ_{exc} , nm	$\lambda_{\text{em max}}$, nm	Fluorescence intensity (a.u.)	Fluorescence enhancement
Blank	388	452	13.02	--
Al(III)	427	462	319.2	23.5
Zr(IV)	442	498	63.67	3.9
Cd(II)	419	495	28.61	1.2
Zn(II)	439	498	55.79	3.3
La(III)	438	508	63.67	3.9

Measurement conditions: Excitation and emission slit of 5 nm; scan speed of 30000 nm/min, solution of 0.5 mL of DMA, 0.5mL of MilliQ water buffered at pH = 4.5, 0.25 mL of a 0.1 M solution corresponding cation in MilliQ water buffered at pH = 4.5, 0.25 mL of a 0.01 M DMA solution of (3).

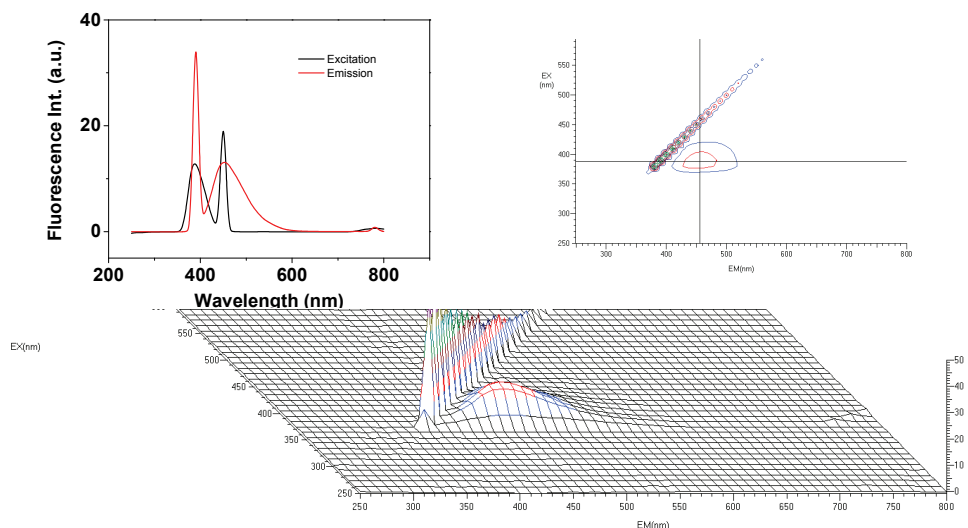


Figure S14. 2D and 3D fluorescence spectra of organic/aqueous solutions (DMA/H₂O, 50/50, v/v) of (3). Measurement conditions: Excitation and emission slit of 5 nm; scan speed of 30000 nm/min, solution of 0.5 mL of DMA, 0.75 mL of MilliQ water buffered at pH = 4.5, 0.25 mL of a DMA 0.01 M solution of (3).

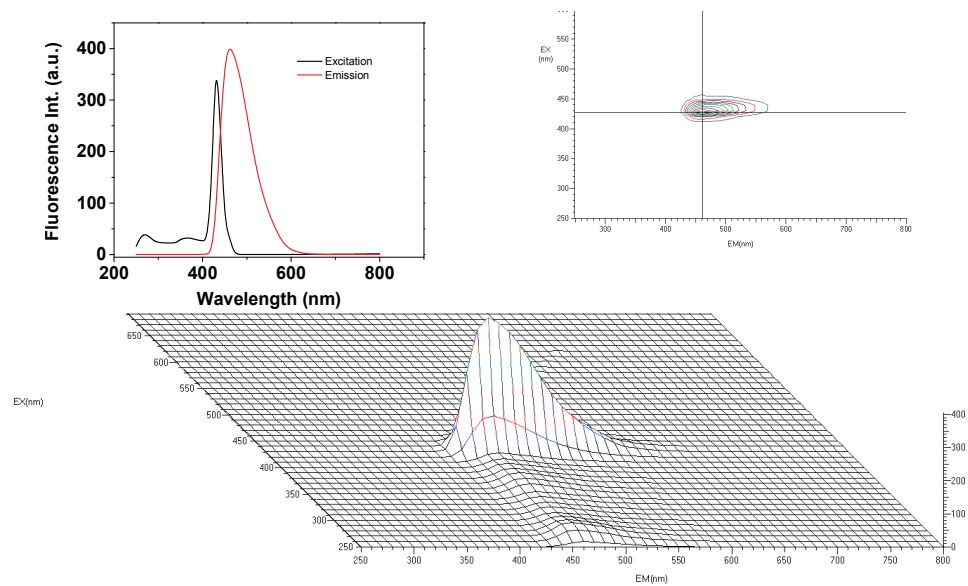


Figure S15. 2D and 3D fluorescence spectra of organic/aqueous solutions (DMA/H₂O, 50/50, v/v) of (3) upon adding Al(III). Measuring conditions: Excitation and emission slit of 5 nm; scan speed of 30000 nm/min, solution of 0.5 mL of DMA, 0.5 mL of MilliQ water buffered at pH = 4.5, 0.25 mL of a 0.1 M solution of Al(NO₃)₃ in MilliQ water buffered at pH = 4.5, 0.25 mL of a DMA 0.01 M solution of (3).

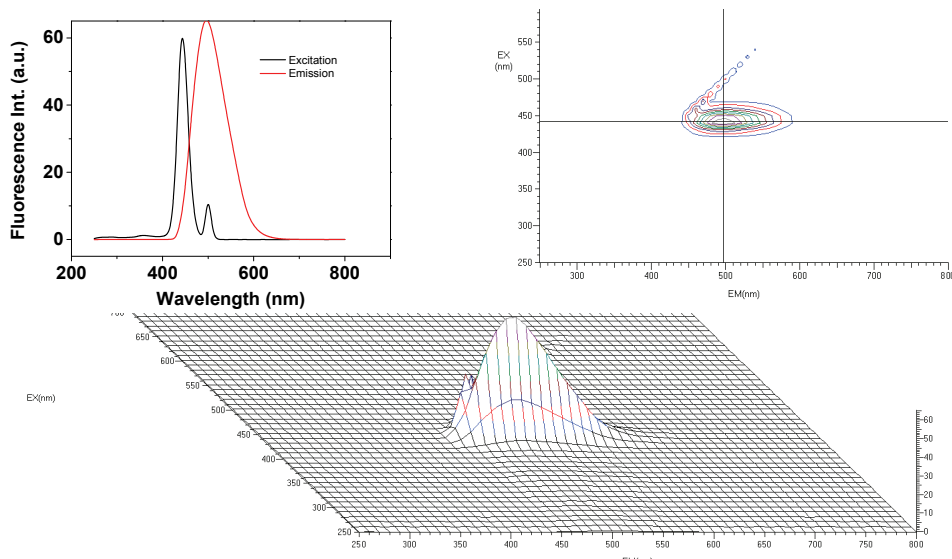


Figure S16. 2D and 3D fluorescence spectra of organic/aqueous solutions (DMA/H₂O, 50/50, v/v) of (**3**) upon adding Zr(IV). Measurement conditions: Excitation and emission slit of 5 nm; scan speed of 30000 nm/min, solution of 0.5 mL of DMA, 0.5 mL of MilliQ water buffered at pH = 4.5, 0.25 mL of a 0.1M solution of ZrCl₄ in MilliQ water buffered at pH = 4.5, 0.25 mL of a DMA 0.01 M solution of (**3**).

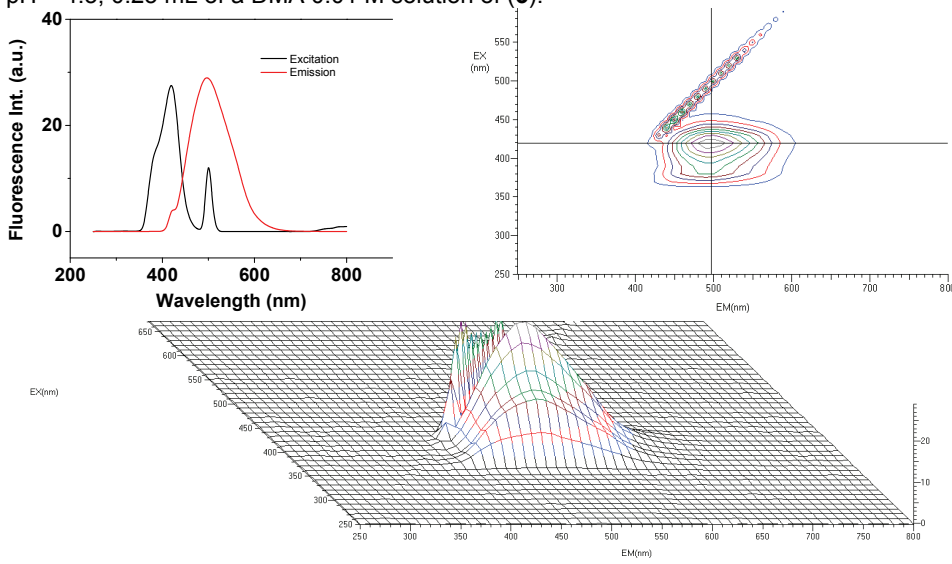


Figure S17. 2D and 3D fluorescence spectra of organic/aqueous solutions (DMA/H₂O, 50/50, v/v) of (**3**) upon adding Cd(II). Measurement conditions: Excitation and emission slit of 5 nm; scan speed of 30000 nm/min, solution of 0.5 mL of DMA, 0.5 mL of MilliQ water buffered at pH = 4.5, 0.25 mL of a 0.1 M solution of Cd(NO₃)₂ in MilliQ water buffered at pH = 4.5, 0.25 mL of a DMA 0.01 M solution of (**3**).

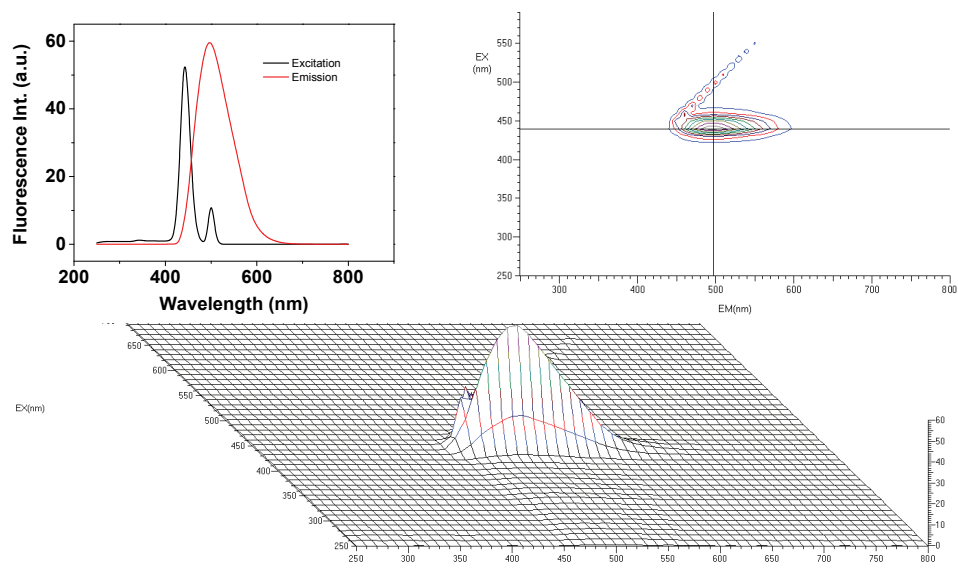


Figure S18. 2D and 3D fluorescence spectra of organic/aqueous solutions (DMA/H₂O, 50/50, v/v) of (3) upon adding Zn(II). Measurement conditions: Excitation and emission slit of 5 nm; scan speed of 30000 nm/min, solution of 0.5 mL of DMA, 0.5 mL of MilliQ water buffered at pH = 4.5, 0.25 mL of a 0.1 M solution of Zn(NO₃)₂ in milliQ water buffered at pH = 4.5, 0.25 mL of a 0.01 M DMA solution of (3).

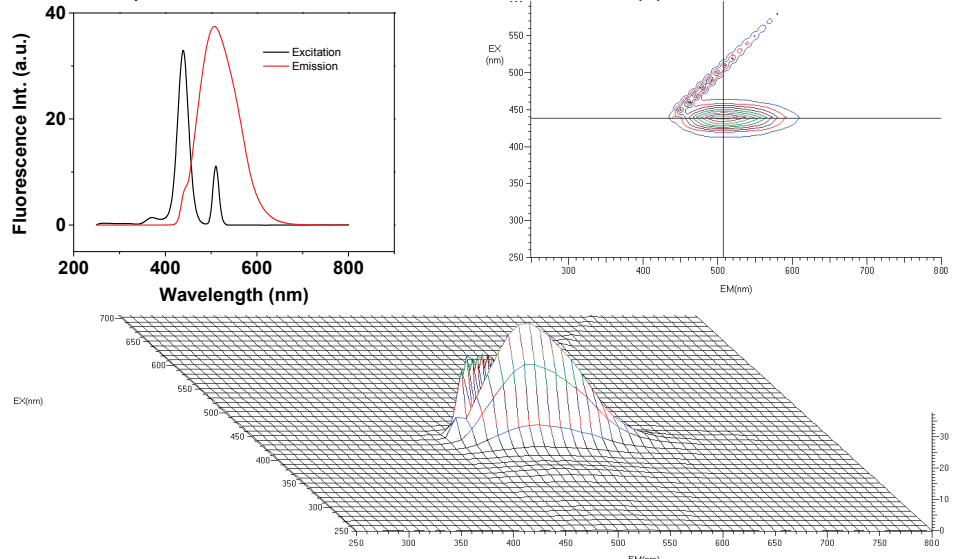


Figure S19. 2D and 3D fluorescence spectra of organic/aqueous solutions (DMA/H₂O, 50/50, v/v) of (3) upon adding La(III). Measurement conditions: Excitation and emission slit of 5 nm; scan speed of 30000 nm/min, solution of 0.5 mL of DMA, 0.5 mL of MilliQ water buffered at pH = 4.5, 0.25 mL of a 0.1 M solution of La(NO₃)₃ in MilliQ water buffered at pH = 4.5, 0.25 mL of a DMA 0.01 M solution of (3).

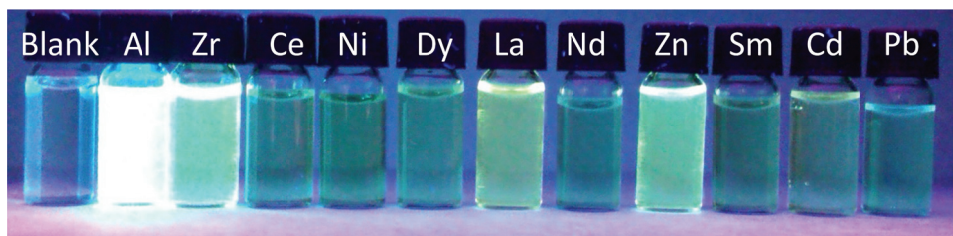


Figure S20. Photograph of DMA/water (50/50, v/v) solutions of (**3**) captured under UV light (366 nm). Conditions: MilliQ water buffered at pH = 4.5; concentration of (**3**) = 3.3×10^{-3} M, concentration of each cation 3.3×10^{-2} M.

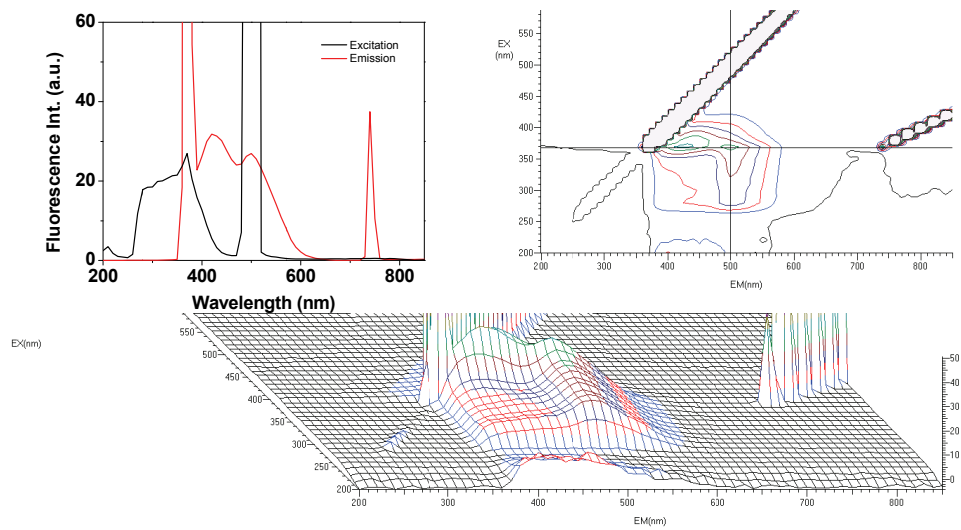


Figure S21. 2D and 3D fluorescence spectra of **Msen** in water (MilliQ water buffered at pH = 4.5). Measurement conditions: Excitation and emission slit of 5 nm; scan speed of 30000 nm/min.

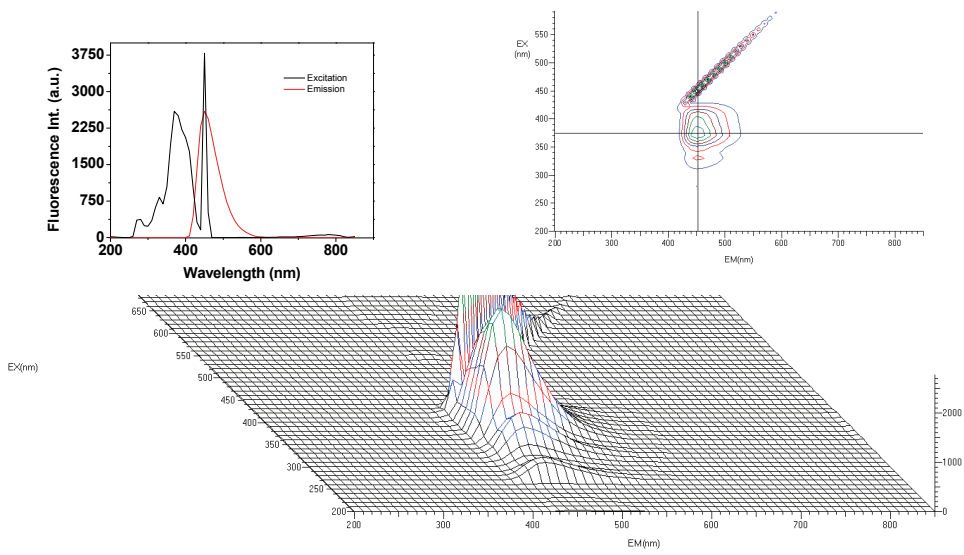


Figure S22. 2D and 3D fluorescence spectra of **Msen** dipped in water (MilliQ water buffered at pH = 4.5) with an $\text{Al}(\text{NO}_3)_3$ concentration of 4.8×10^{-2} M. Measurement conditions: Excitation and emission slit of 5 nm; scan speed of 30000 nm/min, volume = 2.1 mL.

CONCLUSIONES

El anclaje químico de grupos que actúan como receptores de analitos en materiales poliméricos hidrofílicos permite su empleo en medios acuosos, con independencia tanto de la naturaleza química del receptor como de su afinidad hacia dicho medio. Por otra parte, la estructura del polímero se puede diseñar para que provea una apropiada difusión del analito en el material sensor y para conseguir una adecuada velocidad de respuesta, junto con una selectividad eficaz en la interacción analito-receptor.

Las conclusiones particulares derivadas del trabajo son las siguientes:

- El diseño monómeros con grupos receptores de aniones derivados de fluoreno, y de cationes derivados de 2,5-dicetopiperazina, 8-hidroxiquinolina y acilhidrazona permite la preparación de polímeros orgánicos lineales y entrecruzados para su empleo como materiales sensores.
- El diseño químico de la estructura de polímeros para aplicaciones como sensores cromogénicos y fluorogénicos permite la obtención de materiales sensores manejables, con buenas propiedades mecánicas, para su empleo en medios acuosos.
- La sensibilidad y manejabilidad de los polímeros sensores se puede ajustar de forma precisa para satisfacer demandas tecnológicas concretas.

ANEXOS

ANEXO I

En el presente Anexo se expone la primera página (Figura A1) y se comentan las conclusiones a las que se llegaron al realizar el trabajo publicado en la revista *Macromolecular Chemistry and Physics* y que lleva por título "*Determination of oxygen permeability in Acrylic-Based hydrogels by proton NMR Spectroscopy and imaging*". Se llevó a cabo en colaboración con el grupo de investigación dirigido por el Prof. Dr. Julio Guzmán del Instituto de Ciencia y Tecnología de Polímeros del CSIC, y en él se describe el estudio de la permeabilidad frente al oxígeno de los polímeros sintetizados con el monómero *N*-(2-(2-hidroxietoxi)ethyl)metacrilamida (HEEMAM). Las conclusiones son:

- ❖ Se determinó la permeabilidad al oxígeno de los hidrogeles. A partir de las cinéticas de absorción de oxígeno en los materiales se evaluaron los coeficientes de solubilidad y difusión, y con ellos la permeabilidad.
- ❖ Las cinéticas de absorción de oxígeno se obtuvieron mediante un nuevo método que emplea la RMN de protón. Así, éste se basa en el efecto paramagnético del oxígeno en los tiempos de relajación espín-red de los protones evaluable mediante RMN convencional y de imagen. El método se verificó con agua destilada, comprobando cómo los valores obtenidos se correspondían con los de la bibliografía.
- ❖ Los valores obtenidos para los geles poliméricos ensayados se compararon los con que se obtuvieron por técnicas potenciosztáticas convencionales, llegando a una coincidencia aceptable de los parámetros de difusión.
- ❖ Aunque el método de formación de imágenes de RMN permite una estimación directa de la difusión usando la ecuación diferencial de Fick, el enfoque se ve obstaculizado por las grandes incertidumbres asociadas al cálculo de las derivadas correspondientes.

Determination of Oxygen Permeability in Acrylic-Based Hydrogels by Proton NMR Spectroscopy and Imaging

Vicente Compañ, Sergio Mollá, Saúl Vallejos, Félix García, José Miguel García, Julio Guzmán, Leoncio Garrido*

Polymer network membranes with a high capacity for water absorption are obtained by radical polymerization of *N*-[2-(2-hydroxyethoxy)ethyl]methacrylamide (HEEMAM). The permeability, solubility, and diffusion coefficients of oxygen in hydrogels are determined using nuclear magnetic resonance (NMR) methods based on the paramagnetic effect of dissolved oxygen gas on the proton spin-lattice relaxation times of water, and the results are compared with those obtained with electrochemical procedures. The results of NMR measurements of oxygen transport coefficients in distilled water show excellent agreement with corresponding literature values. The results of the potentiostatic and NMR oxygen transport measurements in hydrogels are in reasonable agreement and support the viability of the NMR method.

1. Introduction

Hydrophilic and hydrosoluble polymers have received a considerable attention due to their vast range of applications. Particularly, water absorbent crosslinked materials have been widely investigated in the last decades for use as contact lenses and super absorbent hydrogels for applications in different fields.^[1–7]

Generally, chemical structures having hydrophilic or hydrosoluble (meth)acrylic monomers constitute the base polymers to prepare hydrogels and, particularly, membranes for soft contact lenses. Concerning the later, current research efforts are leading to the development of materials with improved water absorption and minimal dehydration during the wear cycle. An improvement in both properties, compared with conventional lenses of poly(2-hydroxyethylmethacrylate), may be obtained with polymers where strong intermolecular interactions between water and the hydrophilic moieties in the polymer chain occur as, for example, in glycerol methacrylates.^[8,9]

A key property, a polymer material must display for use as soft contact lenses, is optical transparency. However, other characteristics are also needed, such as suitable mechanical properties, a relatively high permeability to oxygen in order to avoid corneal diseases, and adequate hydrolytic stability. The later can be attained with monomers containing amide groups, which are more resistant than the ester groups.^[10] Thus, hydrogels of poly(*N*-[2-(2-hydroxyethoxy)ethyl]methacrylamide) (PHEEMAM) with

Prof. V. Compañ, Dr. S. Mollá
Departamento de Termodinámica Aplicada,
Universidad Politécnica de Valencia
C/Camino de Vera s/n, 46020 Valencia, Spain
S. Vallejos, Prof. F. García, Prof. J. M. García
Departamento de Química, Facultad de Ciencias,
Universidad de Burgos
Plaza Misael Bañuelos s/n, 09001 Burgos, Spain
Prof. J. Guzmán, Dr. L. Garrido
Departamento de Química Física, Instituto de Ciencia y
Tecnología de Polímeros
Consejo Superior de Investigaciones Científicas (ICTP-CSIC)
Juan de la Cierva 3, 28006 Madrid, Spain
E-mail: lgarrido@ceteef.csic.es

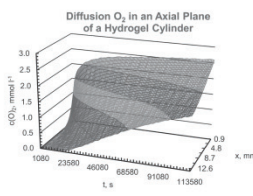


Figura A1. Primera página del artículo “*Determination of Oxygen Permeability in Acrylic-Based Hydrogels by Proton NMR Spectroscopy and Imaging*” publicado en la revista *Macromolecular Chemistry and Physics*.

ANEXO II

En este Anexo se expone la primera página (Figura A2) y se comentan las conclusiones a las que se llegaron al realizar el trabajo publicado en la revista *Macromolecules* y que lleva por título “*Effect of the Dipole–Dipole Interactions in the Molecular Dynamics of Poly(vinylpyrrolidone)-Based Copolymers*”. Se llevó a cabo en colaboración con el grupo de investigación dirigido por la Prof. María Jesús Sanchís del Departamento de Termodinámica Aplicada de la Universidad Politécnica de Valencia, y en él se describe el estudio de las interacciones dipolares en los copolímeros preparados a partir de distintas proporciones de los monómeros *N*-vinilpirrolidona (VP) y acrilato de butilo (BA), así como su influencia en diversas propiedades macroscópicas, como por ejemplo las propiedades mecánicas y las temperaturas de transición vítrea y de descomposición. Las conclusiones son:

- ❖ Los filmes de polivinilpirrolidona lineal obtenidos por evaporación del disolvente fueron frágiles, transparentes y con un brillo característico. Estas propiedades no variaron con una reticulación moderada. Por otra parte, la elevada hidrofilia del polímero hizo que en ausencia de reticulante se disolviera en agua y que ligeramente reticulado, en forma de membrana o filme, se hinchara hasta valores próximos al 1000%, destrozando este hinchamiento al propio material y perdiendo, por tanto, toda posibilidad de uso.
- ❖ El polímero de acrilato de butilo es un polímero muy hidrofóbico y con una temperatura de transición vítrea muy inferior a la ambiente (con una reticulación moderada, 1% en moles de reticulante en la alimentación, esta temperatura fue de -44°C). Estos hechos conllevaron a que las membranas preparadas absorbieran menos del 1% en agua y que el material fuera excesivamente blando, por lo que tampoco se puede emplear como material con mínimas propiedades estructurales.

- ❖ La copolimerización de VP con BA ofrece un abanico de materiales con excelentes propiedades que se pueden modular a la carta mediante la distinta proporción de los comonomeros. Se observó compatibilidad en todas las proporciones estudiadas, así como copolimerización al azar. Las propiedades se evaluaron y se correlacionaron con la estructura mediante diferentes técnicas analíticas, como la termogravimetría (TGA), calorímetría diferencial de barrido (DSC), espectroscopía de infrarrojo (FTIR), análisis mecánico de tracción (TMA), espectroscopía de relajación dieléctrica (DRS).
- ❖ De acuerdo con la TGA y con los ensayos de tracción, la estabilidad mecánica y térmica se incrementa con el porcentaje de VP.
- ❖ El grado de hinchamiento estuvo directamente relacionado con el porcentaje de VP.
- ❖ Todos los copolímeros mostraron tres relajaciones dipolares (γ , β , y α) y un proceso de conducción importante a baja frecuencia y alta temperatura.
- ❖ Las interacciones dipolo-dipolo entre grupos amida del anillo lactámico de la VP, que se estudiaron por FTIR, afectan directamente a la movilidad molecular, obteniéndose las siguientes conclusiones: a) la temperatura de transición vítrea se incrementa con el aumento de la proporción de VP por disminución de la movilidad molecular. Los valores de la transición se obtuvieron por DSC y DRS; b) el mayor incremento en la capacidad calorífica en la T_g se produjo en el homopolímero de BA, y la menor en el de VP, que está relacionado con la fuerte interacción dipolo-dipolo entre unidades de VP; c) la rigidez dieléctrica del copolímero con 50% de VP es más alta que la de los copolímeros con mayor

porcentaje de VP, hecho que también se relacionó con las interacciones dipolo-dipolo entre anillos lactama; d) la energía de activación del proceso γ relacionado con los movimientos locales del grupo butilo se incrementa con el contenido en VP. Por el contrario, la energía de activación de la relajación β , que es un proceso de relajación Johari y Goldstein (JG)^{71,72} relacionado con la movilidad del anillo lactámico junto con segmentos de la cadena principal, permanece constante con el porcentaje de comonómeros, hecho que también se relacionó con las interacciones dipolo-dipolo mencionadas previamente; e) los valores de fragilidad, relacionados íntimamente con las interacciones intermoleculares, indicaron que los copolímeros son vidrios frágiles. Así, el índice de fragilidad (m) se incrementó con la proporción de VP, hecho que se atribuyó al aumento consiguiente de las interacciones dipolo-dipolo.^{73,74}

- ❖ La conductividad depende mucho de la temperatura y de la composición. Los copolímeros mostraron un comportamiento Vogel–Fucher–Tamman–Hesse (VFTH), lo que probó la contribución de la relajación segmental a la conductividad.

⁷¹ G. P. Johari, M.J. Goldstein, *J. Chem. Phys.* **1970**, 53, 2372.

⁷² G. P. Johari, M.J. Goldstein, *J. Chem. Phys.* **1972**, 56, 4411

⁷³ D. Cangialosi, A. Alegría, J. Colmenero, *J. Chem. Phys.* **2006**, 124, 024906.

⁷⁴ C. M. Roland, P. G. Santangelo, K. L. Ngai, *J. Chem. Phys.* **1999**, 111, 5593.

Effect of the Dipole–Dipole Interactions in the Molecular Dynamics of Poly(vinylpyrrolidone)-Based Copolymers

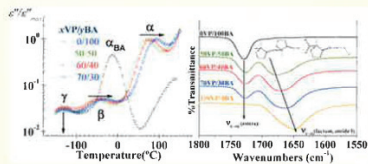
B. Redondo-Foj,[†] M. Carsí,[†] P. Ortiz-Serna,[†] and M. J. Sanchis^{†,*}

[†]Instituto Tecnológico de la Energía, Departamento de Termodinámica Aplicada, Universitat Politècnica de València, Camí de Vera s/n, 46022, Valencia, Spain

S. Vallejos,[‡] F. García,[‡] and J. M. García[‡]

[‡]Departamento de Química, Facultad de Ciencias, Universidad de Burgos, Plaza Misael Bañuelos s/n, 09001 Burgos, Spain

ABSTRACT: Poly(vinylpyrrolidone-*co*-butyl acrylate) samples with different proportions of monomers were prepared as tractable and hydrophilic materials. An analysis of the intermolecular interactions between the polymer groups was carried out by FTIR. The dependence of the C=O bands (lactam and pendant butyl ester) with the composition suggests a strong interaction between the lactam groups. They exert an important influence in the molecular mobility, which was studied by DSC and DRS. A single narrow glass transition temperature (T_g) is observed in each random copolymer, consistent with a single phase of low compositional nanoheterogeneity. The dependence of the T_g with the composition suggests significant interactions between polymer components. The dielectric spectra show γ , β , and α relaxations in increasing order of temperature, followed by conductive contributions. The apparent activation energies for secondary relaxations have similar values for all the samples. The γ -process is related to the local motions of the butyl units and the β -process is a Johari–Golstein secondary relaxation that is related to the local motions of the pyrrolidone group together with the motion of polymer backbone segments.



1. INTRODUCTION

N-Vinyl-2-pyrrolidone (VP) is a cheap and widely available chemical, prepared industrially from acetylene and formaldehyde following the Reppe's procedure.^{1,2} VP is a high boiling point liquid (92–95 °C at 1.3 kPa), highly miscible in water and in organic solvents, and with other vinyl or acrylic monomers. VP linear polymerization, either in bulk, in solution or in suspension, gives rise to linear polyvinylpyrrolidone (PVP). PVP is also known as Povidone, an amphiphilic polymer soluble in water and in polar organic solvents but insoluble in esters, ethers, ketones and hydrocarbons.³ It cannot be melt processed due to its low decomposition temperature. Its T_g reaches a constant value (approximately 175 °C) when its average molecular weight is 100 000 g·mol⁻¹.⁴ The films prepared from PVP solution are brittle, clear, and glossy. Its popcorn polymerization, i.e., proliferous polymerization, gives rise to highly cross-linked PVP, called Crospovidone, completely insoluble, and of the great industrial importance. Both, linear and cross-linked PVP have a wide range of applications. Because of its biocompatibility, PVP is used in pharmacological and biomedical applications. Furthermore, it is also utilized in numerous industrial fields like adhesives, ceramic, coatings, food, etc.^{2,3}

The relation between the structure of polymers and their properties has been widely studied in the literature. In this way, the copolymerization is presented as an effective method to prepare macromolecules with specific chemical structures and

to control some properties such as hydrophilic/hydrophobic balances, solubility, polarity, etc.⁵ Hence, copolymers have attracted a great attention because they can be frequently used to tune the properties of a material between those of the corresponding homopolymers. Copolymers comprised of VP and acrylic or vinyl comonomers are commercially produced to modify, to improve, and to adapt the properties of PVP to specific applications. In the same way, the water affinity of the PVP, or even the water solubility, which can be too high for certain applications, has been reduced by copolymerizing with vinyl acetate or vinyl propionate.^{3,6} Thus, acrylic chemicals are among the most versatile and inexpensive comonomers to prepare materials with specific properties.

The dynamic mechanical and dielectrical properties are intrinsically correlated and they are associated with a structural polymer feature.^{7–12} The dynamic relaxation properties of cross-linked polymer networks are highly sensitive to network composition and polymer chain architecture. The cooperative segmental motions (T_g) and the more localized processes observed below T_g can be dramatically affected by (i) changes in the backbone structure, (ii) cross-link density, or (iii) the introduction of pendant groups or branches. One of the most powerful and versatile methods for the study of molecular

Received: April 16, 2014

Revised: July 8, 2014

Published: July 18, 2014

Figura A2. Primera página del artículo “Effect of the Dipole–Dipole Interactions in the Molecular Dynamics of Poly(vinylpyrrolidone)-Based Copolymers” publicado en la revista *Macromolecules*.

ANEXO III

A continuación se realiza el listado de publicaciones científicas, patentes y aportaciones a congresos que se han conseguido durante la realización de esta tesis doctoral:

Publicaciones Científicas

- 1) S. Vallejos, P. Estévez, F. C. García, F. Serna, J. L. de la Peña, J. M. García, *Putting to work organic sensing molecules in aqueous media: fluorene-derivative containing polymers as sensory materials for the colorimetric sensing of cyanide in water*, *Chem. Commun.* **2010**, 46, 7951.
- 2) S. Vallejos, H. El Kaoutit, P. Estévez, F. C. García, J. L. de la Peña, F. Serna, J. M. García, *Working with water insoluble organic molecules in aqueous media fluorene derivate-containing polymers as sensory materials for the colorimetric sensing of cyanide in water*, *Polym. Chem.* **2011**, 2, 1129.
- 3) S. Vallejos, P. Estévez, S. Ibeas, A. Muñoz, F. C. García, F. Serna, J. M. García, *A selective and highly sensitive fluorescent probe of Hg²⁺ in organic and aqueous media: The role of a polymer network in extending the sensing phenomena to water environments*, *Sens. Actuators, B* **2011**, 157, 686.
- 4) S. Vallejos, P. Estévez, S. Ibeas, F. C. García, F. Serna, J. M. García, *An Organic/Inorganic Hybrid Membrane as a Solid “Turn-On” Fluorescent Chemosensor for Coenzyme A (CoA), Cysteine (Cys), and Glutathione (GSH) in Aqueous Media*, *Sensors* **2012**, 12, 2969.
- 5) S. Vallejos, A. Muñoz, F. C. García, F. Serna, S. Ibeas, J. M. García, *Methacrylate copolymers with pendant piperazinedione-sensing motifs as fluorescent chemosensory materials for the detection of Cr(VI) in aqueous media*, *J. Hazard. Mater.* **2012**, 227-228, 480.
- 6) S. Vallejos, A. Muñoz, S. Ibeas, F. Serna, F. C. García, J. M. García, *Solid sensory polymer substrates for the quantification of iron in blood, wine and water by a scalable RGB technique*, *J. Mater. Chem. A* **2013**, 1, 15435.
- 7) S. Vallejos, A. Muñoz, S. Ibeas, F. Serna, F. C. García, , J. M. García, *Selective and sensitive detection of aluminium ions in water via fluorescence “turn-on” of both solid and water soluble polymer substrates*, *J. Hazard. Mater.* **2014**, 276, 52.
- 8) V. Compañ, S. Mollá, S. Vallejos, F. García, J. M. García, J. Guzmán, L. Garrido, *Determination of oxygen permeability in Acrylic-Based hydrogels*

- by proton NMR Spectroscopy and imaging, *Macromol. Chem. Phys.* **2014**, 215, 624.
- 9) B. Redondo-Foj, M. Carsí, P. Ortiz-Serna, M. J. Sanchís, S. Vallejos, F. García, J. M. García, *Effect of the Dipole-Dipole Interactions in the Molecular Dynamics of Poly(vinylpyrrolidone)-Based Copolymers*, *Macromolecules* **2014**, 47, 5334.
 - 10) S. Vallejos, A. Muñoz, S. Ibeas, F. Serna, F. García, J. M. García, *Forced solid-state interactions for the rapid, highly sensitive and selective “turn-on” fluorescence sensing of aluminium ions in water using a sensory polymer substrate*, Artículo enviado para su publicación.

Propiedad intelectual. Patentes

- 1) S. Vallejos, P. Estévez, M. Trigo, H. El Kaoutit, S. Ibeas, A. Muñoz, F. García, F. Serna, J. L. de la Peña, J. M. García, *Monómeros vinílicos y membranas poliméricas densas como sensores fluorogénicos de cationes pesados y de moléculas biológicas*, Universidad de Burgos. 2011, solicitud nº: P201100041.
- 2) M. Trigo, S. Vallejos, P. Estévez, S. Ibeas, A. Muñoz, F. García, F. Serna, J. L. de la Peña, J. M. García, *Sensores fluorogénicos de humedad y de agua en disolventes orgánicos*, Universidad de Burgos. 2012, solicitud nº: P201201139.
- 3) S. Vallejos, M. Trigo, J. L. Pablos, M. A. Muñoz, F. C. García, F. Serna, J. M. García, *Sensor colorimétrico de hierro en medios acuosos y biológicos, como aguas industriales, vino, y sangre*, Universidad de Burgos. 2013, solicitud nº: P201300575.
- 4) J. M. García, F. C. García, F. Serna, J. L. de la Peña, M. Trigo, P. A. Estévez, S. Vallejos, R. Ferrer, *Cross-linked aramid*, First Jet International LTD (China). 2013, patente nº: WO 2013/190023.
- 5) J. L. Pablos, M. Trigo, S. Vallejos, M. A. Muñoz, L. A. Sarabia, M. C Ortiz, A. Mendía, F. C. García, F. Serna, J. M. García, *Materiales poliméricos para la detección colorimétrica visual y cuantificación de explosivos nitroaromáticos y utilización de los mismos*, Universidad de Burgos. 2013, solicitud nº: P201301187.
- 6) J. L. Pablos, M. Trigo, S. Vallejos, M. A. Muñoz, L. A. Sarabia, M. C Ortiz, A. Mendía, F. C. García, F. Serna, J. M. García, *Materiales poliméricos sólidos para la detección fluorogénica de explosivos nitroderivados y utilización de los mismos*, Universidad de Burgos. 2014, solicitud nº: P201400073.

- 7) F. C. García, A. Mendía, J. M. García, M. Trigo, F. Serna, S. Vallejos, P. Martínez, J. L. Pablos, M. A. Muñoz, M. J. Rojo, *Sensores cromogénicos para aminas*, Universidad de Burgos. 2014, solicitud nº: P201400595.
- 8) J. M. García, F. C. García, S. Vallejos, C. Represa, J.M. Cámara, I. Ros, Procedimiento de medida de la concentración de especies químicas, Universidad de Burgos. 2014, solicitud nº: P201400514.

Trabajos presentados en congresos nacionales e internacionales

- 1) S. Vallejos, P. Estévez, F. C. García, F. Serna, J. L. de la Peña, J. M. García, *Copolímeros que contienen derivados de fluoreno en su estructura como sensores colorimétricos de cianuro en agua*, presentación póster, *IV Workshop on Sensors and Molecular Recognition*, Valencia (España), 8-9 de julio de 2010, Libro de resúmenes: O17, 33.
- 2) F. Serna, P. Estévez, S. Vallejos, J. M. García, F. García, *Resistencia a la humedad de tableros aglomerados hidrófugos. Comparación de métodos de análisis*, presentación oral, *XI Congreso de Adhesión y Adhesivos*, Madrid (España), 16-17 de septiembre de 2010, Libro de resúmenes: 70.
- 3) S. Vallejos, P. Estévez, F. C. García, F. Serna, J. L. de la Peña, J. M. García, *Putting to work organic sensing molecules in aqueous media: hydrophilic dense hybrid membranes as fluorogenic sensory materials for detection of mercury ions and biomolecules in water environments*, presentación oral, *Second International Conference on Multifunctional, Hybrid and Nanomaterials*, Estrasburgo (Francia), 6-9 de marzo de 2011, Libro de resúmenes: A43.
- 4) P. Estévez, S. Vallejos, H. El Kaoutit, M. Trigo, F. Serna, F. García, J.L. de la Peña, J.M. García, *Síntesis de resinas urea-formaldehído con baja Emisión de formaldehído y su aplicación en la Fabricación de tableros de partículas*, presentación oral, *XVI French-Spanish Meeting of Organic Chemistry*, Burgos (España), 19-24 de junio de 2011, Libro de resúmenes: 32.
- 5) S. Vallejos, P. Estévez, H. El Kaoutit, M. Trigo, F. Serna, F. García, J. L. de la Peña, J. M. García, *Sensory coumarin-containing polymers*, presentación póster, *XVI French-Spanish Meeting of Organic Chemistry*, Burgos (España), 19-24 de junio de 2011, Libro de resúmenes: 74.
- 6) M. Trigo, A. Gómez, P. Estévez, S. Vallejos, H. El Kaoutit, F. Serna, F. García, J. L. de la Peña, J. M. García, *Linear and crosslinked acrylic polymers bearing pendant receptor motifs. application to the extraction/elimination of heavy metals from aqueous media*, presentación poster, *XVI French-Spanish Meeting of Organic Chemistry*, Burgos (España), 19-24 de junio de 2011, Libro de resúmenes: 75.

-
- 7) M. Trigo, S. Vallejos, P. Estévez, H. El Kaoutit, F. Serna, J. L. de la Peña, F. García, J. M. García, *Fluorogenic and chromogenic polymer Chemosensors*, presentación poster, *XVI French-Spanish Meeting of Organic Chemistry*, Burgos (España), 19-24 de junio de 2011, Libro de resúmenes: 61.
- 8) H. El Kaoutit, P. Estévez, S. Vallejos, M. Trigo, F. García, F. Serna, J. L. de la Peña, J. M. García, *Aromatic polyamides with pendant fluorene moieties as sensory materials for the colorimetric and fluorogenic sensing of analytes*, presentación poster, *XVI French-Spanish Meeting of Organic Chemistry*, Burgos (España), 19-24 de junio de 2011, Libro de resúmenes: 70.
- 9) S. Vallejos, P. Estévez, H. El Kaoutit, M. Trigo, F. Serna, F. García, J. L. de la Peña; J. M. García, *Working with water insoluble organic molecules in aqueous media: piperazinedione derivative containing polymers as sensory materials for the fluorogenic sensing of biomolecules*, presentación oral, *European Polymer Congress – European Polymer Federation (EPF)*, Granada (España), 26-30 de junio de 2011, Libro de resúmenes: T4, OP24.
- 10) P. Estévez, S. Vallejos, H. El Kaoutit, M. Trigo, F. Serna, F. García, J. L. de la Peña, J. M. García, *Synthesis of Low Formaldehyde Emission Urea-Formaldehyde Resins and Their Application to the Manufacturing of Particleboards*, presentación poster, *European Polymer Congress – European Polymer Federation (EPF)*, Granada (España), 26-30 de junio de 2011, Libro de resúmenes: T1, 31.
- 11) S. Vallejos, P. Estévez, H. El Kaoutit, M. Trigo, F. Serna, F. García, J. L. de la Peña, J. M. García, *Sensory Coumarin-Containing Polymers*, presentación póster, *European Polymer Congress – European Polymer Federation (EPF)*, Granada (España), 26-30 de junio de 2011, Libro de resúmenes: T4, 114.
- 12) M. Trigo, A. Valdemoro, P. Estévez, S. Vallejos, H. El Kaoutit, F. Serna, F. García, J. L. de la Peña, J. M. García, *Novel Polymetacrylamides Containing a Triazole Moiety. Application to the Extraction/Elimination of Metal Cations from Aqueous Media*, presentación póster, *European Polymer Congress – European Polymer Federation (EPF)*, Granada (España), 26-30 de junio de 2011, Libro de resúmenes: T4, 125.
- 13) H. El Kaoutit, P. Estévez, S. Vallejos, M. Trigo, F. García, F. Serna, J. L. de la Peña, J. M. García, *Fluorene-derivative containing polymers as sensory materials for the colorimetric and fluorogenic sensing of analytes*, presentación póster, *European Polymer Congress – European Polymer*
-

- Federation (EPF), Granada (España), 26-30 de junio de 2011, Libro de resúmenes: T4, 132.
- 14) P. Estévez, H. El Kaoutit, S. Vallejos, M. Trigo, F. García, F. Serna, J. L. de la Peña; J. M. García, *Copolímero que contiene un derivado de pirimidina en su estructura como sensor colorimétrico de mercurio en agua*, presentación oral, *V Workshop on Sensors and Molecular Recognition*, Valencia (España), 1-3 de julio de 2011, Libro de resúmenes: 19.
 - 15) F. Serna, P. Estévez, S. Vallejos, J. M. García, F. García, *Seguimiento de una reacción de síntesis de cola base urea-formol mediante FTIR*, presentación oral, *XII Congreso de Adhesión y Adhesivos*, San Sebastián (España), 29-30 de septiembre de 2011, Libro de resúmenes: 81.
 - 16) M. Trigo, P. Estévez, S. Vallejos, H. El Kaoutit, F. Serna, F. García, J. L. de la Peña, J. M. García, *Reacciones "Click" en la síntesis de monómeros acrílicos*, presentación oral, *Jóvenes Investigadores en Polímeros (JIP)*, Islantilla (España), 22-26 de abril de 2012, Libro de resúmenes: 105.
 - 17) S. Vallejos, P. Estévez, M. Trigo, H. El Kaoutit, F. Serna, F. García; J. L. de la Peña, J. M. García, *Polímeros sensores derivados de la 8-hidroxiquinolina*, presentación oral, *Jóvenes investigadores en Polímeros (JIP)*, Islantilla (España), 22-26 de abril de 2012, Libro de resúmenes: 107
 - 18) F. Serna, P. Estévez, M. Sevilla, S. Vallejos, J. M. García, F. García, *Ensayos de fabricación de tableros de aglomerados obtenidos con dos tipos de colas base Urea-Formaldehído*, presentación oral, *XIII congreso de adhesión y adhesivos*, Barcelona (España), 13-14 de septiembre de 2012, Libro de resúmenes: 147.
 - 19) T. Torroba, J. Garcia, B. Diaz de Guereñu, P. Calvo; J. M. Garcia, S. Vallejos, F. C. Garcia, M. Trigo, *Materiales fluorogénicos para la detección medioambiental de compuestos neurotóxicos*, presentación oral, *VIII Reunión Científica de Bioinorgánica*, Burgos (España), 7-10 de julio de 2013.
 - 20) A. Muñoz, S. Ibeas, S. Vallejos, M. Trigo, J. L. Pablos, A. Mendia, F. García, J. M. García, *Study of Some Complexation Reactions in the Design and Synthesis of New Hybrid Polymeric Materials*, presentación oral, *International symposium on metal complexes*, Burgos (España), 16-20 de junio de 2013.
 - 21) J. García, B. Diaz de Guereñu, P. Calvo, J. M. García, S. Vallejos, F. García, M. Trigo, T. Torroba, *Fluorogenic materials for the environmental detection of neurotoxic compounds*, presentación póster, *International symposium on metal complexes*, Burgos (España), 16-20 de junio de 2013.
 - 22) T. Torroba, J. Garcia Calvo, B. Diaz de Guereñu, P. Calvo, J. M. Garcia S. Vallejos, F. C. Garcia, *Fluorogenic materials for the environmental*

- detection of neurotoxic mercury derivatives*, presentación oral, *X Simposio Investigadores Jóvenes RSEQ-Sigma Aldrich*, Madrid (España), 6-9 de noviembre de 2013, Libro de resúmenes: 232, ISBN 978-84-695-8511-5.
- 23) R. Colleoni, L. Allegri, M. Urrutia, G. Alberti, R. Biesuz, S. Vallejos, F. C. García, J. M. García, *Novel Kojic acid-based polymeric membrane for iron sensing*, presentación oral, *International Symposium on Metal Complexes*, Pavia (Italia), 8-12 de junio de 2014, Libro de resúmenes: 28.
- 24) S. Vallejos, A. Muñoz, S. Ibeas, F. Serna, F. García and J. M. García, *Forced solid-state interactions for the rapid, highly sensitive and selective "turn-on" fluorescence sensing of aluminium ions in water using a sensory polymer substrate*, presentación póster, *XIII Reunión del Grupo Especializado de Polímeros (GEP) de la RSEQ y RSEF*, Girona (España), 7-10 de septiembre de 2014, Libro de resúmenes: 188, ISBN: 978-84-697-0702-9.
- 25) J. L. Pablos, M. Trigo, S. Vallejos, F. Serna, F. C. García, J. M. García, *Polímeros sensores y tejidos inteligentes para la detección colorimétrica de TNT en medio acuoso y fase vapor*, presentación oral, *XIII Reunión del Grupo Especializado de Polímeros (GEP) de la RSEQ y RSEF*, Girona (España), 7-10 de septiembre de 2014, Libro de resúmenes: 55, ISBN: 978-84-697-0702-9.
-